

TECHNO-ECONOMIC ASSESSMENT STUDY FOR ROGUN HYDROELECTRIC CONSTRUCTION PROJECT

PHASE II: PROJECT DEFINITION OPTIONS

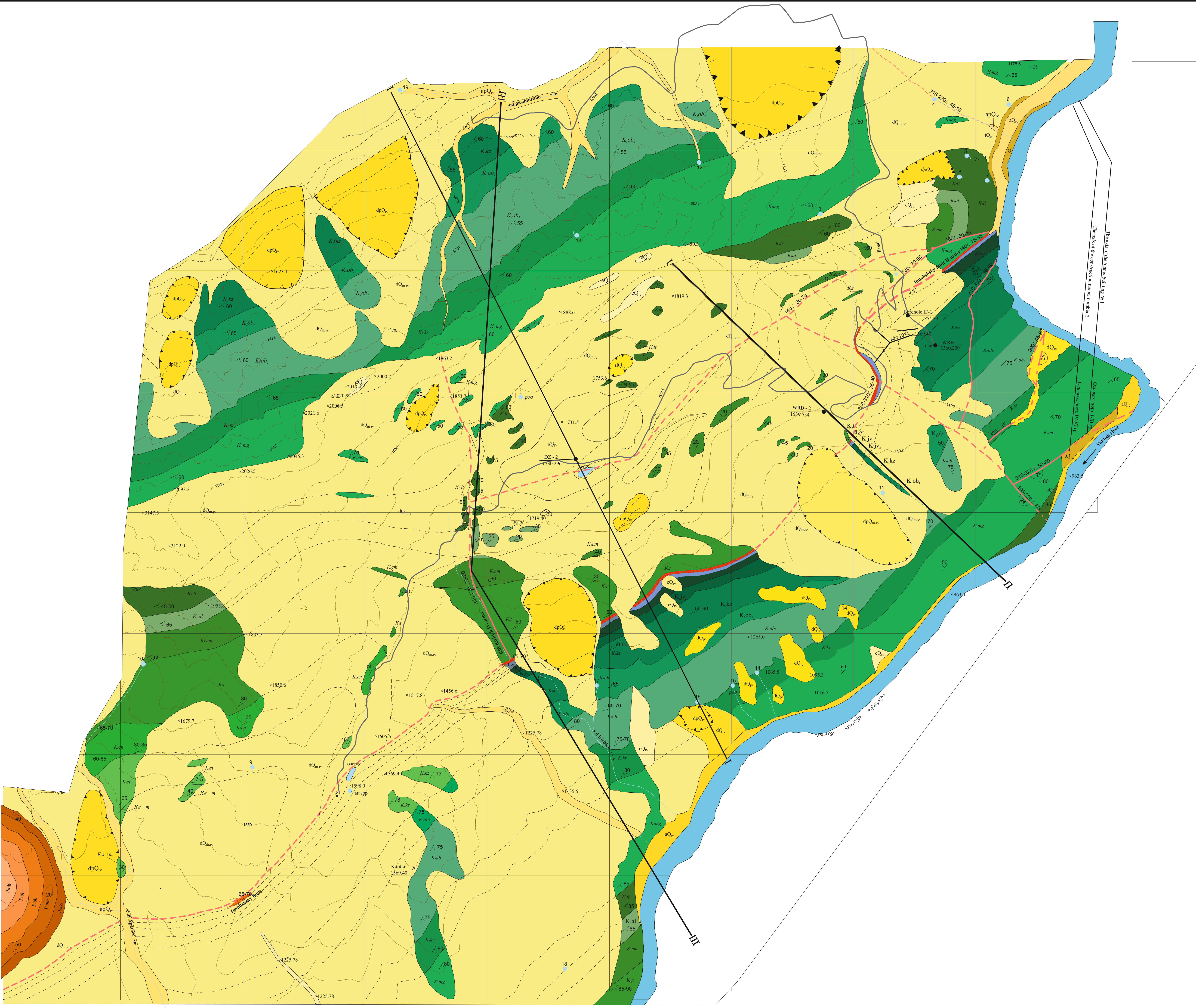
Volume 2: Basic Data

Chapter 2: Geology

Part B - Geological Investigation in the Right Bank

Annex 1 Geological map

March 2014



- LEGEND**
- Amudarya complex**
- lQ_m Man-made deposits.
 - elQ_m Eluvial deposits. Presented drevnyano clay soils with the inclusion of different fractional fragments up to 5%. Ingredients: mudstones and siltstones
 - aQ_m Alluvial deposits of channel and floodplain. Consist mainly of boulders, sometimes coarse gravel. Assorted filler sand (20%). Power 3-8m
 - dpQ_m Landslide-landslide deposits. Separate blocks (30%) ranging in size from 0.5 to 5 m, gravel, grass (50%) with a loose sandy-loam filler (20%). Power 1.0-10.0 m
 - pQ_m Proluvial deposits. Presented subrounded grass detritus deposits with sandy-clay aggregate
 - cQ_m Colluvial deposits. Loose debris: crushed stone, gravel. Power from 0.5 to 1.0 m
- Quaternary system**
- dQ_m Talus deposits. Slope deposits: gravel, grass with sandy-loam filler (20%). Capacity of 0.5-2.0 m
 - $dpQ_{m,iv}$ Deluvial-proluvial deposits. Lumps of gravel, sand and loam
 - $dQ_{m,iv}$ Talus deposits. Grassy-sandy-loam soil with fragments of limestone, sandstone and mudstone
- Paleogene system**
- P_{bh} Bukhara layers
 - P_{bh} Upper unit. Argillity marls and greenish-gray
 - P_{bh} Average stack. Gray limestone with layers and lenses of white gypsum, marl bluish-gray color
 - P_{bh} The lower member. Massive dense, cryptocrystalline limestone, light gray
 - P_{ak} Akdzharskie layers
 - P_{ak} Upper unit. Massive white plaster with a few layers of gray limestone and dolomite
 - P_{ak} The lower member. Sandstones and siltstones of red, with streaks of gray marl and white gypsum
- Cretaceous system**
- Upper series**
- K_{m} Maastricht tier. The massive limestone interbedded with sandstones
 - K_{cp} Campanian yarus. Serovato green mudstone, slightly sandy, sandy limestones with organic residues and interbedded marls
 - K_{st} Cantonsky tier. Interbedded sandstone, siltstone and shale layers
 - K_{cn} Konyaksky tier. Sandstone, limestone, mudstone and rakushnyaki
 - K_{t} Turonian stage. Dark-gray and greenish-gray mudstone interbedded with gray argillaceous limestones and marls
 - K_{cn} Cenoman. Interbedded dark-gray and gray shales with inclusions and lenses of gray limestone, rakushnyakov
- Lower series**
- K_{al} Alban subsuite. Interbedded mudstone and gypsum, with layers of gray sandstone and mudstone plastered
 - K_{lb} Latabanskaya Formation. Interbedded dark-gray and greenish-gray mudstones with thin layers of light-gray, cryptocrystalline sandstones
 - K_{mg} Minghatmanskaya Formation. Interbedded reddish-brown and light gray, fine-to medium-grained sandstones and mudstones
 - K_{kr} Karakuzskaya Formation. Small-and medium-grained sandstone brown-brown, with inclusions of mica layers of mudstone and siltstone
 - K_{ob} Obigarmkaya suite
 - K_{ob} The upper layers. Small-and medium-grained, massive sandstone light brown, brown-brown with occasional thin interbedded mudstone
 - K_{ob} The lower layers. Brownish siltstone and reddish-brown mudstones with thin layers and lenses of white gypsum
 - K_{ks} Kyzyltaszkaya Formation. Brownish-red, fine-grained, micaceous sandstones interbedded with siltstones and mudstones
 - K_{ju} Javanese formation.
 - K_{ju} Upper unit. Uneven striping of red mudstone and brown-brown siltstone
 - K_{ju} The lower member. The reddish-brown mudstone with rare gypsum veins
 - J_{gr} Gaurdak formation. Reddish-brown plastered, massive siltstones and mudstones
- Other symbols:**
- ~ 55 Dips and strikes
 - Tectonic faults, their number, the items of bedding and the number of order: a-credible, b-expected
 - Tectonic zone crushing accompanied faults. Rocks within zones of intense kataklazirovana, split into fragments of size 0.5 cm Seams are made of tectonic breccia breaks friction which is a gravel and rubble significantly weakened rocks in dense sand and loamy filler. Power fault breccias II order is up to 1.5 meters in fractures III order of 0.2-0.3 cm
 - Land collapse-landslide
 - Line of geologic section
 - Place a drilled borehole, its number and altitude
 - Elevation
 - Road
 - Spring and its number
 - The river and its naprvlenie
 - Currents: a-constant, b-time

Main Department of Geology under the Government of Republic of Tajikistan, Unitary Enterprise "South Tajik prospecting"		Report: "Detailed study of geological structure of the right bank of Rogun hydrosystem"	
Attachment		Responsible person: Chief Geologist / J.O.M. Bobomurodov	2012y.
Page No.		GEOLOGICAL MAP right bank of the Rogun hydroelectric	
Scale 1:5000			
Amounted	Geologists	Rustambekov A.	
Computer design		Ibragimov N.	
		Rustambekov G.	

TECHNO-ECONOMIC ASSESSMENT STUDY FOR ROGUN HYDROELECTRIC CONSTRUCTION PROJECT

PHASE II: PROJECT DEFINITION OPTIONS

Volume 2: Basic Data

Chapter 2: Geology

Part B - Geological Investigation in the Right Bank

Annex 2-1 Field book

March 2014

The Ministry of Energy and Industry

Republic of Tajikistan

Subsidiary "Complex-prospecting expedition-3"

The work area Hydra Rogun power stations

Message book №1

Geological survey scale 1:5000

Artist: Chief Geologist Rustambekov A.

Started: 13.08.2012r.

Completed: 12.10.2012r.

Observation points from № 1 to № 185

Rogun-2012.

Дата 13.08.12

Дата _____
Страница _____

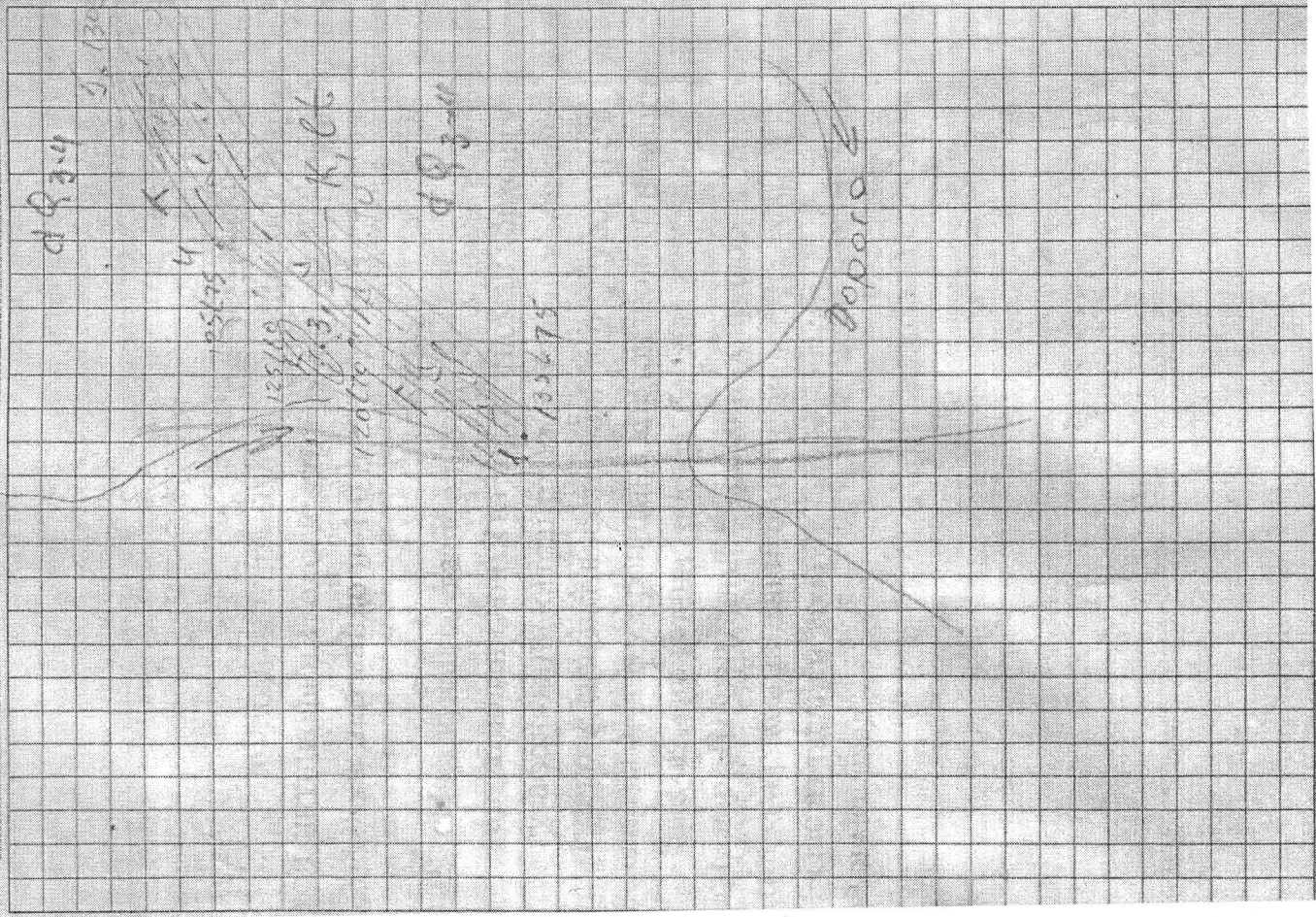
Geological survey scale 1: 5000.

The observation point №1 K₁ It

Exit gypsum plastered and mudstones. Dip azimuth 135°, angle __. Gypsum power up to 0.6 m. Heavily weathered rocks.

The observation point №2 dip azimuth 120, angle 70. Outcrops mudstones and argillites and gypsum plastered. Breed heavily trampled and eroded.

The observation point №3 Dip azimuth 125, angle 60. Claystone dark gray thin-bedded, strongly weathered.



The observation point № 4. K₁lt. Dip azimuth 125, corner of 75. Alternation of mudstone, siltstone and gypsum layers. Gypsum-0, 3m. Weathered rock.

The observation point № 5 K₁lt. Azimut 130, corner of 70. Mudstones plastered. Fractured and weathered rock.

The observation point № 6. K₁lt. Dip azimuth 130, corner of 70. Alternation of siltstone and mudstone weight of 0,6 m Fissured rock the ruins to blocks of 7h10sm.

The observation point number 7. K₁lt. Dip azimuth 165, corner of 85. Sandstones and siltstones, with layers mudstone. Total power - 1.5 m

The observation point number 8. K₁lt. Dip azimuth 110, corner of 58. Mudstones and siltstones highly fractured and weathered. Capacity of 0.4 m.

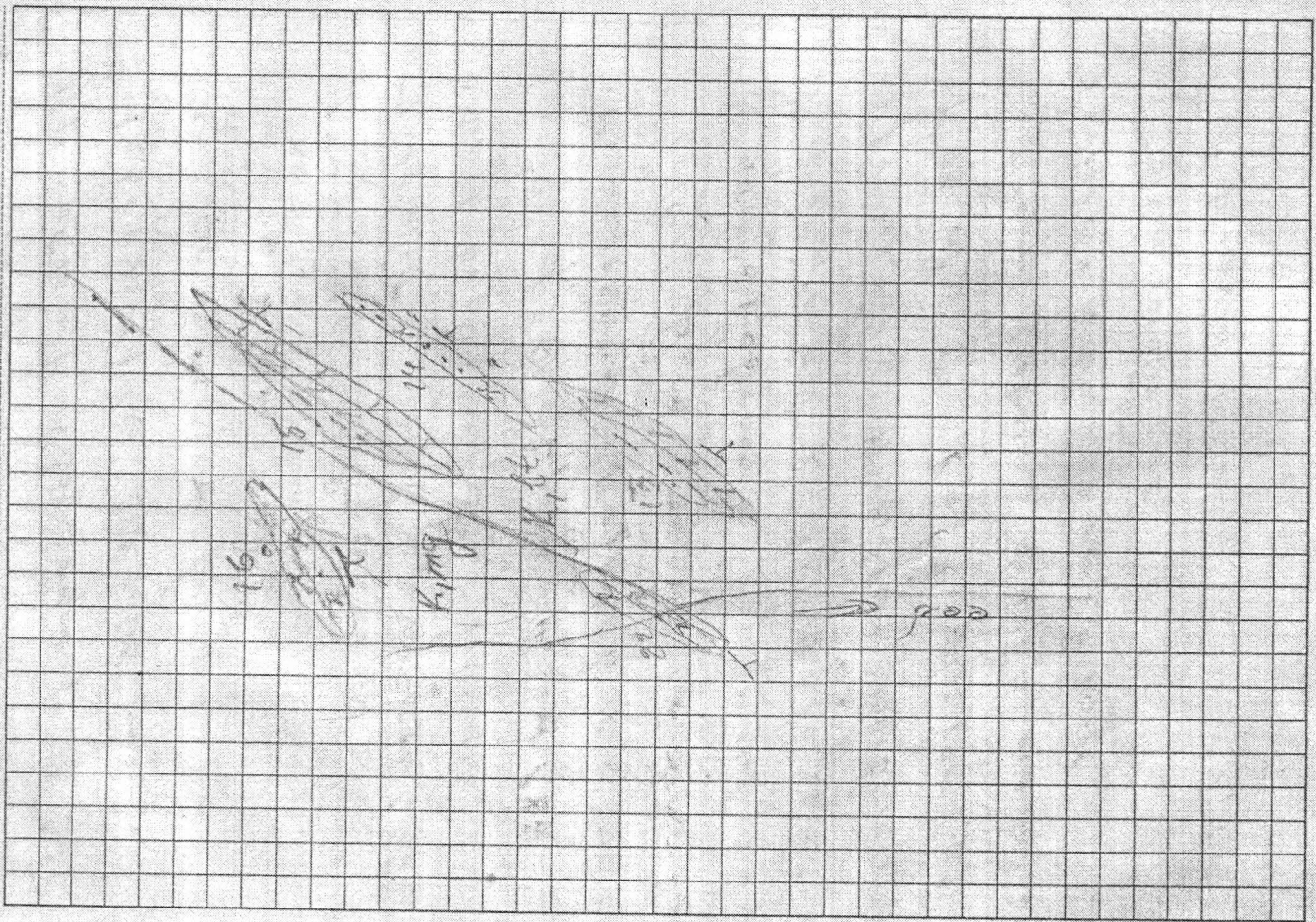
The observation point № 9. K₁lt. Dip azimuth 115, corner of 65. Mudstone with layers of limestone, with a capacity of 2.0 m Mudstones are dark gray, strongly weathered.

The observation point № 10. K₁lt. Dip azimuth 110, corner of 75. Alternation of shales and limestones. Gray, thin-bedded, not clay cement. The total capacity of 2.3 m.

The observation point № 11. K₁lt. Dip azimuth 110, corner of 75. Gray, highly fractured. Capacity of 0.3 m.

12.08.12.

The observation point № 12. K₁lt. Dip azimuth 170, corner of 85. Alternation of shales and marls. Highly weathered rock. Capacity of 2.5 m.



The observation point № 12. K₁lt. Dip azimuth 170, corner of 85°. Alternation of shales and marls. Highly weathered rock. Capacity of 2.5 m.

The observation point № 13. K₁lt. Dip azimuth 150, corner of 75°. Alternation of shales and marls. Dominated mudstone. Weathered rock.

The observation point № 14. K₁lt. Dip azimuth 130, corner of 85°. Contact between K₁mg and K₁lt. Sandstone siltstone, dark-brown, micaceous, fractured.

The observation point № 15. Contact between K₁lt and K₁mg. 130° dip azimuth, angle 80°. Alternation of marly limestones, marls and mudstones. Fissured rock.

The observation point № 16. K₁mg. 130° dip azimuth, angle 87°. Reddish-brown sandstone, medium, fractured.

The observation point № 17. K₁mg. 125° dip azimuth, angle 60°. Brown sandstones with thin interbedded mudstone, with a capacity of 0.2 m (20 cm). Fissured rock.

The observation point № 22. K₁mg. Dip azimuth 125, corner of 70. Fine-grained sandstones, fractured.

The observation point № 23. K₁mg. Dip azimuth 180, corner 80-85. Fine-grained sandstones, slightly fractured.

The observation point № 24. The body of a local landslide. Exit K₁mg. Dip azimuth 315, corner of 40. Rock (sandstone) is highly fragmented. Places to boulders the size of 1m x 0,7 m.

The observation point № 25. K₁mg. Dip azimuth 125, corner of 60. Sandstone rocks of small-and medium-grained, slightly fractured. The fracture tough.

The observation point № 26. K₁mg. The body of a local landslide.

Average length - 1200m.

Average width - 60m.

The average height - 3m.

Volume - 21800m³.

On the body observed damaged layers (K₁mg). Dip azimuth 340, corner of 40. Rock (sandstone) is highly fragmented.

The observation point № 27. K₁mg. Dip azimuth 120, corner of 70. Medium-grained sandstone rocks, slightly fissured fracture strong.

The observation point № 28. K₁lt. Dip azimuth 145, corner of 75. Interbedded mudstone, marl and limestone. Mudstones plastered. Marly limestone with layers of gray sandstone. Heavily weathered rocks.

The observation point № 29. K₁lt. Dip azimuth 135, corner of 55. Mudstone and limestone dominated by mudstone. Breed highly fractured and weathered.

The observation point № 30. K₁lt. Dip azimuth 135, corner of 80. Interbedded thin-bedded marls. Highly weathered rock.

The observation point № 31. K₁lt. Dip azimuth 145, corner of 70. Mudstones plastered with layers of plaster, capacity of 0.2 m. Highly weathered rock.

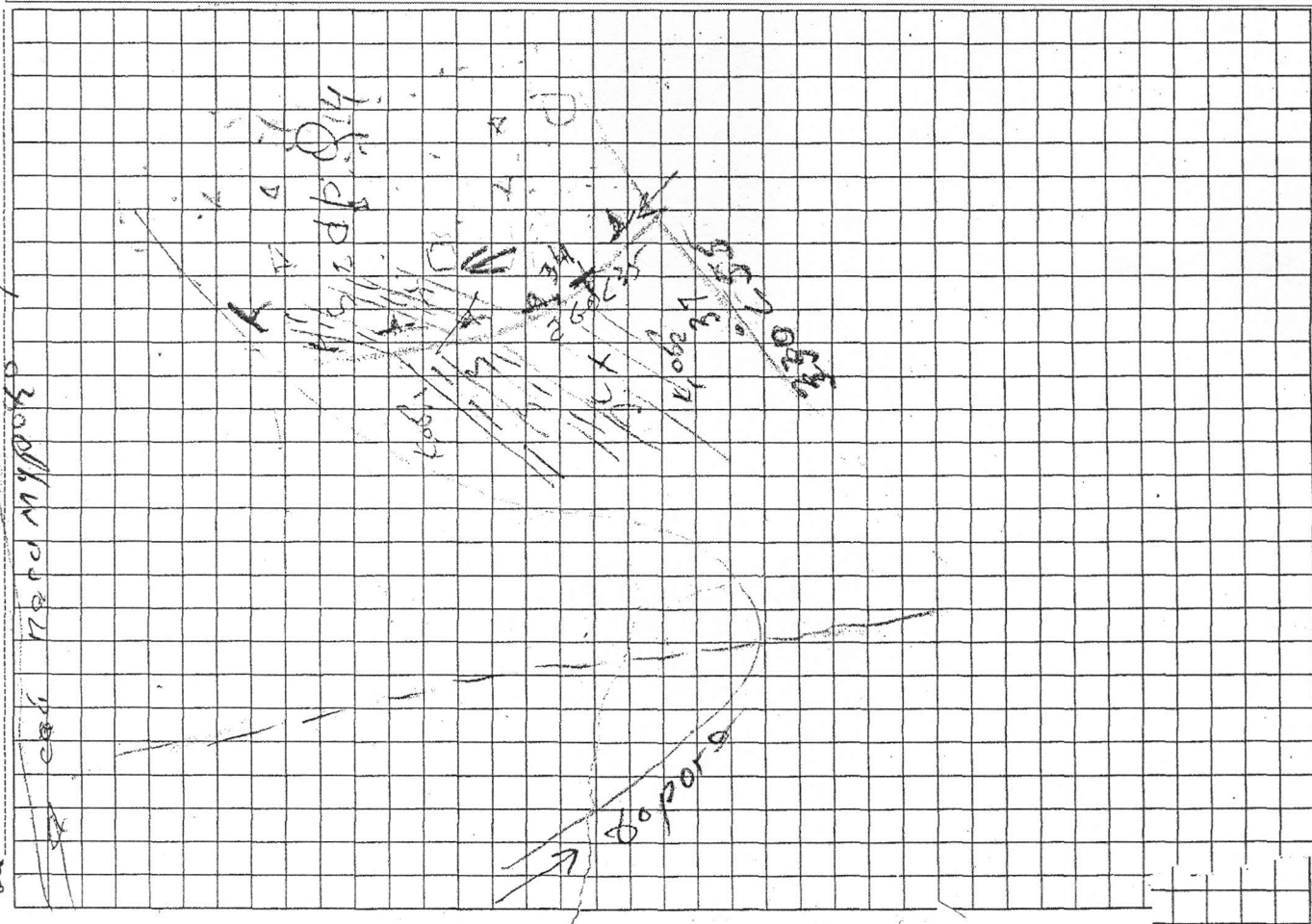
The observation point № 34. (dpQ₄) the watershed landslide from the north-west side of the mixing of sediments on indigeno breeds and tear. Dip azimuth 260, corner of 35. Mixing breeds 10.5 m Breed for contact badly damaged. In the upper part of the section to the blocky grained material with wood filler loamy.

The average length of a landslide - 412m.

Average width - 280 m.

The average height - 3m.

Volume - 34680m³.



The observation point № 34. (dpQ₄) the watershed landslide from the north-west side of the mixing of sediments on indigenous breeds and tear. Dip azimuth 260, corner of 35. Mixing breeds by 0.5 m Breed for contact badly damaged. In the upper part of the section to the blocky grained material with wood filler loamy.

The average length of a landslide - 412m.

Average width - 280 m.

The average height - 3m.

Volume - 34680m³.

The observation point № 35. Dip azimuth 135, corner of 40. K₁ob₁. Interbedded siltstone and mudstone brown-brown, heavily fractured, fine-to medium layered, highly weathered.

The observation point № 36. K₁ob₁. Dip azimuth 140, corner of 40. Sandstones with interbedded mudstone rare. The sandstones are light brown, brownish, medium and medium thick layered, very strong.

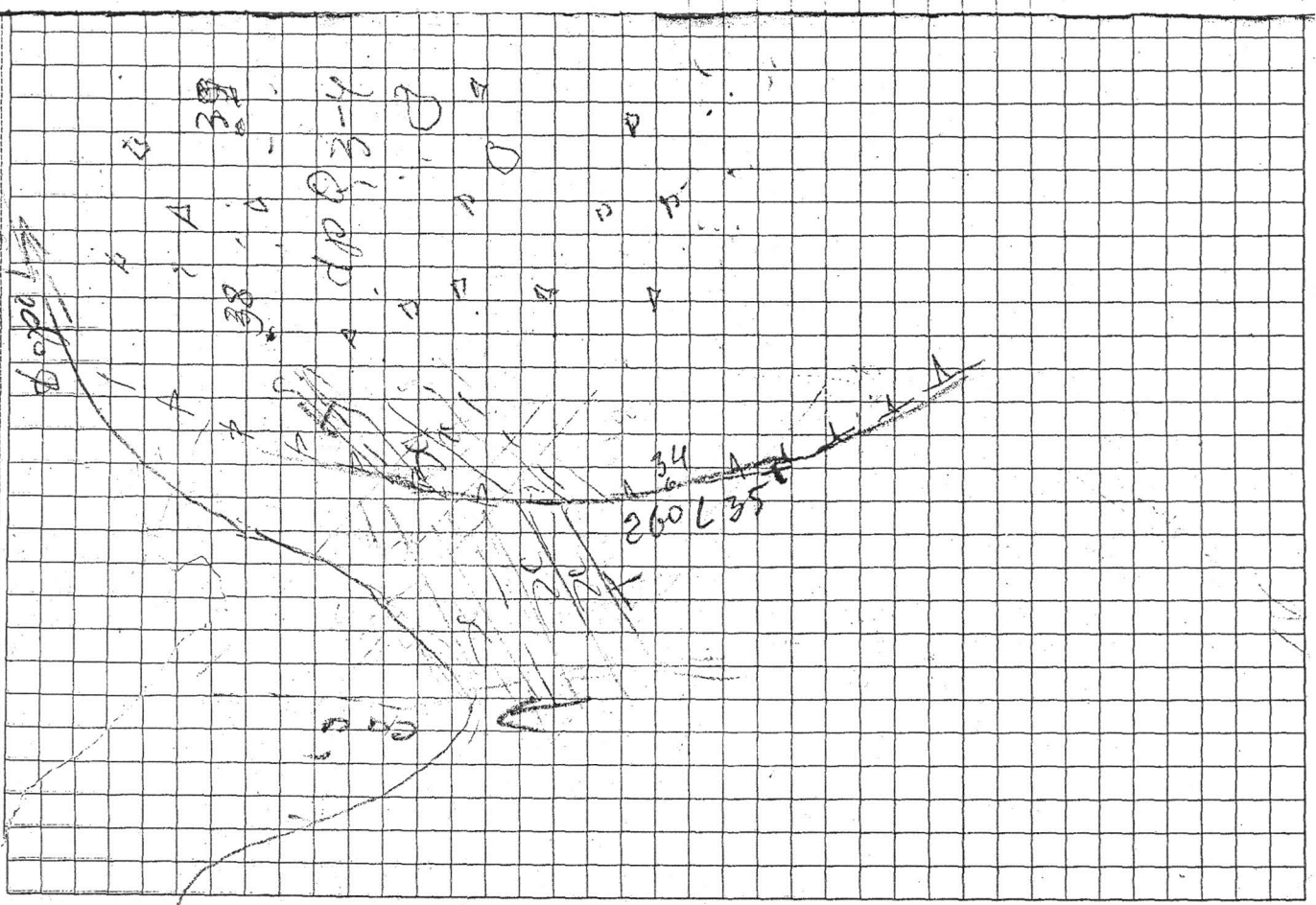
The observation point №37. Tectonic crack. Dip azimuth 330, corner of 55. Mixing amplitude is observed. The influence zone of 2.0 m

The observation point № 38. dpQ3-4. Landslide zone. Block detrital material grussy clay filler. The composition of sandstone and 80% less likely to siltstones and mudstones.

The observation point № 39. dpQ3-4. Landslide zone. Block stony soil with clay filler grussy.

The observation point № 40. K₁lt. Dip azimuth 130, corner o 85. Private crystalline limestone to calcareous cement firm. The total mass of 3.2 m.

→ 200
→ 1000



The observation point № 41. K₁lt. Dip azimuth 186, corner of 55. Interbedded mudstone and gypsum. Gypsum from light gray to white. Power - 0.4 m The breed is highly fragmented and eroded.

The observation point № 42. K₁lt. Dip azimuth 120, corner of 60. Mudstones plastered. Highly weathered rock.

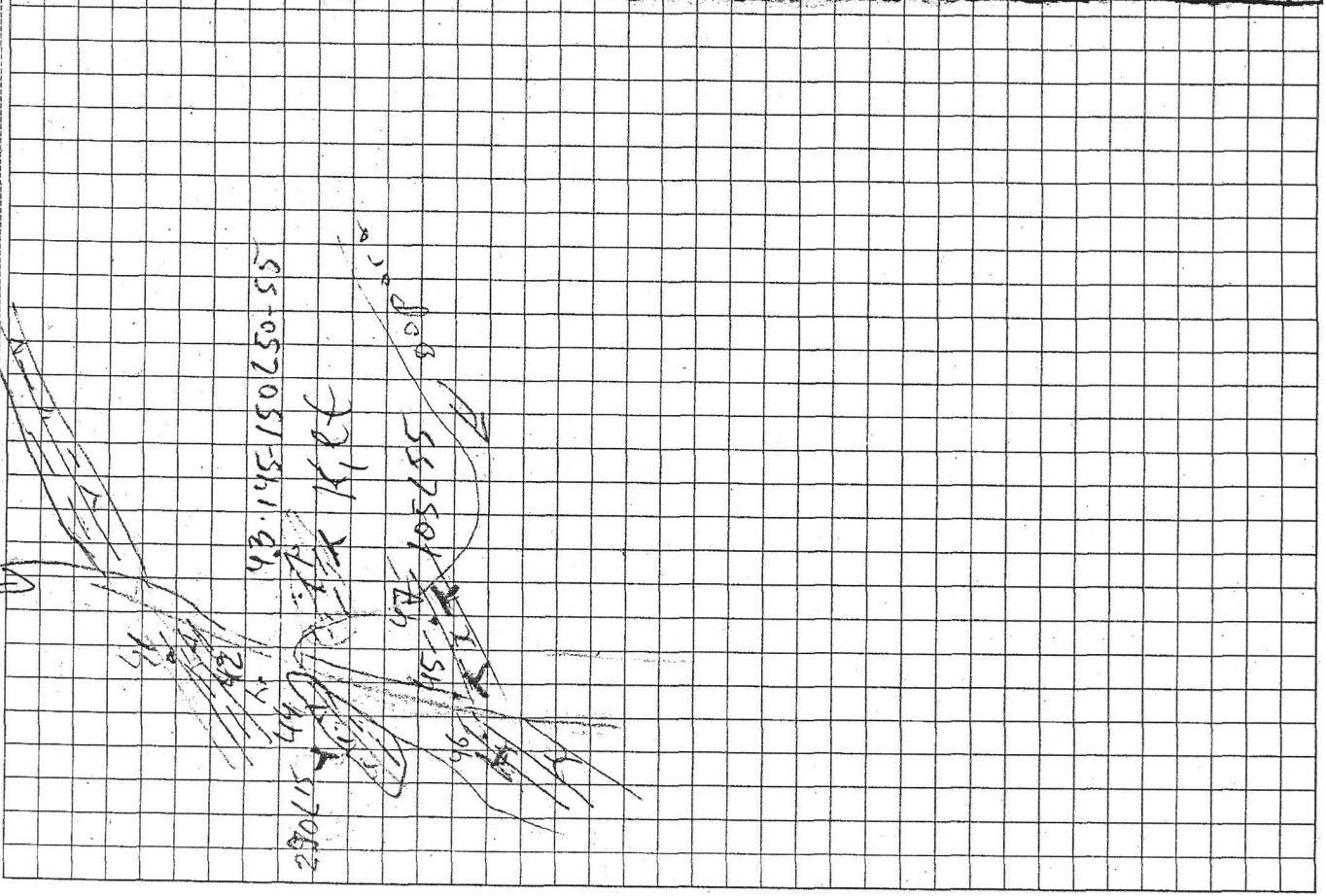
The observation point № 43. K₁lt. Dip azimuth 140-150, corner of 50-55. Alternation of shales and marls, with a predominance of mudstone. Thin-bedded rock and strongly weathered.

The observation point № 44. K₁lt. Dip azimuth 290, corner of 15. Mudstone and gypsum, highly fractured and weathered.

The observation point № 45. K₁lt. Dip azimuth 100, corner of 45. In ditch gray sandstone. medium grained, thin-bedded, on clay cement.

The observation point № 46. Dip azimuth 150, corner of 65. Sandstones (K₁lt) medium grained, thinly layered, fractured.

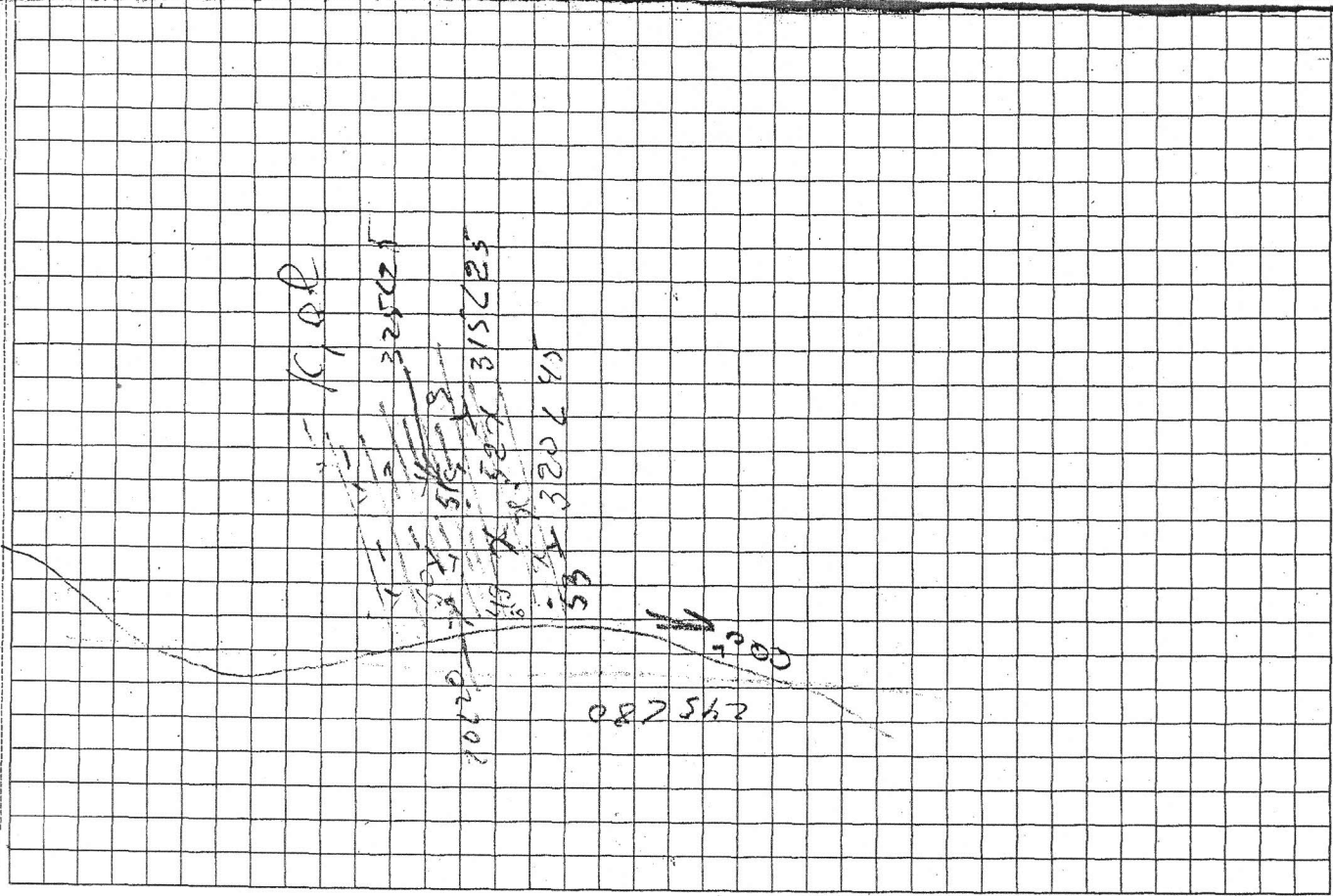
The observation point № 47. To port sai (K₁lt). Sandstones are small and medium grained, finely layered and fractured.



The observation point № 48. K₁al. Dip azimuth 110, corner of 20. Uneven interbedded mudstone and gypsum. Gypsum from light gray to white, with a predominance of mudstone. Highly weathered rock.

The observation point № 49. K₁al. 76 dip azimuth, angle of 20. Sandstone siltstone, fine-grained, thinly layered, fractured.

The observation point № 50. K₁al. 20 dip azimuth, angle of 20. Mudstones plastered. Gypsum and mudstones with a capacity of up to 2.0 m. Highly weathered rock.



The observation point № 51. K_{1al} . Dip azimuth 325, corner of 25. Mudstones plastered with capacity of 25m. Breed highly fractured and weathered.

The observation point № 52. K_{1al} . Dip azimuth 315, corner of 25. Thin-bedded sandstone, fine-grained, fractured.

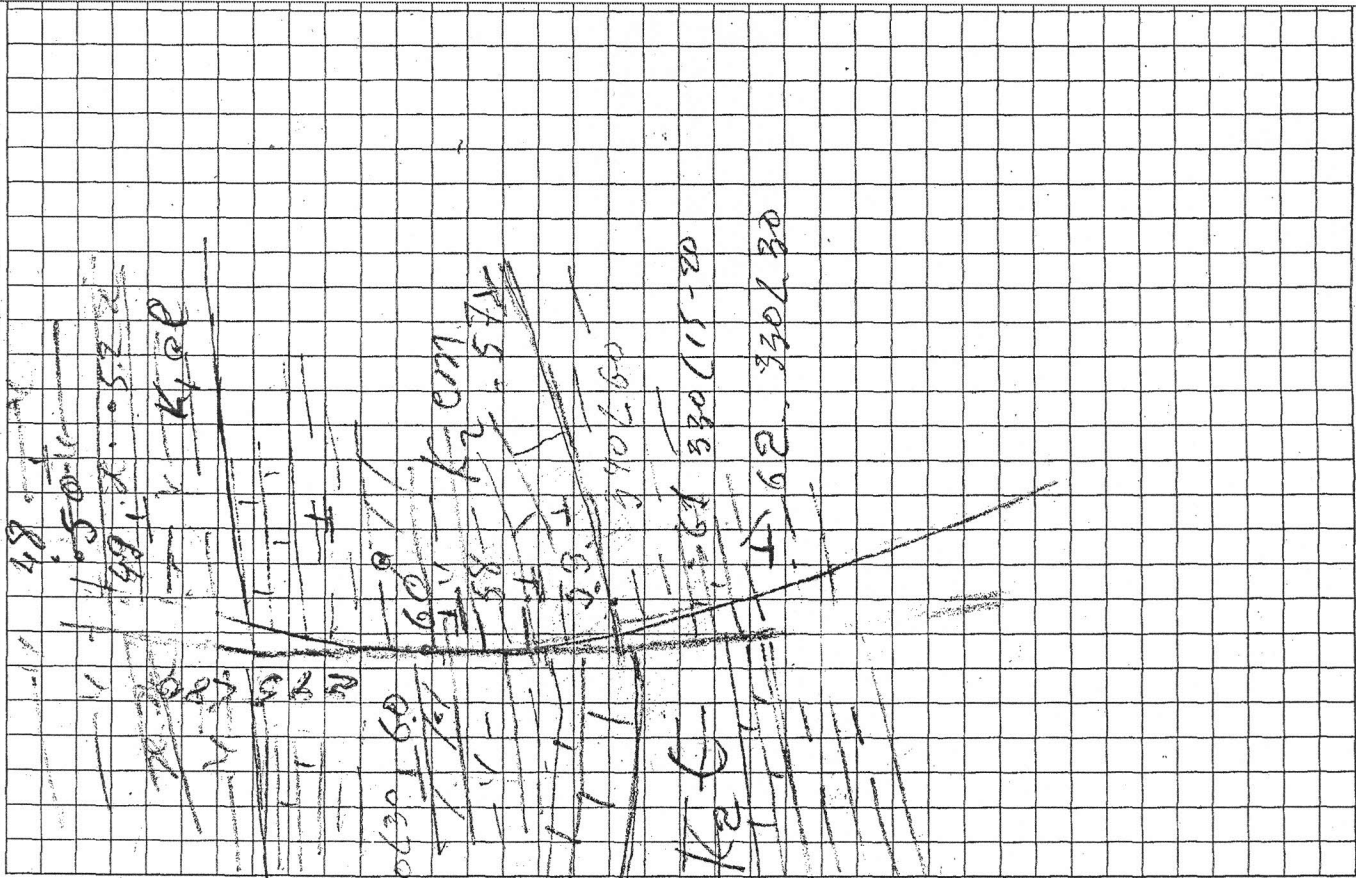
The observation point № 53. K_{1al} . Dip azimuth 320, corner of 45. The sandstones are gray, thin-bedded, fractured, cemented by clay cement.

The observation point № 54. Dip azimuth 205, corner of 50 (K_{1al}). Little way out of sandstone. The total capacity of 0.6 m. Fine-grained sandstones, fractured.

The observation point № 55. K_{2t} (Turonian). Dip azimuth 340, corner of 70. Limestone gray hidden crystalline carbonate cement on clay, on a break strong. The total capacity of 3.5 m.

The observation point № 56. K_{2cm} (Cenomanian). Dip azimuth 30, corner of 45. Gray, hidden crystalline carbonate cement on clay, very dense, slightly fractured.

The observation point № 57. K_{2cm} . Dip azimuth 320, corner of 55. Gray, very strong, slightly fractured.



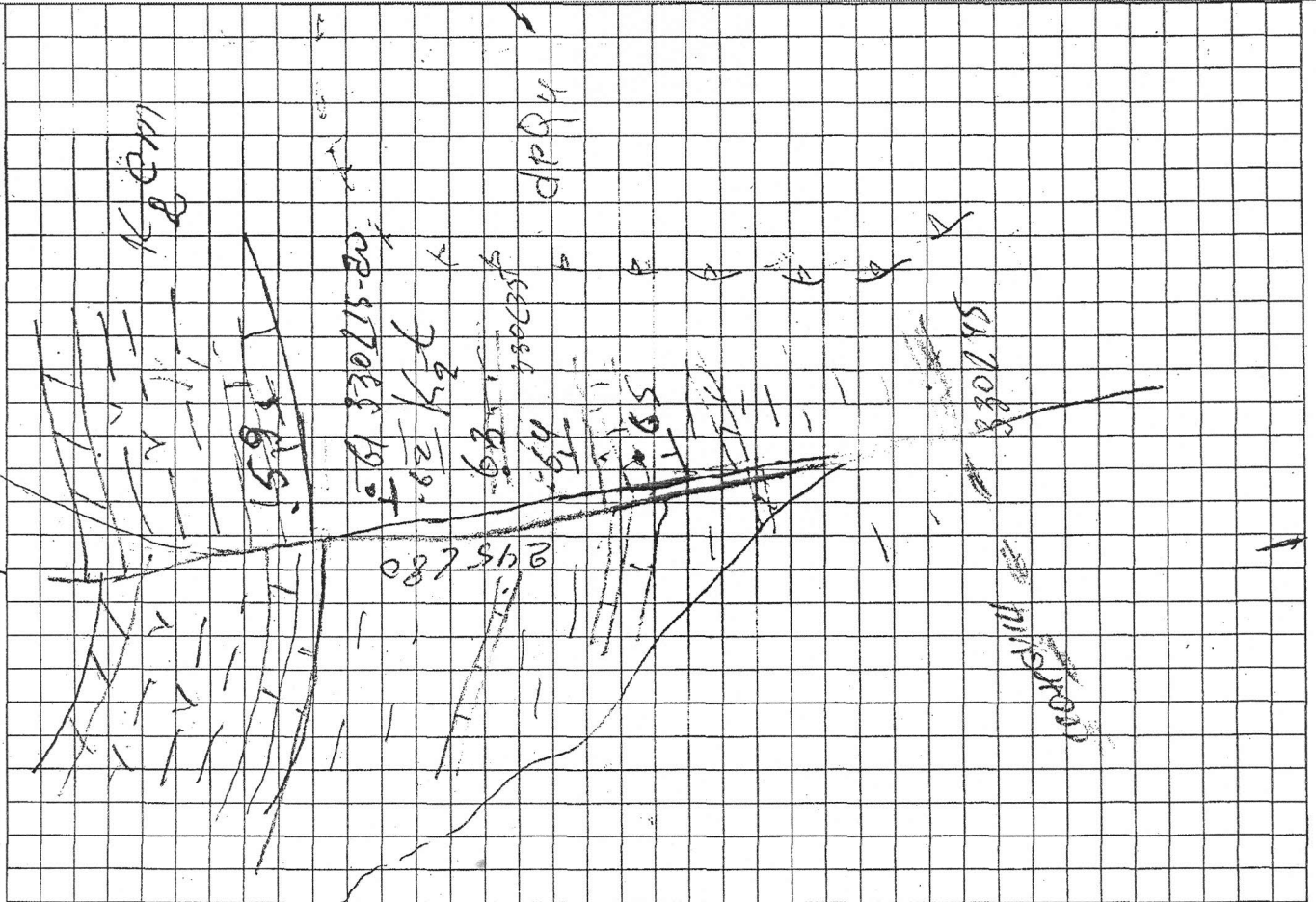
The observation point № 58. K₂cm. Dip azimuth 360, corner of 60. Uneven alternation: mudstone, marl, with layers of plaster. Gypsum power 0.7m. Fractured and weathered rock.

The observation point № 59. K₂cm. 340 azimuth angle 60. Gray, massive, slightly fractured. The fracture strong.

The observation point № 60. K₂cm. Azimut 330, corner of 30. Mudstones and marly limestones. Fractured and weathered rock.

The observation point № 60a. Tectonic disturbance IV order. Azimut 245, corner 80. Weld size to 6cm. The influence zone of up to 3m. The nature of the wall - rough. The amplitude of mixing - 0.4 m Sequence number - IV.

K₁OC



The observation point № 61. K₂t. Dip azimuth 330, corner 15-20. Mudstones are dark gray, thin-bedded, strongly weathered.

The observation point № 62. K₂t. Mudstones are gray, dark gray, with rare and veins of gypsum. Highly weathered rock. Power 7m.

The observation point № 63. K₁t. Dip azimuth 330, corner of 35. Gray limestone with a few streaks of calcite capacity 2m.

The observation point № 64 K₂t. Dip azimuth 325, corner 30-35. Mudstone with occasional veins of gypsum. Gypsum is white.

The observation point № 65. K₂t. Dip azimuth 340, corner of 20. Gray limestone for cement and clay mudstones power 7m. The total capacity of 23m.

The observation point № 66. Dip azimuth 330, corner of 30. K_{2t}. Thin-bedded mudstones, heavily weathered with rare gypsum. The total capacity of 15m.

The observation point № 67. K_{1t}. Dip azimuth 325, corner of 45. Mudstones and limestones. Mudstones are gray, dark gray, thin-bedded, strongly weathered. Gray limestone with layers of marl, fractured.

The observation point № 68. Dip azimuth 335, corner of 50. Ionahshsky tectonic fault II order. The breed is highly fragmented. Seam fault 2m. Filler clay. Mudstone and gypsum. The influence zone of 30m.

The observation point № 69. K_{1jv}. Dip azimuth 325, corner 45-50. Breed mudstones and siltstones strongly fractured to gravel and clay.

The observation point № 70. K_{1kz}. Dip azimuth 340, corner 50-60. Sandstone with layers of mudstone and siltstone.

The observation point № 71. K_{1ob1}. Dip azimuth 350, corner of 65. Breed mudstones and siltstones. Mudstones brick-red color, highly fragmented and weathered.

The observation point № 71^a. K_{1ob2}. Dip azimuth 345, angle of 65-70. Sandstone light brown, brown-brown, small and medium-grained, slightly fractured.

08/21/12

The observation point № 72. K_{1al}. Dip azimuth 285, corner of 20. Small outcrops. Thin layers of shale and mudstone, greenish-gray, strongly weathered. Total power 2.0 m.

The observation point № 73. K_{1al}. Dip azimuth 265, corner of 30. Mudstone and clay gray, greenish-gray, much destroyed, places to gravel.

The observation point № 74. K_{1al}. Dip azimuth 250, corner of 20. Similarly, the observation point № 73.

The observation point № 75. K_{1al}. Dip azimuth 190, corner of 35. A little way. Thin-bedded mudstones, greenish-gray clay. Breed badly damaged and weathered.

The observation point № 76. dQ₃. Four breeds broken up blocks h4m size 3.5 or less. Ingredients: gray, fracture strong.

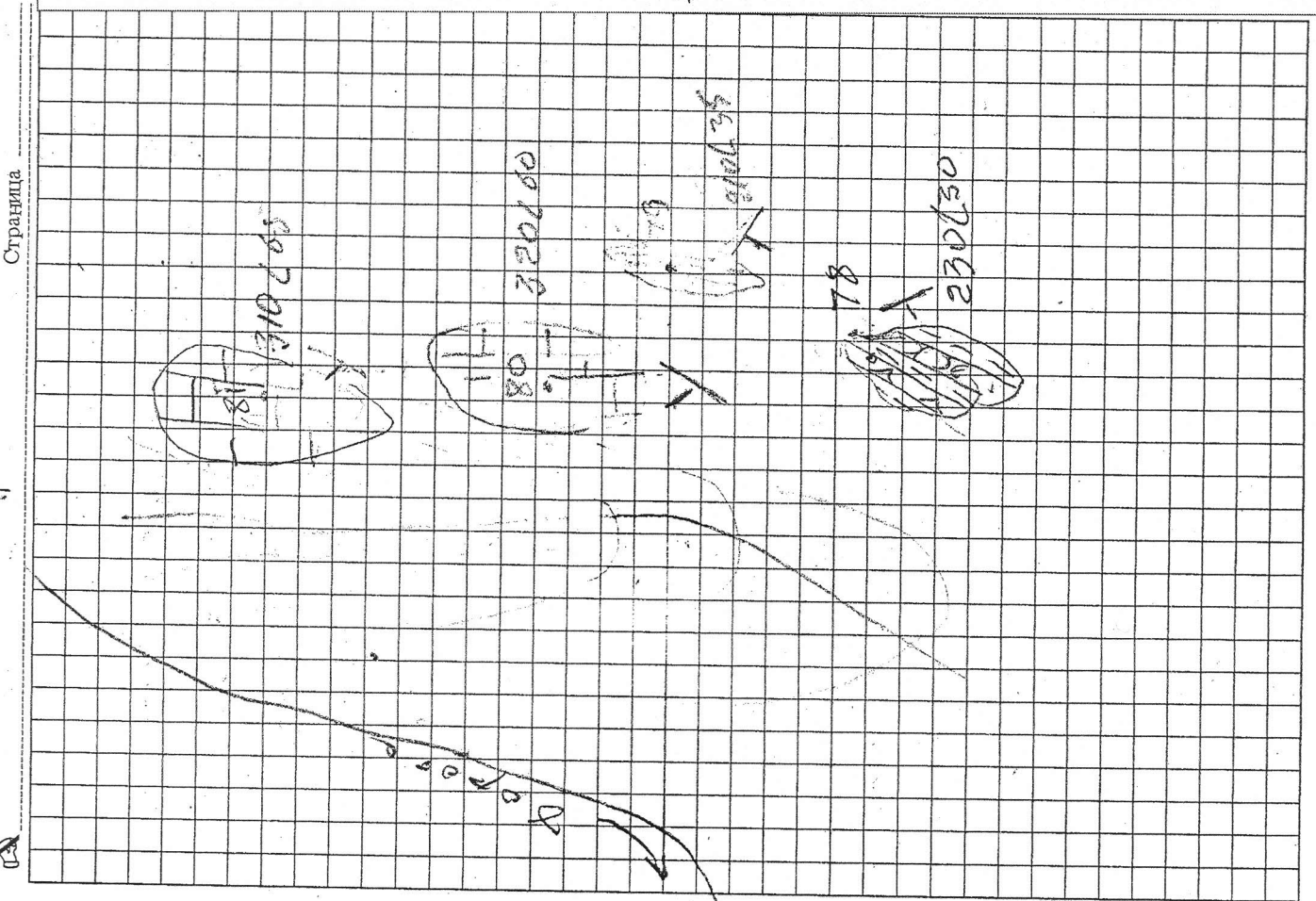
The observation point № 77. K_{2cm}. Dip azimuth 140, corner of 40. Small outcrops. Gray, hidden crystal, fracture, fracture strong.

The observation point № 78. K₂cm. Dip azimuth 230, corner of 30. Alternation of gypsum, mudstone and sandstone. Highly fractured rocks. The total capacity of 2m. Power plaster 0,4 m.

The observation point № 79. K₂cm. Dip azimuth 210, corner of 35. A little way. Mudstone with layers of gray clay. Highly weathered rock. The total capacity of 2.5-3m.

The observation point № 80. K₂cm. Dip azimuth 320, corner of 60. On the surface there is a flat surface, the limestone area of 3.5 m². Gray, to break strong.

The observation point № 81. K₂cm. Dip azimuth 310, corner of 65. Similarly, the observation point number 80. Flat plane of gray limestone. Area of 3.7 m². The fracture tough.



The observation point № 82. dQ_{3-4} . Block-grained material of different sizes. Ingredients: Gray, fracture strong.

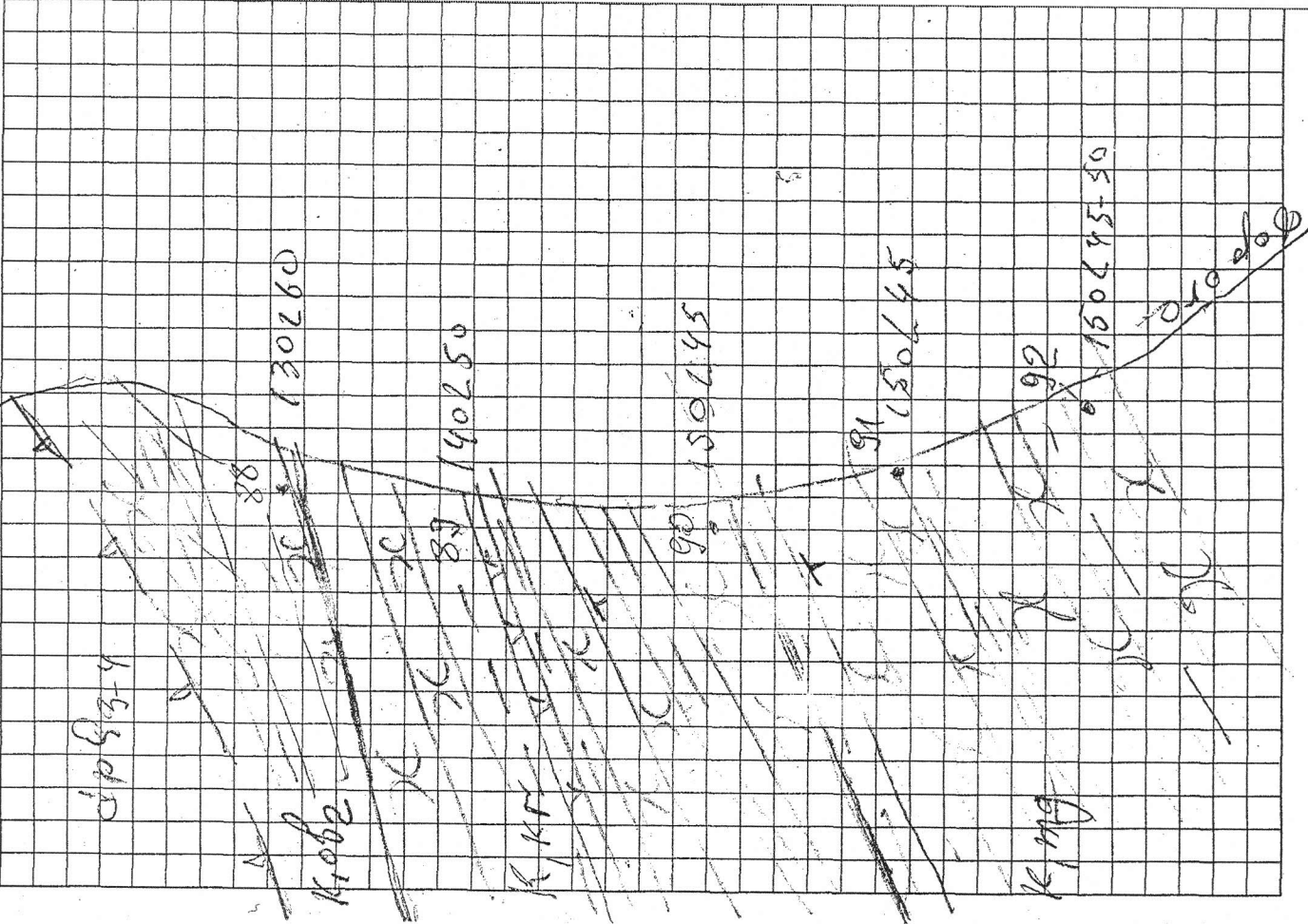
The observation point № 83. dQ_{3-4} . In the north a distance 45-50m from the observation point № 82. Rocks similar to the observation point № 82.

The observation point № 84. dQ_{3-4} . Located in the north-east from the observation point № 83 at a distance of 70m. Rocks similar to the observation point № 83.

The observation point № 85. dQ_{3-4} . Block-grained material. Composition: limestone gray.

The observation point № 86. K_1cm . Dip azimuth 290, corner of 20. Small outcrops of limestone gray. Fissured rock. The total capacity of 1.8 m.

The observation point № 87. K_1cm . Dip azimuth 300, corner of 50. Limestone outcrops of gray. Fissured rock, fracture strong. Capacity of 2.5 m.



The observation point № 88. K_{1ob_2} . 20 dip azimuth, angle of 40. Breed Gray, highly fractured. Power 3m.

22/08/12

The observation point № 88^a. K_{1kr} . Dip azimuth 130, corner of 60. Sandstones with a few layers of mudstone. Highly fractured rock.

The observation point № 89. K_{1kr} . Dip azimuth 140, corner of 50. Interbedded sandstone and mudstone with layers of plaster, up to 35cm. Gypsum is white. Breed highly fractured and weathered.

The observation point № 90. K_{1kr} . Dip azimuth 150, corner of 45. Sandstones interbedded with mudstone. Fine-grained sandstones, reddish-brown clay to the cement.

The observation point № 91. K_{1mg} . Dip azimuth 150, corner of 45. Sandstones and mudstones, with a predominance of mudstone. Fissured rock.

The observation point № 92. K_{1mg} . Dip azimuth 150, corner 45-50. Sandstone with layers of mudstone, siltstone less. Medium-grained sandstones, fractured.

TECHNO-ECONOMIC ASSESSMENT STUDY FOR ROGUN HYDROELECTRIC CONSTRUCTION PROJECT

PHASE II: PROJECT DEFINITION OPTIONS

Volume 2: Basic Data

Chapter 2: Geology

Part B - Geological Investigation in the Right Bank

Annex 2-2-1 WRB1_Photos of core boxes for submission

March 2014

TECHNO-ECONOMIC ASSESSMENT STUDY FOR ROGUN HYDROELECTRIC CONSTRUCTION PROJECT

PHASE II: PROJECT DEFINITION OPTIONS

Volume 2: Basic Data

Chapter 2: Geology

Part B - Geological Investigation in the Right Bank

Annex 2-2-2 WRB-1_Photographs of core boxes for submission

March 2014



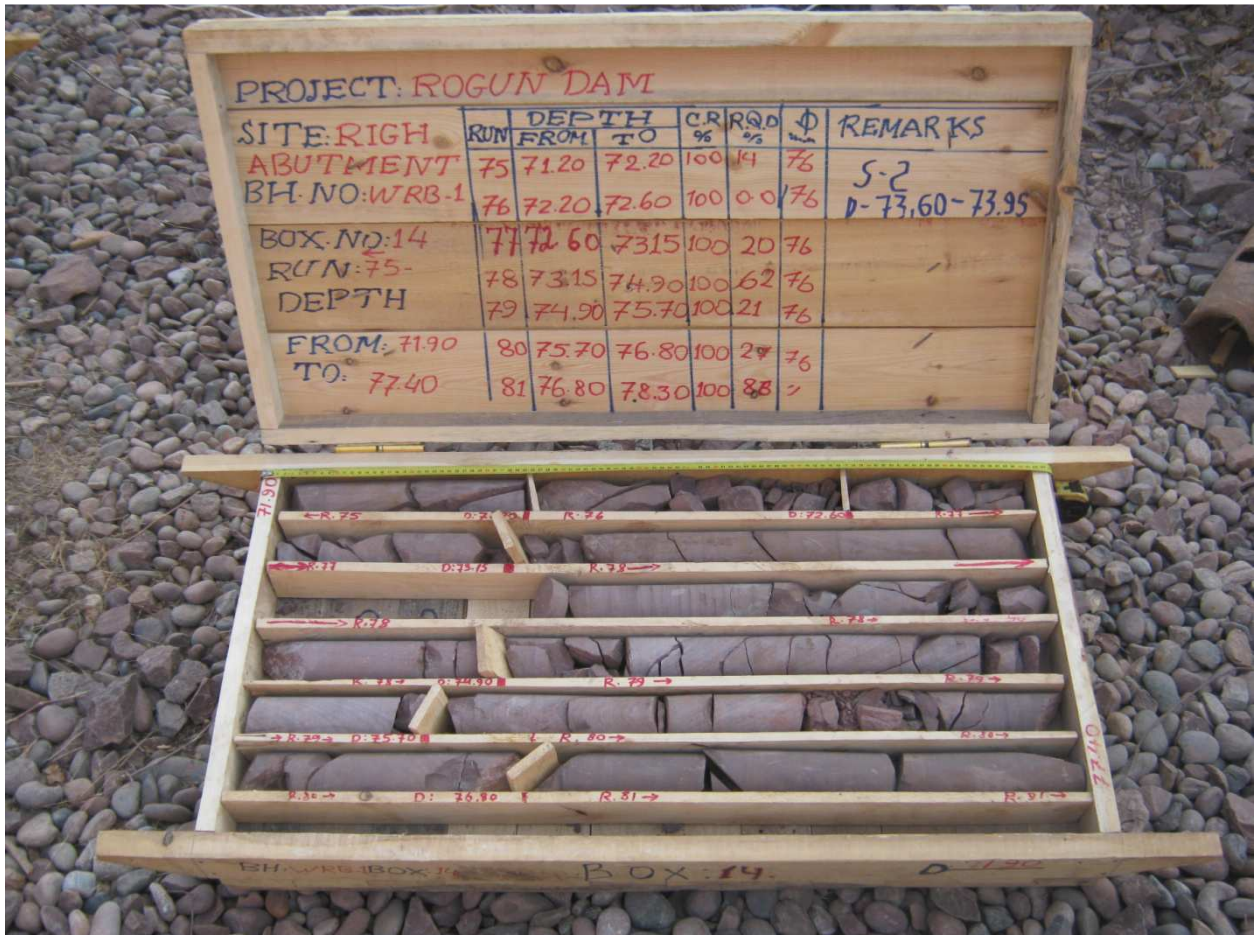




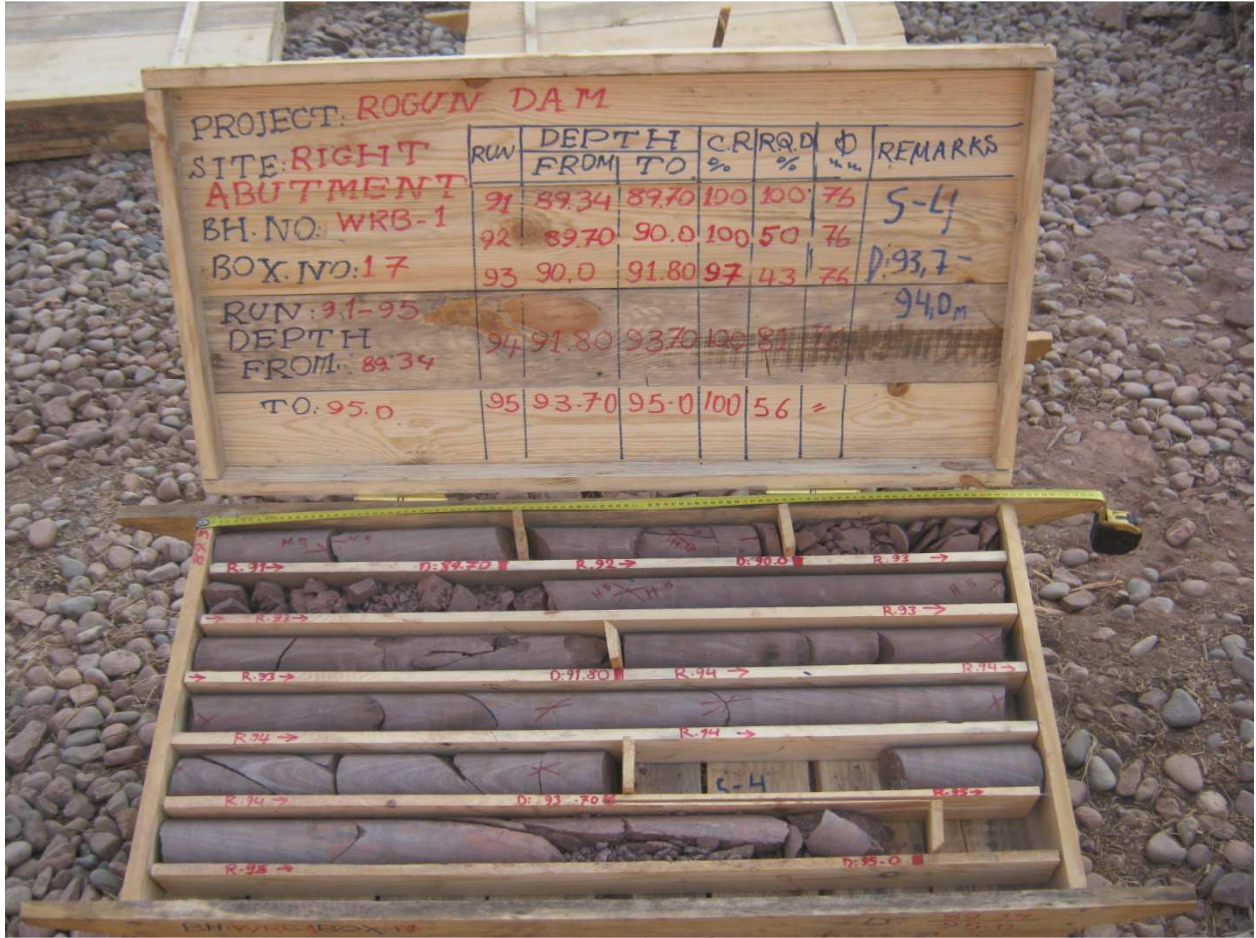














TECHNO-ECONOMIC ASSESSMENT STUDY FOR ROGUN HYDROELECTRIC CONSTRUCTION PROJECT

PHASE II: PROJECT DEFINITION OPTIONS

Volume 2: Basic Data

Chapter 2: Geology

Part B - Geological Investigation in the Right Bank

Annex 2-3 Geotechnical studies of borehole WRB-2

March 2014

TECHNO-ECONOMIC ASSESSMENT STUDY FOR ROGUN HYDROELECTRIC CONSTRUCTION PROJECT

PHASE II: PROJECT DEFINITION OPTIONS

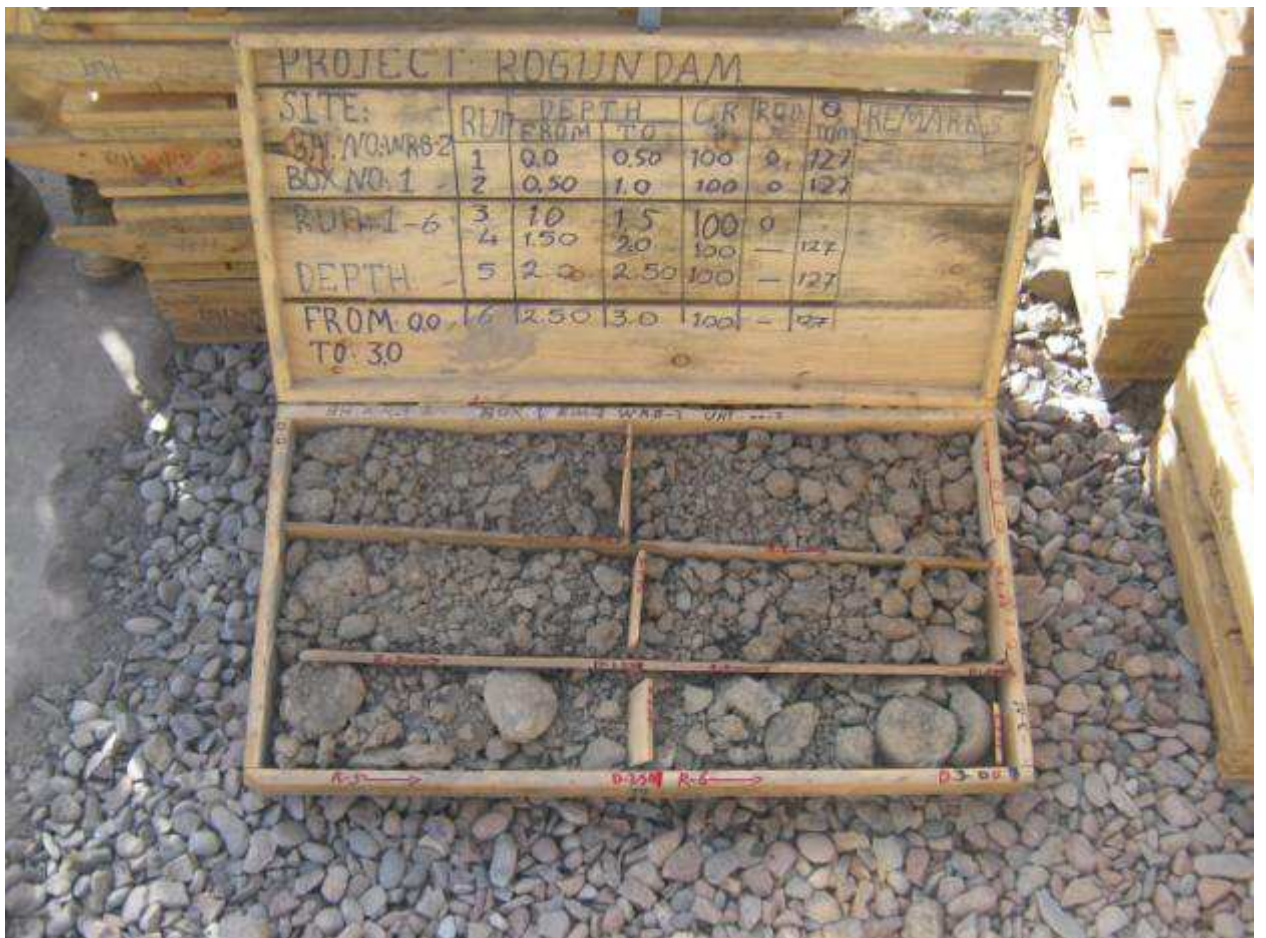
Volume 2: Basic Data

Chapter 2: Geology

Part B - Geological Investigation in the Right Bank

Annex 2-2-3 WRB2_Photos of core boxes for submission

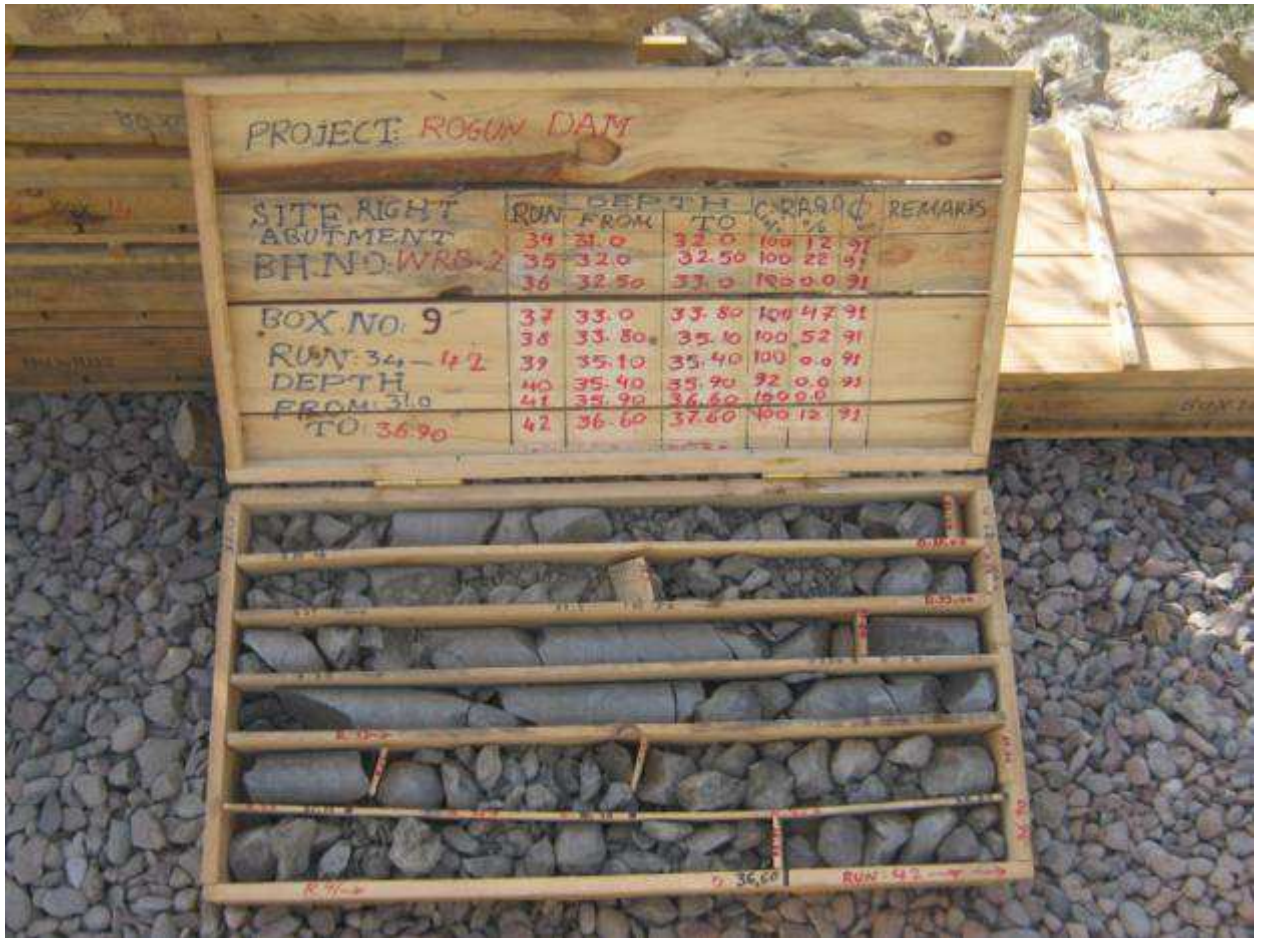
March 2014

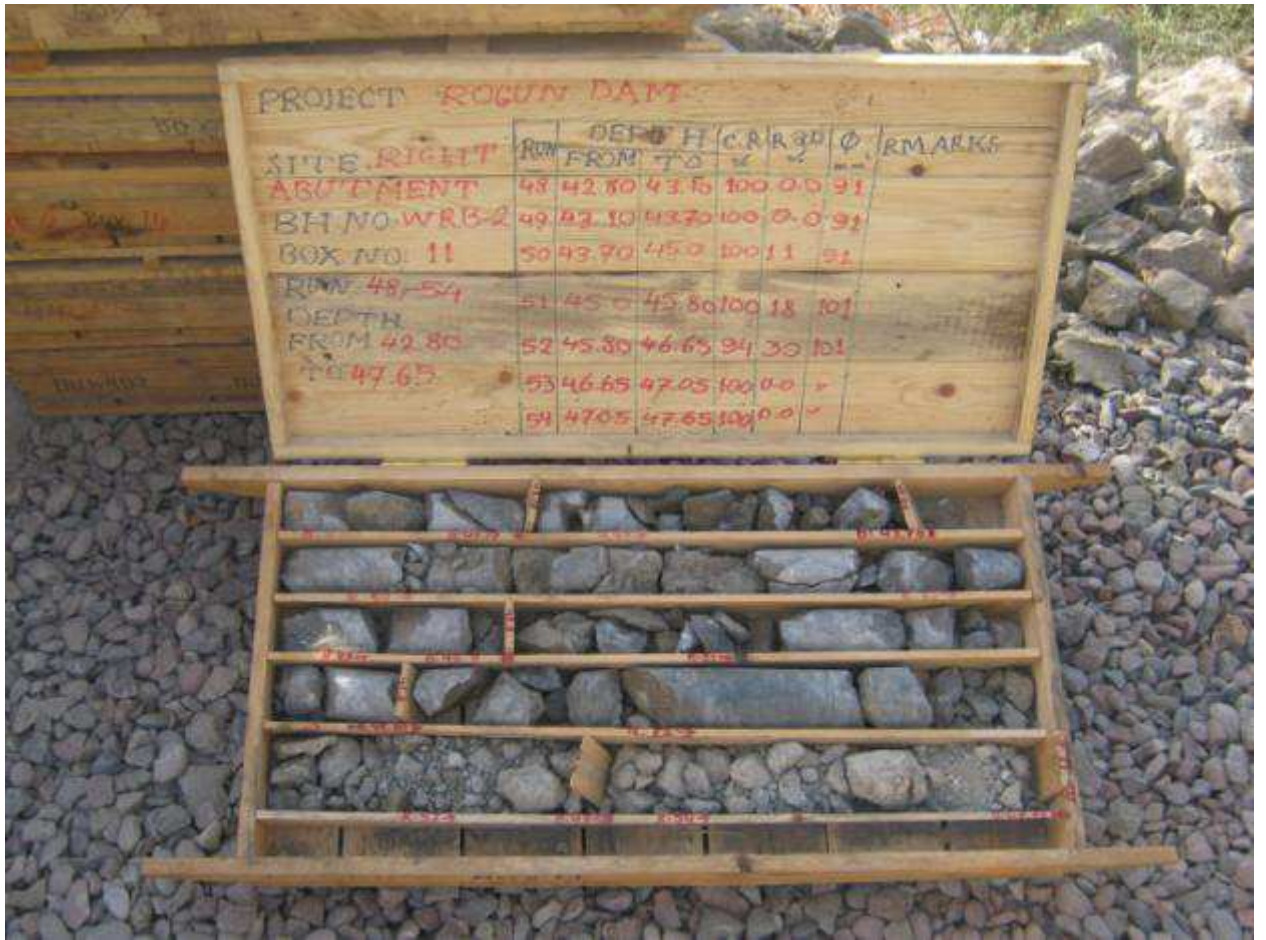


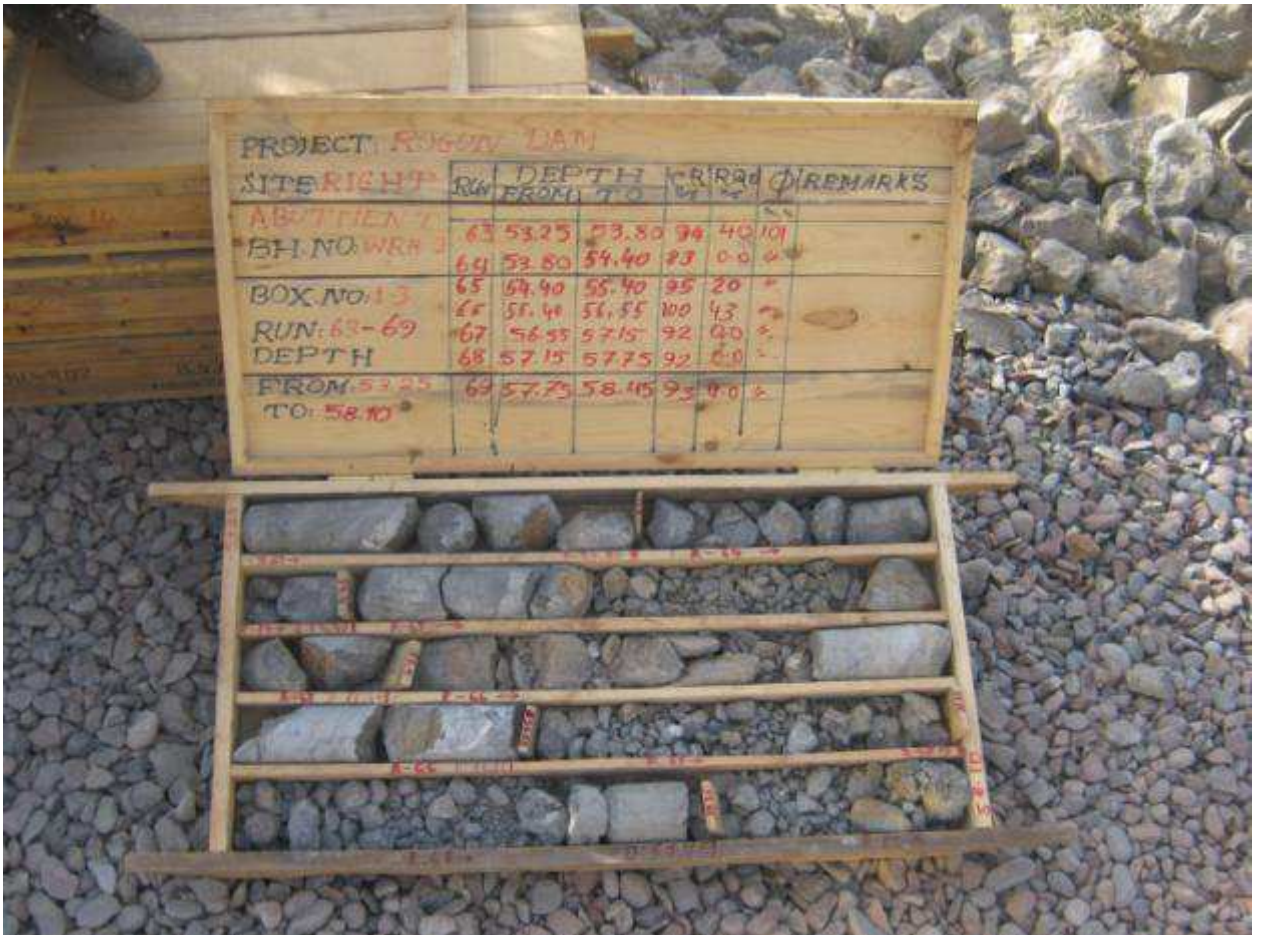


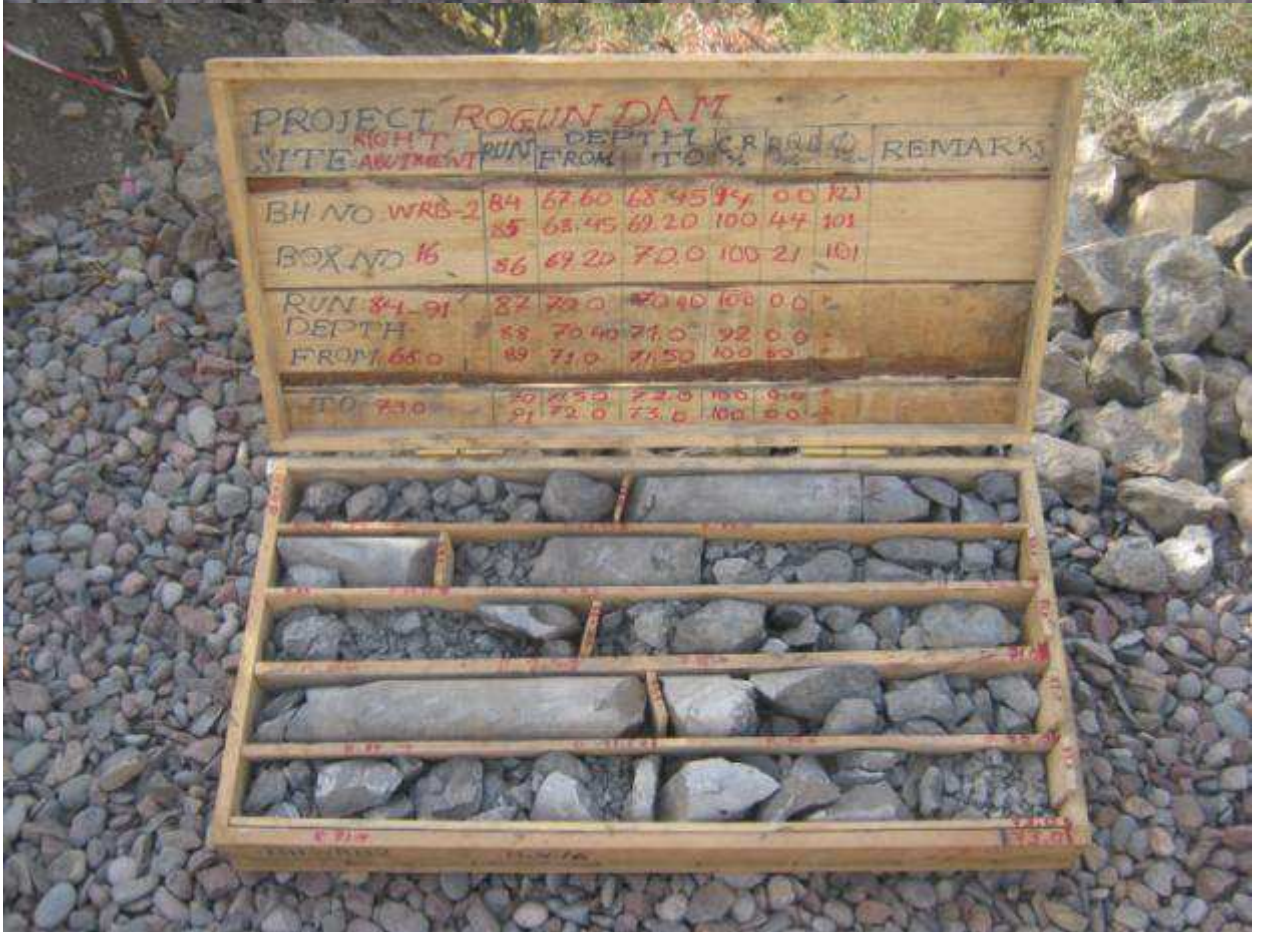












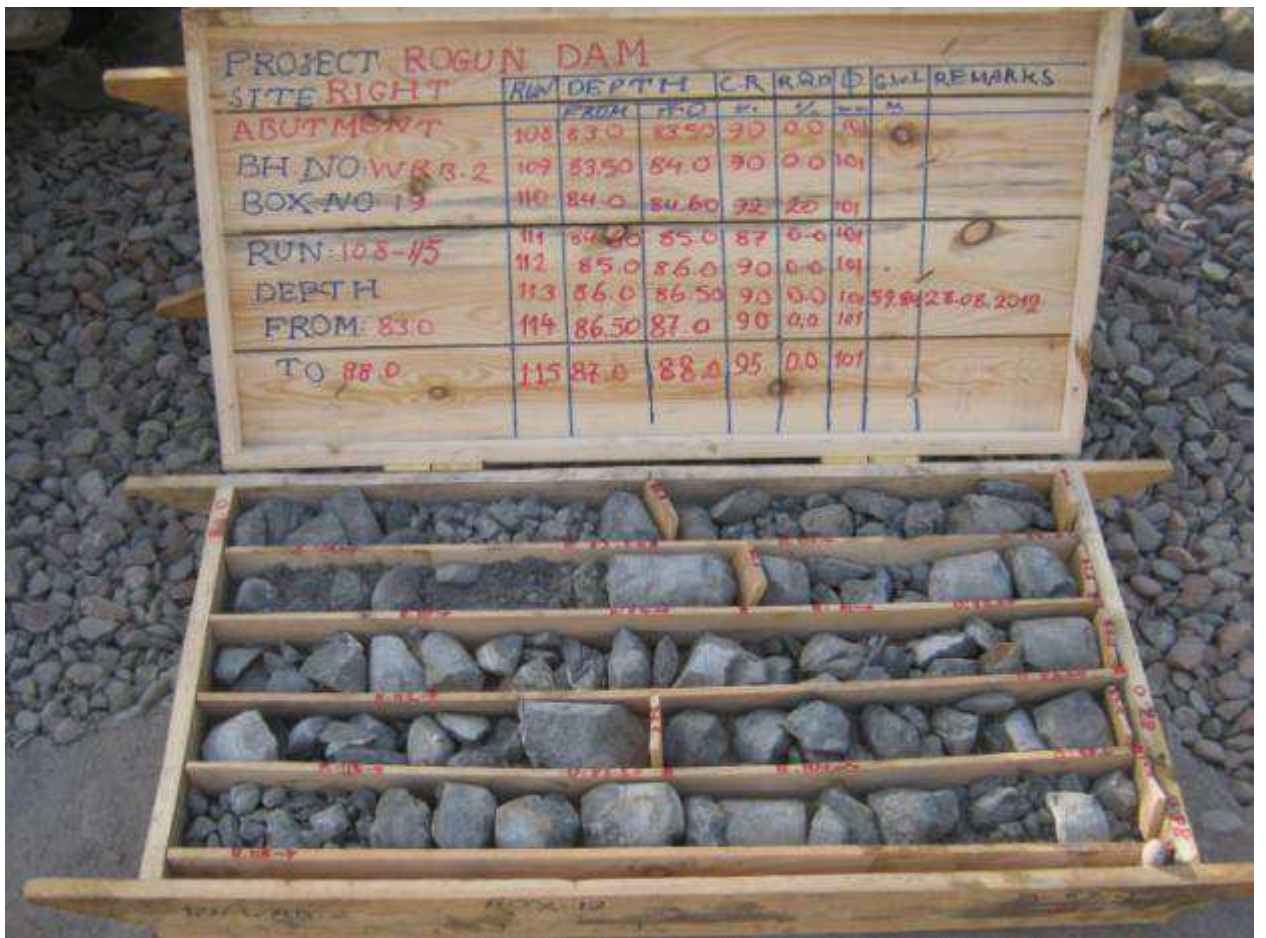


PROJECT: ROGUN DAM

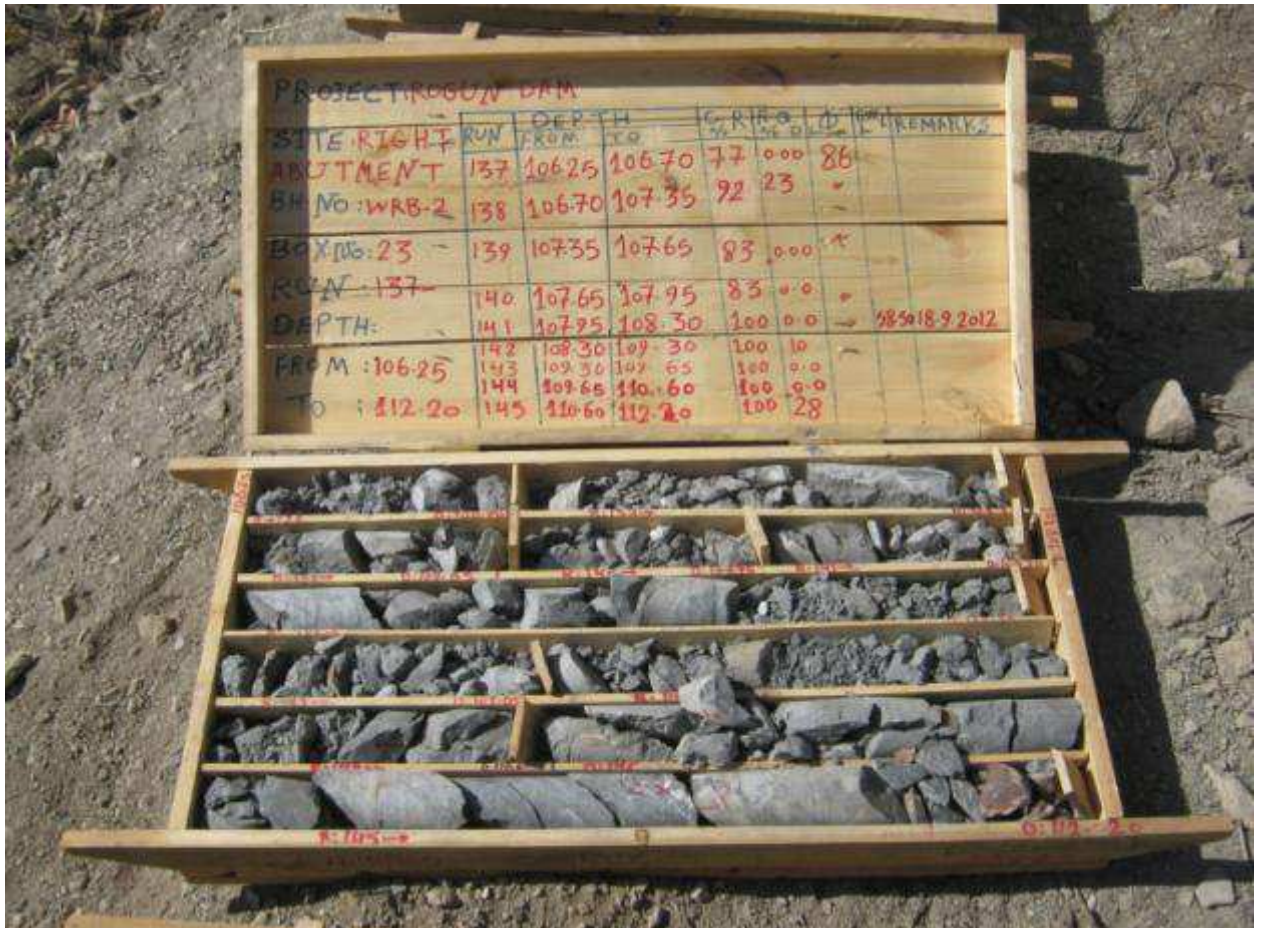
SITE RIGHT	RUN	DEPTH		CR RD Φ		REMARKS	
		FROM	TO	%	%		
ABUTMENT	92	73.0	73.60	100	0.0	101	
BH NO WRB-2							
BOX NO	17	93	73.60	75.0	100	0.0	101
RUN: 92-96	94	75.0	76.40	100	0.0	101	
DEPTH							
FROM: 73.0	95	76.40	77.40	100	0.0	101	
TO: 77.95	96	77.40	78.25	88	0.0	=	

PROJECT: ROGUN DAM

SITE RIGHT	RUN	DEPTH		CR RD Φ		REMARKS	
		FROM	TO	%	%		
ABUTMENT	96	77.40	78.25	88	0.0	101	
BH NO WRB-2	97	78.25	78.55	83	0.0	101	
BOX NO	18	98	78.55	79.0	89	0.0	101
RUN: 96-107	99	79.0	79.50	80	0.0	101	
DEPTH	100	79.50	80.0	60	0.0	101	
FROM: 77.95	101	80.0	80.35	85	0.0	101	
	102	80.35	80.70	100	0.0	101	
	103	80.70	81.0	100	0.0	101	
	104	81.0	81.50	90	0.0	101	
	105	81.50	82.0	70	0.0	101	
	106	82.0	82.45	89	0.0	101	
	107	82.45	83.0	91	0.0	101	



















PROJECT: ROGUN DAM

SITE: RIGHT
ABUTMENT

BH NO: 14 RB 2

BOX NO: 38

RUN: 230 - 239

DEPTH

FROM: 206.32

TO: 212.35

RUN	DEPTH		CORR QD		Φ	CWD	REMARKS
	FROM	TO	%	%			
230	206.20	207.0	100	31	76	5.3	12.10.08
231	207.0	207.30	100	0.0	76		
232	207.30	208.51	100	33	76		
233	208.91	209.40	81	0.0	76		
234	209.40	209.60	100	100	76		
235	209.60	210.10	100	0.0	76		
236	210.10	210.53	100	0.0	76		
237	210.50	210.95	56	0.0	76		
238	210.95	211.90	100	74	76		
239	211.90	212.35	100	0.0	76		



212.35

PROJECT: ROGUN DAM

SITE RIGHT	RUN	DEPTH		C.R.R.Q.D		Φ GWL		REMARKS
		FROM	TO	%	CM	MIN.	IN.	
ABUTMENT BH. NO. WRB-2	240	212.35	213.20	75	14	76		
BOX NO. 39 RUN: 240-243	241	213.20	214.20	100	59	76		
DEPTH FROM: 212.35	242	214.20	216.55	100	78	76		
TO: 217.20	243	216.55	217.20	100	37	76		



TECHNO-ECONOMIC ASSESSMENT STUDY FOR ROGUN HYDROELECTRIC CONSTRUCTION PROJECT

PHASE II: PROJECT DEFINITION OPTIONS

Volume 2: Basic Data

Chapter 2: Geology

Part B - Geological Investigation in the Right Bank

Annex 2-4-1 Geotechnical studies of borehole DZ2

March 2014

TECHNO-ECONOMIC ASSESSMENT STUDY FOR ROGUN HYDROELECTRIC CONSTRUCTION PROJECT

PHASE II: PROJECT DEFINITION OPTIONS

Volume 2: Basic Data

Chapter 2: Geology

Part B - Geological Investigation in the Right Bank

Annex 2-4-2 DZ-2_ Photographs of core boxes for submission

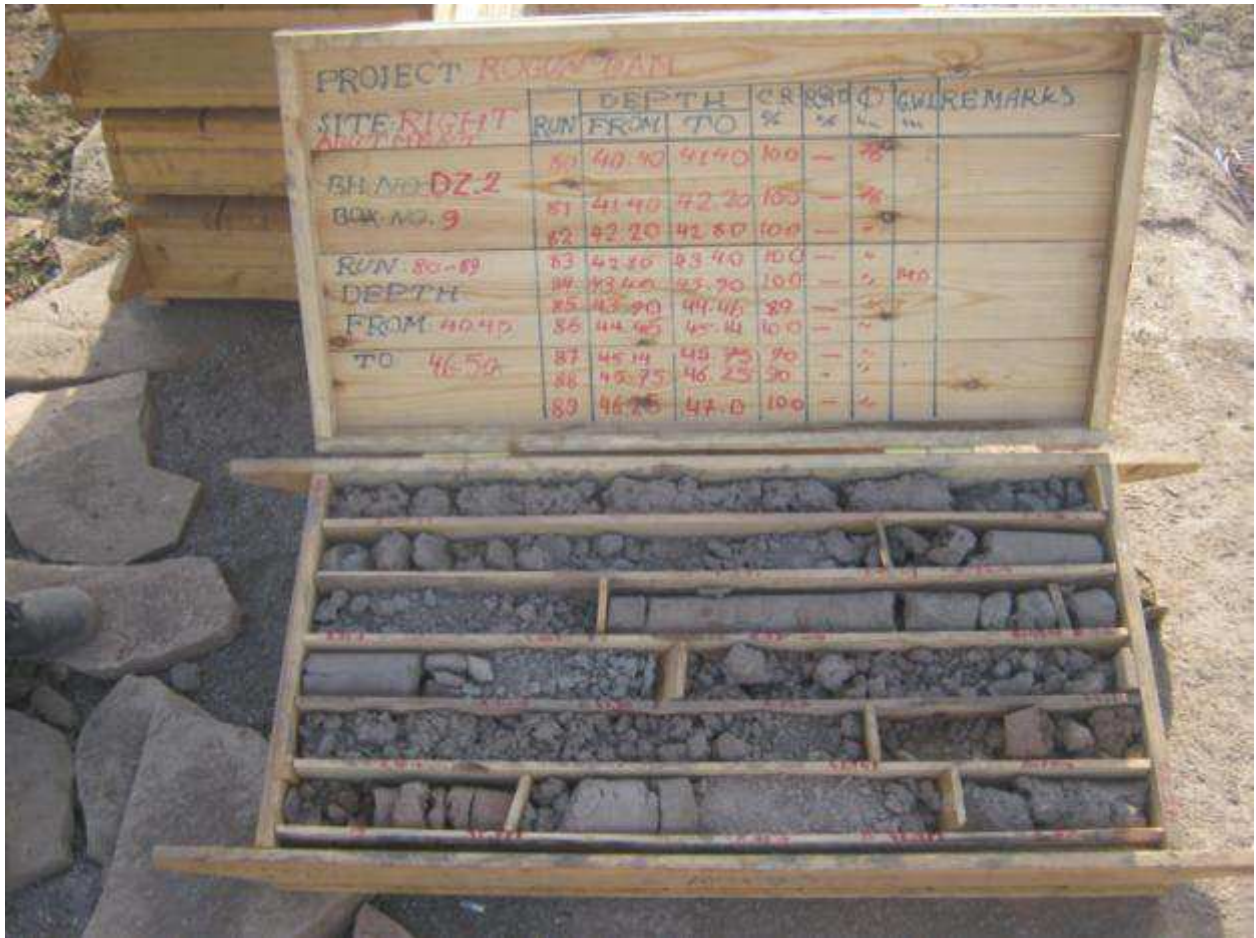
March 2014



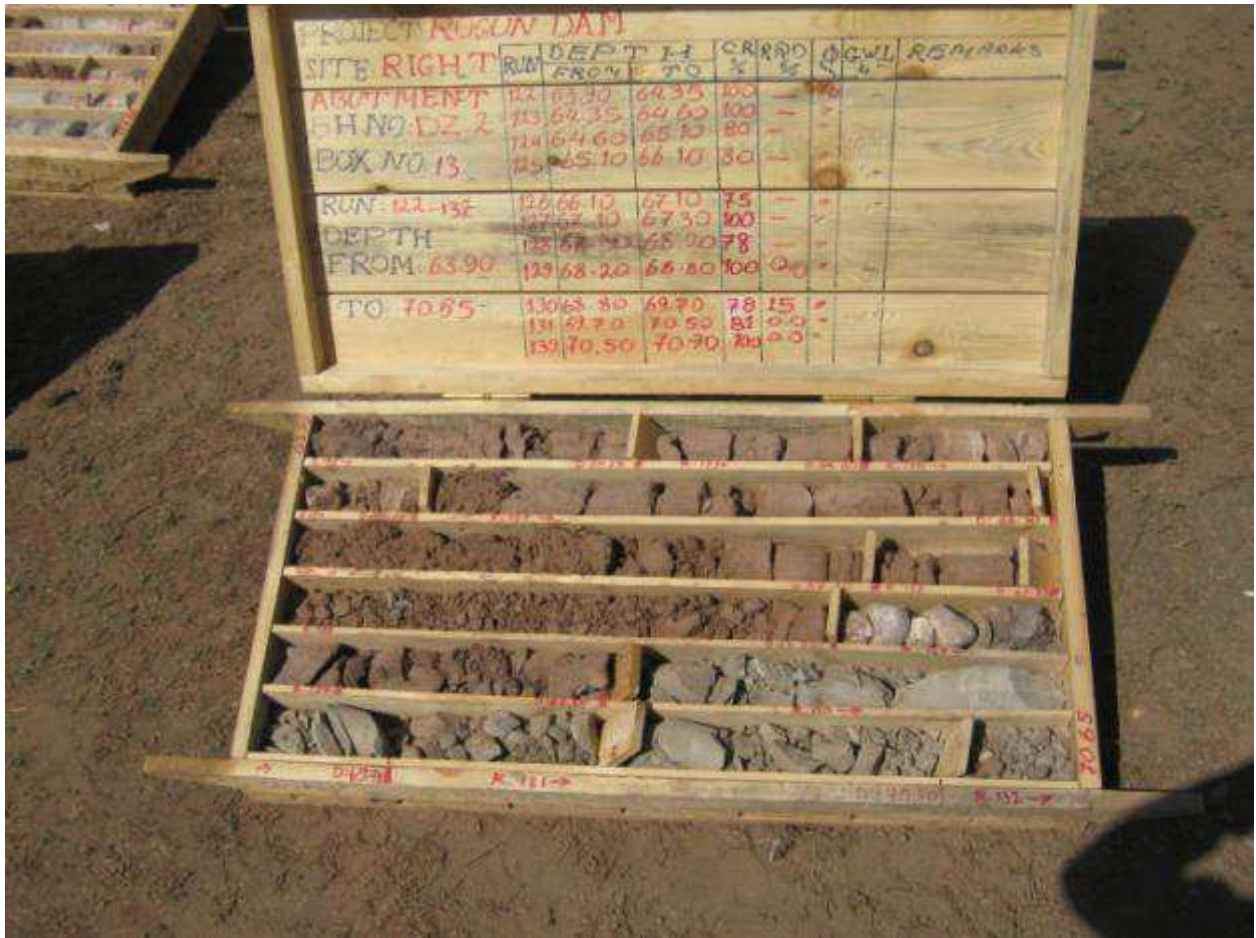




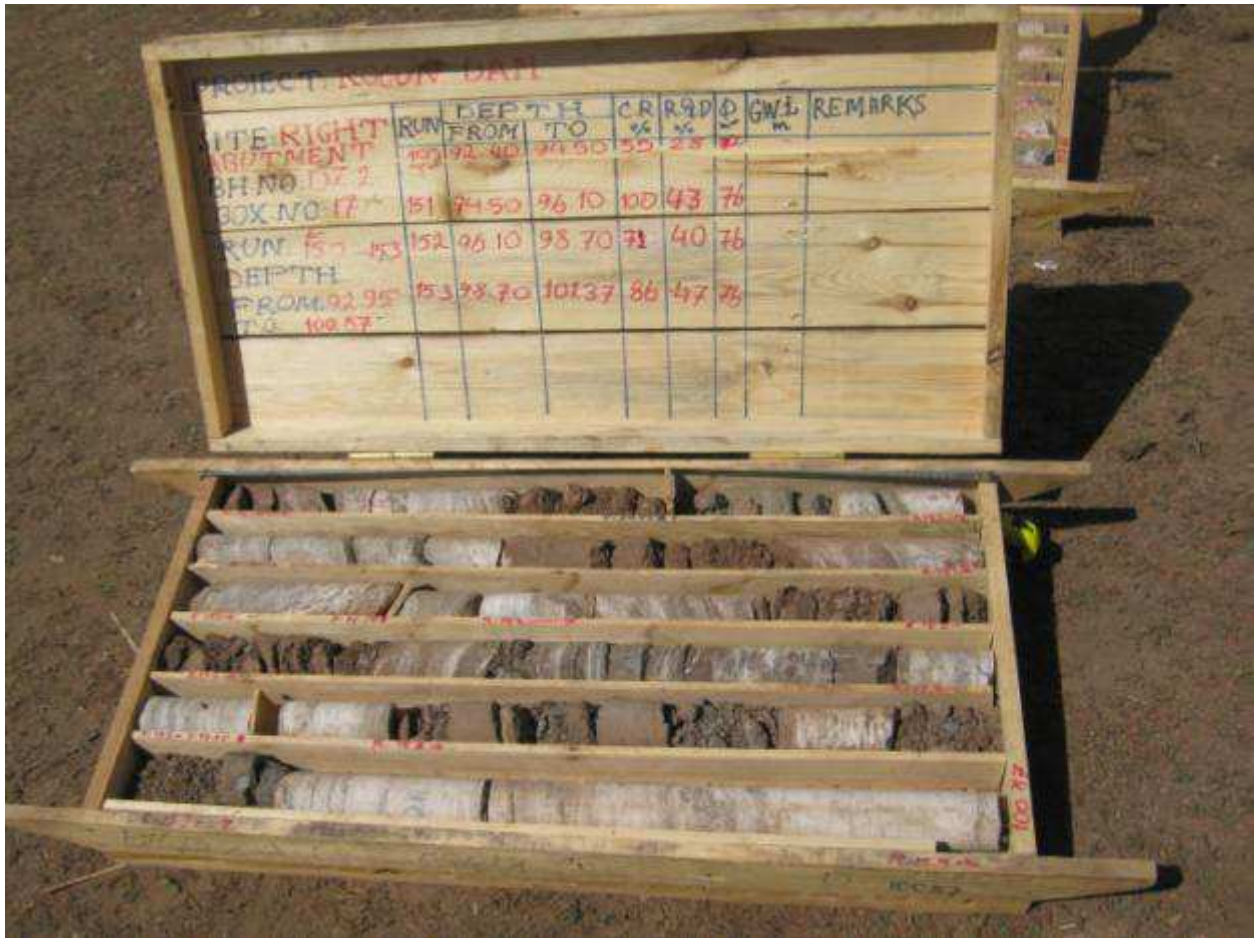


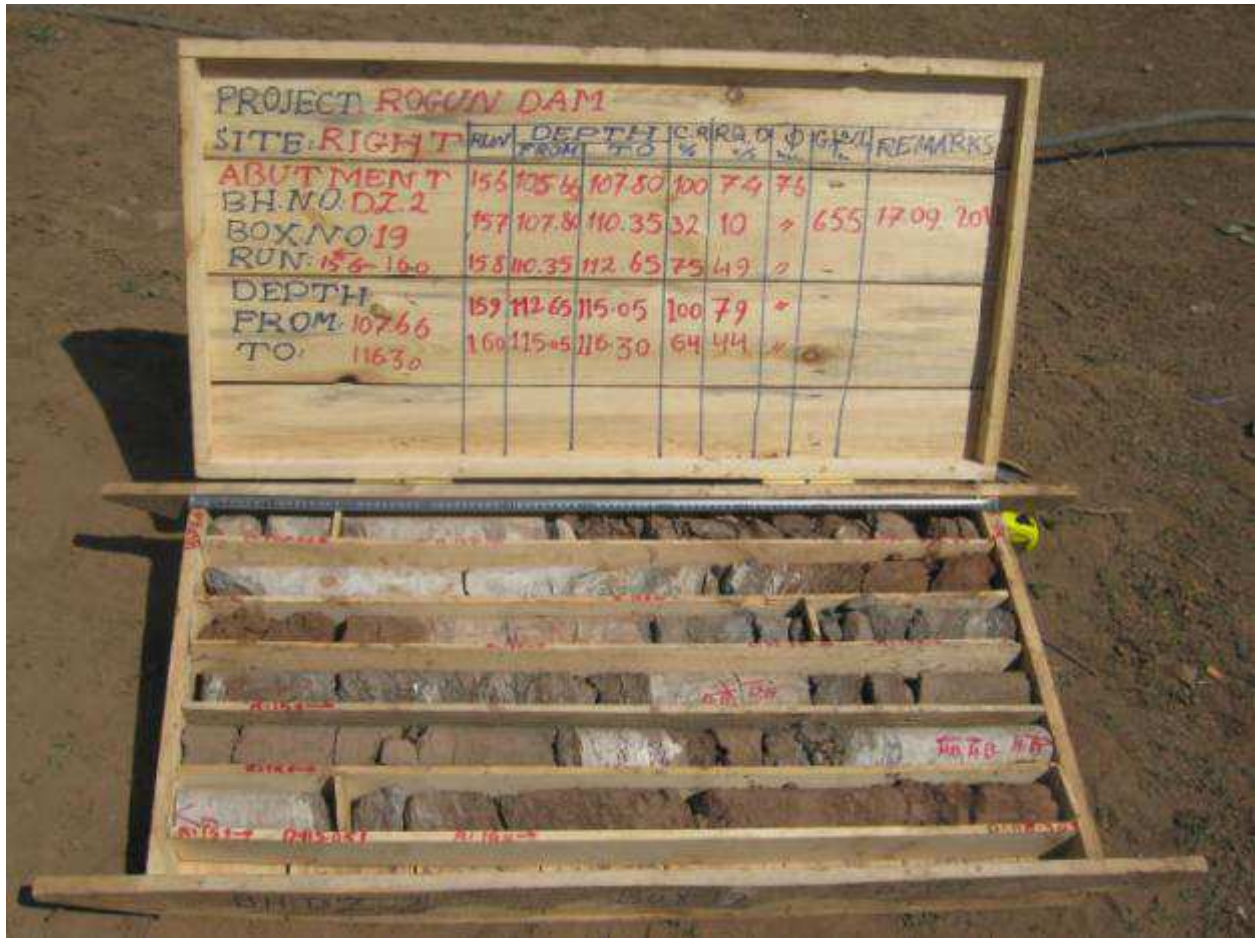


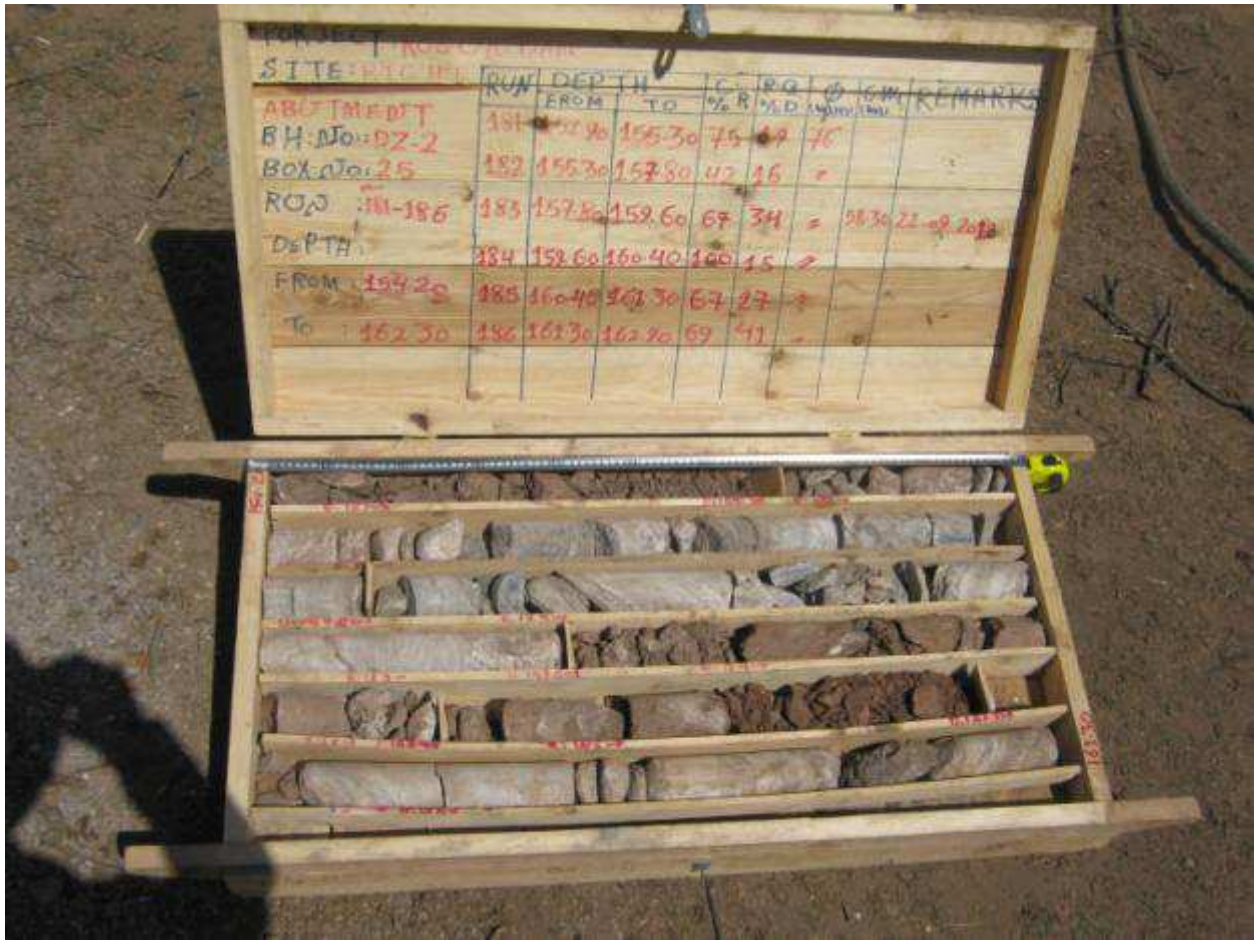












TECHNO-ECONOMIC ASSESSMENT STUDY FOR ROGUN HYDROELECTRIC CONSTRUCTION PROJECT

PHASE II: PROJECT DEFINITION OPTIONS

Volume 2: Basic Data

Chapter 2: Geology

Part B - Geological Investigation in the Right Bank

Annex 3-1-1 Geotechnical studies of borehole IF-1

March 2014

267332.67 22956.604 1354.33
Elevation 1054.3

PASSPORT
of borehole №IF-1
Rogan HPP
Right bank of the Vakhsh River

Started 28.06.2012.
Completed 23.07.2012.

Interval	Depth (m)	Height (m)	Category of rocks	Description of rocks	Core sample No.	Core length (m)	Core diameter (mm)	Core quality	System	Angle of dip	Quantity of cracks	Width of cracks (mm)	Filling aggregate	Drilling date	Schedule of deepening (hole No.)		
1	0-1.5	1353.03	1.5	Interval 0-1.5 m. Brownish-brown clay, mixed with sand and with inclusions of coarse gravel, sandstone and gravel.													
2	1.5-10.6	1336.69	1.1	Interval 1.5-10.6 m. Greenish-brown clay with inclusions of coarse gravel, limestone, argillite and sandstone.													
3	10.6-19.1	1337.79	8.5	Interval 10.6-19.1 m. Dark and dark green sandy clay with inclusions of coarse gravel, gravel, argillite and limestone.													
4	19.1-20.2	1336.69	1.1	Interval 19.1-20.2 m. Rubbles of greenish-gray limestone thick laminated, with cracks, strong.													
5	20.2-20.6	1336.69	0.4	Interval 20.2-20.6 m. Greenish-gray clay with inclusion of sand.													
6	20.6-22.9	1334.85	2.3	Interval 20.6-22.9 m. Brown clay with inclusion of poorly sorted sand and coarse gravel, argillite.													
7	22.9-29.0	1329.22	6.1	Interval 22.9-29.0 m. Greenish brown clay mixed with poorly sorted sand and coarse gravel, as well as gravel, limestone and argillite. In the lower part - brownish of limestone.													
8	29.0-36.0	1329.22	6.1	Interval 29.0-36.0 m. Large coarse gravel and blocks of limestone, 2-6.0 m with interlayers of gray clay (5-7), sometimes the clay is red, with gravel and coarse gravel. Brown limestone, with cracks, along cracks signs of ferruginization. In lower part in the interval 31.5-36.0 m sandy clay with fine crushed stone of limestone.													
9	36.0-38.5	1323.16	7.0	Interval 36.0-38.5 m. Sandy clay, yellow and greenish-brown with gravel, coarse gravel and argillite.													
10	38.5-39.0	1320.98	7.5	Interval 38.5-39.0 m. Rubby soil composed of pieces of limestone and brownish sandstone.													
11	39.0-41.4	1318.18	2.4	Interval 39.0-41.4 m. Brownish-brown sandy siltstone, strong on break.													
12	41.4-47.3	1313.37	6.9	Interval 41.4-47.3 m. Brownish-gray siltstone, finely laminated, creviced with rare inclusions of sandstone bodies (2-3cm) of brownish-brown color. Cores are in the form of a column 80-90cm (11 pcs). The angle of crack towards the axis of cores 60°.													
13	47.3-48.2	1313.37	6.9	Interval 47.3-48.2 m. Brownish brown sandy siltstone finely laminated, creviced. Width of cracks up to 2mm, filling aggregate is calcite. The angle of crack towards the axis of cores 65-60°.													
14	48.2-52.0	1309.3	3.8	Interval 48.2-52.0 m. Dark brown siltstone, finely laminated, average creviced. The angle of crack towards the axis of cores 65-60°.													
15	52.0-54.95	1306.75	2.95	Interval 52.0-54.95 m. Brownish-gray argillite, medium grained, finely laminated, creviced (cracks 5-65), with rear streak (0.5-2mm) of gypsum and interlayer of dark brown siltstone.													
16	54.95-56.05	1305.02	2.0	Interval 54.95-56.05 m. Brownish-gray fine grained sandstone, finely laminated, creviced, poor rigidity.													
17	56.05-60.0	1302.36	3.0	Interval 56.05-60.0 m. Brownish-brown siltstone finely-averaged laminated, creviced, of crack towards axis of cores 65°. In the lower part in the interval the rock is highly creviced with streak (3 mm) of gypsum.													
18	60.0-63.55	1299.31	3.55	Interval 60.0-63.55 m. Dark brown siltstone finely laminated, creviced, of cracks 65-80 with rare inclusions (0.3-4 cm) of brownish-gray sandstone. Sometimes there are interlayers (0.2-0.3cm) of sandy siltstone.													
19	63.55-69.1	1294.51	5.55	Interval 63.55-69.1 m. Dark brown siltstone finely- medium laminated, creviced, with streaks 1-2 mm of membranes of gypsum in the interval 64.5-66.0 m. The rock is highly creviced and fragmented. Cores is in the form of pieces and column 60-37 cm, (9 pcs).													
20	69.1-70.4	1293.26	1.3	Interval 69.1-70.4 m. Dark brown siltstone, finely laminated, creviced, laminated.													
21	70.4-74.0	1290.29	3.6	Interval 70.4-74.0 m. Dark brown siltstone finely laminated, creviced, with streaks (2-3mm) of gypsum. The rock is of medium rigidity.													
22	74.0-80.0	1285.07	6.0	Interval 74.0-80.0 m. Brownish brown argillite, medium laminated, creviced with streaks (3-5 mm) and nests (0.5-2 cm) of gypsum.													
23	80.0-84.0	1281.67	4.0	Interval 80.0-84.0 m. Brownish-brown argillite, brecciated with streaks (2-3 mm) of gypsum nests (2-5 cm) of gypsum.													
24	84.0-88.3	1277.88	4.3	Interval 84.0-88.3 m. Brownish-brown siltstone, finely laminated, slightly creviced with streaks (2-3 mm) and rare nests (1-2 cm) of gypsum, sometimes there are cracks from 2-3 to 7-8mm, filled with coarse gravel and clay. Core is in the form of column 82 cm, 14 pcs.													
25	88.3-94.9	1267.07	6.6	Interval 88.3-94.9 m. Dark brown siltstone, thick laminated, slightly creviced with streaks (4 mm) and nests (0.5-1.5 cm) of gypsum. The rock is of high and average rigidity.													
26	94.9-95.7	1267.07	6.6	Interval 94.9-95.7 m. Brownish silty sandstone, medium grained, thick laminated, slightly creviced, of laminations 60-65°, L of cracks 80°.													
27	95.7-100.1	1267.07	4.4	Interval 95.7-100.1 m. Dark brown siltstone, medium laminated, sometimes highly plastered with interlayers of (0.1-0.2 m) of sandy siltstones.													
28	100.1-100.8	1267.07	0.7	Interval 100.1-100.8 m. Brown siltstone, average laminated, creviced with cracks up to 2 mm. L cracks 75-80°.													
29	100.8-102.5	1265.6	1.7	Interval 100.8-102.5 m. Dark brown siltstone thick laminated, creviced with streaks (4 mm) of gypsum. The rock of medium rigidity.													
30	102.5-105.1	1263.3	2.6	Interval 102.5-105.1 m. Brown siltstone, medium laminated, creviced with streaks (0.5-2 cm) of gypsum. L of cracks 65-70 from the axis of cores, in some places there are cracks (1-2 to 4-5cm) filled with coarse gravel of siltstone and argillite.													
31	105.1-106.5	1262.14	1.4	Interval 105.1-106.5 m. Brownish-brown brecciated argillite.													
32	106.5-107.3	1261.45	0.8	Interval 106.5-107.3 m. Pinkish-white gypsum with nests for brown argillite (poro anera).													
33	107.3-109.1	1259.87	1.8	Interval 107.3-109.1 m. The zone of faulting tectonic fault. Breccia is composed of gravel and coarse gravel of argillite, siltstone, anhydrite and sandstone. Filling aggregate is concretion sandstone.													
34	109.1-111.2	1258.07	2.1	Interval 109.1-111.2 m. Fault zone. Dark brown brecciated argillite.													
35	111.2-115.0	1257.29	0.9	Interval 111.2-115.0 m. Tectonic fault zone. Brown gravelite composed of fragments of argillite, siltstone, sandstone with interlayer (2-3 cm) of anhydrite.													
36	115.0-125.4	1254.74	2.9	Interval 115.0-125.4 m. Brownish-gray fine grained sandstone, finely laminated, creviced. In the interval 112.1-113.0 m with interlayers (0.2 m) of dark brown argillite.													

Comments
Piezometer is installed in the borehole 60mm
Plastic pipe PWS
0.5-0.0 concrete curbstone
1) 0.0-0.0 m Blind part
2) 60-115.0 m Drilling every 3.0 m
3) Setting tank 0.0 m. Lower part is damped

Ar - Argillite
Fe - Ferruginized
G - Gypsum
Ca - Calcium
Гп - Clay with gravel
Гм - Clay with sand
bp - Brecciated argillite
- empty

Zone of Inakshskiy tectonic fault

Main Department of Geology under the Government of Republic of Tajikistan
Unitary Enterprise "Sant Tajik Prospecting Expedition"
In charge Chief geologist of Vakhsh Geological Prospecting Party /Niezov K. 2012
Attachment Page Copy № Scale: 1:100
Amounted Geologists: Niezov K., Gaidumshayev S.
Computer design: Bragimov N.

TECHNO-ECONOMIC ASSESSMENT STUDY FOR ROGUN HYDROELECTRIC CONSTRUCTION PROJECT

PHASE II: PROJECT DEFINITION OPTIONS

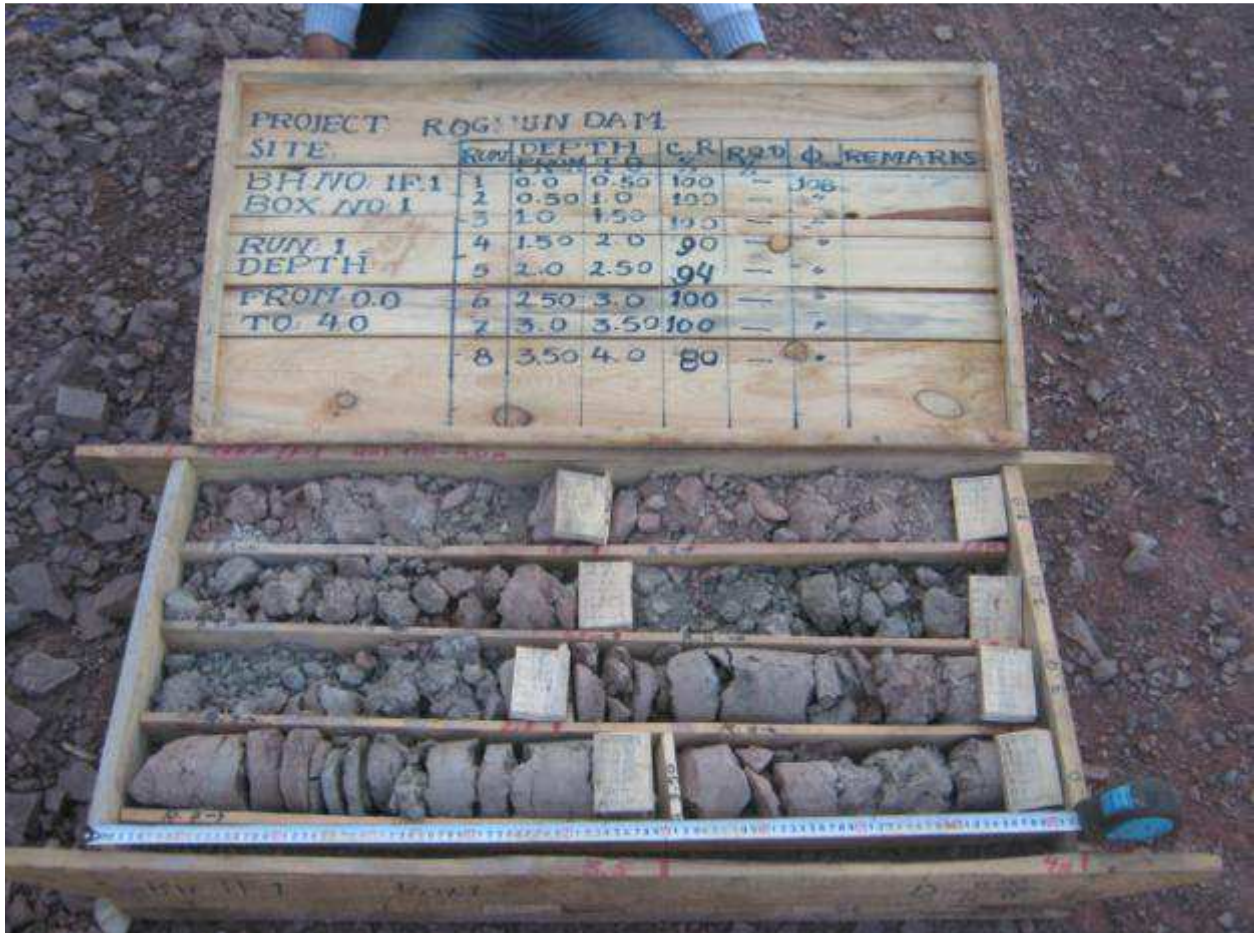
Volume 2: Basic Data

Chapter 2: Geology

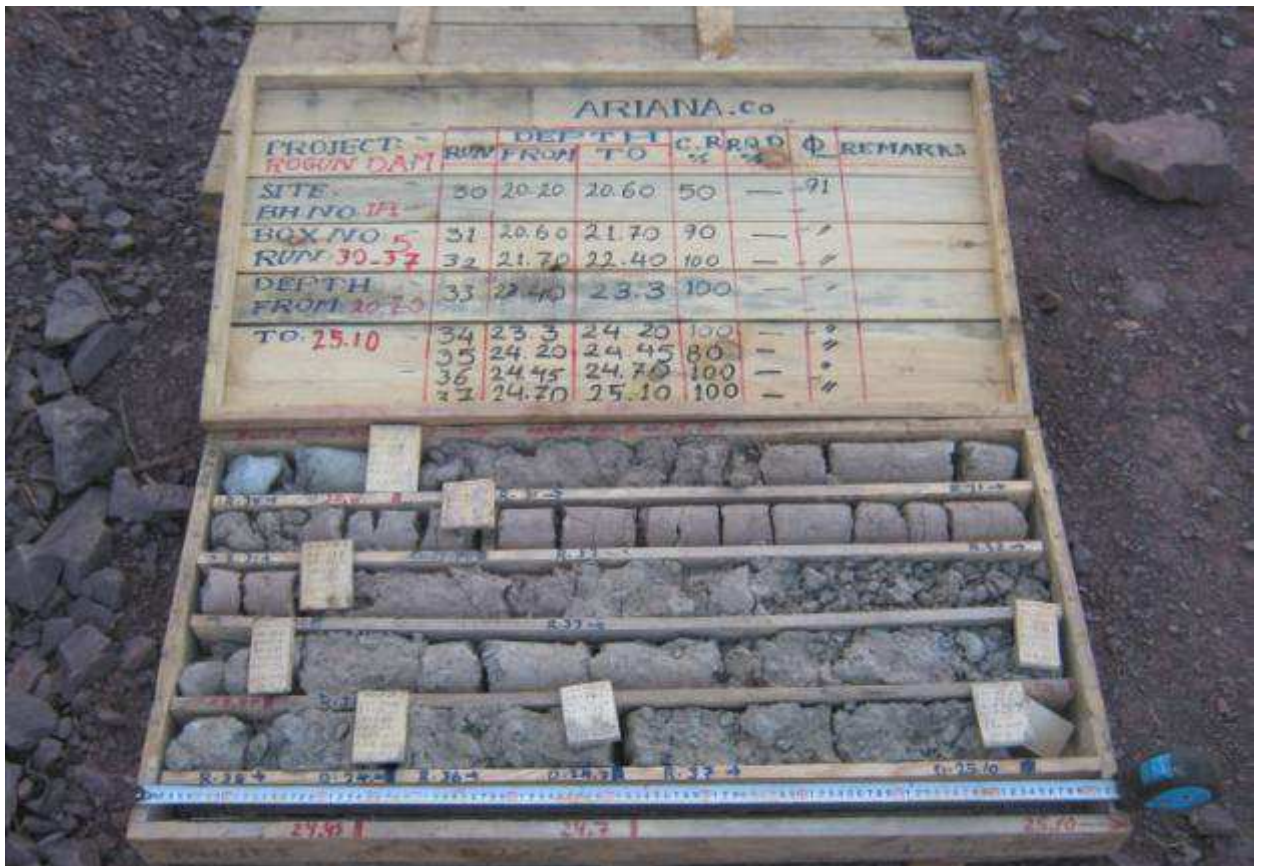
Part B - Geological Investigation in the Right Bank

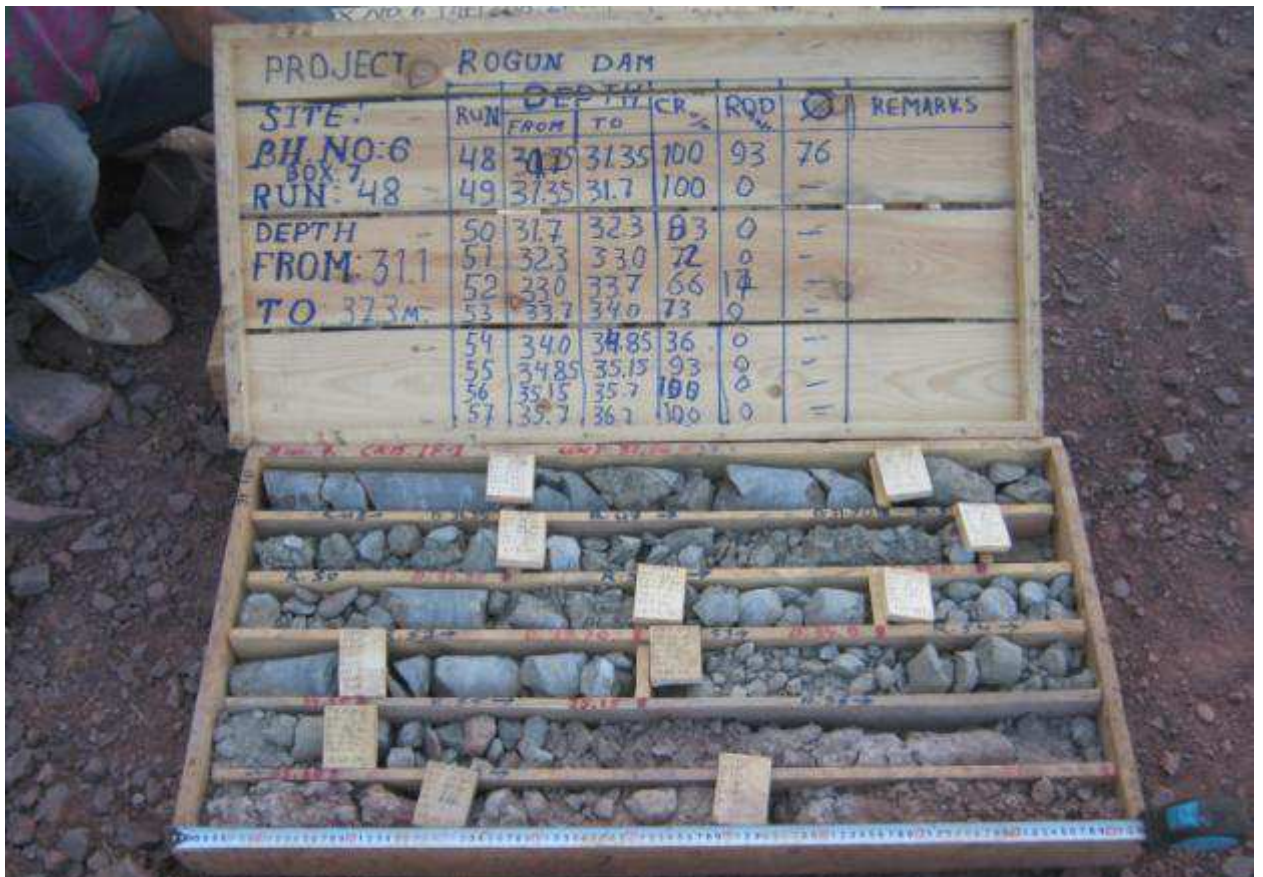
Annex 3-1-2 IF1_Photos of core boxes for submission

March 2014











PROJECT: ROGUN DAM 2012 rod

SITE	Run	DEPTH		C.R %	ROD %	Ø mm	REMARKS
		FROM	TO				
BH NO: IF-1	67	42.6	43.3	100	85	76	
BOX NO: 9	68	43.3	45.6	48	17	76	
RUN	69	45.6	47.0	96	56	76	
DEPTH	70	47.0	47.75	100	73	76	
FROM	71	47.75	49.05	100	77	76	
TO		49.05					



PROJECT: ROGUN DAM 2012r

SITE	Run	DEPTH		C.R %	ROD %	Ø mm	REMARKS
		FROM	TO				
BH NO: IF-1	72	49.05	50.7	100	0	76	
BOX NO: 10	73	50.7	52.0	96	29	-	
RUN	74	52.0	52.7	100	14	-	
DEPTH FROM	75	52.7	53.3	100	42	-	
49.05 TO	76	53.3	53.6	100	0	-	
54.95	77	53.6	54.95	98	30	-	



DEPTH	87	620	630	100	0	-
FROM	88	620	630	100	0	-
TO	89	630	640	97	0	-
	90	640	661	100	0	-
	85	649	661	100	0	-
	86	661	670	91	0	-

PROJECT - ROGUN DAM

SITE	RUN	DEPTH		CR	RQD	REMARKS
		FROM	TO	%		
BH NO IF1	87	670	676	100	25	76
BOX NO	13					
RUN	88	676	690	100	0	-
DEPTH	89	690	704	100	25	-
	90	704	721	100	0	-
FROM	67	91	721	729	100	29
TO	7290					

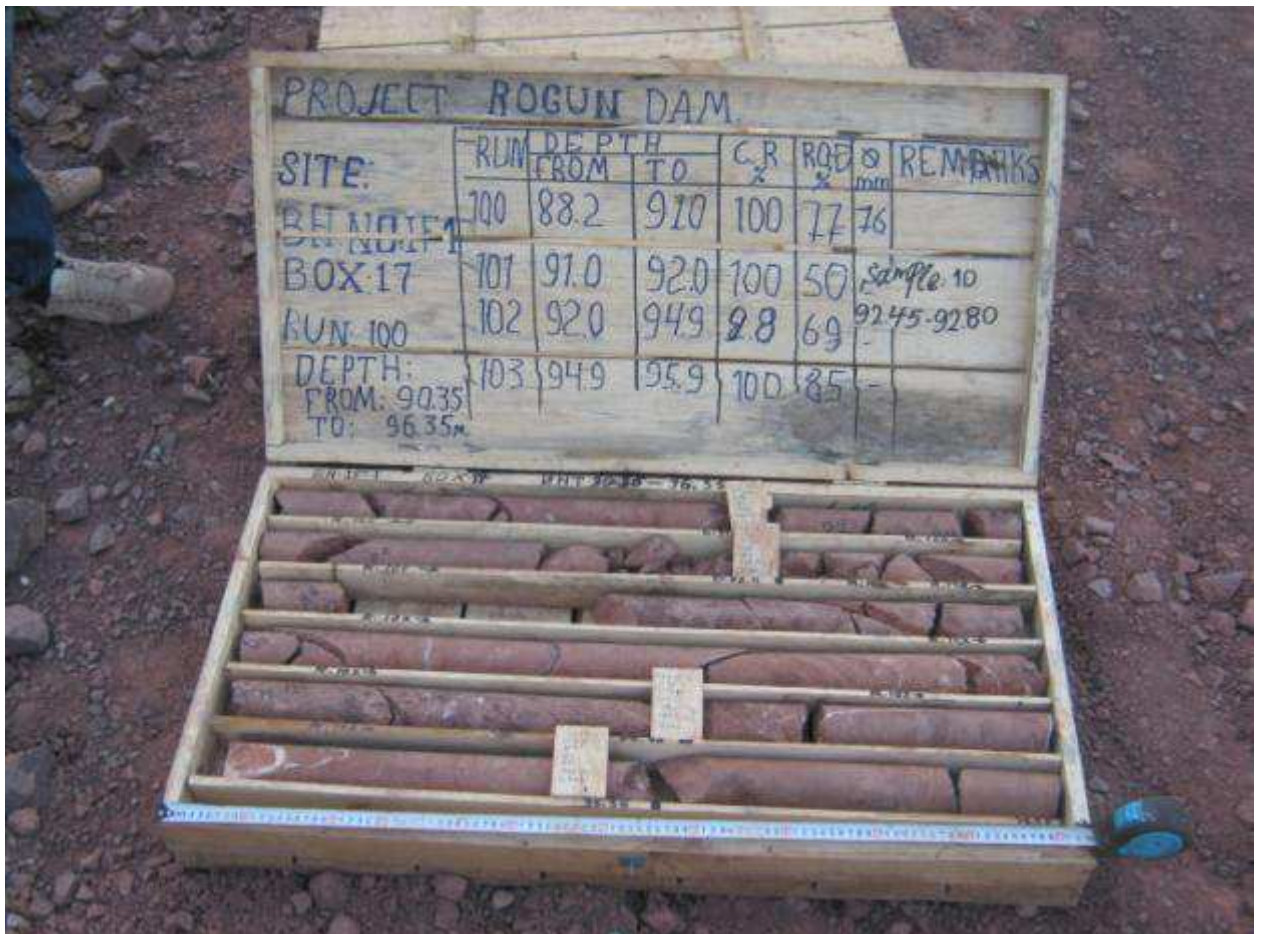
Box 13 contains several cylindrical rock samples held in wooden frames. A blue measuring tape is visible at the bottom right.

PROJECT - ROGUN DAM

SITE	RUN	DEPTH		CR	RQD	REMARKS
		FROM	TO	%		
BH NO IF1	92	72.90	73.50	100	00	76. 72.9-73.5
BOX NO	14					
RUN	93	73.50	75	100	42	76 sample 7
DEPTH	94	75	77	100	70	76. 75-76.50
FROM	77	95	785			
TO						

Box 14 contains several cylindrical rock samples held in wooden frames. A blue measuring tape is visible at the bottom right.







TECHNO-ECONOMIC ASSESSMENT STUDY FOR ROGUN HYDROELECTRIC CONSTRUCTION PROJECT

PHASE II: PROJECT DEFINITION OPTIONS

Volume 2: Basic Data

Chapter 2: Geology

Part B - Geological Investigation in the Right Bank

Annex 4-1 Report on Seismic Refraction

March 2014



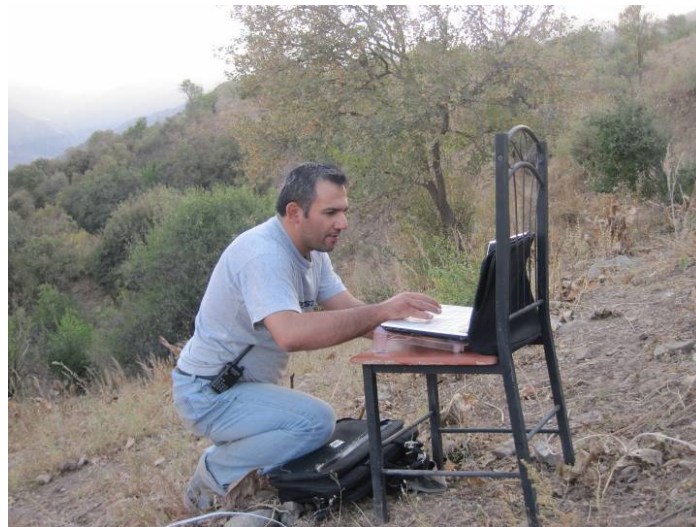
Joint Stock Company "ROGUN HYDROELECTRICAL POWER PLANT"
The Republic of Tajikistan



Tunnel Dam Ariana Engineering Co.

Rogun Dam - Complementary Geotechnical Investigations at Right Bank

Final Report on Seismic Refraction Investigations



SADD TUNNEL PARS
Consulting Engineers



SAMANIAN
Technical and Engineering Co.

Report and Revision No.	Date	Prepared by	Checked by Team Leader	Reviewed by Supervisors	Approved by Project Manager
STP No.: Geoph/Rep.02/Rev.0	Nov. 2012	Dr. D. Hariri	H. A. Chehreh	A. Mehinrad A. Farazmand	Kh. Binazadeh
ATD No.:					



Table of content

1.	Introduction.....	10
1.1.	Location of the Site.....	10
1.2.	Site Geology.....	11
2.	Introduction To Seismic Refraction Method	14
2.1.	Basic Field Experiment	14
2.2.	Elements Of Elasticity: Stress, Strain And Elastic Moduli	14
2.3.	Seismic Waves	15
2.4.	Seismic Wave Velocities	16
3.	Seismic Refraction Investigations At Right Bank of Rogun Dam Site	20
3.1.	Line 1 Profile A.....	21
3.2.	Line 1 Profile B.....	30
3.3.	Line 1 Porofile C.....	40
3.4.	Line 1 Porofile D	49
3.5.	Line 1 Porofile E.....	59
3.6.	Line 1 Porofile F	67
3.7.	Line 2 Porofile A	74
3.8.	Line 2 Porofile B.....	83
3.9.	Line 2 Porofile C.....	91
3.10.	Line 2 Porofile D	96
3.11.	Line 3 Porofile A	106
4.	Conclusions.....	114



Table of Figures

Fig. 1: General view of the location of refraction seismic investigations	11
Fig. 2: Geological map of Rogun dam site	12
Fig. 3: Schematic design of geophones location	18
Fig. 4 : Locations of seismic profiles along the lines 1, 2 and 3	20
Fig. 5: Shot is located at 70 meters before the first geophone in the profile A of line 1	21
Fig. 6: Shot is located at 50 meters before the first geophone in the profile A of line 1	21
Fig. 7: Shot is located at 30 meters before the first geophone in the profile A of line 1	22
Fig. 8: Shot is located at 10 meters before the first geophone in the profile A of line 1	22
Fig.9: Shot is located at 1 meter before the first geophone in the profile A of line 1	23
Fig. 10: Shot is located at 55 meters after the first geophone in the profile A of line 1	23
Fig. 11: Shot is located at 155 meters after the first geophone in the profile A of line 1	24
Fig. 12: Shot is located at 1 meter after the 24th geophone in the profile A of line 1	24
Fig. 13: Shot is located at 260 meters after the first geophone in the profile A of line 1	25
Fig. 14: Shot is located at 280 meters after the first geophone in the profile A of line 1	25
Fig. 15: Shot is located at 300 meters after the first geophone in the profile A of line 1	26
Fig. 16: Travelttime curves of 12 shots in the profile A of line 1	26
Fig. 17: Obtained velocity model not affected by topography in the profile A of line 1	27
Fig. 18: Obtained velocity model affected by topography in the profile A of line 1	28
Fig. 19: Obtained velocity model affected by topography in the profile A of line 1 with detection of layer margins	29
Fig. 20: Shot is located at 70 meters before the first geophone in the profile B of line 1	30
Fig. 21: Shot is located at 50 meters before the first geophone in the profile B of line 1	30
Fig. 22: Shot is located at 33 meters before the first geophone in the profile B of line 1	31



Fig. 23: Shot is located at 10 meters before the first geophone in the profile B of line 1	31
Fig. 24: Shot is located at 1 meter before the first geophone in the profile B of line 1	32
Fig. 25: Shot is located at 55 meters after the first geophone in the profile B of line 1	32
Fig. 26: Shot is located at 115 meters after the first geophone in the profile B of line 1	33
Fig. 27: Shot is located at 175 meters after the first geophone in the profile B of line 1	33
Fig. 29: Shot is located at 231 meters after the first geophone in the profile B of line 1	34
Fig. 30: Shot is located at 260 meters after the first geophone in the profile B of line 1	34
Fig. 31: Shot is located at 280 meters after the first geophone in the profile B of line 1	35
Fig. 32: Shot is located at 300 meters after the first geophone in the profile B of line 1	35
Fig. 33: Traveltime curves of 10 shots in the profile B of line 1	36
Fig. 34: Obtained velocity model not affected by topography in the profile B of line 1	37
Fig. 35: Obtained velocity model affected by topography in the profile B of line 1	38
Fig. 36: Obtained velocity model affected by topography in the profile B of line 1 with detection of layer margins	39
Fig. 37: Shot is located at 70 meters before the first geophone in the profile C of line 1	40
Fig. 38: Shot is located at 50 meters before the first geophone in the profile C of line 1	40
Fig. 39: Shot is located at 10 meters before the first geophone in the profile C of line 1	41
Fig. 40: Shot is located at 1 meter before the first geophone in the profile C of line 1	41
Fig. 41: Shot is located at 51 meters after the first geophone in the profile C of line 1	42
Fig. 42: Shot is located at 175 meters after the first geophone in the profile C of line 1	42
Fig. 43: Shot is located at 231 meters after the first geophone in the profile C of line 1	43
Fig. 44: Shot is located at 240 meters after the first geophone in the profile C of line 1	43
Fig. 45: Shot is located at 280 meters after the first geophone in the profile C of line 1	44
Fig. 46: Shot is located at 300 meters after the first geophone in the profile C of line 1	44
Fig. 47: Traveltime curves of 11 shots in the profile C of line 1	45



Fig. 48: Obtained velocity model not affected by topography in the profile C of line 1.....	46
Fig. 49: Obtained velocity model affected by topography in the profile C of line 1	47
Fig. 50: Obtained velocity model affected by topography in the profile C of line 1 with detection of layer margins.....	48
Fig. 51: Shot is located at 70 meters before the first geophone in the profile D of line 1.....	49
Fig. 52: Shot is located at 50 meters before the first geophone in the profile D of line 1.....	49
Fig. 53: Shot is located at 30 meters before the first geophone in the profile D of line 1.....	50
Fig. 54: Shot is located at 10 meters before the first geophone in the profile D of line 1.....	50
Fig. 55: Shot is located at 1 meter before the first geophone in the profile D of line 1	51
Fig. 56: Shot is located at 55 meters after the first geophone in the profile D of line 1.....	51
Fig. 57: Shot is located at 115 meters after the first geophone in the profile D of line 1.....	52
Fig. 58: Shot is located at 175 meters after the first geophone in the profile D of line 1.....	52
Fig. 59: Shot is located at 231 meters after the first geophone in the profile D of line 1.....	53
Fig. 60: Shot is located at 240 meters after the first geophone in the profile D of line 1.....	53
Fig. 61: Shot is located at 260 meters after the first geophone in the profile D of line 1.....	54
Fig. 62: Shot is located at 280 meters after the first geophone in the profile D of line 1.....	54
Fig. 63: Shot is located at 300 meters after the first geophone in the profile D of line 1.....	55
Fig. 64: Travel time curves of 10 shots in the profile D of line 1	55
Fig. 65: Obtained velocity model not affected by topography in the profile D of line 1	56
Fig. 66: Obtained velocity model affected by topography in the profile D of line 1.....	57
Fig. 67: Obtained velocity model affected by topography in the profile D of line 1 with detection of layer margins.....	58
Fig. 68: Shot is located at 70 meters before the first geophone in the profile E of line	59
Fig. 69: Shot is located at 40 meters before the first geophone in the profile E of line 1	59
Fig. 70: Shot is located at 10 meters before the first geophone in the profile E of line 1	60



Rogun Dam
Complementary Geotechnical Investigations at
Right Bank



Fig. 71: Shot is located at 1 meter before the first geophone in the profile E of line 1.....	60
Fig. 72: Shot is located at 125 meters after the first geophone in the profile E of line 1	61
Fig. 73: Shot is located at 175 meters after the first geophone in the profile E of line 1	61
Fig. 74: Shot is located at 231 meters after the first geophone in the profile E of line 1	62
Fig. 75: Shot is located at 240 meters after the first geophone in the profile E of line 1	62
Fig. 76: Travel time curves of 8 shots in the profile E of line 1	63
Fig. 77: Obtained velocity model not affected by topography in the profile E of line 1.....	64
Fig. 78: Obtained velocity model affected by topography in the profile E of line 1	65
Fig. 80: Shot is located at 22 meters before the 12th geophone in the profile F of line 1	67
Fig. 81: Shot is located at 1 meter before the 12th geophone in the profile F of line 1.....	67
Fig. 82: Shot is located at 112 meters after the 12th geophone in the profile F of line 1	68
Fig. 83: Travel time curves of 5 shots in the profile F of line 1.....	68
Fig. 84: Obtained velocity model not affected by topography in the profile F of line 1	69
Fig. 85: Obtained velocity model affected by topography in the profile F of line 1	70
Fig. 86: Obtained velocity model affected by topography in the profile F of line 1 with detection of layer margins.....	71
Fig. 87: Obtained velocity model affected by topography along the line 1, interpolated according to Kriging method.....	72
Fig. 88: Obtained velocity model affected by topography along the line 1, interpolated according to Triangular method.....	73
Fig. 89: Shot is located at 70 meters before the first geophone in the profile A of line 2.....	74
Fig. 90: Shot is located at 40 meters before the first geophone in the profile A of line 2.....	74
Fig. 91: Shot is located at 10 meters before the first geophone in the profile A of line 2.....	75
Fig. 92: Shot is located at 1 meter before the first geophone in the profile A of line 2	75
Fig. 93: Shot is located at 300 meters after the first geophone in the profile A of line 2.....	76



Rogun Dam
Complementary Geotechnical Investigations at
Right Bank



Fig. 94: Shot is located at 270 meters after the first geophone in the profile A of line 2.....	76
Fig. 95: Shot is located at 240 meters after the first geophone in the profile A of line 2.....	77
Fig. 96: Shot is located at 230 meters after the first geophone in the profile A of line 2.....	77
Fig. 97: Shot is located at 175 meters after the first geophone in the profile A of line 2.....	78
Fig. 98: Shot is located at 115 meters after the first geophone in the profile A of line 2.....	78
Fig. 99: Shot is located at 55 meters after the first geophone in the profile A of line 2.....	79
Fig. 100: Travel time curves of 10 shots in the profile A of line 2.....	79
Fig. 101: Obtained velocity model not affected by topography in the profile A of line 2.....	80
Fig. 102: Obtained velocity model affected by topography in the profile A of line 2.....	81
Fig. 103: Obtained velocity model affected by topography in the profile A of line 2 with detection of layer margins.....	82
Fig.104: Shot is located at 70 meters before the first geophone in the profile B of line 2.....	83
Fig.105: Shot is located at 40 meters before the first geophone in the profile B of line 2.....	83
Fig.106: Shot is located at 10 meters before the first geophone in the profile B of line 2.....	84
Fig.107: Shot is located at 300 meters after the first geophone in the profile B of line 2.....	84
Fig.108: Shot is located at 270 meters after the first geophone in the profile B of line 2.....	85
Fig. 109: Shot is located at 240 meters after the first geophone in the profile B of line 2.....	85
Fig. 110: Shot is located at 55 meters after the first geophone in the profile B of line 2.....	86
Fig. 111: Shot is located at 165 meters after the first geophone in the profile B of line 2.....	86
Fig. 112: Travel time curves of profile B in line 2.....	87
Fig. 113: Obtained velocity model not affected by topography in the profile B of line 2.....	88
Fig. 114: Obtained velocity model affected by topography in the profile B of line 2.....	89
Fig. 115: Obtained velocity model affected by topography in the profile B of line 2 with detection of layer margins.....	90
Fig. 116: Shot is located at 55 meters before the first geophone in the profile C of line 2.....	91



Fig. 117: Shot is located at 10 meters before the first geophone in the profile C of line 2.....	91
Fig. 118: Shot is located at 1 meter before the first geophone in the profile C of line 2.....	92
Fig. 119: Shot is located at 45 meters after the first geophone in the profile C of line 2.....	92
Fig. 120: Shot is located at 95 meters after the first geophone in the profile C of line 2.....	93
Fig. 121: Travel time curves of 5 shots of profile C in line 2.....	93
Fig. 122: Obtained velocity model not affected by topography of the profile C in line 2.....	94
Fig. 123: Obtained velocity model affected by topography of the profile C in line 2.....	95
Fig. 124: Shot is located at 50 meters before the first geophone in the profile D of line 2.....	96
Fig. 125: Shot is located at 30 meters before the first geophone in the profile D of line 2.....	96
Fig. 126: Shot is located at 1 meter before the first geophone in the profile D of line 2.....	97
Fig. 127: Shot is located at 280 meters after the first geophone in the profile D of line 2.....	97
Fig. 128: Shot is located at 260 meters after the first geophone in the profile D of line 2.....	98
Fig. 129: Shot is located at 240 meters after the first geophone in the profile D of line 2.....	98
Fig. 130: Shot is located at 231 meters after the first geophone in the profile D of line 2.....	99
Fig. 131: Shot is located at 115 meters after the first geophone in the profile D of line 2.....	99
Fig. 132: Shot is located at 165 meters after the first geophone in the profile D of line 2.....	100
Fig. 133: Travel time curves of 10 shots of profile D in line 2.....	100
Fig. 134: Obtained velocity model not affected by topography in the profile D of Line 2.....	101
Fig. 135: Obtained velocity model affected by topography in the profile D of Line 2.....	102
Fig. 136: Obtained velocity model affected by topography in the profile D of line 2 with detection of layer margins.....	103
Fig. 137: Obtained velocity model affected by topography along the line 2, interpolated according to Kriging method.....	104
Fig. 138: Obtained velocity model affected by topography in the line 2, interpolated according to Triangular method.....	105



Rogun Dam
Complementary Geotechnical Investigations at
Right Bank



Fig. 139: Shot is located at 55 meters before the first geophone in the profile A of line 3.....	106
Fig. 140: Shot is located at 10 meters before the first geophone in the profile A of line 3.....	106
Fig. 141: Shot is located at 1 meter before the first geophone in the profile A of line 3	107
Fig. 142: Shot is located at 231 meters after the first geophone in the profile A of line 3.....	107
Fig. 143: Shot is located at 175 meters after the first geophone in the profile A of line 3.....	108
Fig. 144: Shot is located at 115 meters after the first geophone in the profile A of line 3.....	108
Fig. 145: Shot is located at 55 meters after the first geophone in the profile A of line 3.....	109
Fig. 146: Travel time curves of 7 shots of profile A of line 3	109
Fig. 147: Obtained velocity model not affected by topography in the profile A of Line 3.....	110
Fig. 148: Obtained velocity model affected by topography in the profile A of Line 3	111
Fig. 149: Obtained velocity model affected by topography in the profile A of line 3 with detection of layer margins.....	112



CHAPTER 1

INTRODUCTION

1. INTRODUCTION

"Rogun" dam and power plant is under construction on "Vakhsh" river at about 110 kilometers far from north-east of the city of Dushanbe, Tajikistan.

The dam is a rockfill dam with impervious core and in its final stage will be 335 m high. Therefore, it will be the highest dam in the world. Rogun underground powerhouse, with its 6 turbines each with nominal capacity of 600 MW will have a total nominal capacity of 3600 MW for the whole power plant.

According to the planning and scheduling by the Client (Rogun HPP), the first two units (1200 MW) of the Rogun powerhouse shall be commissioned as the first stage of the project. In order to achieve this goal, the river closure shall be done as soon as possible, by which construction of the upstream cofferdam and then stage 1 dam can be effectively started.

This report consists of four chapters. The present chapter is dedicated to "Introduction". In "Chapter 2", the seismic refraction method is introduced. "Chapter 3" explains the seismic refraction investigations at the right bank of Rogun dam and seismic profiles as the results of the investigations are presented. In "Chapter 4", a brief conclusion on the results of refraction seismic investigations is presented.

1.1. LOCATION OF THE SITE

The area under consideration is located in a mountainous region with a rough topography at the Rogun dam site in Tajikistan.

Three lines of refraction seismic surveys were designed at the downstream part of the right bank of Rogun dam (Fig. (1)). The main aim was to investigate the sub-surface geotechnical features of the proposed area.

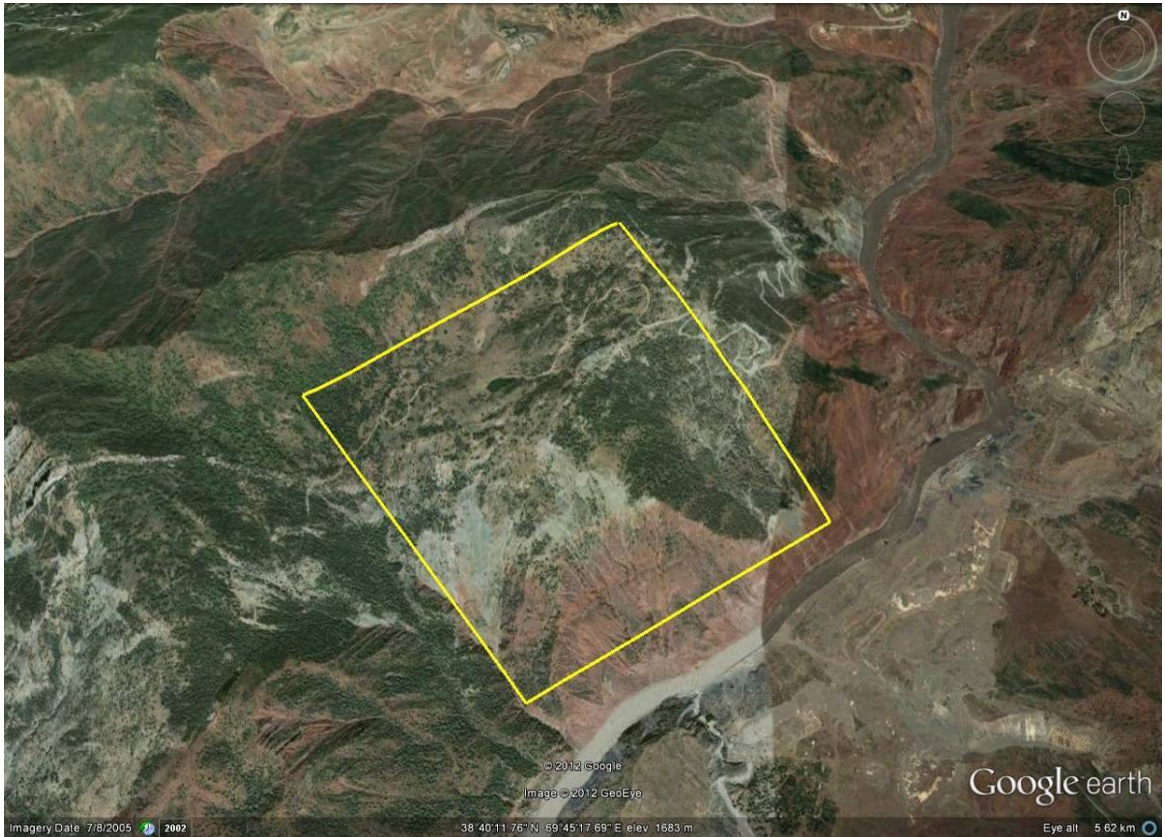


Fig. 1: General view of the location of refraction seismic investigations

1.2. SITE GEOLOGY

The main Geological units in the surveyed area are as follows:

Cretaceous: silt, mud, sandstone, granodiorite, Conglomerate and limestone.

Triassic: Evaporates (Gypsum and Halite).

The geological map is shown in Fig. (2).

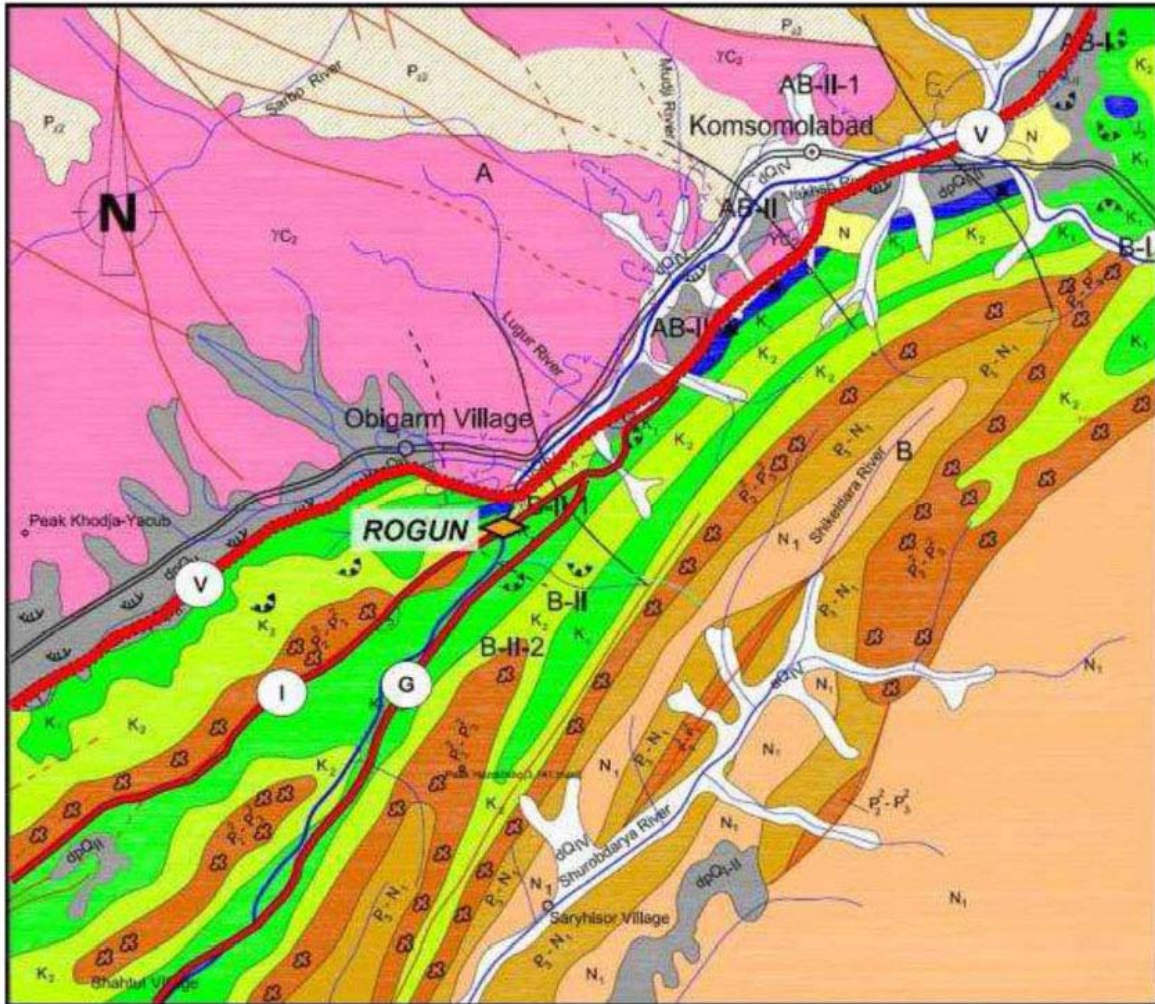


Fig. 2: Geological map of Rogun dam site

V = Vakhsh Fault, I = Ionaksh Fault, G = Gulizindan Fault.

Green and yellow green: Cretaceous made of silt, mud and sandstone;

Pink: Granodiorite;

Brown: Conglomerate and limestone;

Dark blue: Triassic including evaporates (gypsum and halite).



CHAPTER 2

INTERODUCTION TO SEISMIC REFRACTION METHOD

2. INTRODUCTION TO SEISMIC REFRACTION METHOD

2.1. BASIC FIELD EXPERIMENT

Seismic refraction is one of the basic, classical methods of applied geophysics. Whole-earth seismology started in the late 1800's. Perhaps the first significant small-scale work was that of Mohorovicic who analyzed earthquake records in terms of a low-velocity crust over a high-velocity mantle.

The most basic refraction experiment involves a source (earthquake, explosion, hammer blow) and a set of receivers (seismographs, geophones, hydrophones). In many cases the geophones are set out in a straight line originating at the source. The geophones respond in turn as seismic waves pass by them. The geophones are sensitive to the velocity of vertical ground motion, not to the travel velocity of the various waves.

Because of the difficulty of identifying later wiggles on the geophone traces only the "first arrival" times are used in elementary interpretations. The mathematical interpretation yields some pattern of wave velocities in the ground. Geological interpretation involves converting the velocity distribution into a geologic cross-section. In other words, what earth materials correspond to the estimated velocities?

2.2. ELEMENTS OF ELASTICITY: STRESS, STRAIN AND ELASTIC MODULI

Stretching a cylindrical rock sample leads to Hooke's Law. Up to some elastic limit, the applied axial stress (force per unit area measured in Newtons per meter squared or Pascals) is proportional to the axial strain (fractional elongation of the rod; dimensionless). Hooke's Law states that the stress equals the strain times Young's Modulus (Newtons per meter squared or Pascals). This "law" holds only for small strains. In this "elastic region" strains go away when the stress is removed. The law holds for both tension and compression. For sufficiently large strains there is some form

of permanent deformation or even fracture. With respect to seismic waves we experience linear (Hooke's Law) behavior except in the immediate vicinity of the source.

If we examine our stretched rock cylinder more carefully we'll note that it got narrower as well as longer. Poisson's Ratio is simply the negative of the radial strain (fractional change in radius; dimensionless) divided by the axial strain. Conversely, the cylinder gets broader if it is shortened by compressive stress. Poisson's Ratio is dimensionless (as are all ratios) and is always between zero and one half.

For our second experiment let's subject a cube or sphere to uniform stress ("hydrostatic stress"). For small enough stresses we find that the stress is proportional to the volumetric strain (also called cubical dilation). This is just the fractional change in volume (dimensionless). The proportionality constant is called the bulk modulus (Pascals or Newtons per meter squared). In this experiment only the size of the object changes; the shape stays the same.

For a third experiment let's apply tangential stresses (shear stresses) to the faces of a cube. We'll note that the shape changes from a square to a rhombus. The tangent of the total angular change in an original right angle is called the shear strain (dimensionless). For the small shear strains involved in seismic wave propagation, we can equate the tangent of the angle to the angle itself. For elastic materials and behaviour the shear stress (Pascals) is proportional to the shear strain. The constant of proportionality is called the shear modulus or modulus of rigidity (Pascals).

2.3. SEISMIC WAVES

Seismic waves can be divided into two classes. "Body waves" can travel throughout a three dimensional volume. Examples of body waves are compressional waves and shear waves, "Surface waves" (in a broad sense) are restricted to travel along some interface. Ocean waves are surface waves although most ocean surface waves are not seismic waves. Love waves and Rayleigh waves on solids are examples of seismic surface waves.

Traditionally the most significant waves in seismic exploration are compressional waves (also called P-waves, primary waves and push-pull waves). P-waves are body waves and can travel through solids, liquids and gases. The waves used in echo-sounding and sonar in the sea are just P- waves as are sound waves in the air. As the name implies these are the fastest seismic waves and are the first to be picked up after an earthquake or other seismic event. The particle motion ("orbital motion") is back and forth parallel to the direction of wave travel ("ray path") and at right angles to the wavefront.

Shear waves (S-waves, secondary waves, shake waves) have traditionally been little used in exploration seismology although they always have been used in earthquake seismology. This is changing rapidly with S-waves becoming more important every year. S-waves travel more slowly than P-waves and can not travel through liquids and gases. The particle motion is normal to the ray path and parallel to the wavefront. Shear waves can be polarized with horizontal, vertical or some other sense of motion.

In conventional P-wave seismology using vertical geophones we often observe very strong "ground roll" consisting of large, low-frequency waves. The waves are predominantly Rayleigh waves, one of the two major types of seismic surface waves. In the simplest case the orbits are ellipses in a vertical plane. As with other surface waves the motion dies out with depth in the ground. Unlike body waves, surface waves are dispersive. That is, the speed of travel depends on the frequency of the wave.

Love waves are another common type of seismic surface wave. Orbital motion is horizontal and normal to the ray path. Love waves die out at depth and are always dispersive. Unlike Rayleigh waves they can only travel over a layered medium. We would not expect to detect Love waves with the vertical geophones that we normally employ.

2.4. SEISMIC WAVE VELOCITIES

The text has tables of seismic velocities for common earth materials. From these tables and other observations we can draw some general conclusions. For loose sediment the

P-wave velocity is about the same as the velocity in the pore fluid (air or water). For S-waves the pore fluid has little influence on the velocity.

For a grab-bag of rocks the P-wave velocity increases with density. Later we'll see that this statement needs some serious qualifications. S-wave velocities are about two-thirds of compressional wave velocities on the same rocks. Velocities increase as pressure increases. For rocks within a few km of the surface V_p and V_s may be much less than at greater depth where joints and micro cracks are sealed. Near surface weathering can also lead to low velocities.

Sedimentary rocks velocity increases with cementation and compaction but decreases with porosity. Thus V_p and V_s typically increase with depth and age. V_p depends strongly on pore fluid but V_s does not.

Increase of temperature increases the velocity of waves in air, water and some sediments. In solid rocks the seismic velocities decrease as temperature increases.

When a sound wave crosses an interface between layers of two different velocities, the wave is refracted. That is, the angle of the wave leaving the interface will be altered from the incident angle, depending on the relative velocities. Going from a low-velocity layer to a high-velocity layer, a wave at a particular incident angle (the "critical angle") will be refracted along the upper surface of the lower layer. As it travels, the refracted wave spawns up going waves in the upper layer, which impinge on the surface geophones.

Sound moves faster in the lower layer than the upper, so at some point, the wave refracted along that surface will overtake the direct wave. This refracted wave is then the first arrival at all subsequent geophones, at least until it is in turn overtaken by a deeper, faster refraction. The difference in travel time of this wave arrival between geophones depends on the velocity of the lower layer. If that layer is plane and level, the refraction arrivals form a straight line whose slope corresponds directly to that velocity. The point at which the refraction overtakes the direct arrival is known as the "crossover distance", and can be used to estimate the depth to the refracting surface.

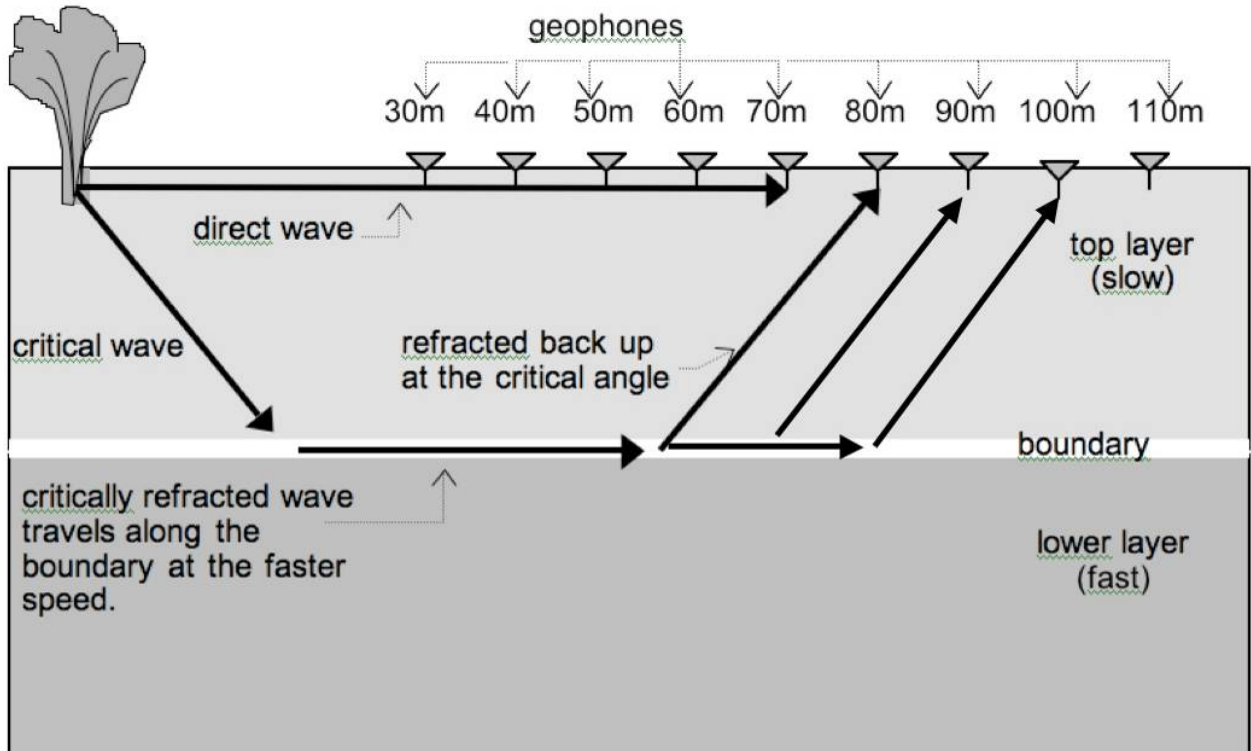


Fig. 3: Schematic design of geophones location



CHAPTER 3

SEISMIC REFRACTION INVESTIGATIONS At RIGHT BANK OF ROGUN DAM SITE

3. SEISMIC REFRACTION INVESTIGATIONS AT RIGHT BANK OF ROGUN DAM SITE

At Rogun Dam site, refraction seismic data were recorded along 3 lines that contain 11 profiles. In each profile shots located in 1 meter beneath the surface. Data recorded in 24 geophones with 10 meters spacing. Format of data is ".sgy" and sampling interval is 2 (ms). Since topography variation along the lines 1 and 2 were sharp so it might create some noisy data. It was tried to use the recorded data in the best manner. In figure (4), locations of seismic profiles along lines 1, 2 and 3 are shown while; in next figures p wave fronts that recorded in the various profiles are shown.



Fig. 4 : Locations of seismic profiles along the lines 1, 2 and 3

3.1. LINE 1 PROFILE A

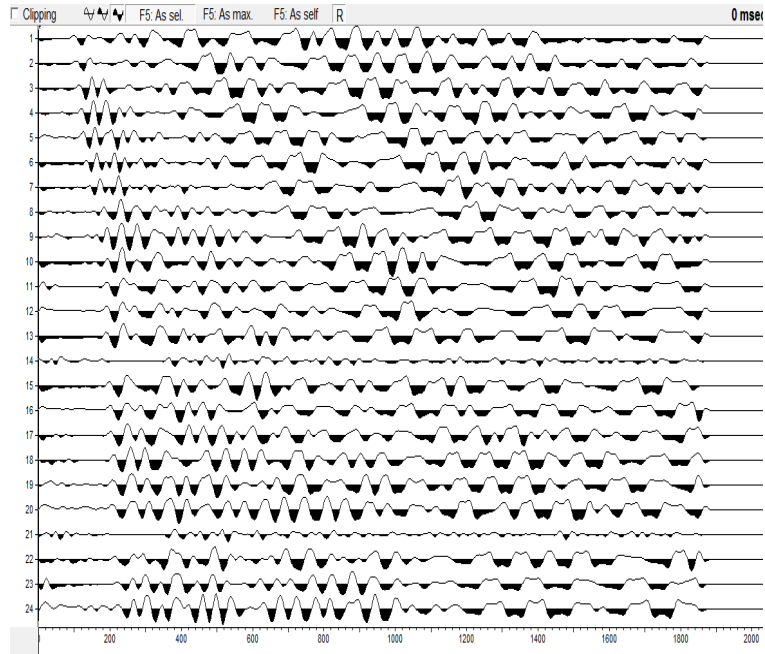


Fig. 5: Shot is located at 70 meters before the first geophone in the profile A of line 1

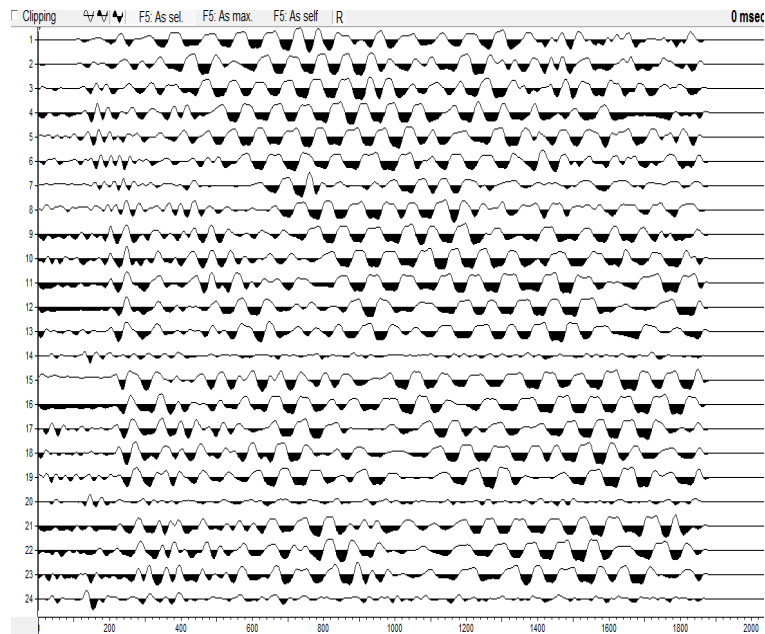


Fig. 6: Shot is located at 50 meters before the first geophone in the profile A of line 1

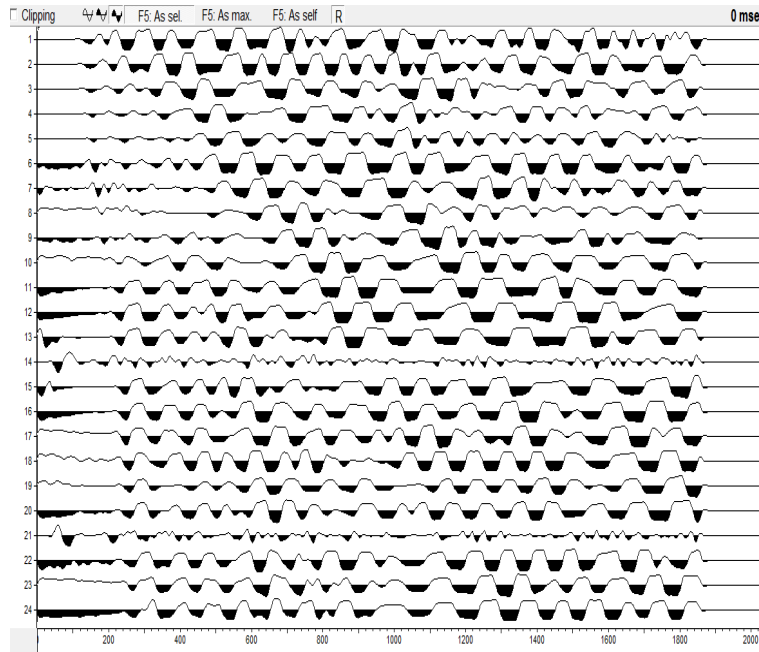


Fig. 7: Shot is located at 30 meters before the first geophone in the profile A of line 1

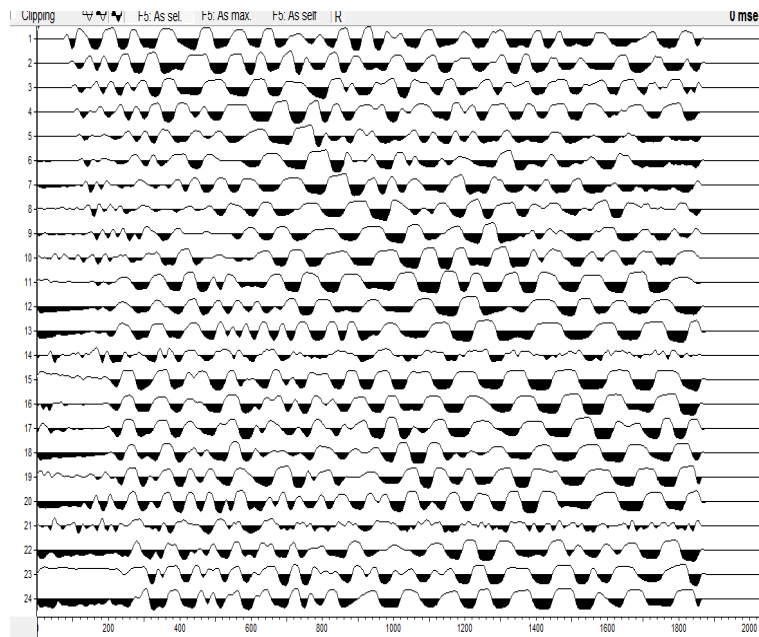


Fig. 8: Shot is located at 10 meters before the first geophone in the profile A of line 1

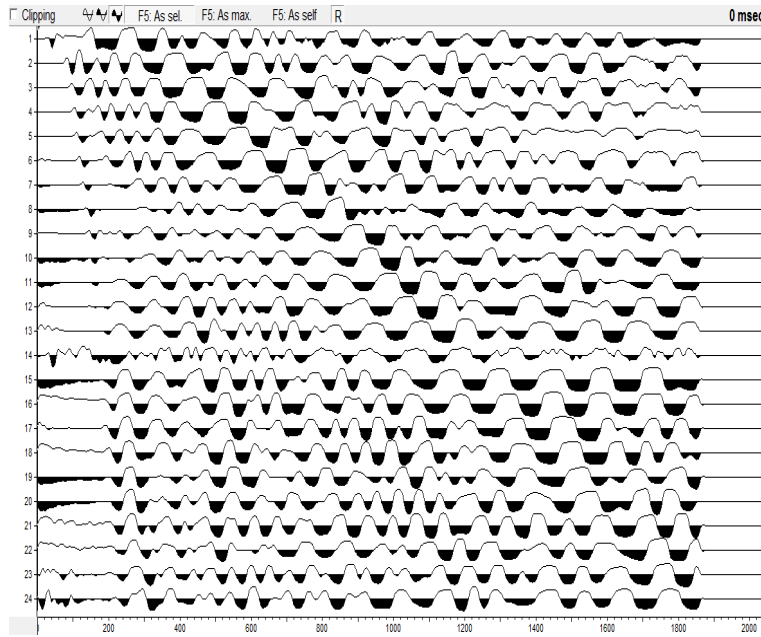


Fig.9: Shot is located at 1 meter before the first geophone in the profile A of line 1

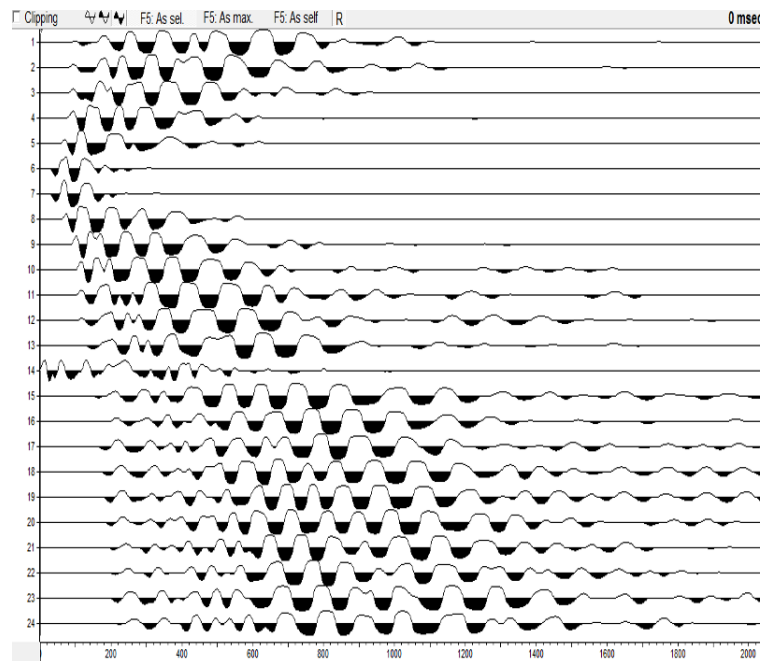


Fig. 10: Shot is located at 55 meters after the first geophone in the profile A of line 1

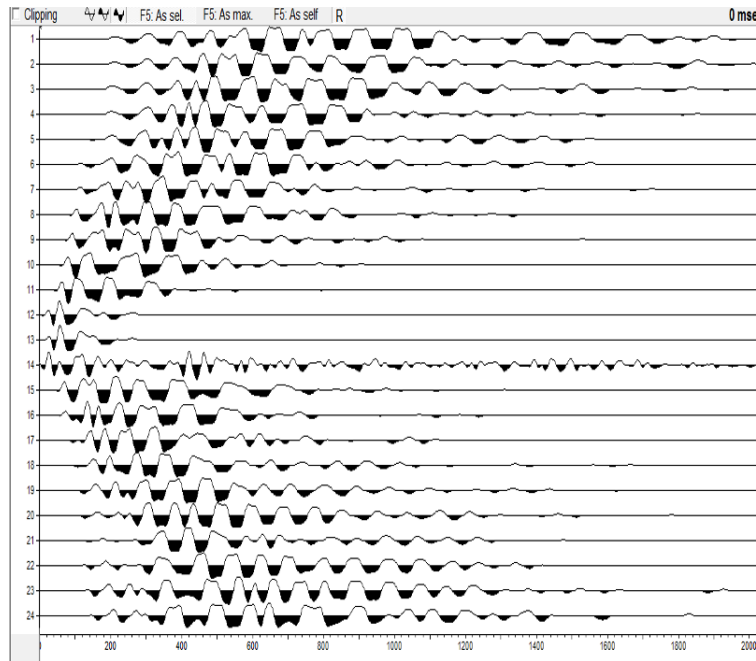


Fig. 11: Shot is located at 155 meters after the first geophone in the profile A of line 1

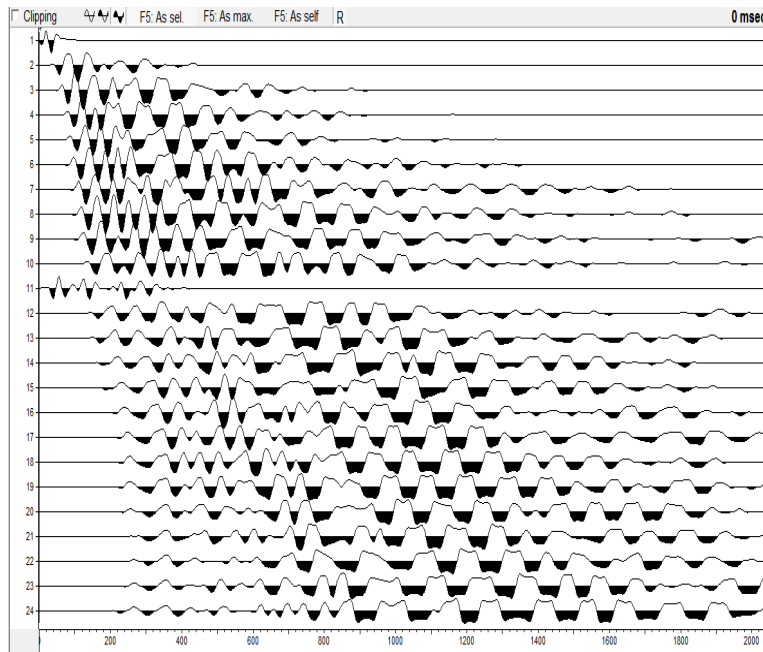


Fig. 12: Shot is located at 1 meter after the 24th geophone in the profile A of line 1

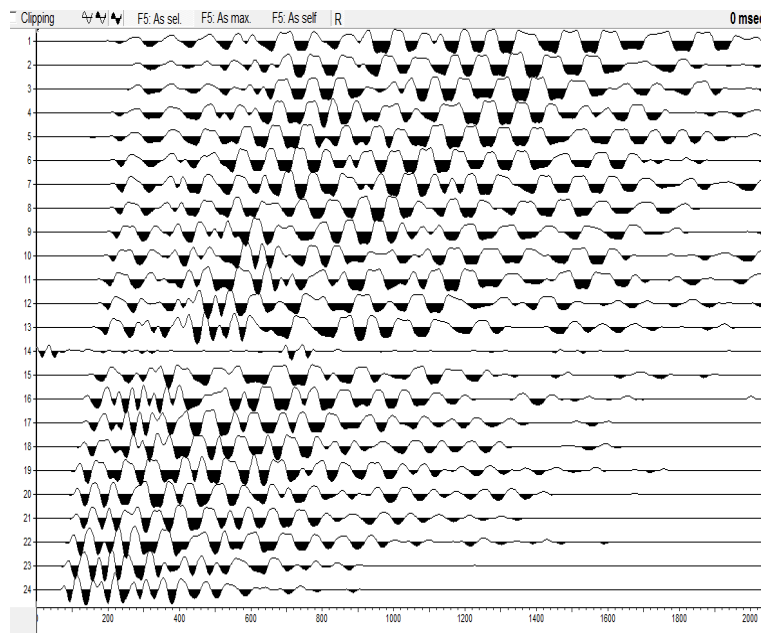


Fig. 13: Shot is located at 260 meters after the first geophone in the profile A of line 1

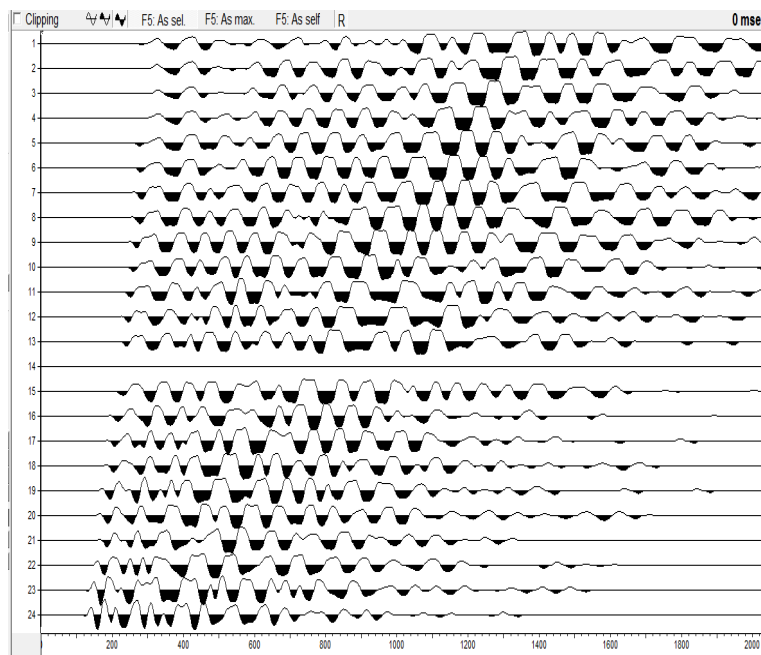


Fig. 14: Shot is located at 280 meters after the first geophone in the profile A of line 1

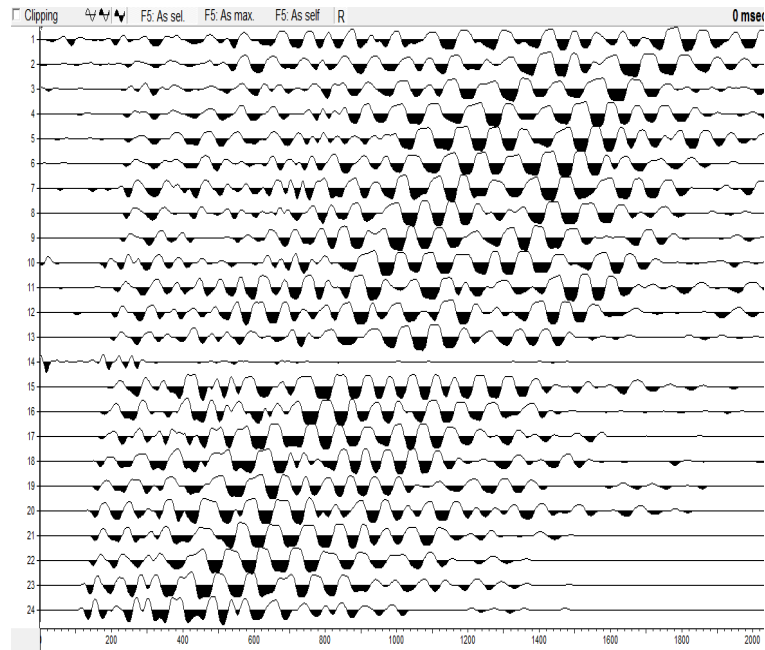


Fig. 15: Shot is located at 300 meters after the first geophone in the profile A of line 1

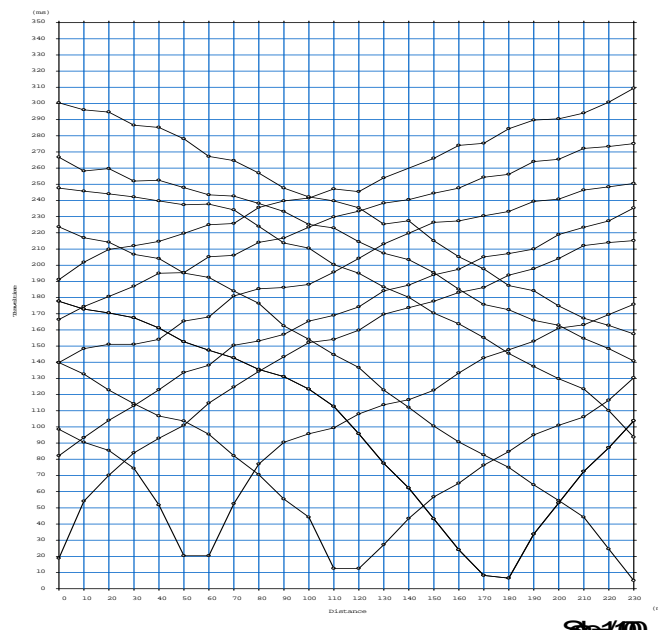


Fig. 16: Traveltime curves of 12 shots in the profile A of line 1

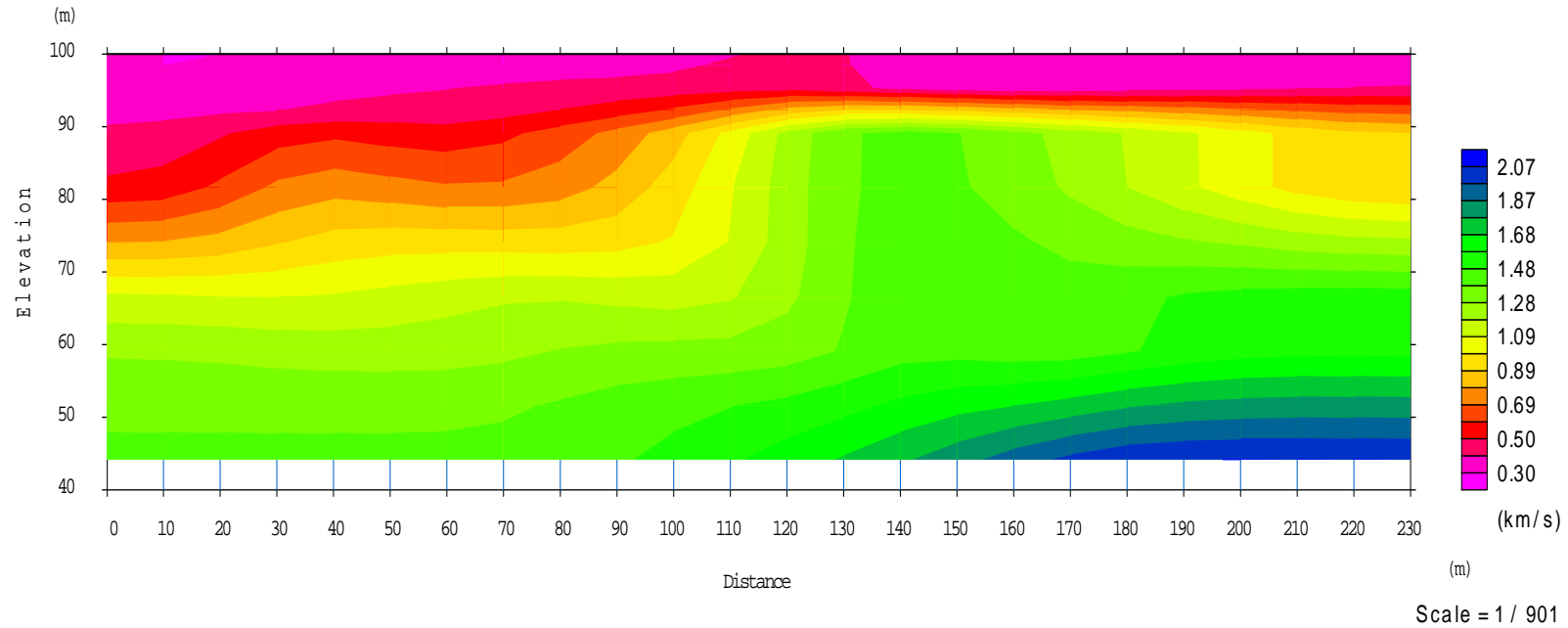


Fig. 17: Obtained velocity model not affected by topography in the profile A of line 1

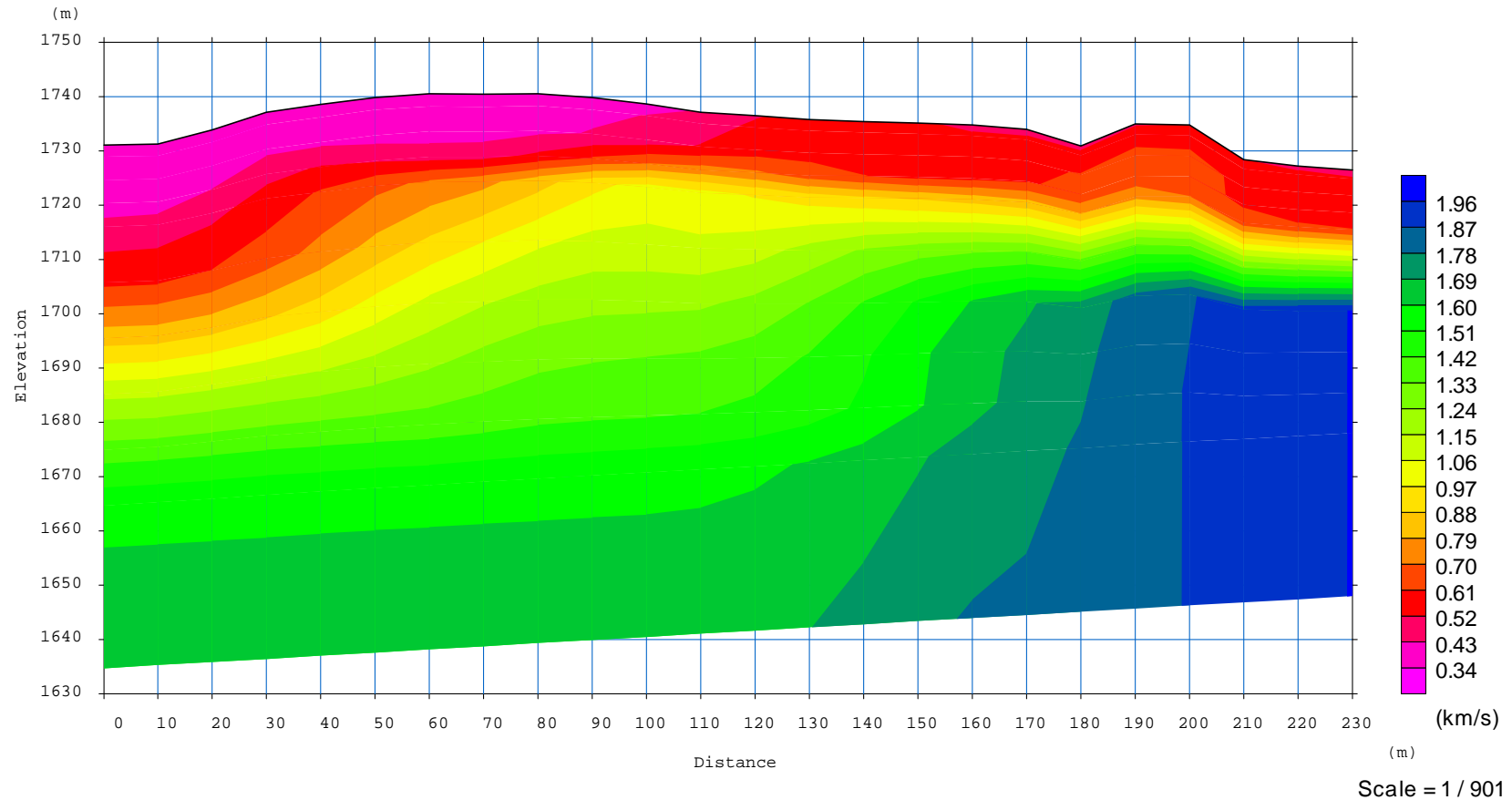


Fig. 18: Obtained velocity model affected by topography in the profile A of line 1

Along the profile A of line 1, three layers with different velocities were detected. These layers, from top to the bottom could be loose soil (overburden), clay and fractured sandstone. Thicknesses of the first and second layers under each Geophone are presented in the below table:

Geophone Number	1	2	3	4	5	6	7	8	9	10	11	12	13	14	15	16	17	18	19	20	21	22	23	24
Thickness of first layer	13.23	12.79	13.52	14.1	12.98	12.45	12.13	11.45	11.11	10.5	10.42	10.55	11.28	12.18	13.4	14.15	14.99	16.2	14.58	19.58	22.44	20.19	21.9	22.81
Thickness of second layer	25.88	26.08	27.55	29.98	32.36	34.14	35.16	35.71	35.96	35.38	33.47	30.83	28	24.47	20.72	17.52	14.41	10.9	8.66	7.73	5.63	2.95	1.79	1.77

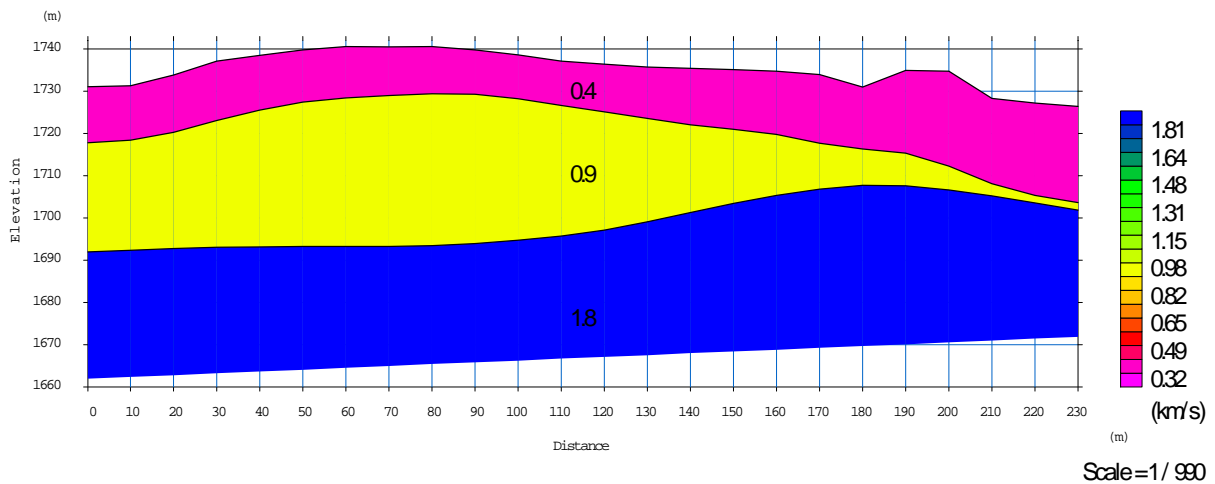


Fig. 19: Obtained velocity model affected by topography in the profile A of line 1 with detection of layer margins

3.2. LINE 1 PROFILE B

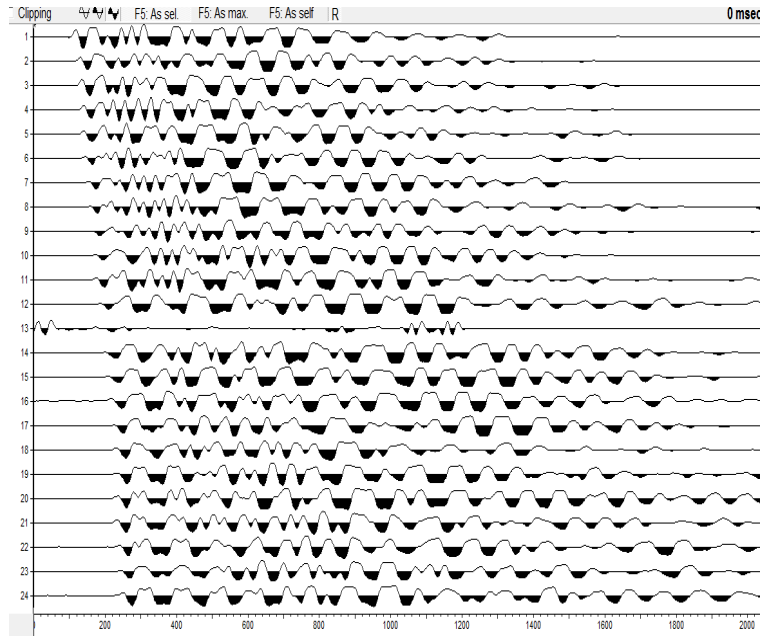


Fig. 20: Shot is located at 70 meters before the first geophone in the profile B of line 1

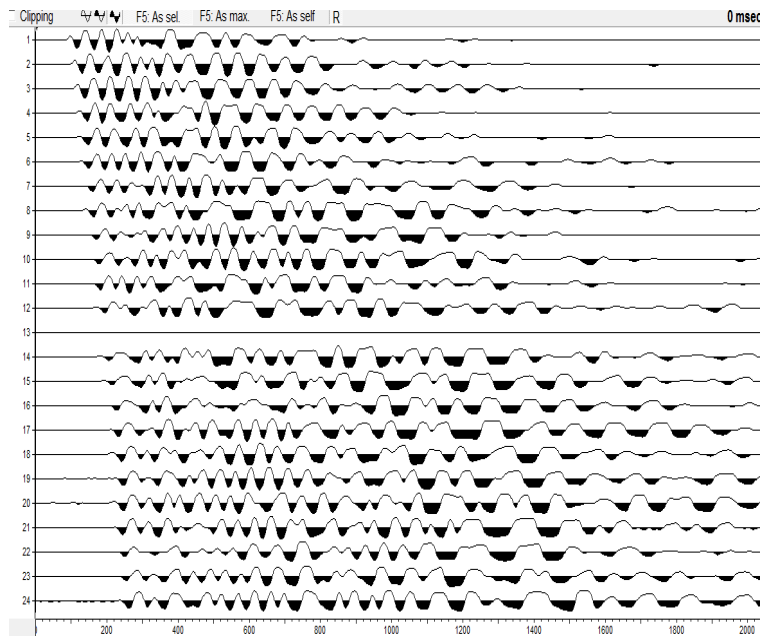


Fig. 21: Shot is located at 50 meters before the first geophone in the profile B of line 1

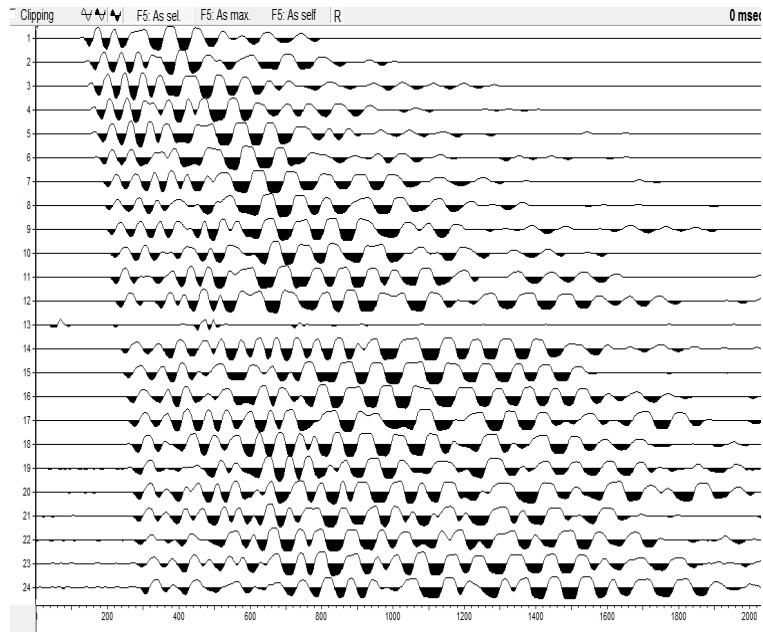


Fig. 22: Shot is located at 33 meters before the first geophone in the profile B of line 1

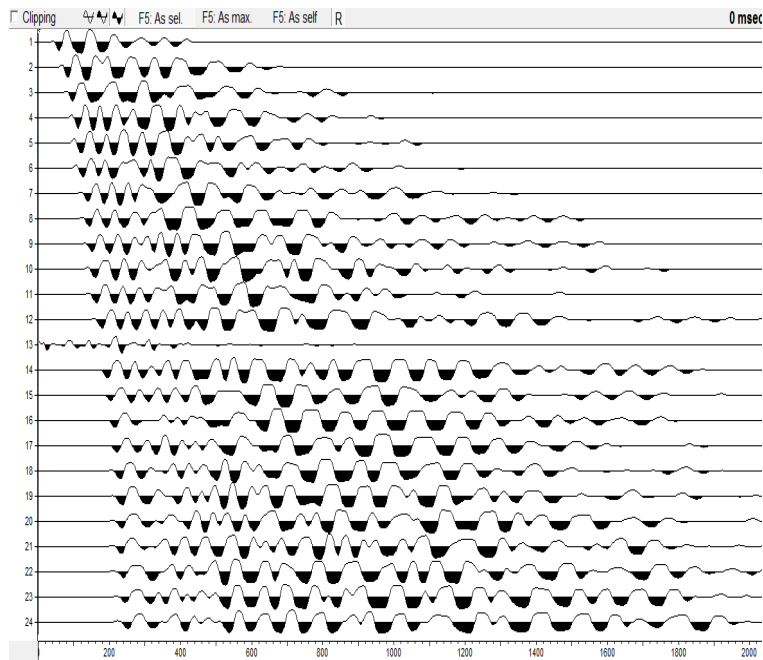


Fig. 23: Shot is located at 10 meters before the first geophone in the profile B of line 1

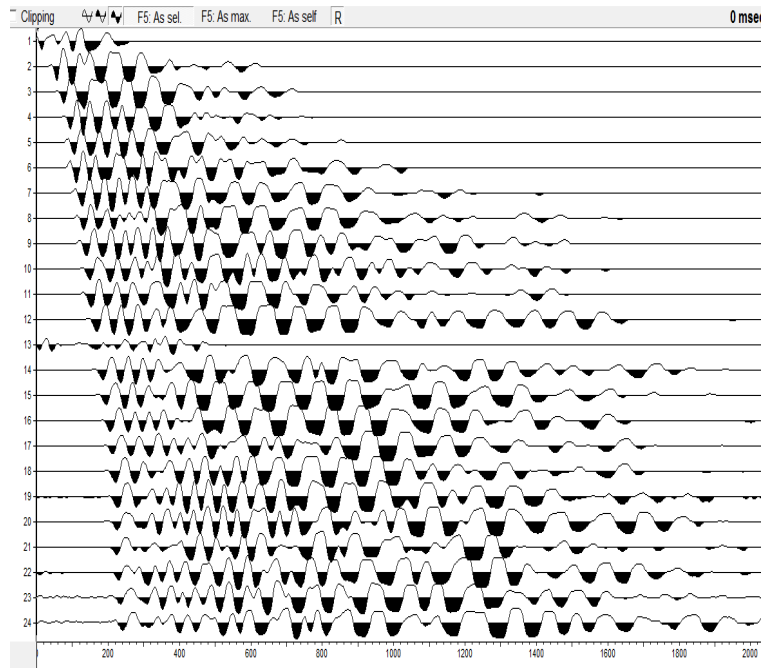


Fig. 24: Shot is located at 1 meter before the first geophone in the profile B of line 1



Fig. 25: Shot is located at 55 meters after the first geophone in the profile B of line 1

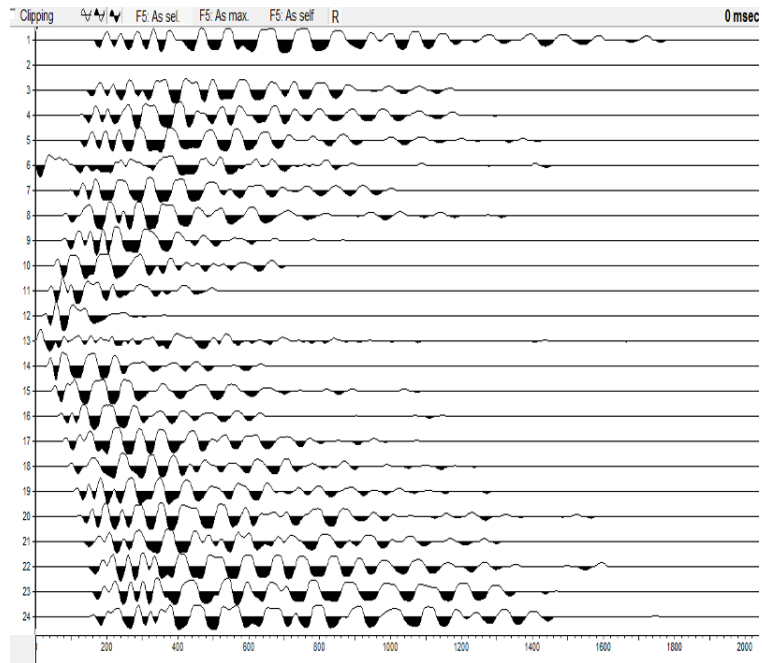


Fig. 26: Shot is located at 115 meters after the first geophone in the profile B of line 1

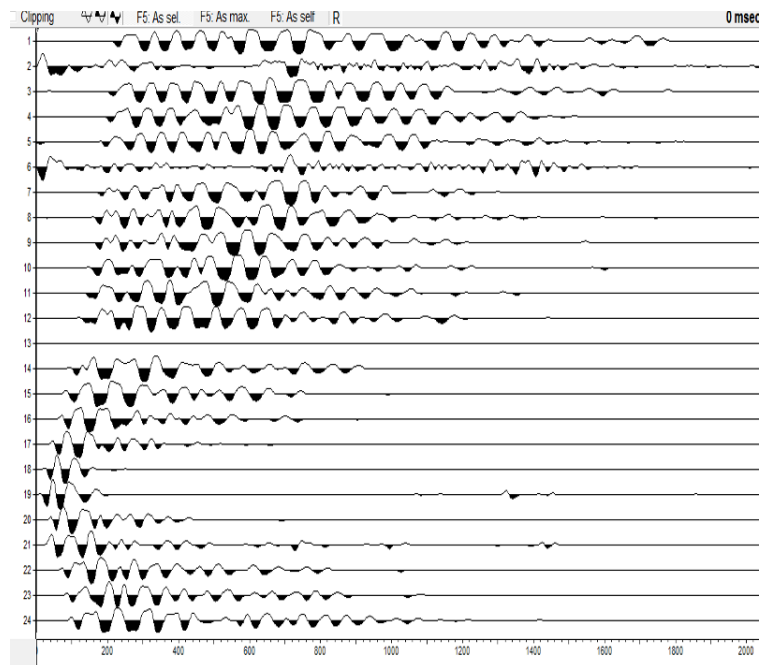


Fig. 27: Shot is located at 175 meters after the first geophone in the profile B of line 1

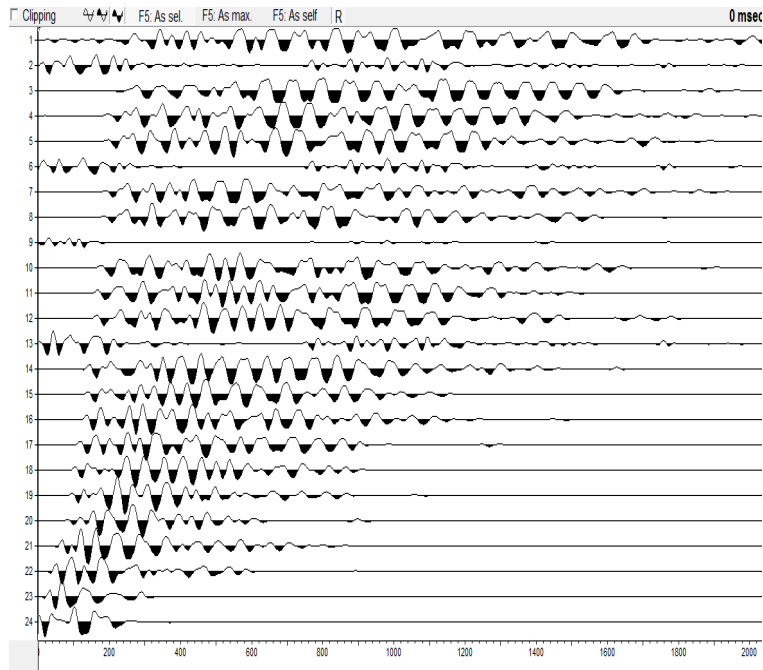


Fig. 29: Shot is located at 231 meters after the first geophone in the profile B of line 1

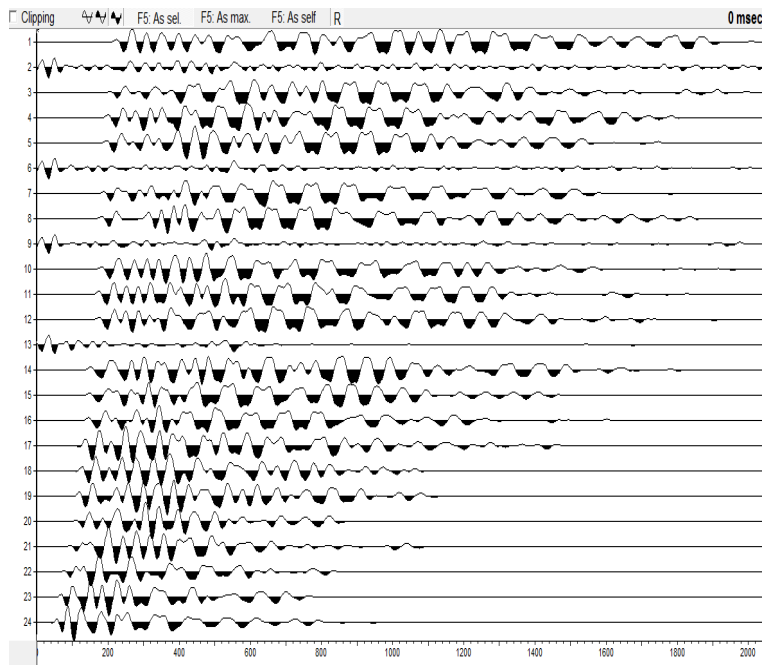


Fig. 30: Shot is located at 260 meters after the first geophone in the profile B of line 1

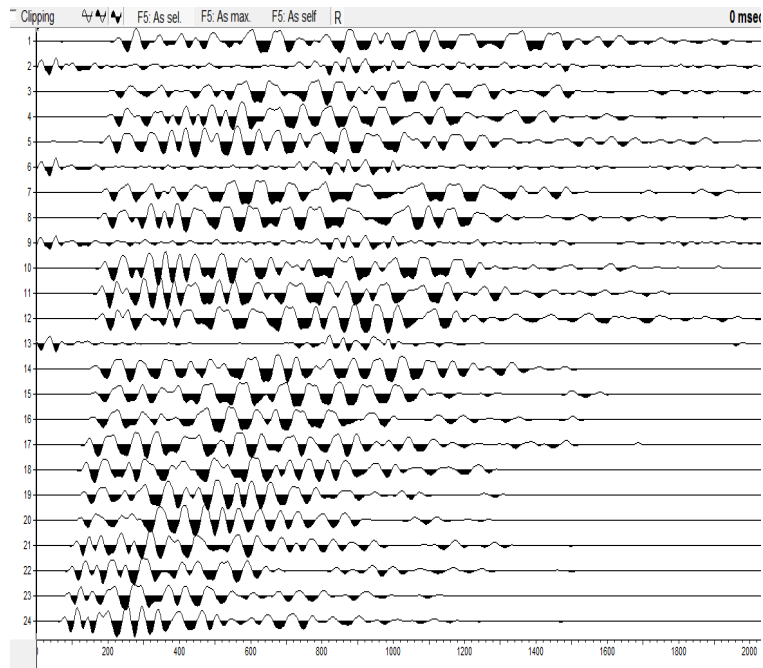


Fig. 31: Shot is located at 280 meters after the first geophone in the profile B of line 1

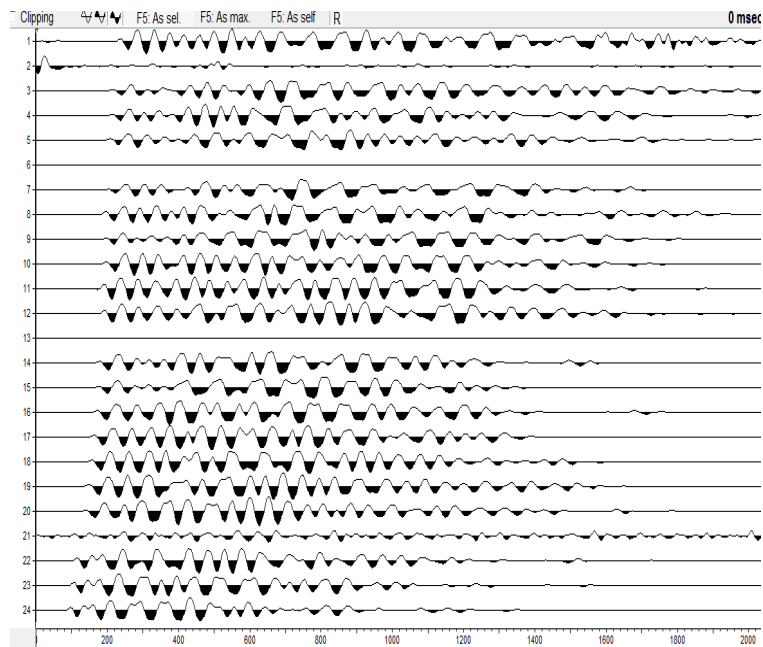


Fig. 32: Shot is located at 300 meters after the first geophone in the profile B of line 1

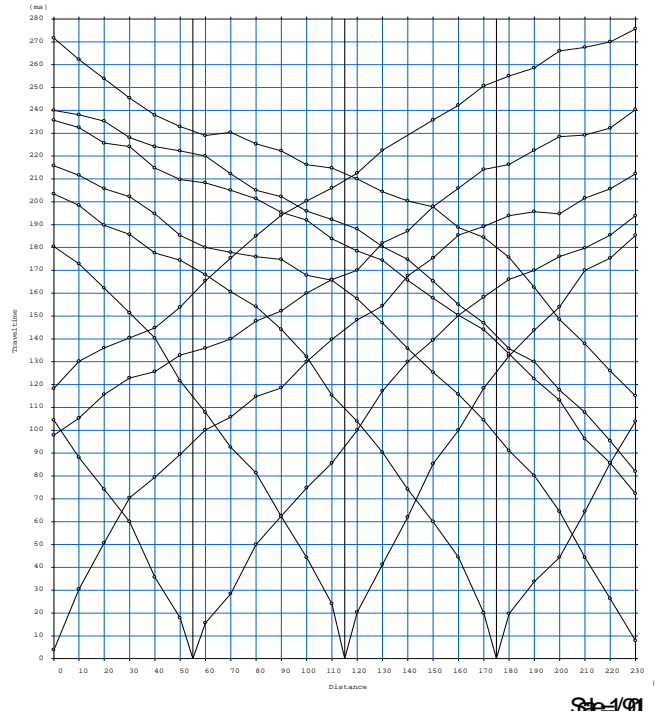


Fig. 33: Traveltime curves of 10 shots in the profile B of line 1

Note: In the profile B of line 1, there were 13 shots but 10 shots were used because of noisy data.

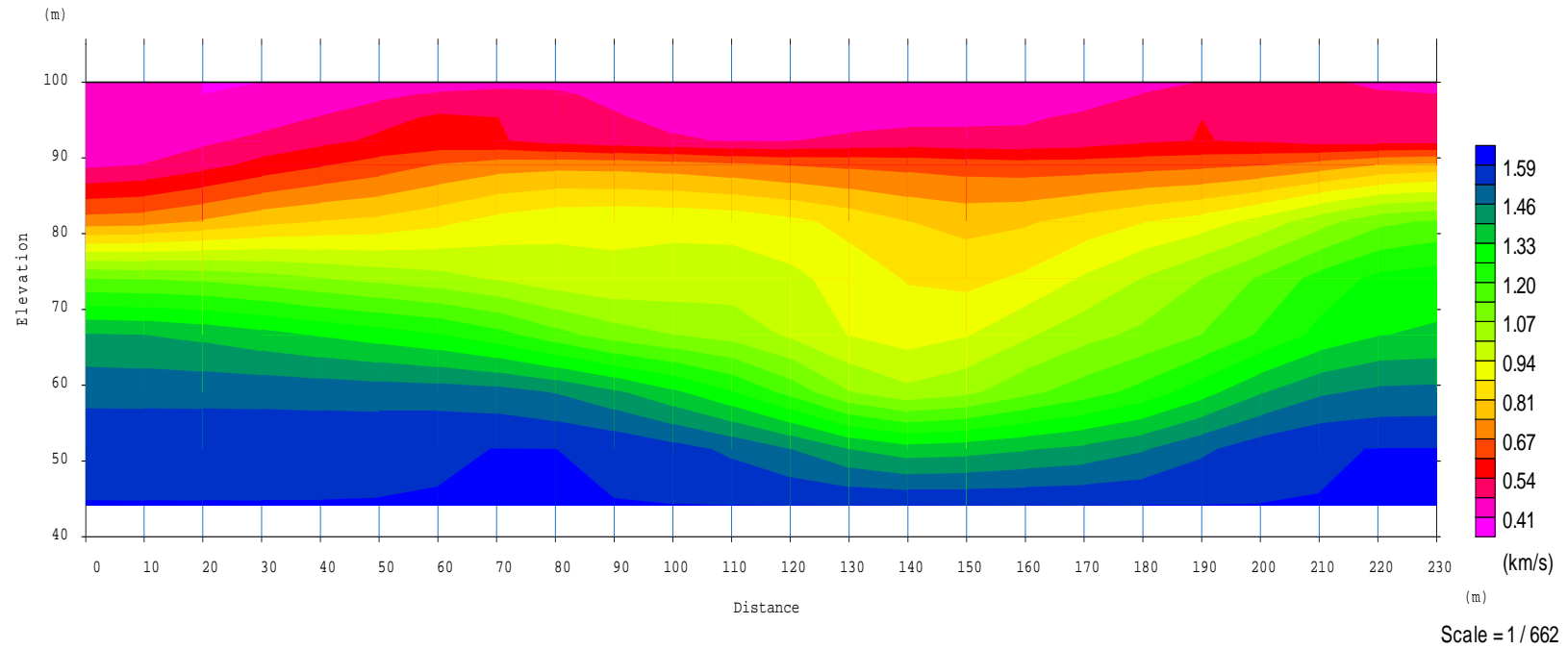


Fig. 34: Obtained velocity model not affected by topography in the profile B of line 1

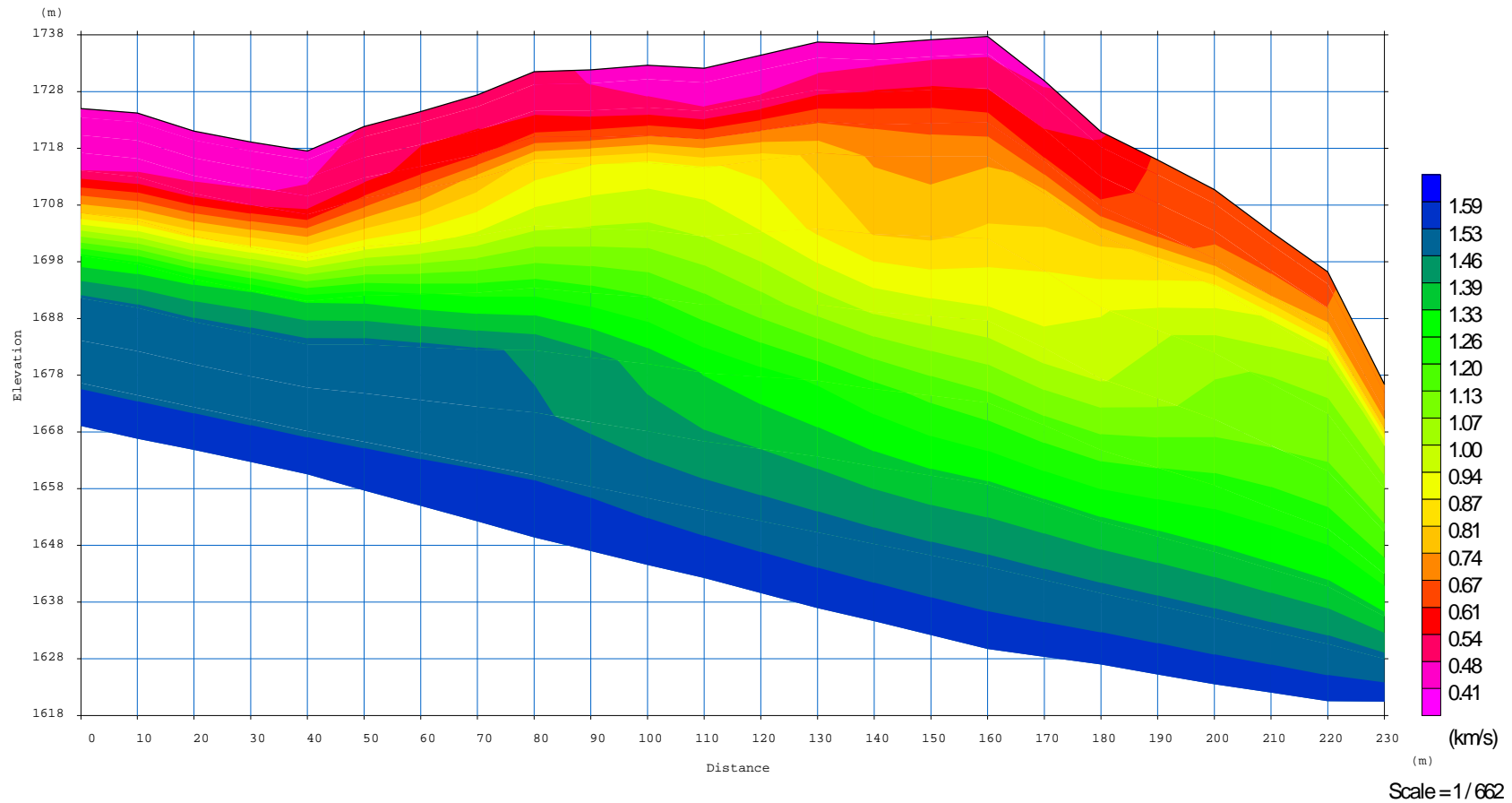


Fig. 35: Obtained velocity model affected by topography in the profile B of line 1

Along the profile B of line 1, three layers with different velocities were detected. These layers, from top to the bottom could be loose soil (overburden), clay and fractured sandstone. Thicknesses of the first and second layers under each Geophone are presented in the below table:

Geophone Number	1	2	3	4	5	6	7	8	9	10	11	12	13	14	15	16	17	18	19	20	21	22	23	24
Thickness of first layer	20.99	20.04	17.52	16.21	14.06	15.69	14.54	13.2	13.36	10.78	9.89	8.46	9.81	11.75	11.82	13.59	18.64	17.72	14.56	14.62	14.95	13.03	9.3	0
Thickness of second layer	3.48	4.1	4.2	4.56	6.17	10.17	15.89	22.69	29.6	35.33	39.14	41.08	42.04	42.09	41.83	41.75	39.13	34.54	30.94	27.71	23.46	18.77	15.9	5.78

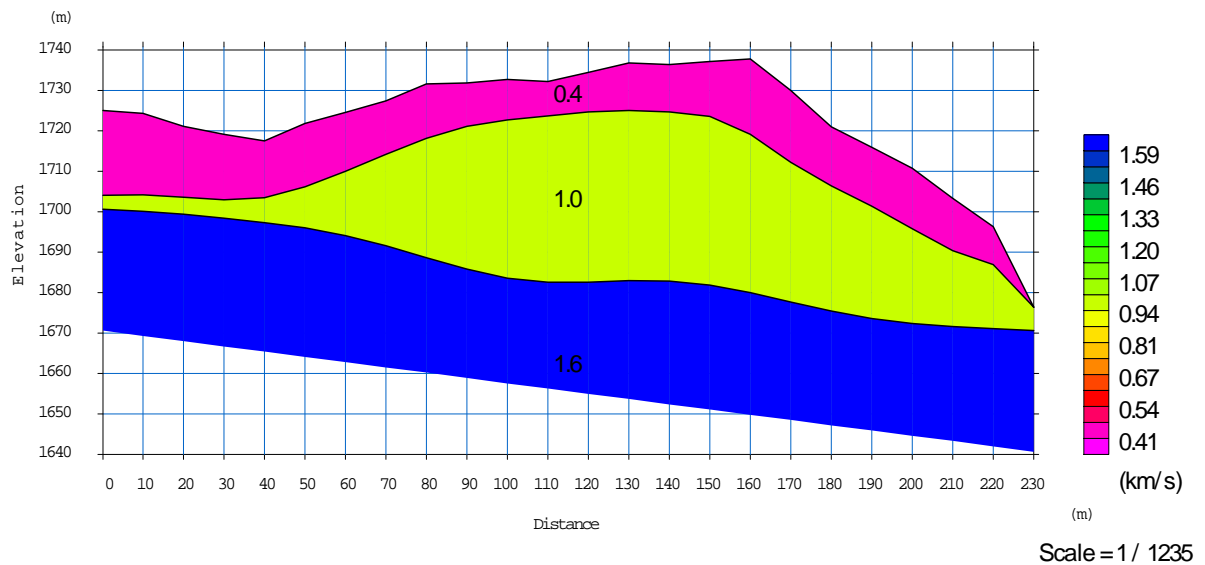


Fig. 36: Obtained velocity model affected by topography in the profile B of line 1 with detection of layer margins

3.3. LINE 1 POROFILE C

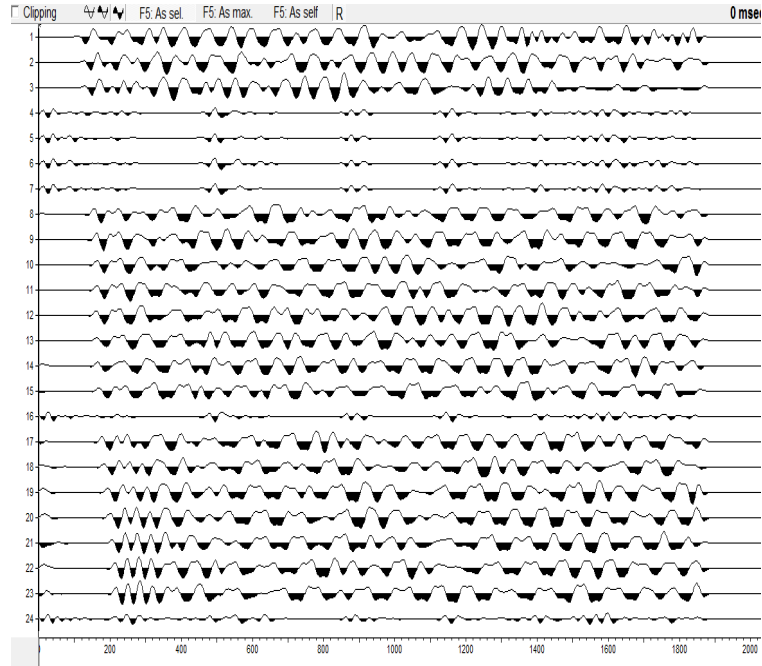


Fig. 37: Shot is located at 70 meters before the first geophone in the profile C of line 1

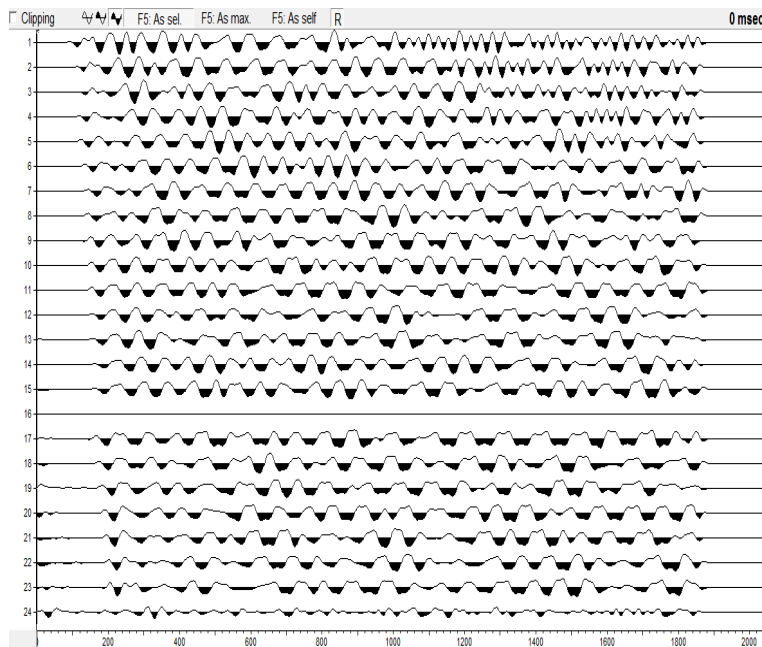


Fig. 38: Shot is located at 50 meters before the first geophone in the profile C of line 1

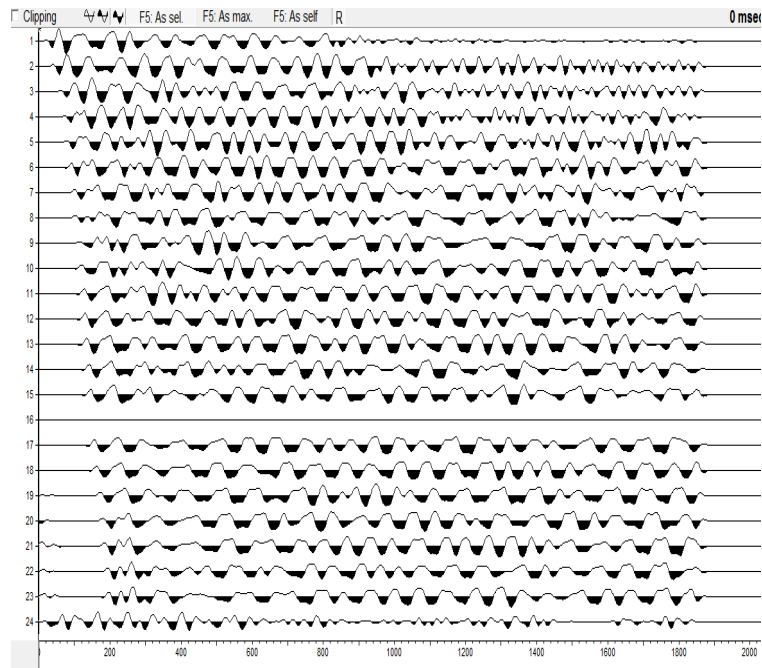


Fig. 39: Shot is located at 10 meters before the first geophone in the profile C of line 1

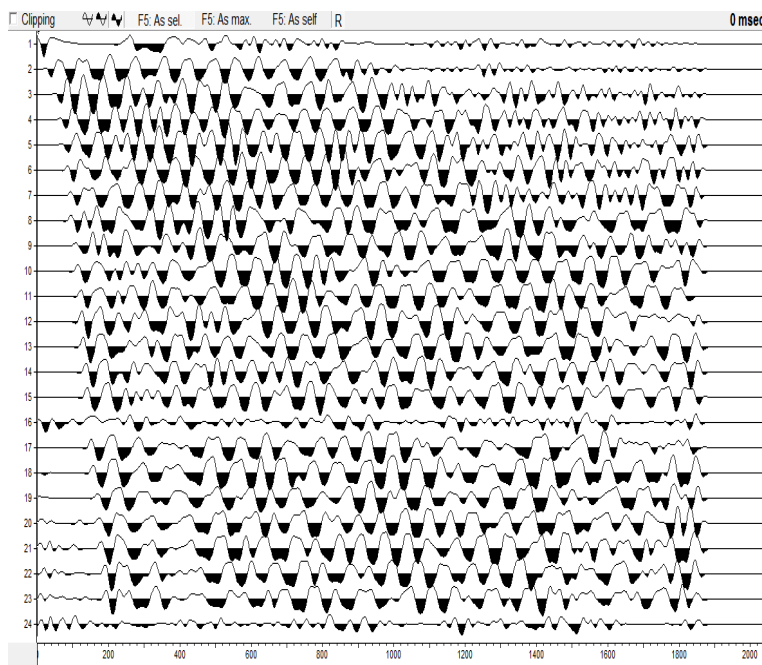


Fig. 40: Shot is located at 1 meter before the first geophone in the profile C of line 1

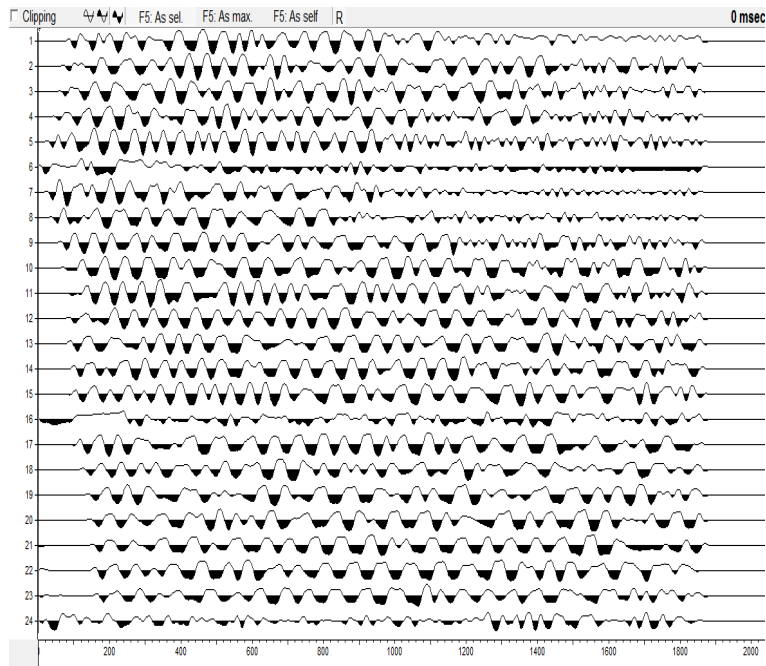


Fig. 41: Shot is located at 51 meters after the first geophone in the profile C of line 1

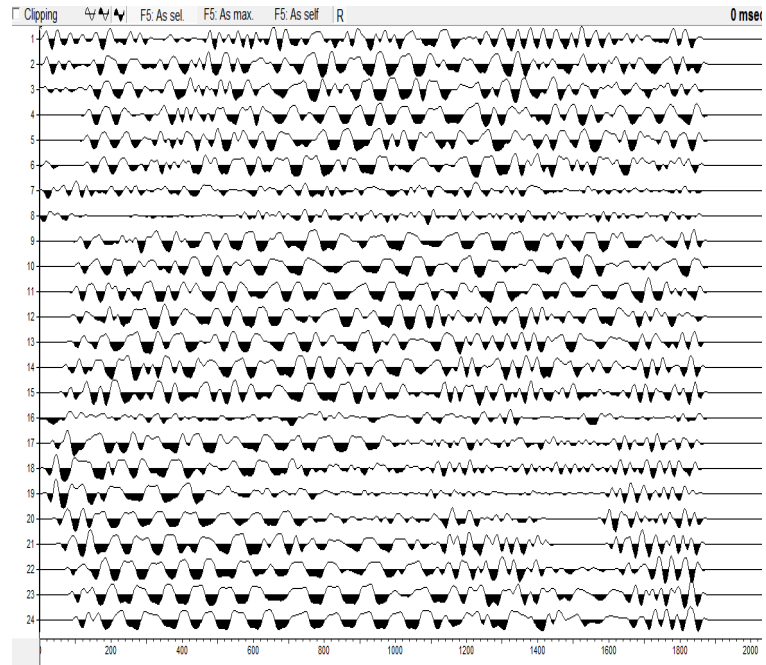


Fig. 42: Shot is located at 175 meters after the first geophone in the profile C of line 1

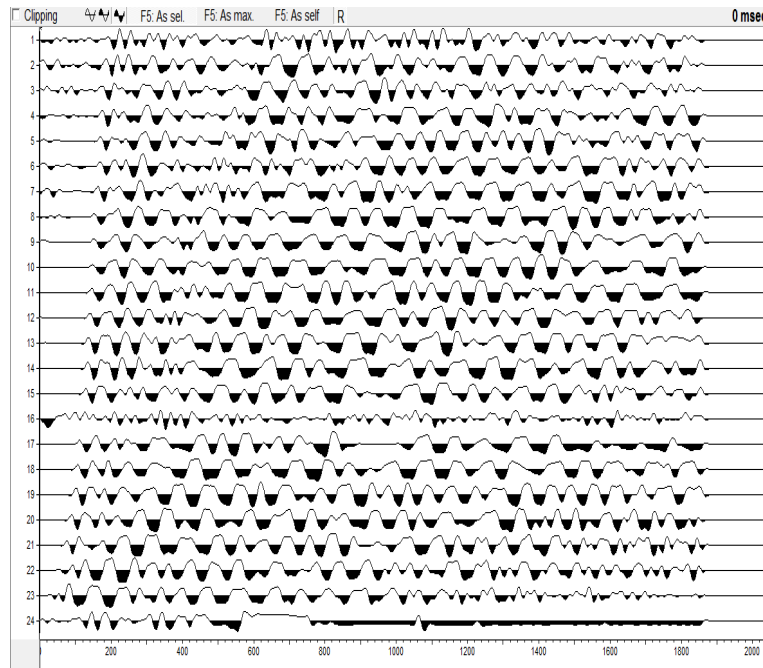


Fig. 43: Shot is located at 231 meters after the first geophone in the profile C of line 1

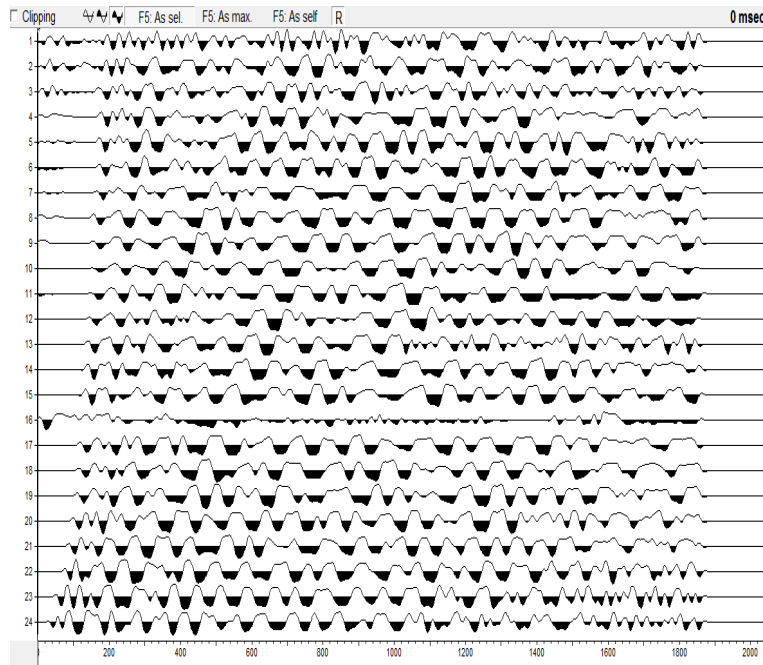


Fig. 44: Shot is located at 240 meters after the first geophone in the profile C of line 1

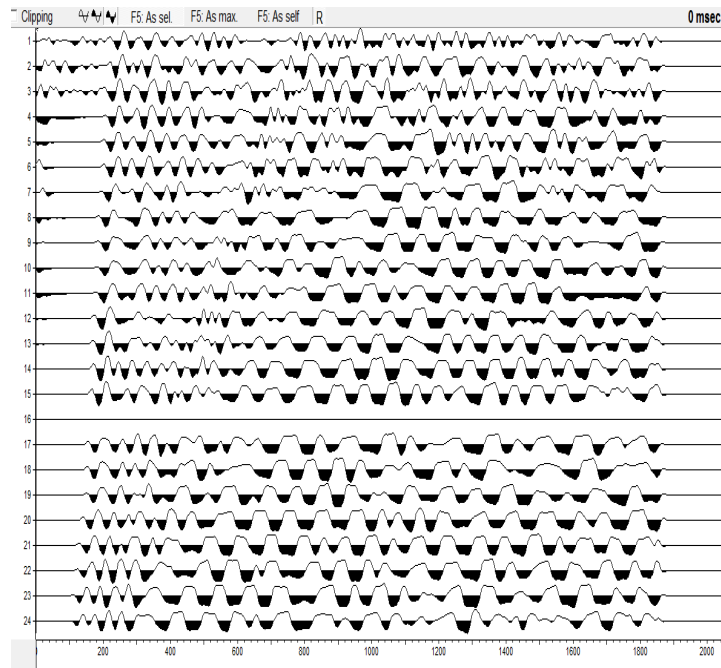


Fig. 45: Shot is located at 280 meters after the first geophone in the profile C of line 1

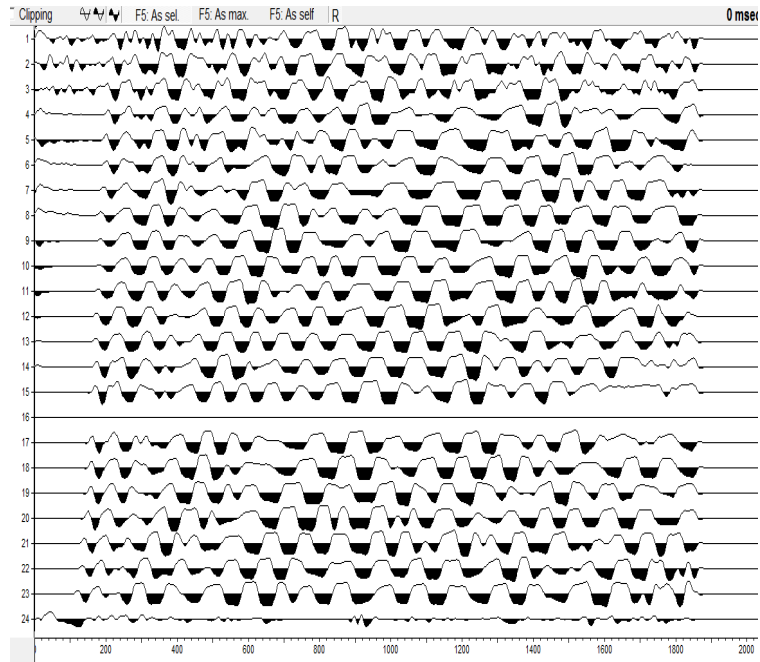


Fig. 46: Shot is located at 300 meters after the first geophone in the profile C of line 1

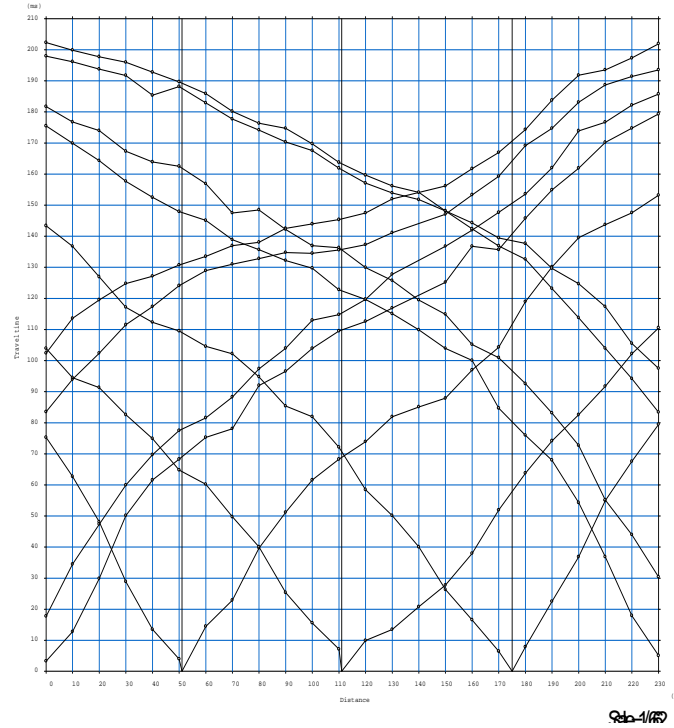


Fig. 47: Traveltime curves of 11 shots in the profile C of line 1

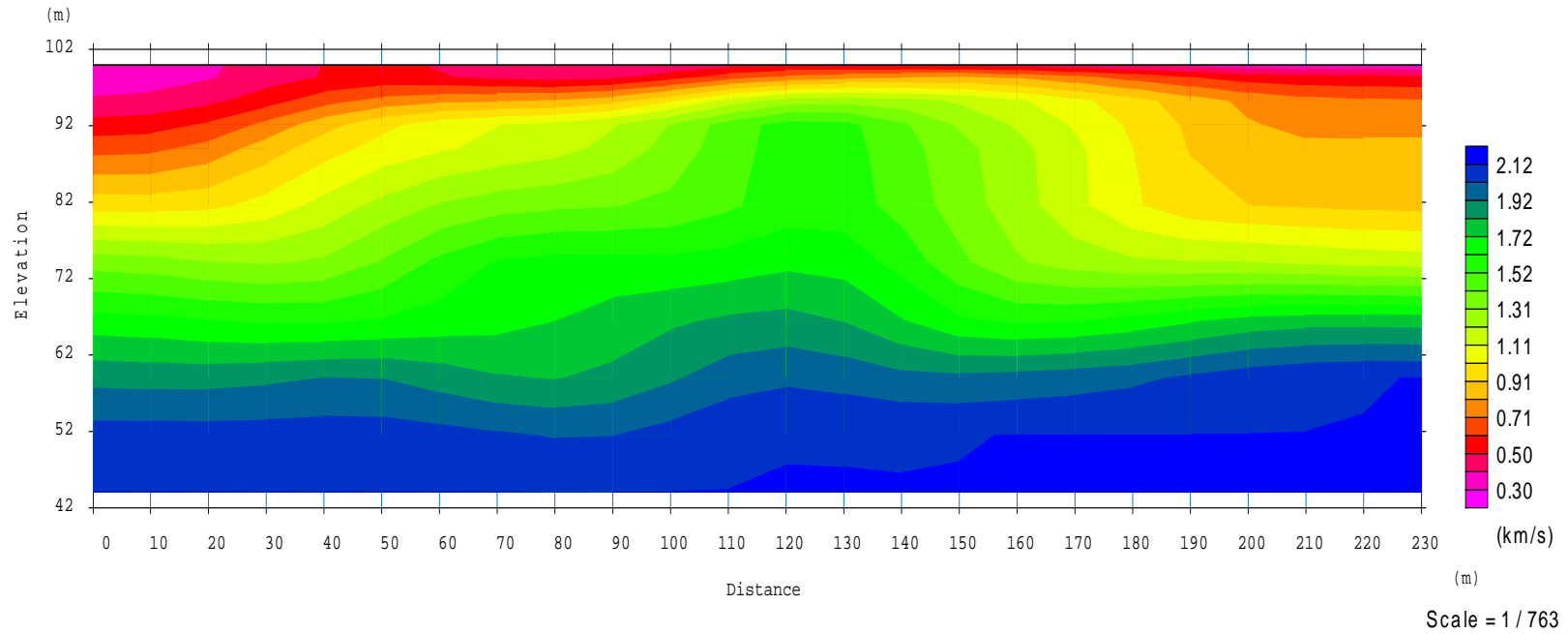


Fig. 48: Obtained velocity model not affected by topography in the profile C of line 1

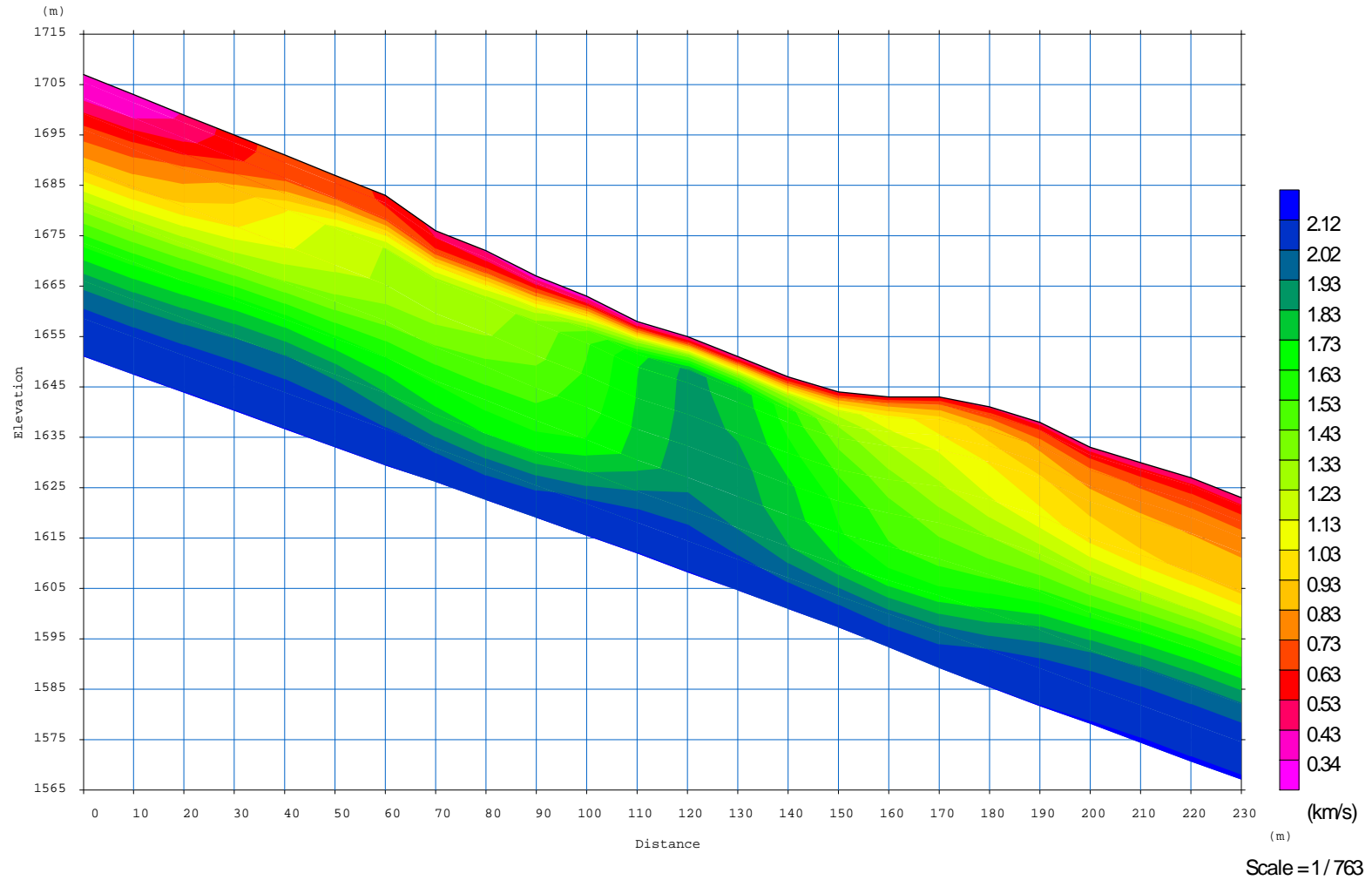


Fig. 49: Obtained velocity model affected by topography in the profile C of line 1

Along the profile C of line 1, three layers with different velocities were detected. These layers, from top to the bottom could be loose soil (overburden), clay and fractured sandstone. Thicknesses of the first and second layers under each Geophone are presented in the below table:

Geophone Number	1	2	3	4	5	6	7	8	9	10	11	12	13	14	15	16	17	18	19	20	21	22	23	24
Thickness of first layer	7.71	7.41	7.29	7.24	6.92	6.49	7	5.33	6.33	5.81	5.59	3.42	3	2.03	0.93	0.34	1	2.78	3.52	4.28	3.41	3.58	2.78	0.51
Thickness of second layer	6.99	7.16	7.51	8.16	9.33	10.68	11.06	10.65	10.8	11.89	14.07	17.3	20.33	21.9	22.36	22.35	22.83	23.6	23.99	23.55	22.3	21.24	20.49	19.96

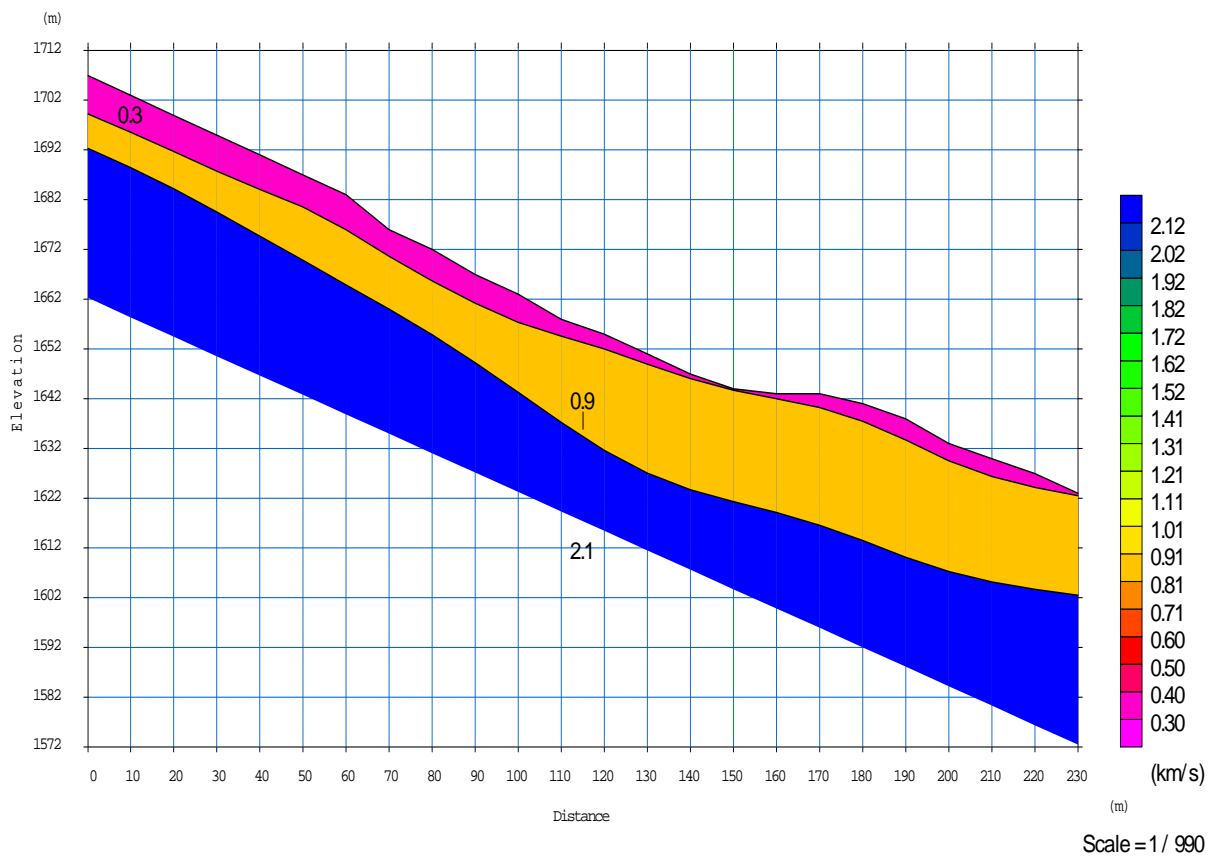


Fig. 50: Obtained velocity model affected by topography in the profile C of line 1 with detection of layer margins

3.4. LINE 1 POROFILE D

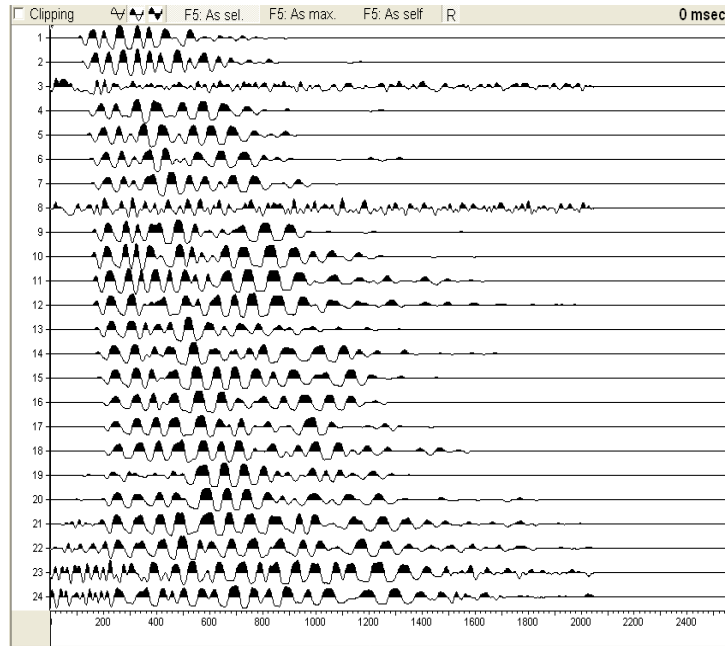


Fig. 51: Shot is located at 70 meters before the first geophone in the profile D of line 1

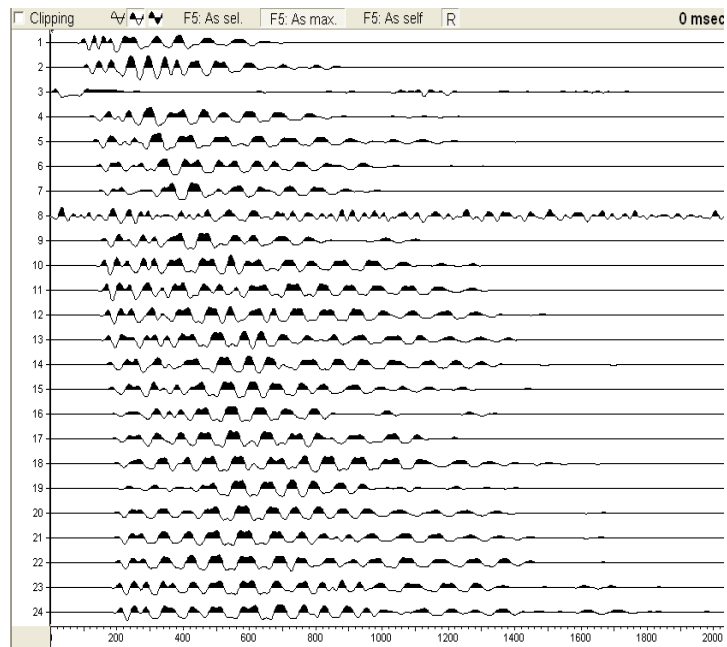


Fig. 52: Shot is located at 50 meters before the first geophone in the profile D of line 1

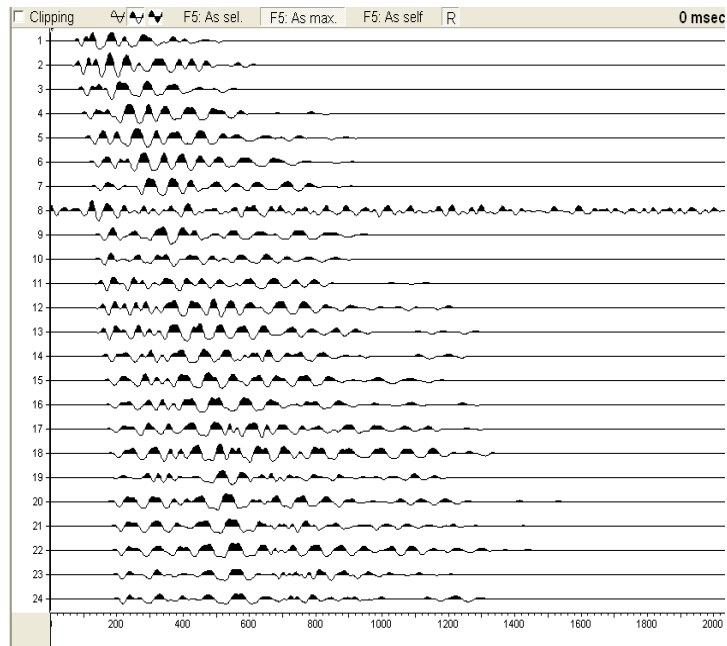


Fig. 53: Shot is located at 30 meters before the first geophone in the profile D of line 1

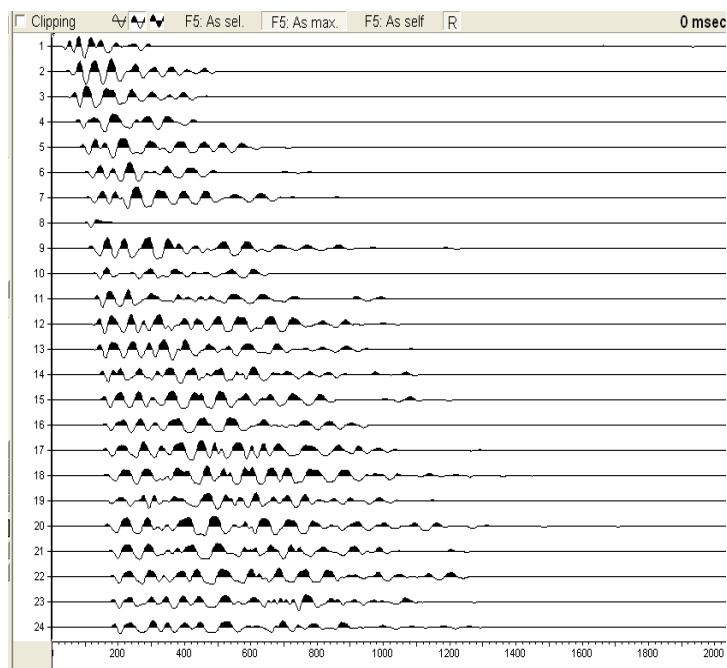


Fig. 54: Shot is located at 10 meters before the first geophone in the profile D of line 1

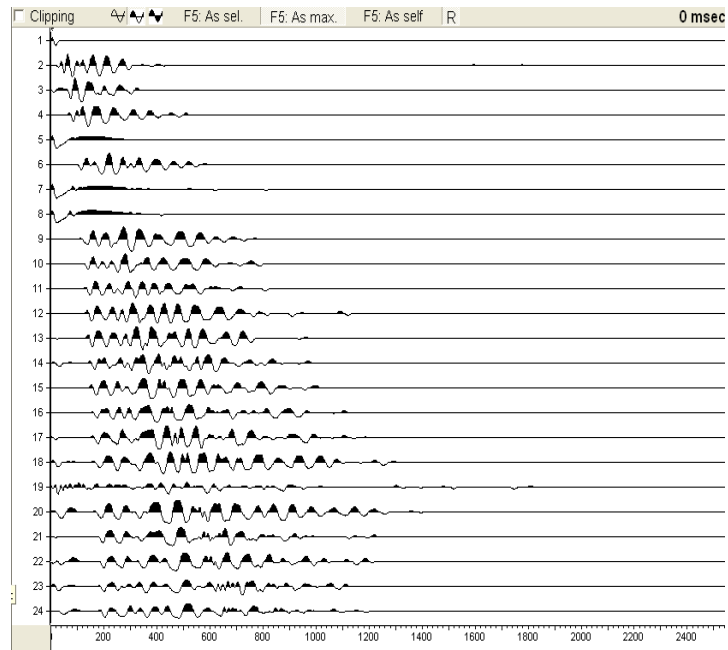


Fig. 55: Shot is located at 1 meter before the first geophone in the profile D of line 1

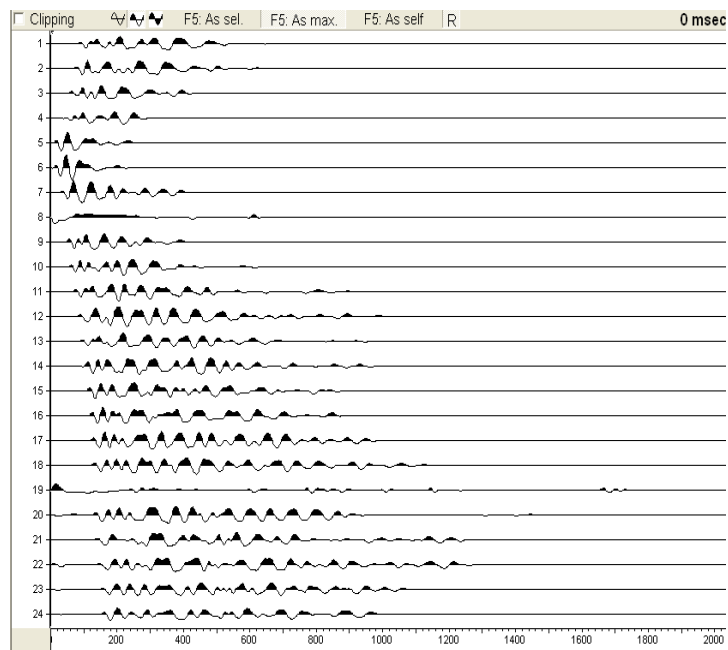


Fig. 56: Shot is located at 55 meters after the first geophone in the profile D of line 1

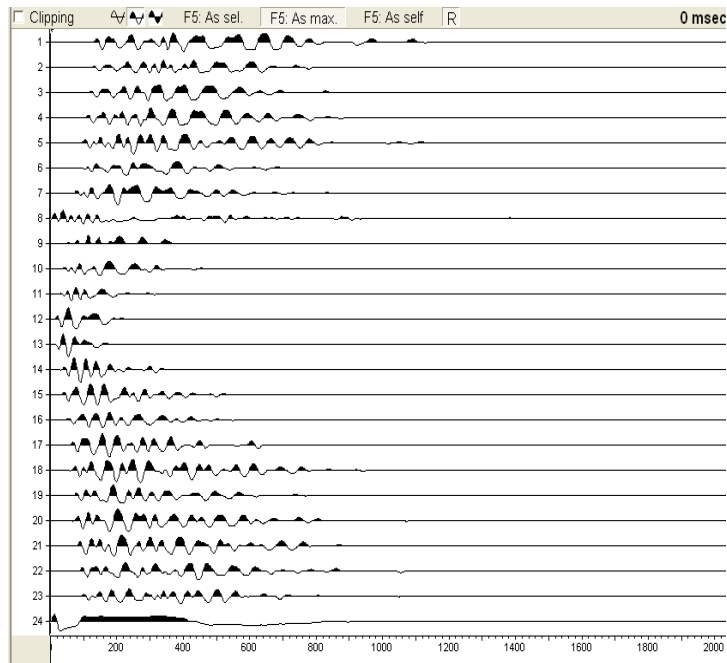


Fig. 57: Shot is located at 115 meters after the first geophone in the profile D of line 1

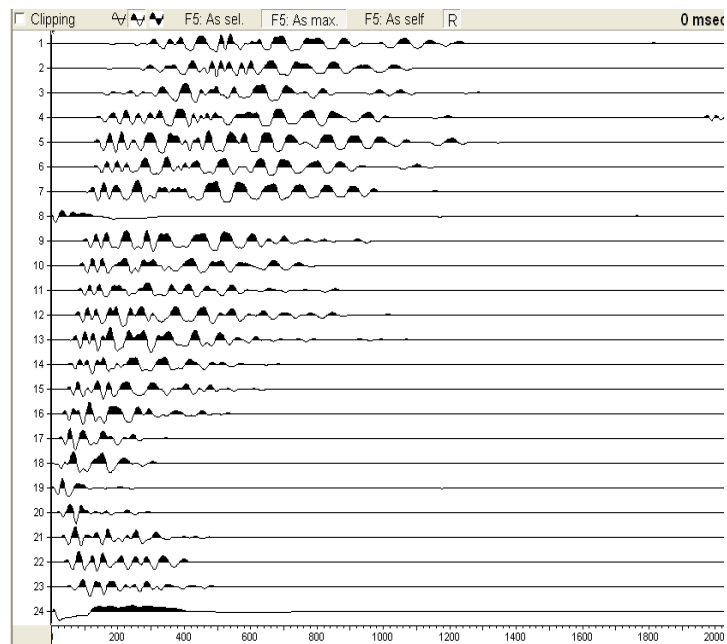


Fig. 58: Shot is located at 175 meters after the first geophone in the profile D of line 1

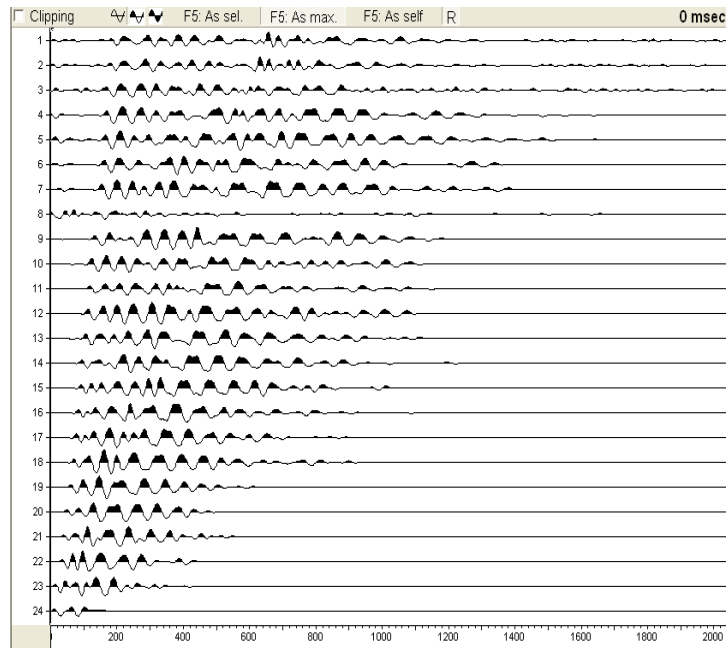


Fig. 59: Shot is located at 231 meters after the first geophone in the profile D of line 1

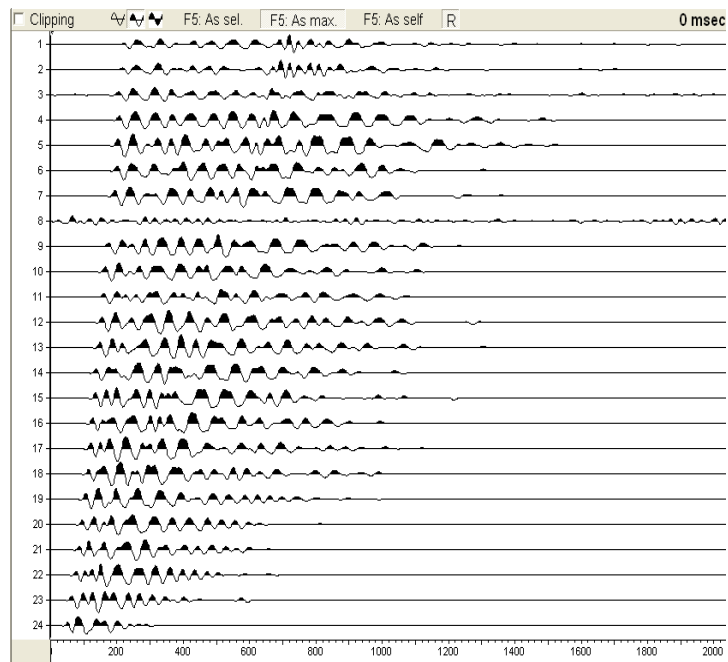


Fig. 60: Shot is located at 240 meters after the first geophone in the profile D of line 1

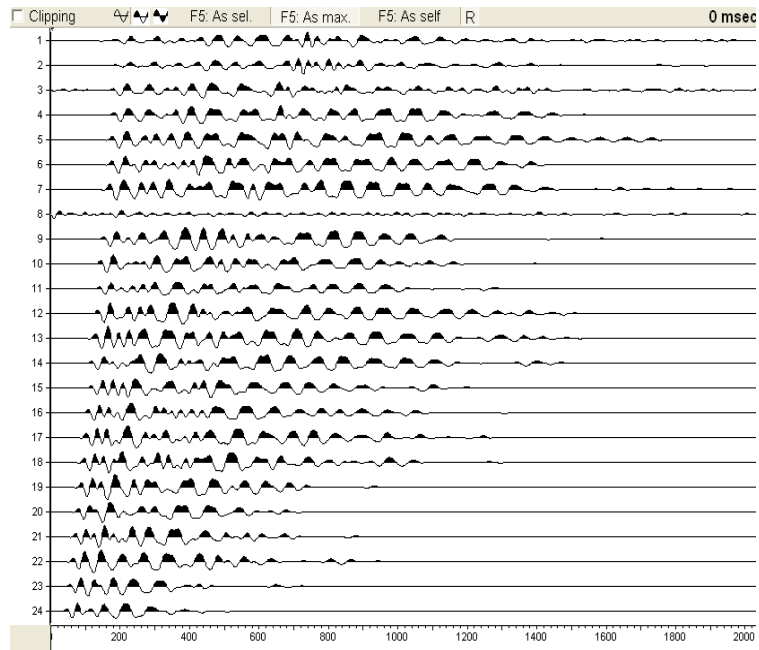


Fig. 61: Shot is located at 260 meters after the first geophone in the profile D of line 1

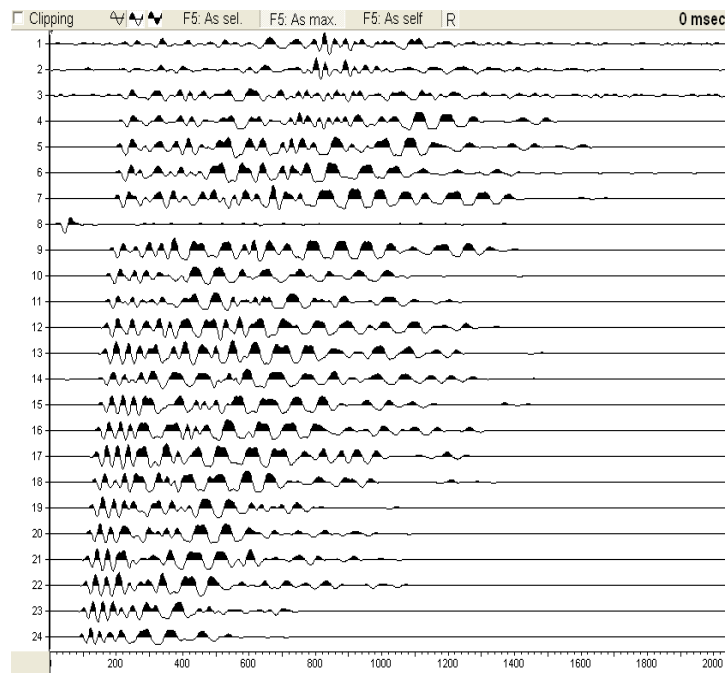


Fig. 62: Shot is located at 280 meters after the first geophone in the profile D of line 1

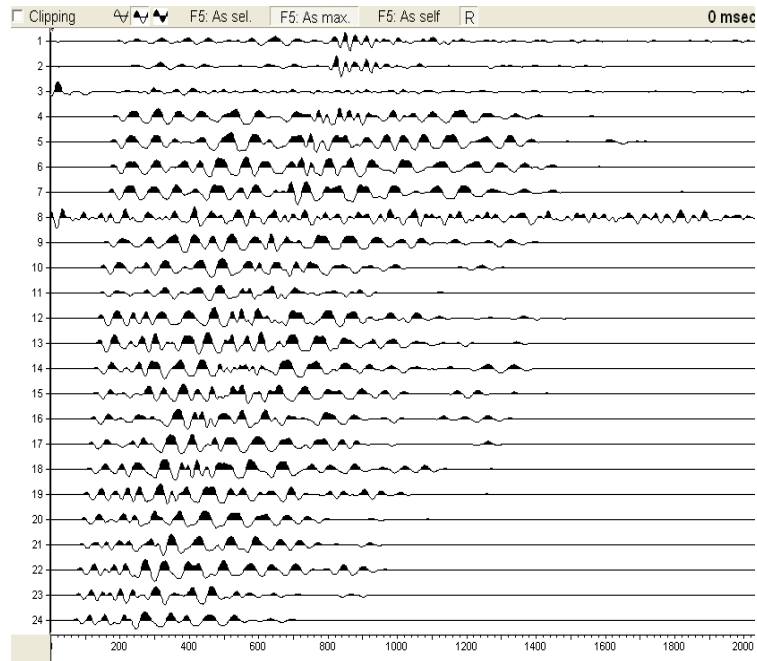


Fig. 63: Shot is located at 300 meters after the first geophone in the profile D of line 1

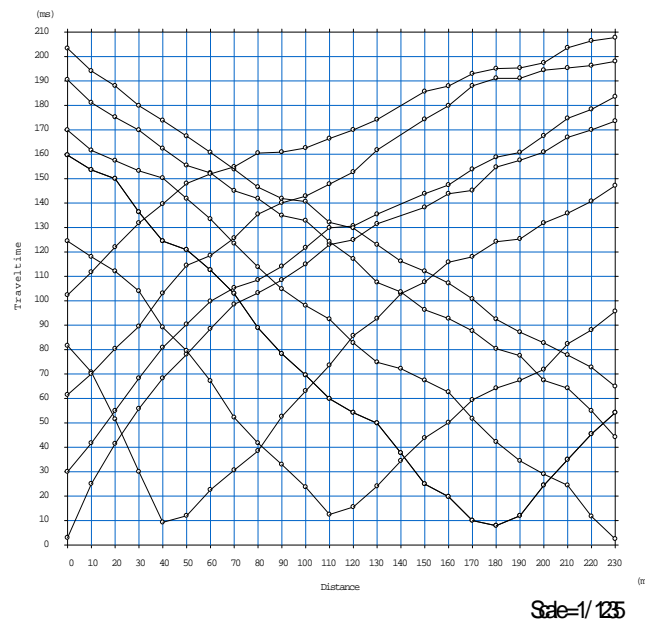


Fig. 64: Travel time curves of 10 shots in the profile D of line 1

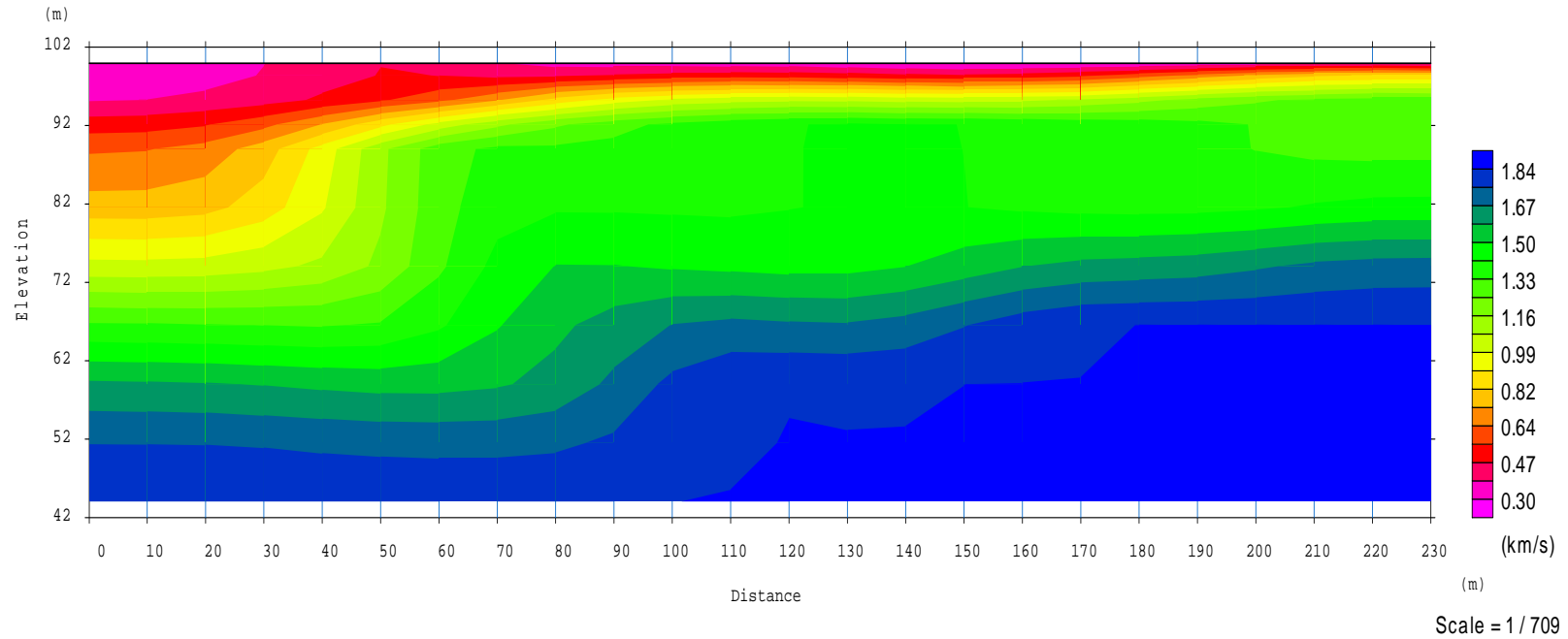


Fig. 65: Obtained velocity model not affected by topography in the profile D of line 1

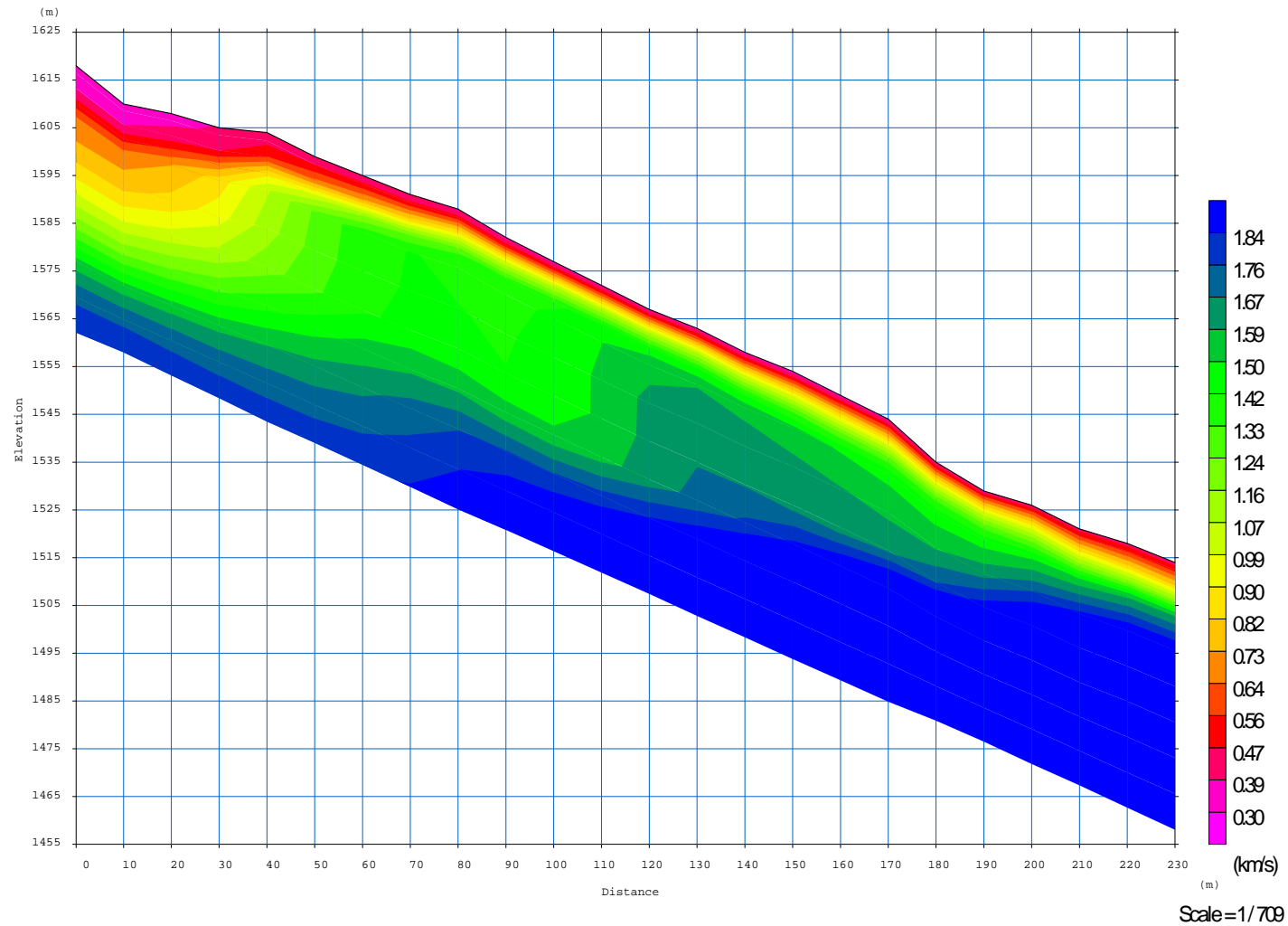


Fig. 66: Obtained velocity model affected by topography in the profile D of line 1

Along the profile D of line 1, three layers with different velocities were detected. These layers, from top to the bottom could be loose soil (overburden), clay and fractured sandstone. Thicknesses of the first and second layers under each Geophone are presented in the below table:

Geophone Number	1	2	3	4	5	6	7	8	9	10	11	12	13	14	15	16	17	18	19	20	21	22	23	24
Thickness of first layer	9.56	6.59	7.86	7.01	8.27	6.35	4.92	3.15	3.9	3.08	3.22	3.44	3.17	3.42	2.94	3.23	2.4	2.99	0.75	1.35	5.34	6.36	6.55	4.35
Thickness of second layer	28.9	26.7	26.27	27.41	29.23	30.79	32.91	35.1	35.44	34.15	32.94	31.88	31.71	32.59	33.6	34.65	34.89	32.21	26.79	20.42	13.26	7.08	3.83	2.02

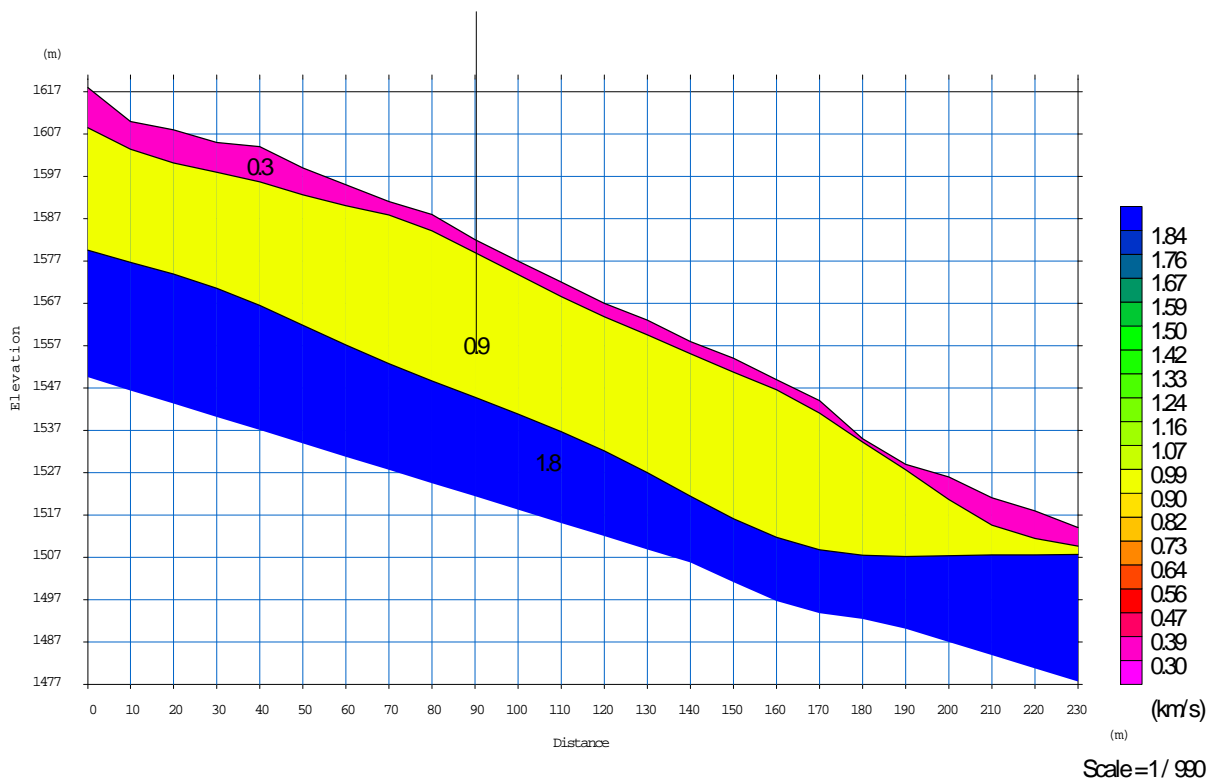


Fig. 67: Obtained velocity model affected by topography in the profile D of line 1 with detection of layer margins

3.5. LINE 1 POROFILE E

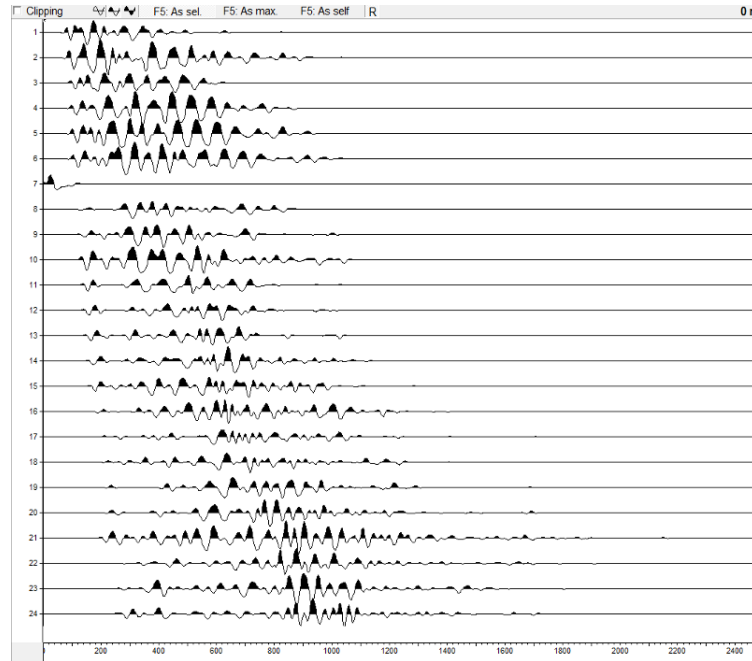


Fig. 68: Shot is located at 70 meters before the first geophone in the profile E of line

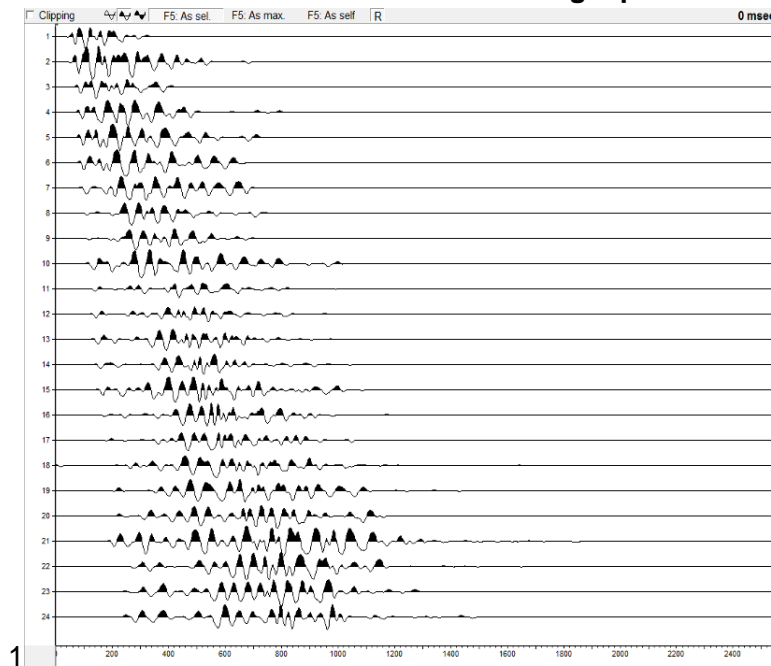


Fig. 69: Shot is located at 40 meters before the first geophone in the profile E of line 1

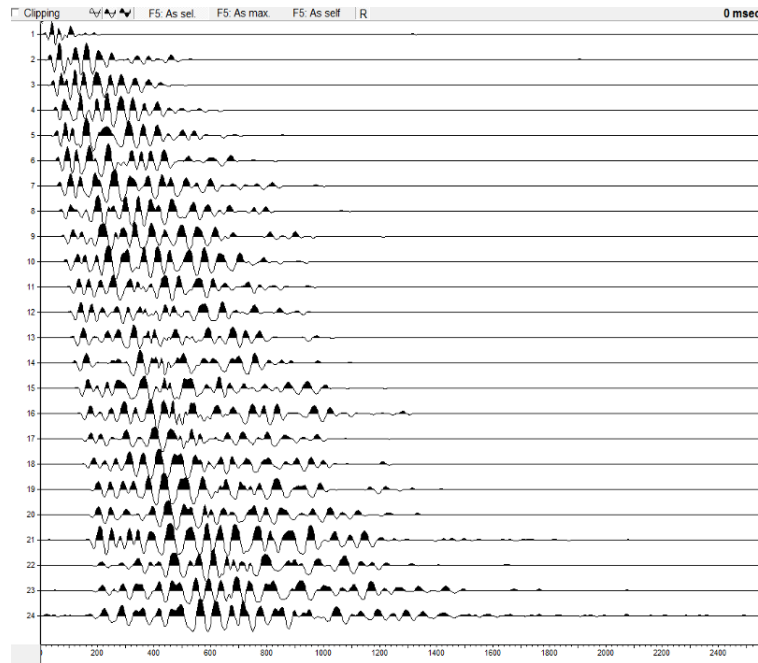


Fig. 70: Shot is located at 10 meters before the first geophone in the profile E of line 1

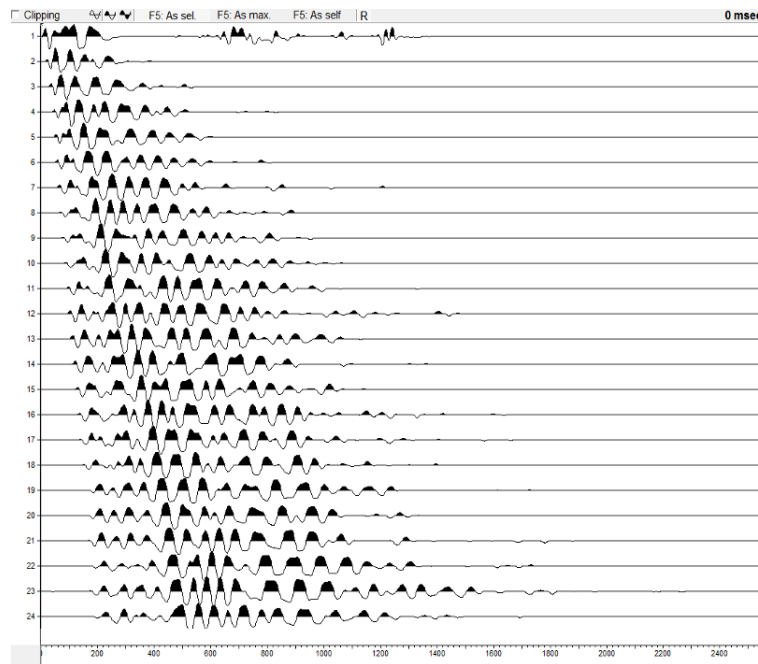


Fig. 71: Shot is located at 1 meter before the first geophone in the profile E of line 1

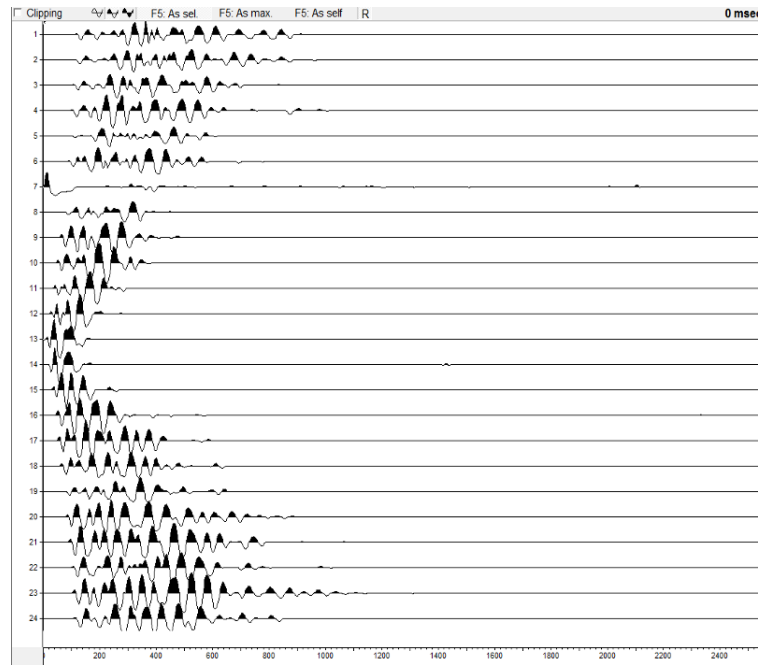


Fig. 72: Shot is located at 125 meters after the first geophone in the profile E of line 1

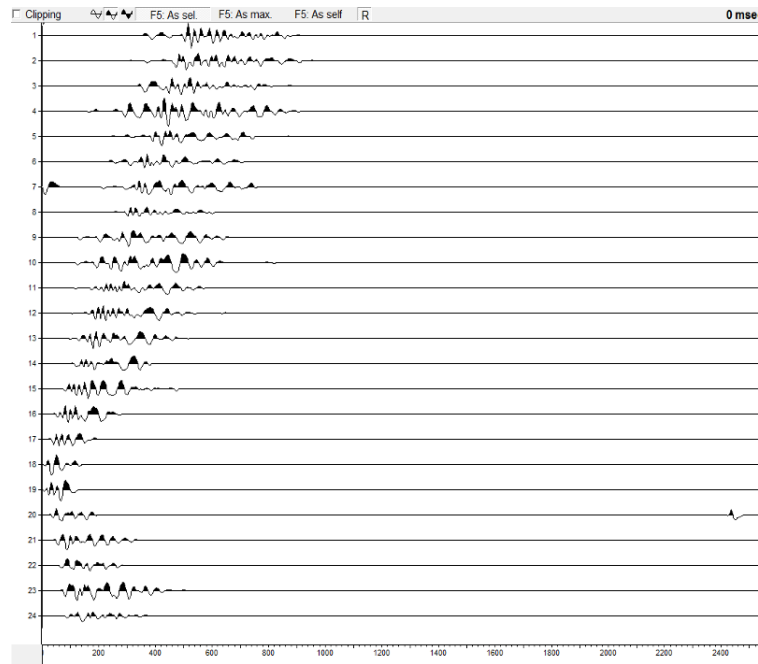


Fig. 73: Shot is located at 175 meters after the first geophone in the profile E of line 1

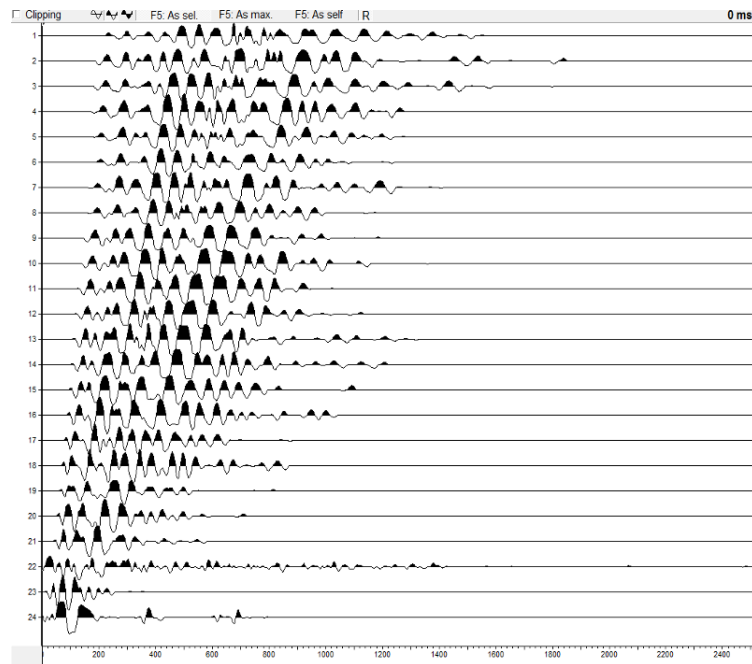


Fig. 74: Shot is located at 231 meters after the first geophone in the profile E of line 1

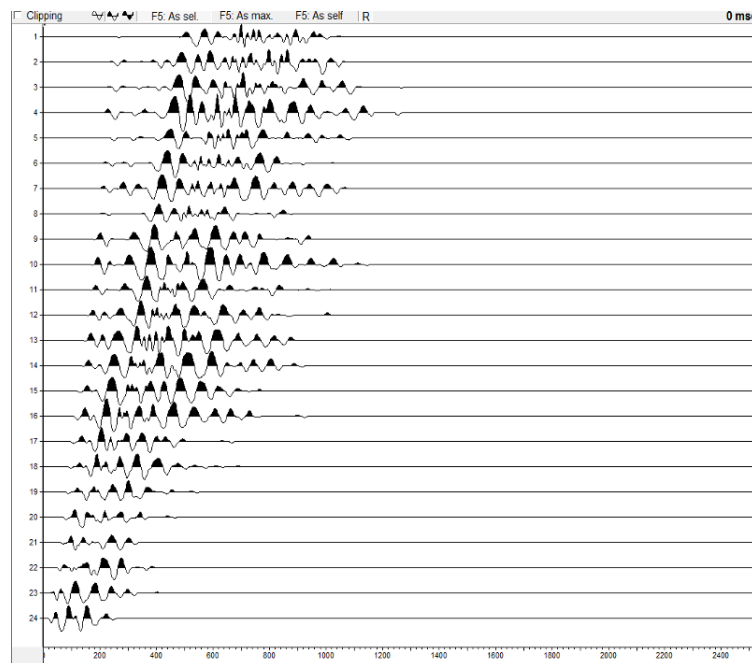


Fig. 75: Shot is located at 240 meters after the first geophone in the profile E of line 1

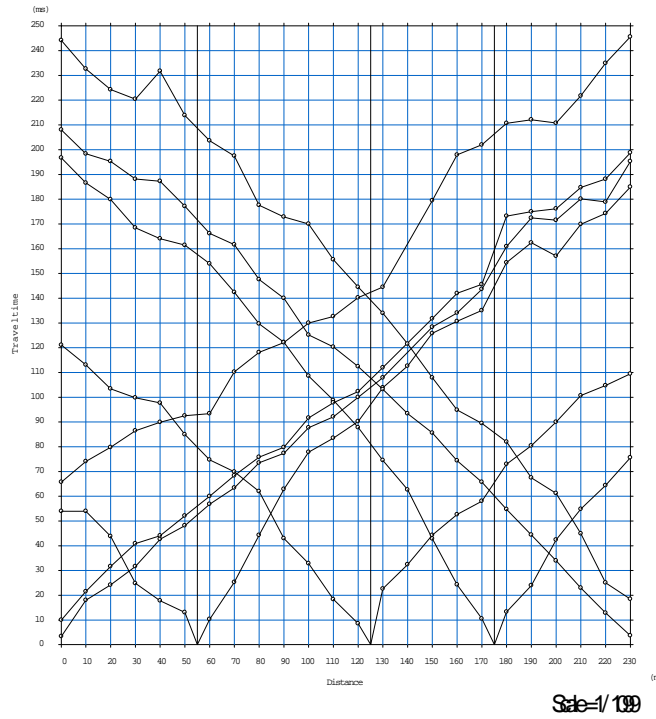


Fig. 76: Travel time curves of 8 shots in the profile E of line 1

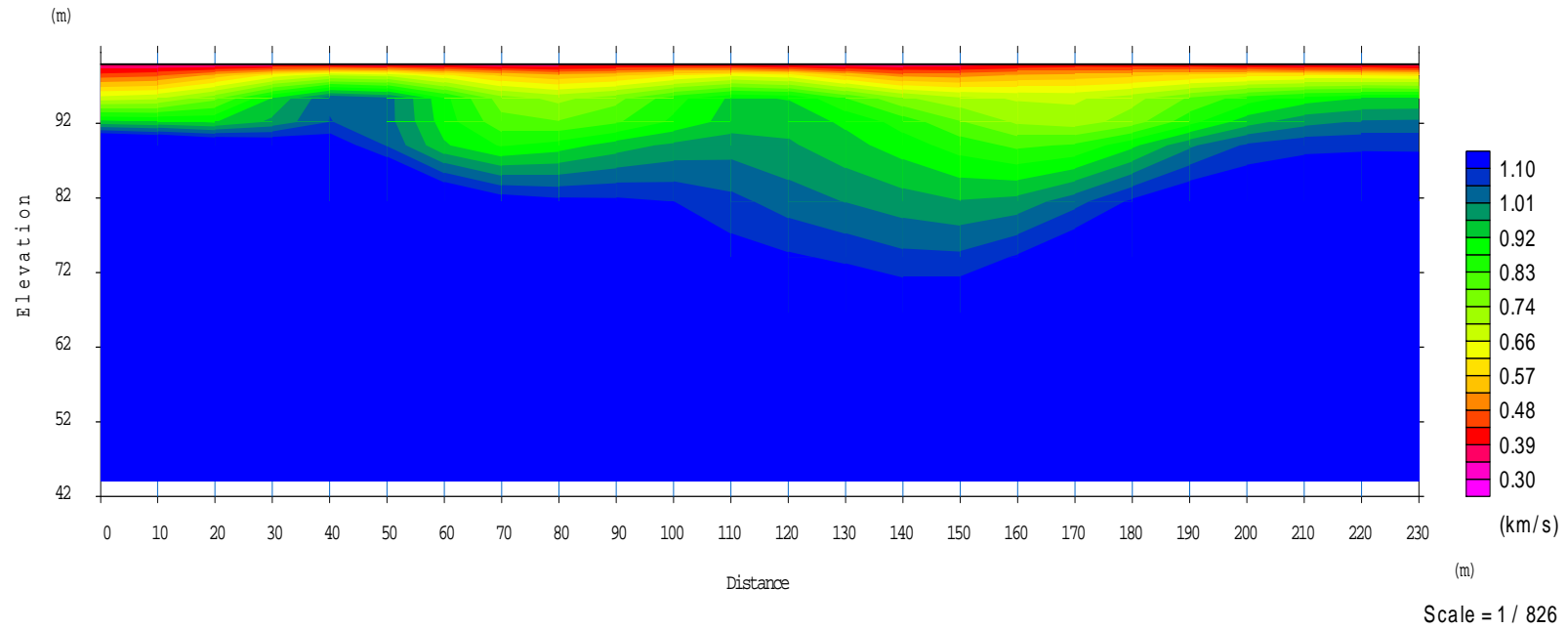


Fig. 77: Obtained velocity model not affected by topography in the profile E of line 1

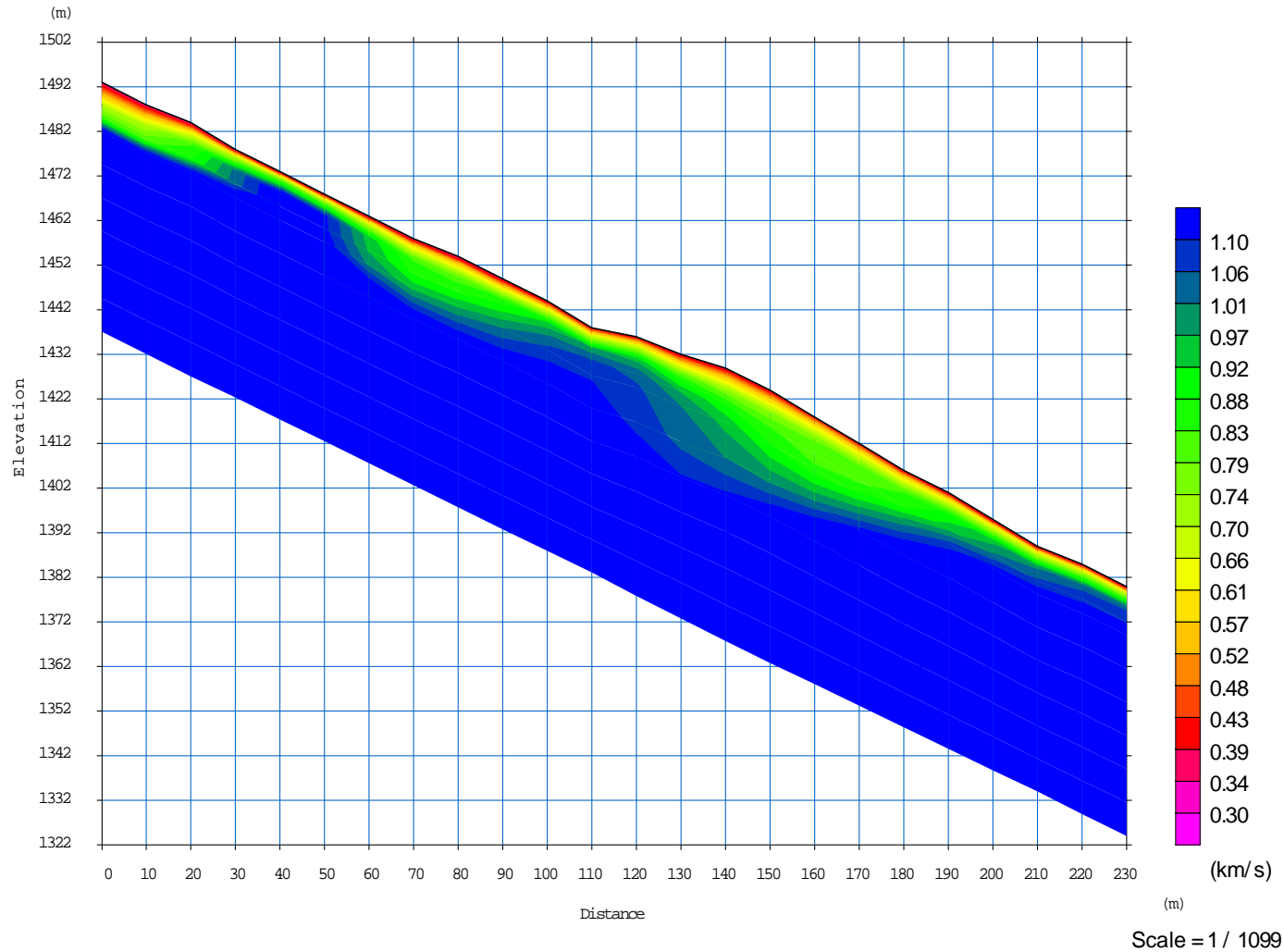


Fig. 78: Obtained velocity model affected by topography in the profile E of line 1

Along the profile E of line 1, three layers with different velocities were detected. These layers, from top to the bottom could be loose soil (overburden), clay and combination of clay with highly fractured sandstone. Thicknesses of the first and second layers under each Geophone are presented in the below table:

Geophone Number	1	2	3	4	5	6	7	8	9	10	11	12	13	14	15	16	17	18	19	20	21	22	23	24
Thickness of first layer	2.8	1.49	1.11	0	0	0	0	0	0	0.46	0.9	0	2.9	3.85	3.83	1.89	0	0	0	0	0.47	0	0	0
Thickness of second layer	0.36	4.93	10.95	16.03	19.72	20.98	19.7	16.85	14.6	11.1	7.85	5.16	3.27	2.49	5.07	8.56	11.05	10.63	8.72	6.75	2.93	0	0	0

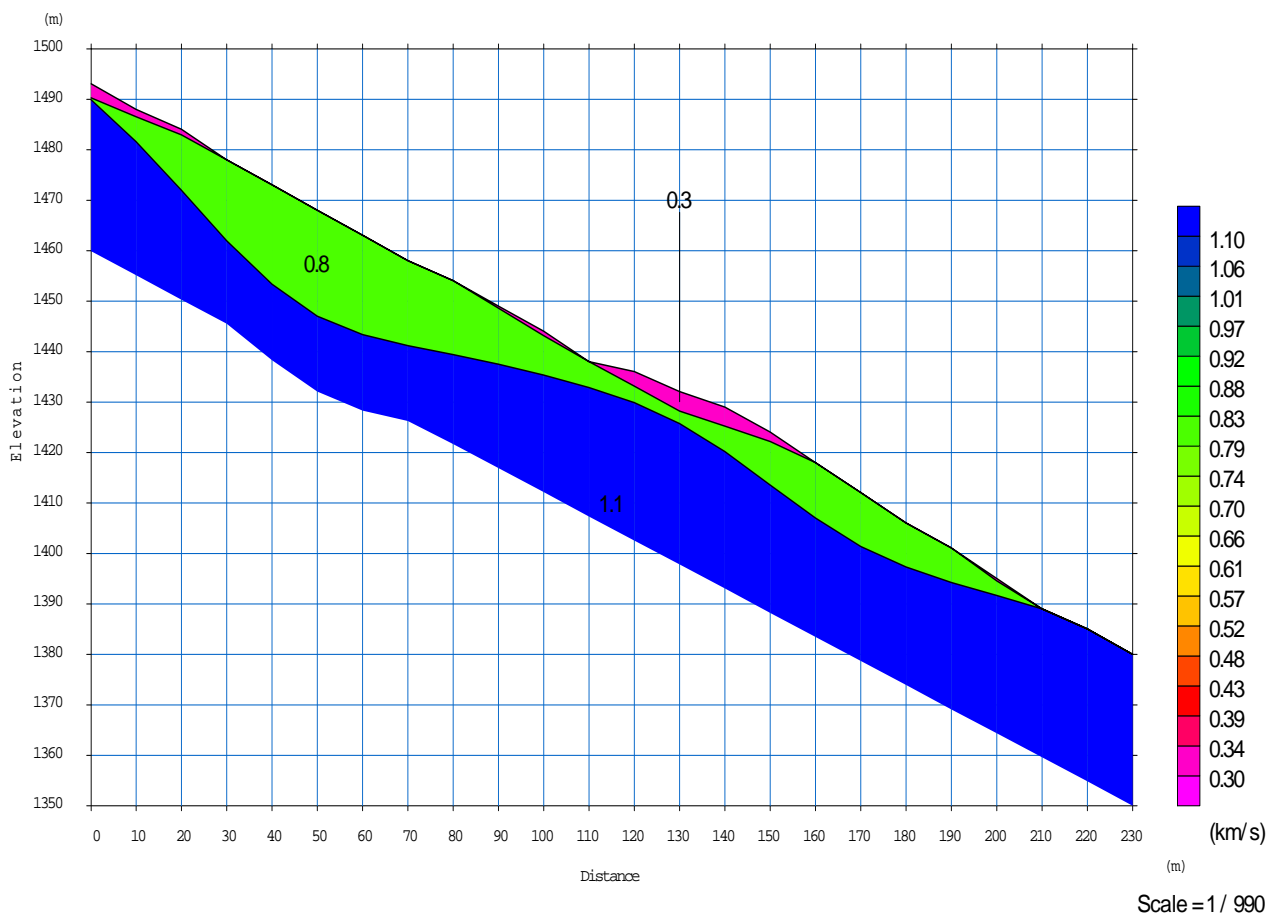


Fig. 79: Obtained velocity model affected by topography in the profile E of line 1 with detection of layer margins

3.6. LINE 1 POROFILE F

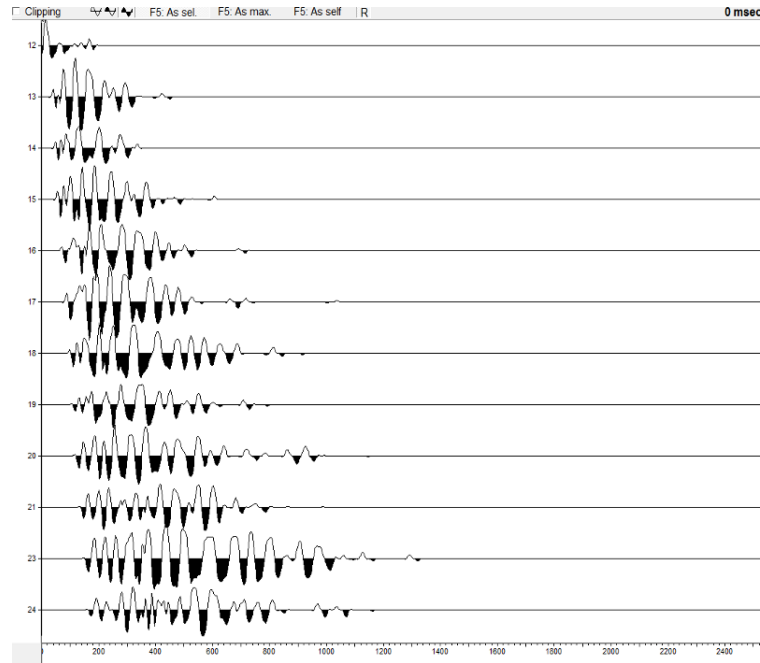


Fig. 80: Shot is located at 22 meters before the 12th geophone in the profile F of line 1

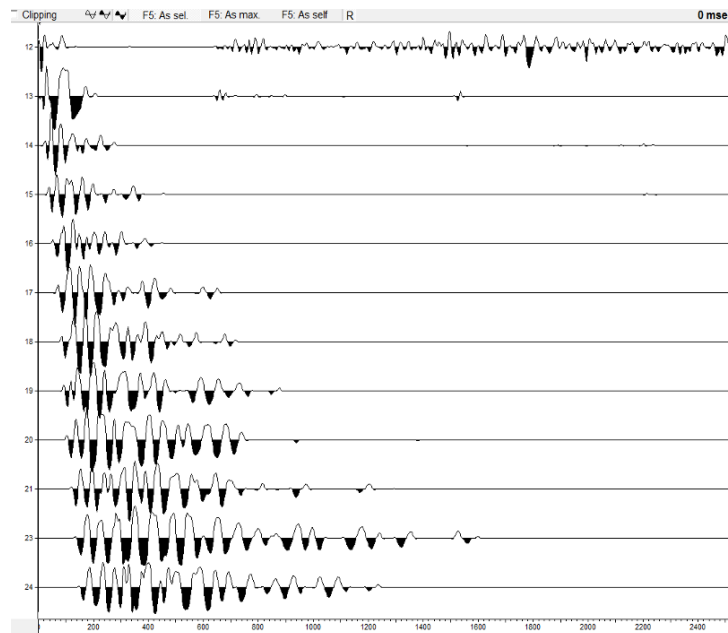


Fig. 81: Shot is located at 1 meter before the 12th geophone in the profile F of line 1

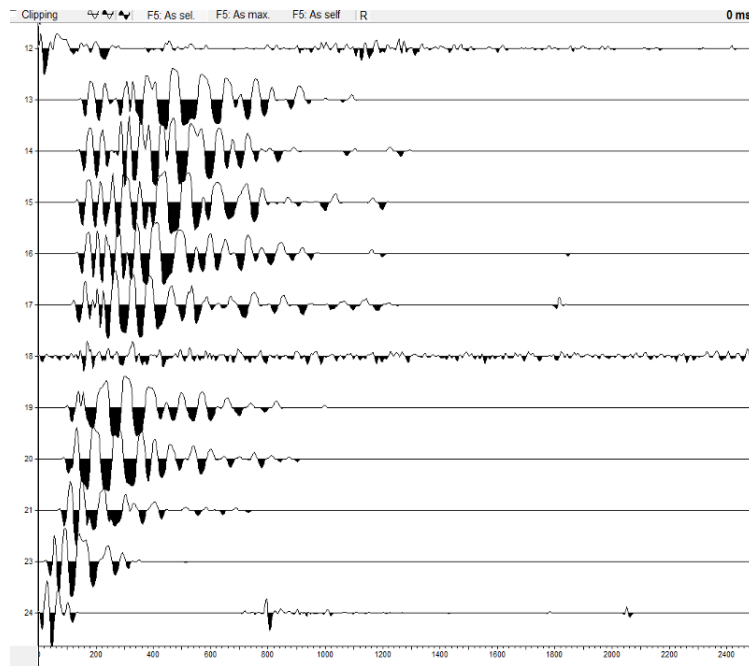


Fig. 82: Shot is located at 112 meters after the 12th geophone in the profile F of line 1

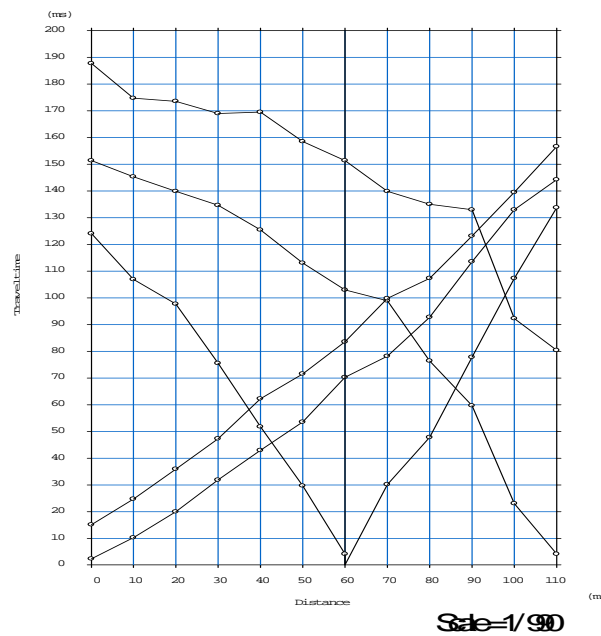


Fig. 83: Travel time curves of 5 shots in the profile F of line 1

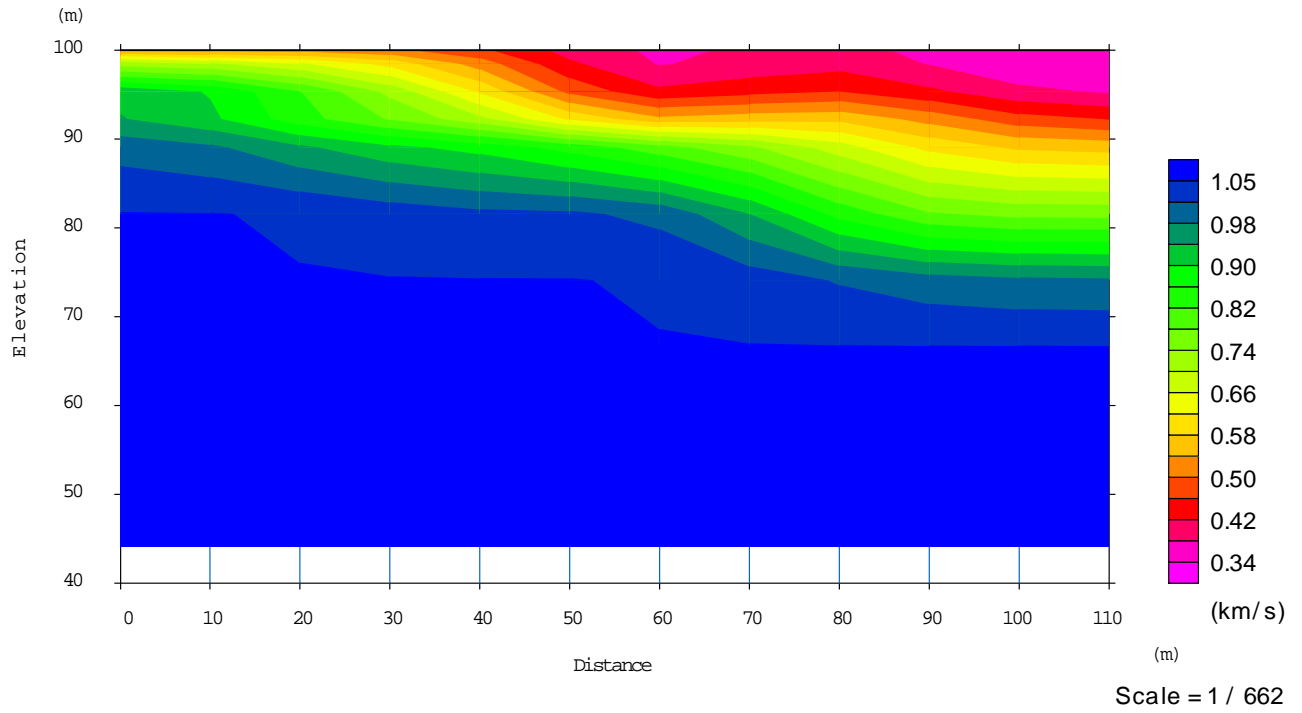


Fig. 84: Obtained velocity model not affected by topography in the profile F of line 1

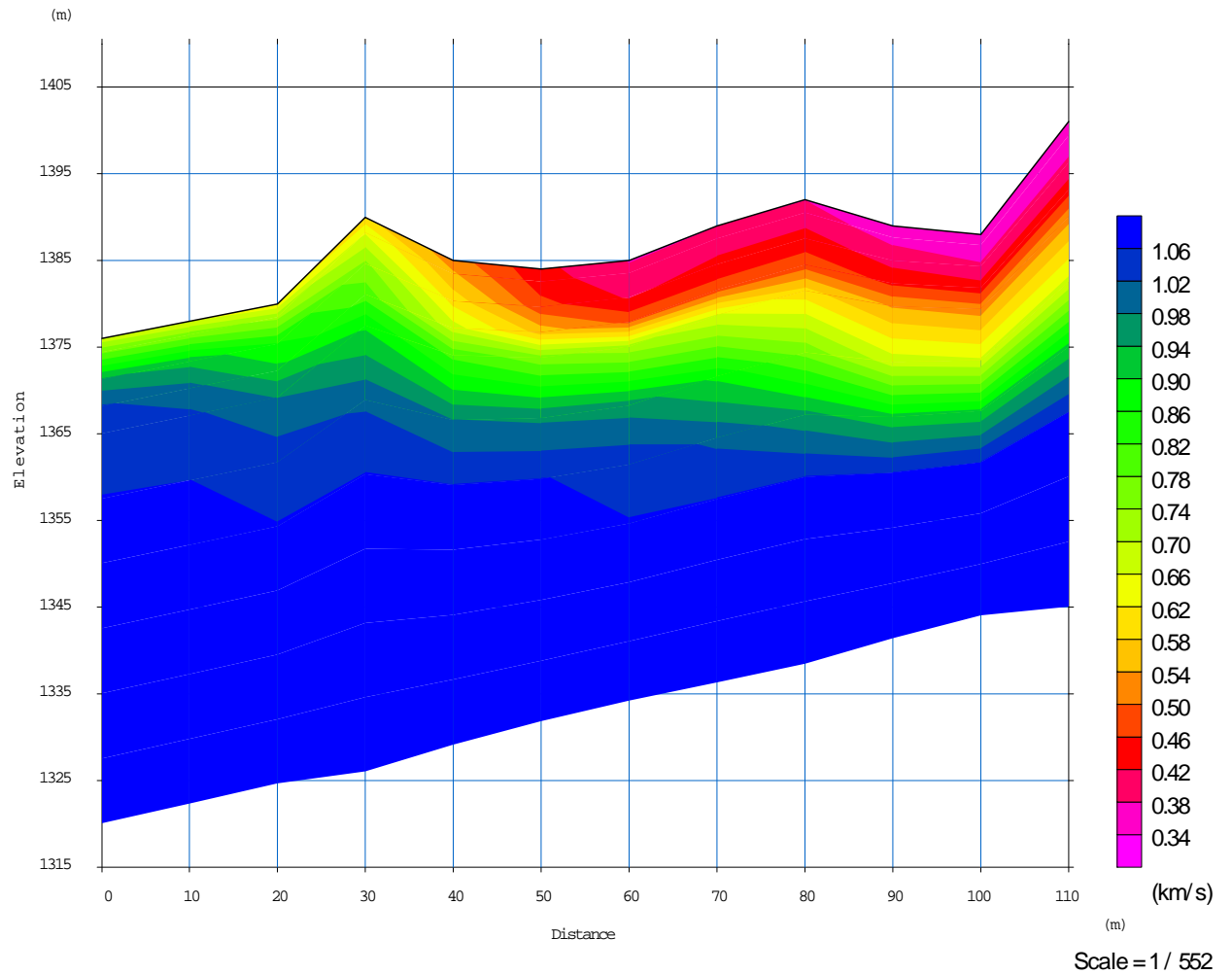


Fig. 85: Obtained velocity model affected by topography in the profile F of line 1

Along the profile F of line 1, three layers with different velocities were detected. These layers, from top to the bottom could be loose soil (overburden), clay and combination of

clay with highly fractured sandstone. Thicknesses of the first and second layers under each Geophone are presented in the below table:

Geophone Number	1	2	3	4	5	6	7	8	9	10	11	12
Thickness of first layer	15.1	10.37	2.81	6.48	0.3	0	0	0.78	2.31	0	0	9.81
Thickness of second layer	0	0.61	11.7	20.03	23.01	23.24	24.29	27.16	28.4	27.84	27.29	31.05

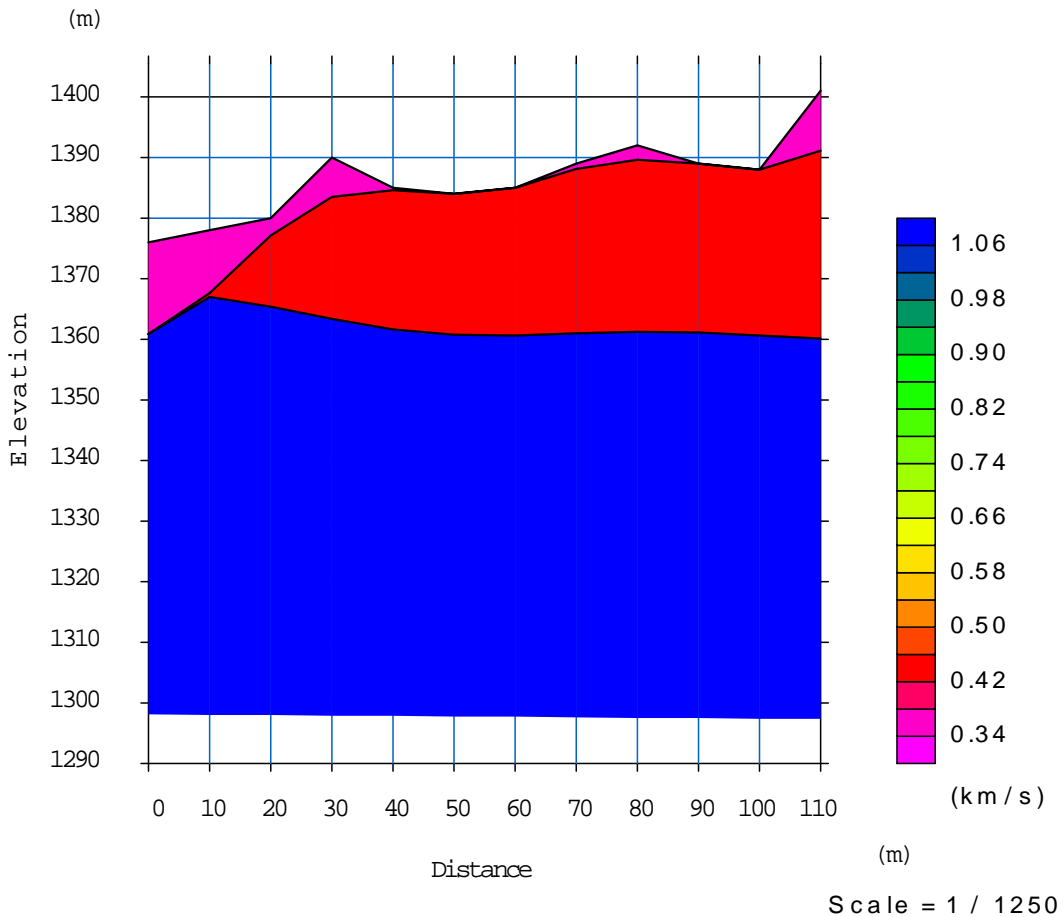


Fig. 86: Obtained velocity model affected by topography in the profile F of line 1 with detection of layer margins

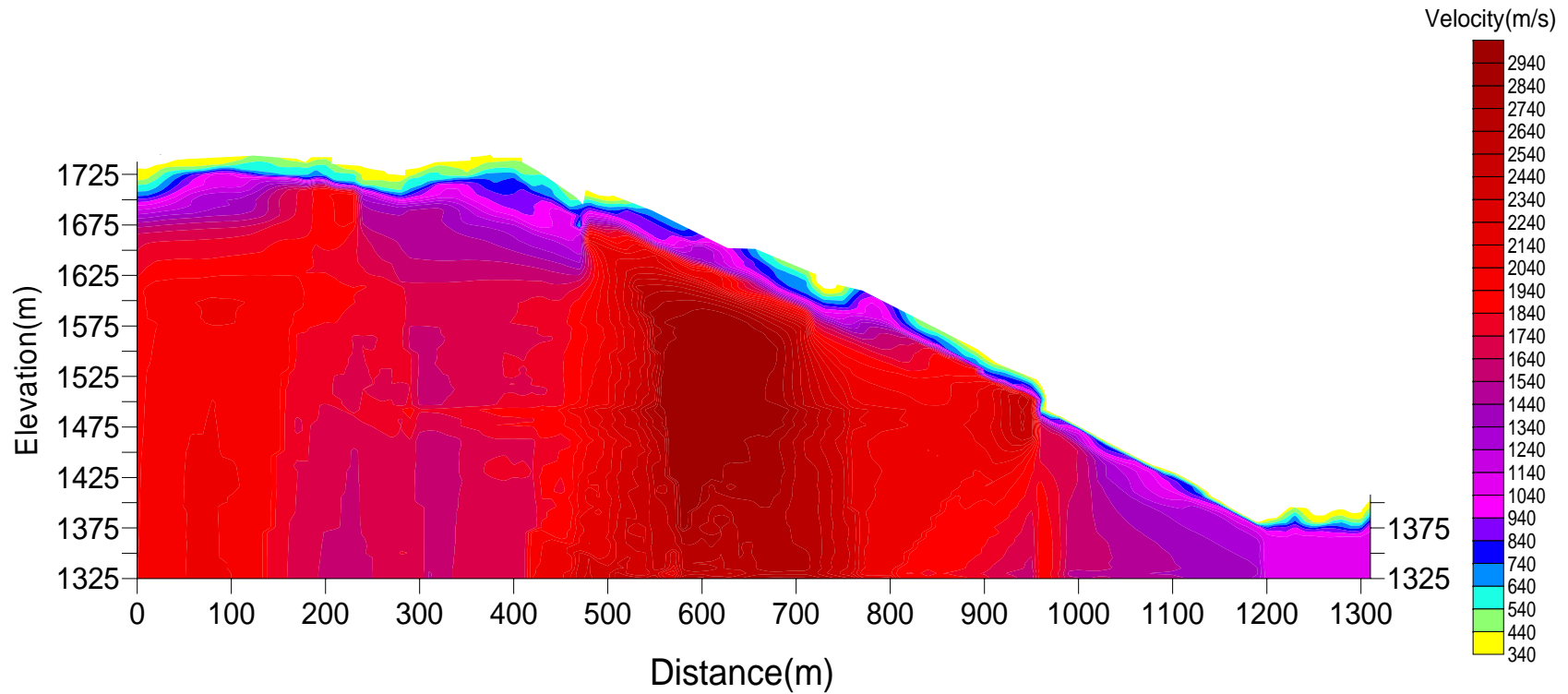


Fig. 87: Obtained velocity model affected by topography along the line 1, interpolated according to Kriging method

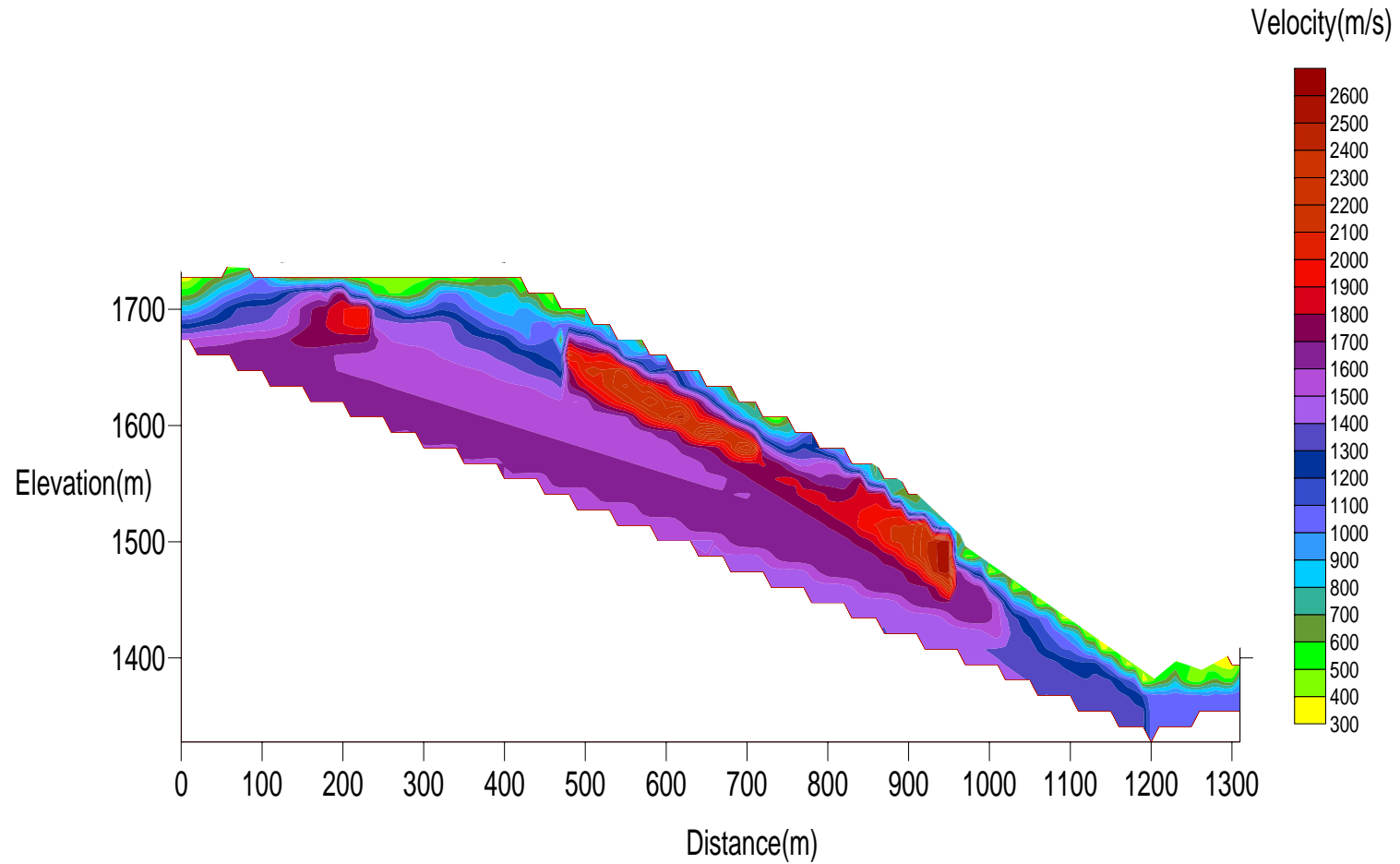


Fig. 88: Obtained velocity model affected by topography along the line 1, interpolated according to Triangular method

3.7. LINE 2 POROFILE A

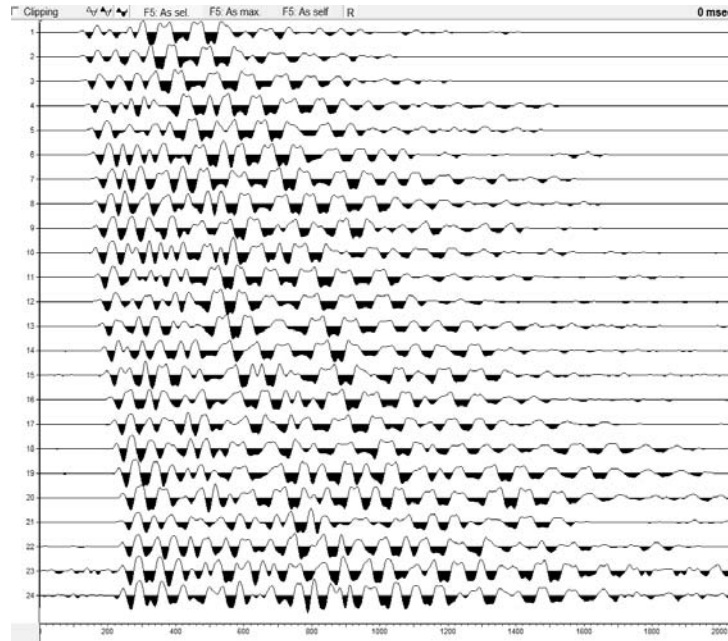


Fig. 89: Shot is located at 70 meters before the first geophone in the profile A of line 2

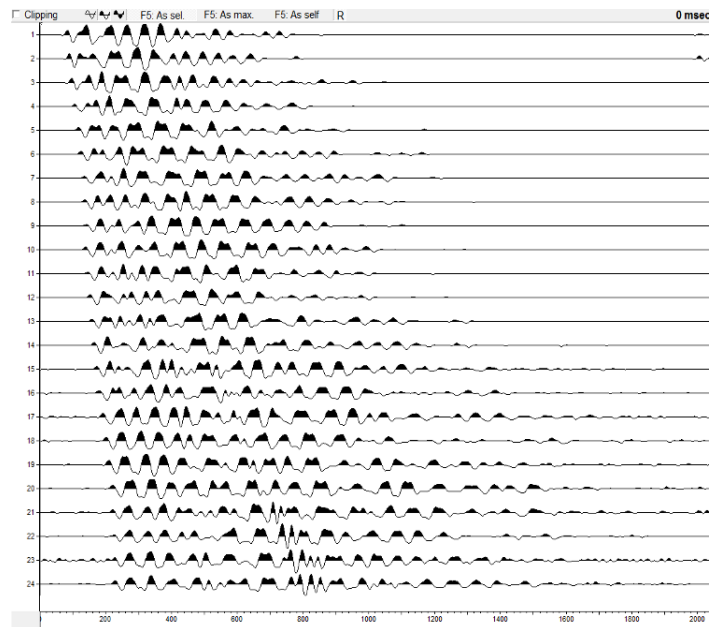


Fig. 90: Shot is located at 40 meters before the first geophone in the profile A of line 2

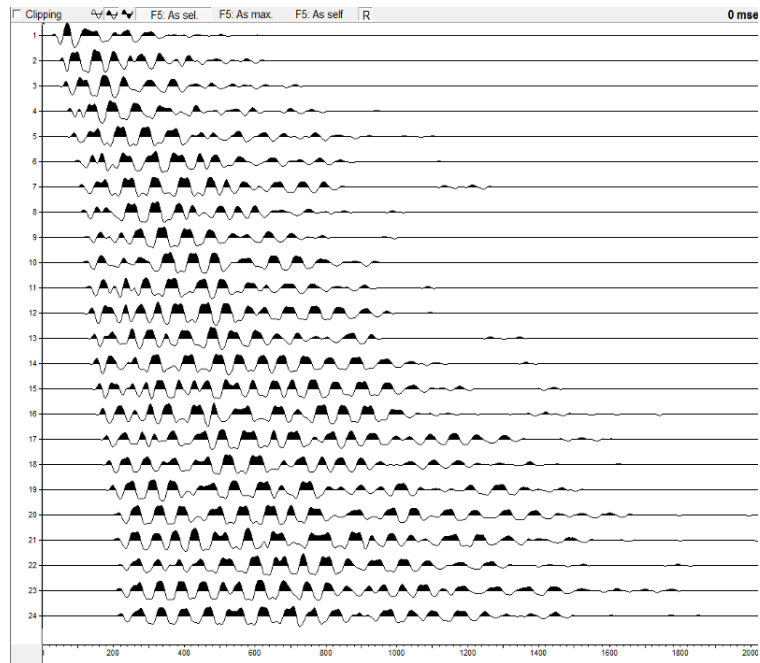


Fig. 91: Shot is located at 10 meters before the first geophone in the profile A of line 2

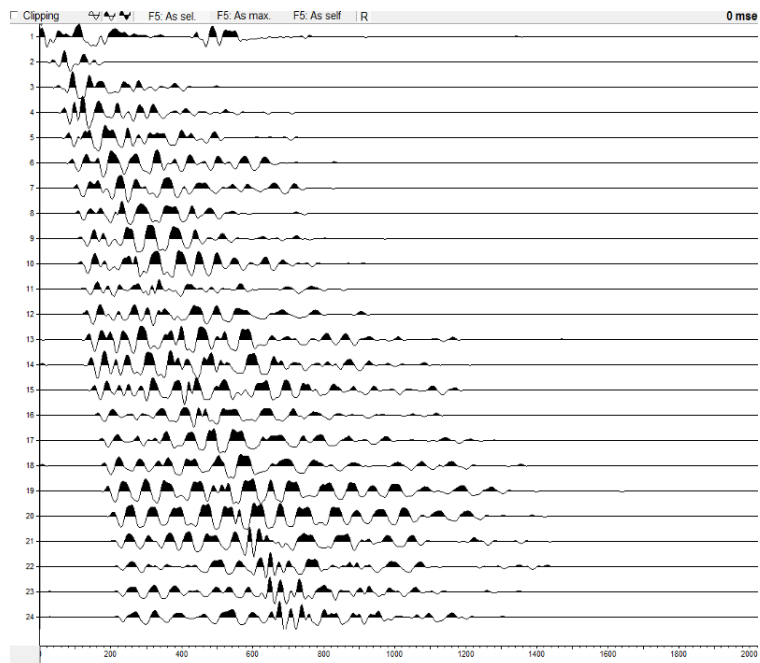


Fig. 92: Shot is located at 1 meter before the first geophone in the profile A of line 2

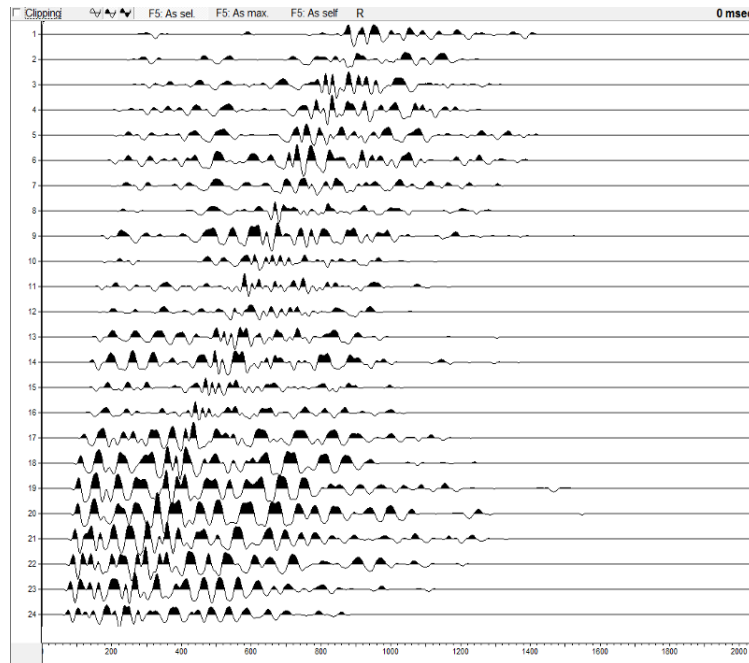


Fig. 93: Shot is located at 300 meters after the first geophone in the profile A of line 2

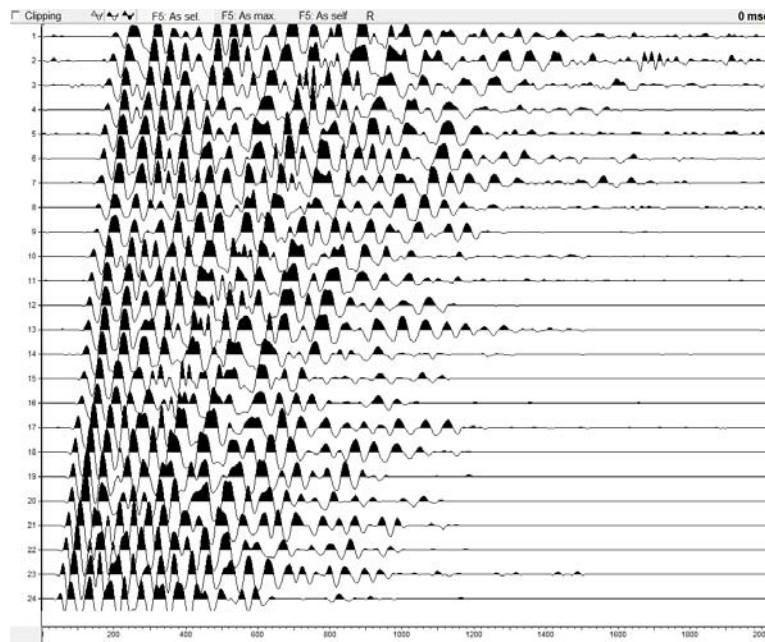


Fig. 94: Shot is located at 270 meters after the first geophone in the profile A of line 2

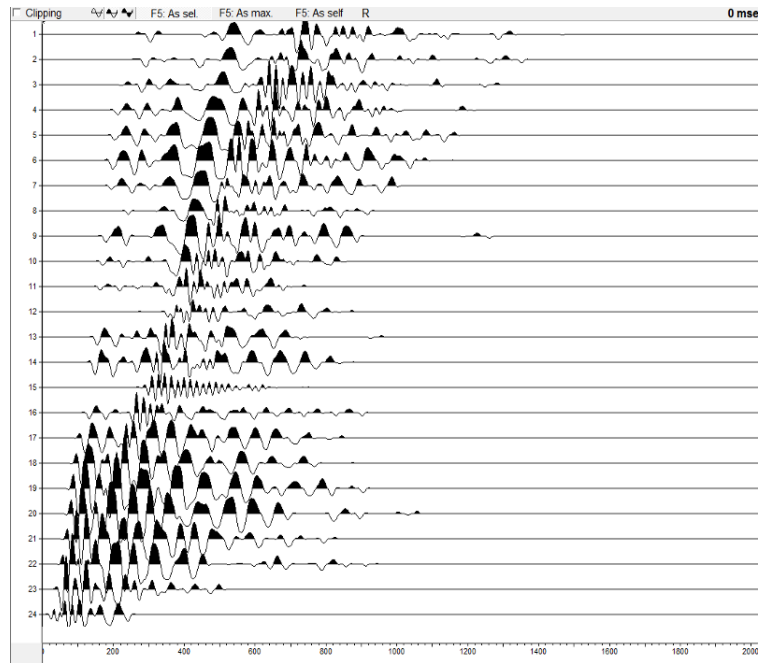


Fig. 95: Shot is located at 240 meters after the first geophone in the profile A of line 2

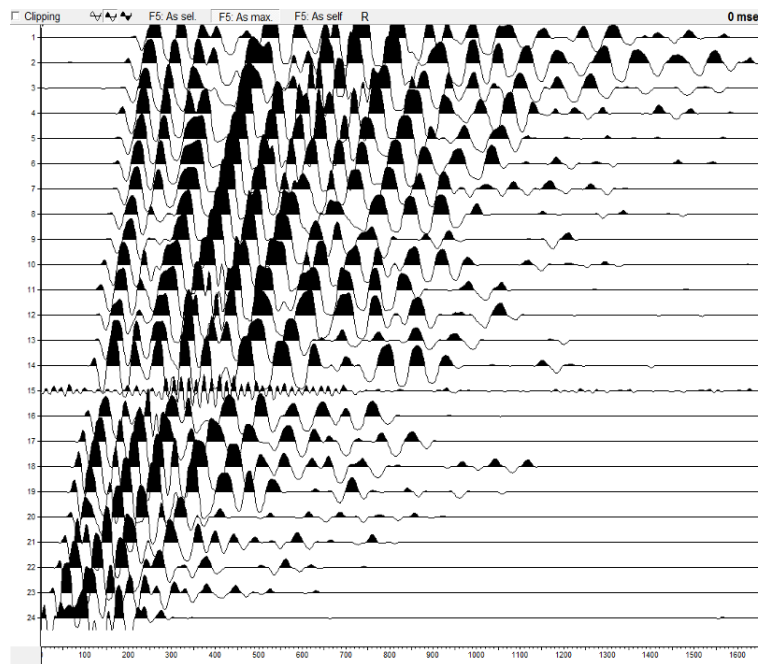


Fig. 96: Shot is located at 230 meters after the first geophone in the profile A of line 2

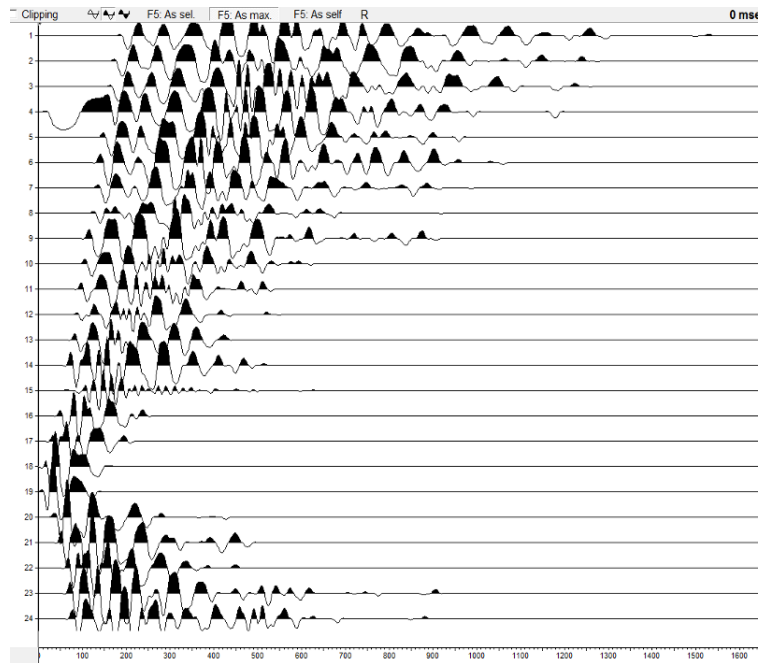


Fig. 97: Shot is located at 175 meters after the first geophone in the profile A of line 2

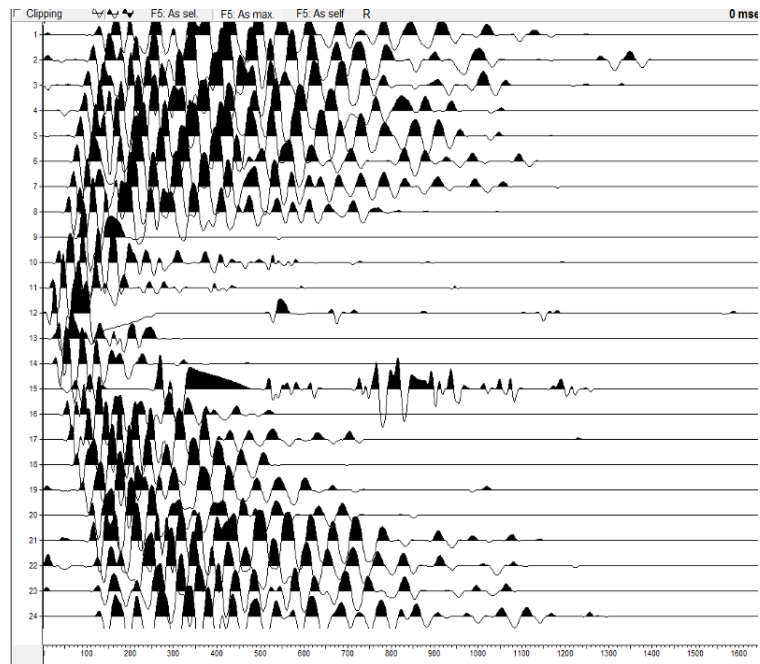


Fig. 98: Shot is located at 115 meters after the first geophone in the profile A of line 2

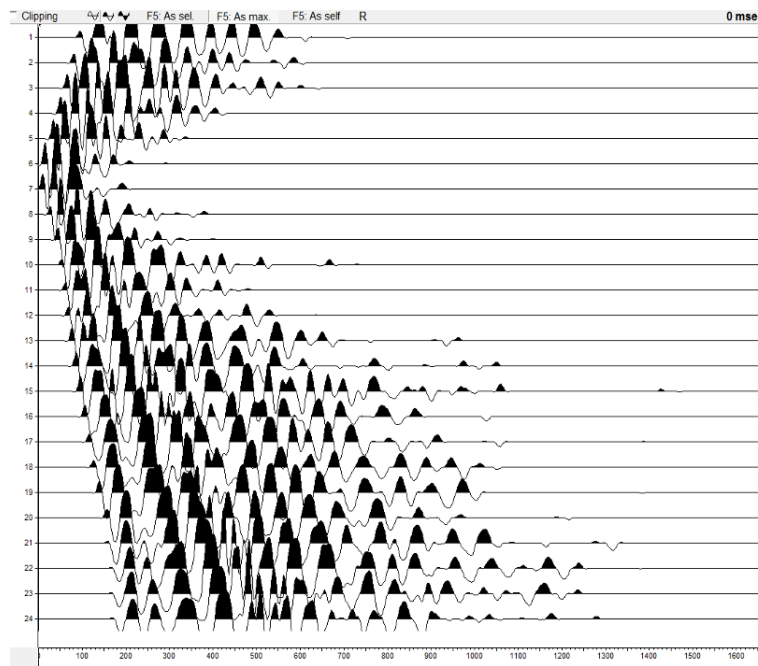


Fig. 99: Shot is located at 55 meters after the first geophone in the profile A of line 2

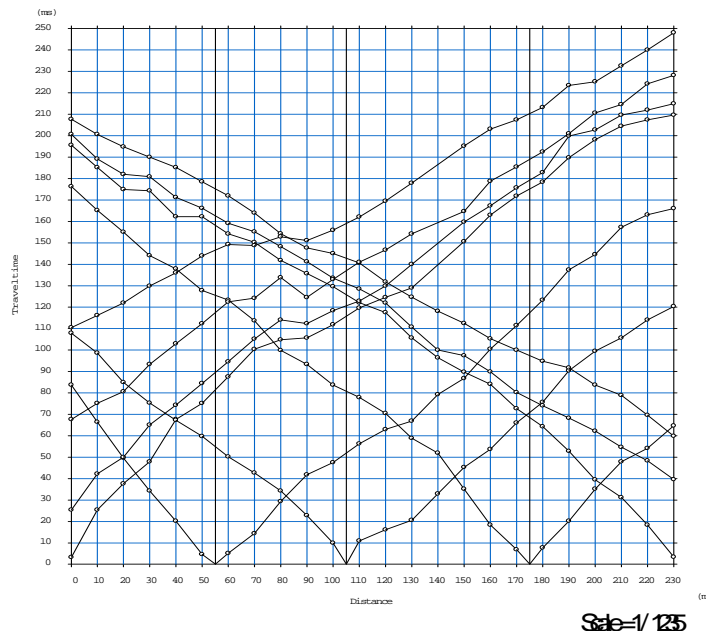


Fig. 100: Travel time curves of 10 shots in the profile A of line 2

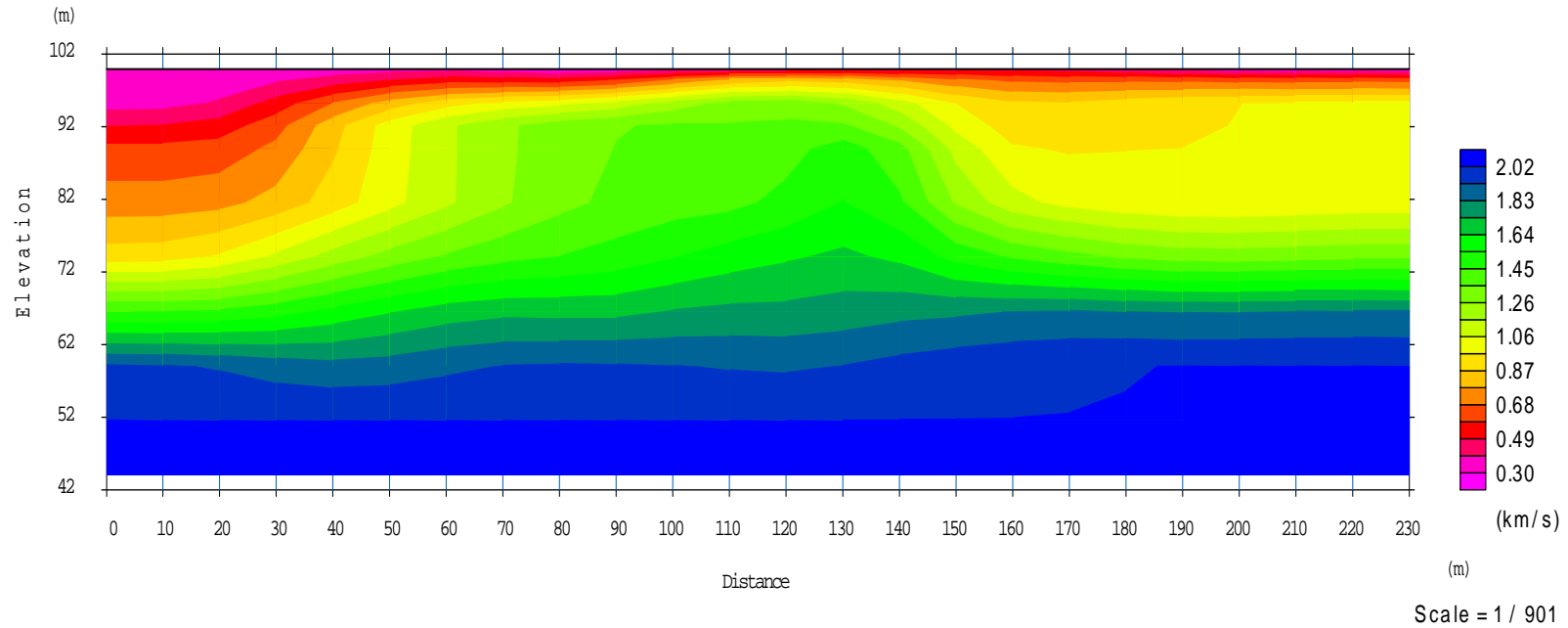


Fig. 101: Obtained velocity model not affected by topography in the profile A of line 2

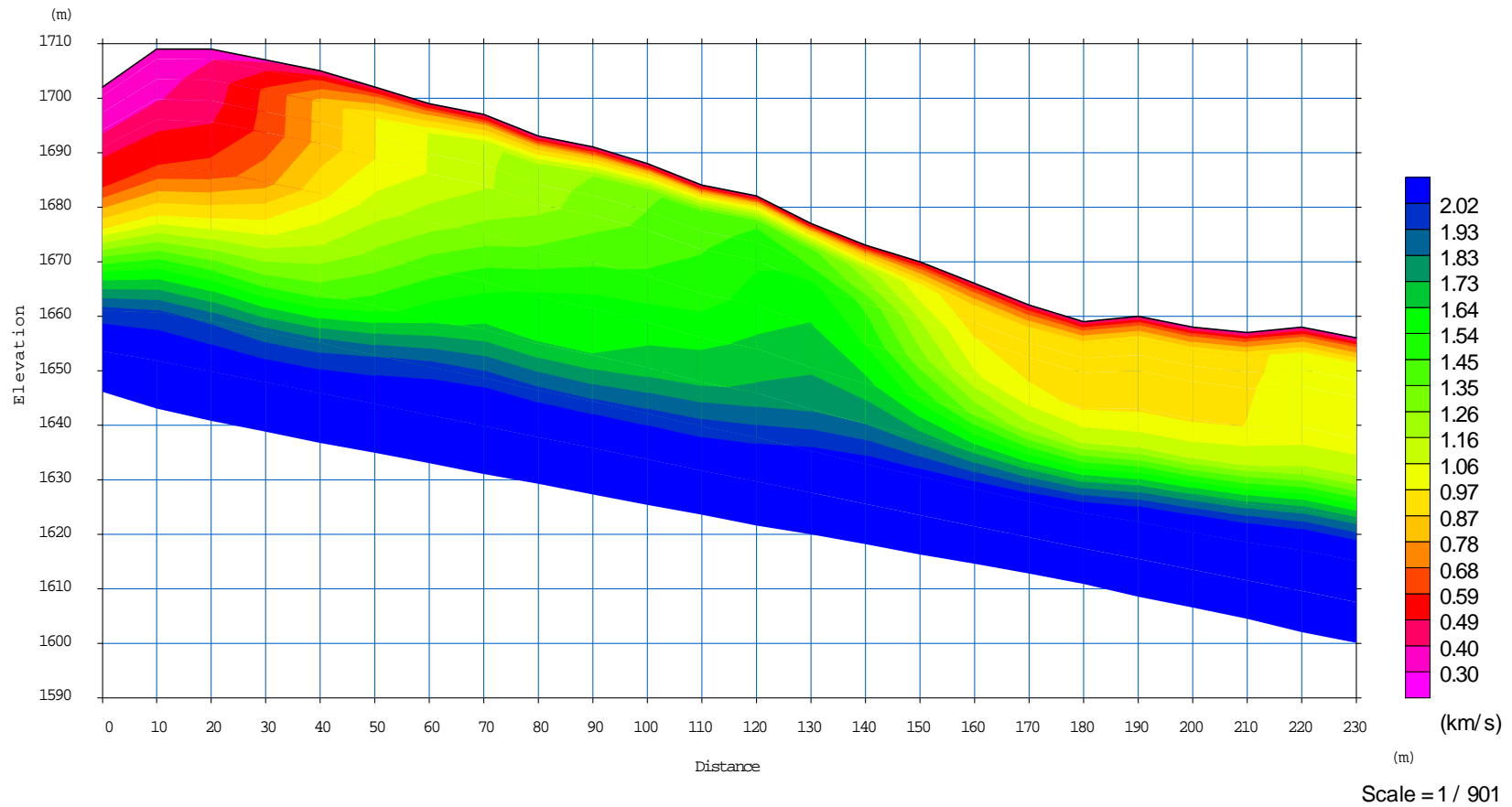


Fig. 102: Obtained velocity model affected by topography in the profile A of line 2

Along the profile A of line 2, three layers with different velocities were detected. These layers, from top to the bottom could be loose soil (overburden), clay and fractured sandstone. Thicknesses of the first and second layers under each Geophone are presented in the below table:

Geophone Number	1	2	3	4	5	6	7	8	9	10	11	12	13	14	15	16	17	18	19	20	21	22	23	24
Thickness of first layer	2.86	6.96	5.68	4.55	4.15	2.99	1.95	2.43	1.49	2.43	2.83	1.43	1.51	0	0	0	0	0	0	0.33	0	0	0.27	0
Thickness of second layer	37.27	34.46	31.34	27.84	25.34	23.75	22.41	20.37	17.63	15.59	14.33	15.21	17.83	20.06	22.26	25.16	26.32	26.61	26.88	29.6	28.71	27.54	27.58	25.02

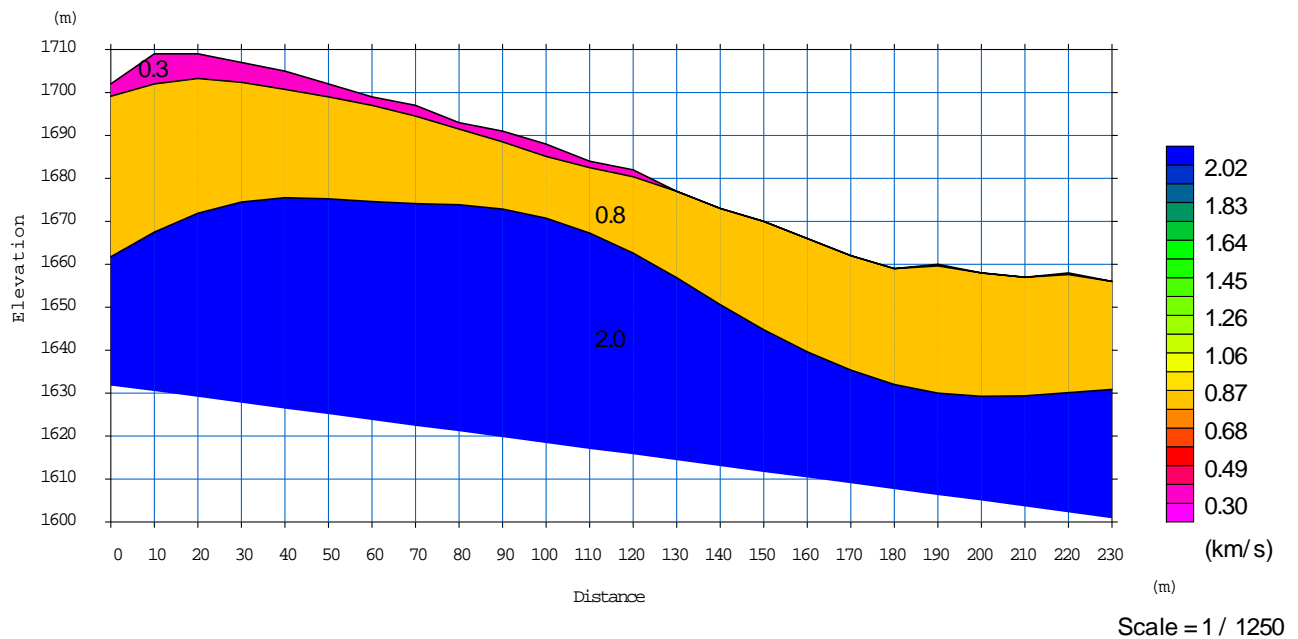


Fig. 103: Obtained velocity model affected by topography in the profile A of line 2 with detection of layer margins

3.8. LINE 2 POROFILE B

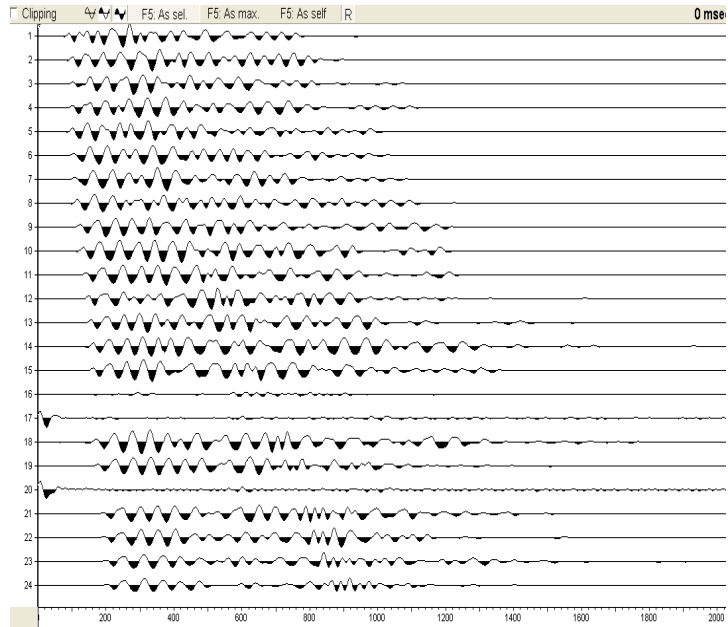


Fig.104: Shot is located at 70 meters before the first geophone in the profile B of line 2

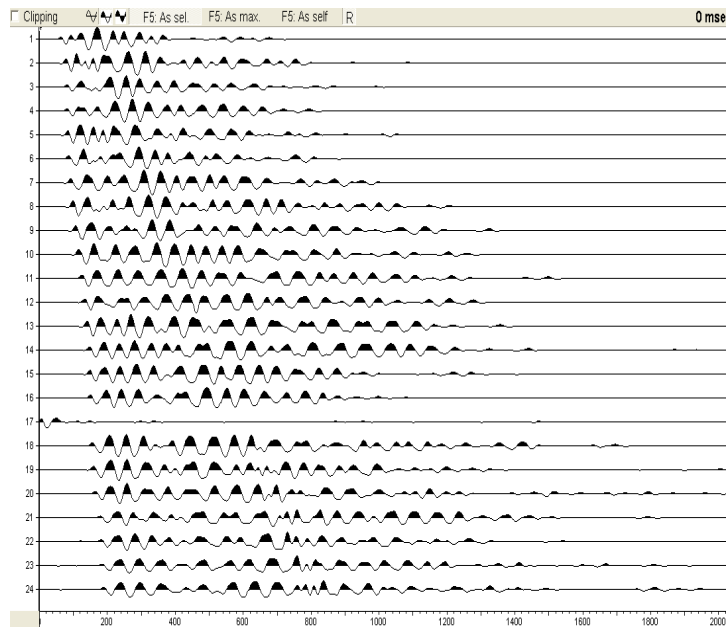


Fig.105: Shot is located at 40 meters before the first geophone in the profile B of line 2

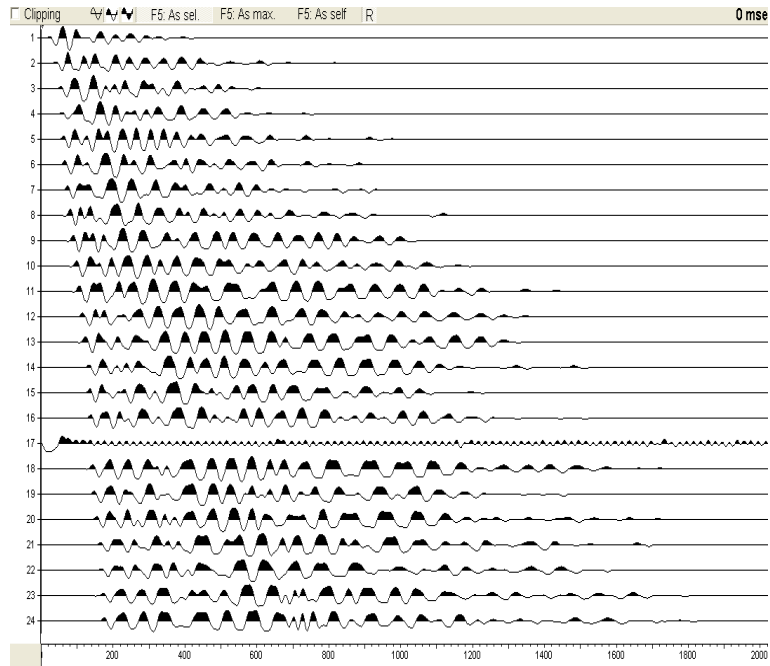


Fig.106: Shot is located at 10 meters before the first geophone in the profile B of line 2

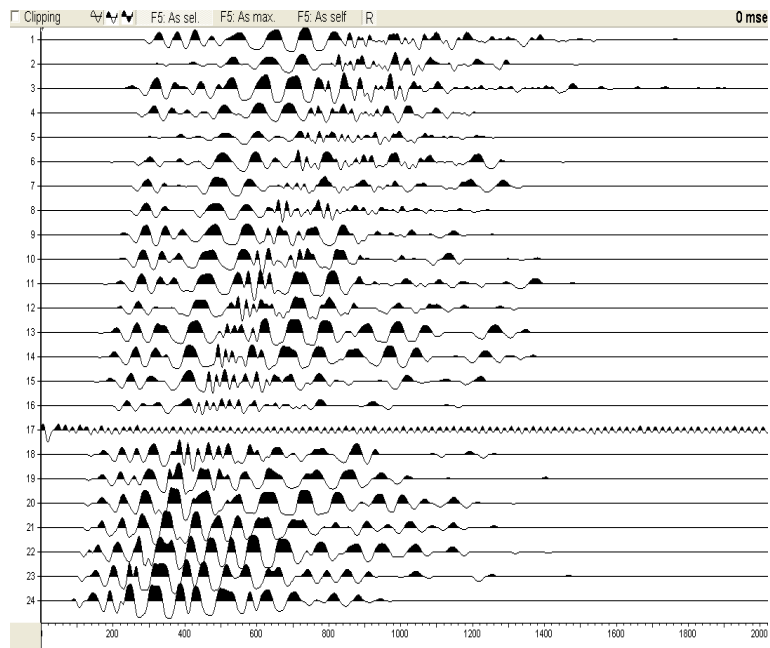


Fig.107: Shot is located at 300 meters after the first geophone in the profile B of line 2

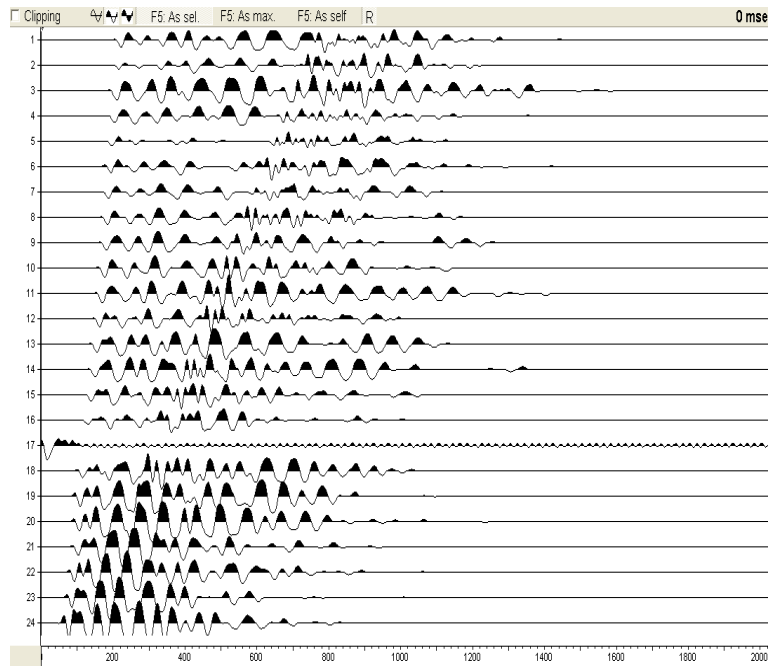


Fig.108: Shot is located at 270 meters after the first geophone in the profile B of line 2

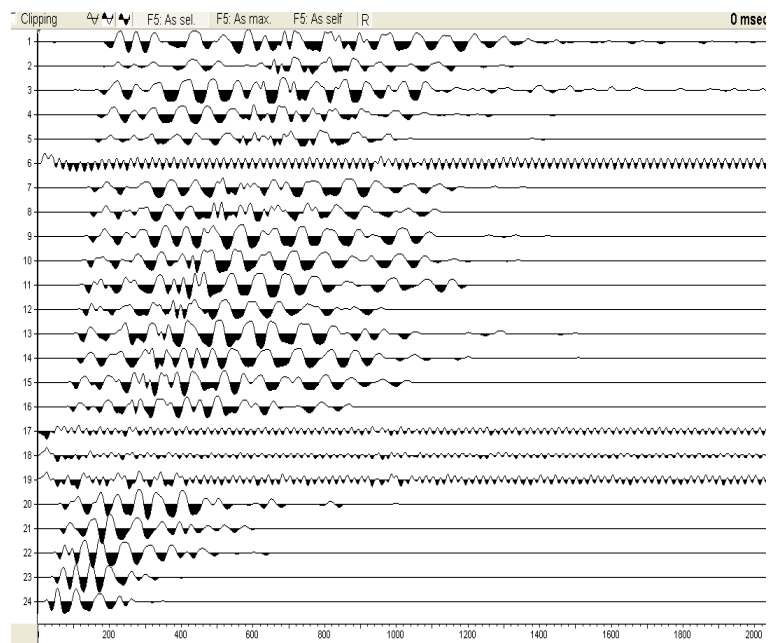


Fig. 109: Shot is located at 240 meters after the first geophone in the profile B of line 2

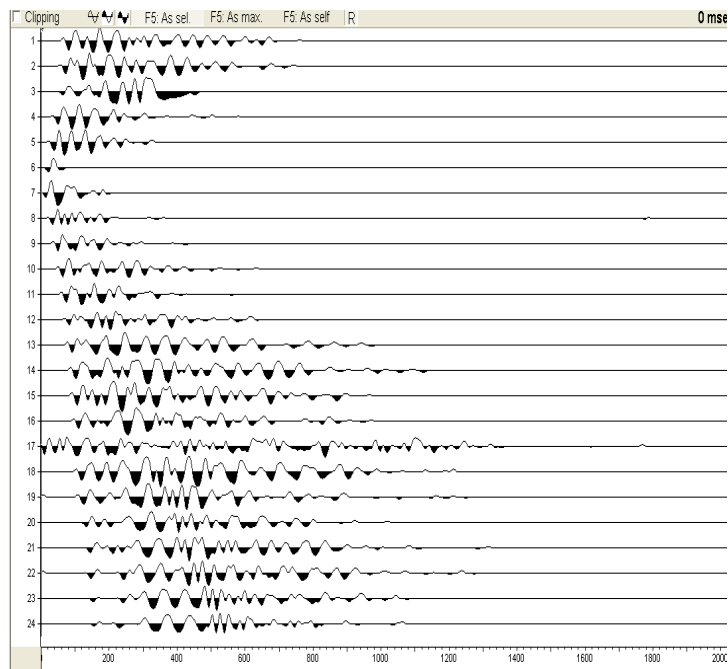


Fig. 110: Shot is located at 55 meters after the first geophone in the profile B of line 2

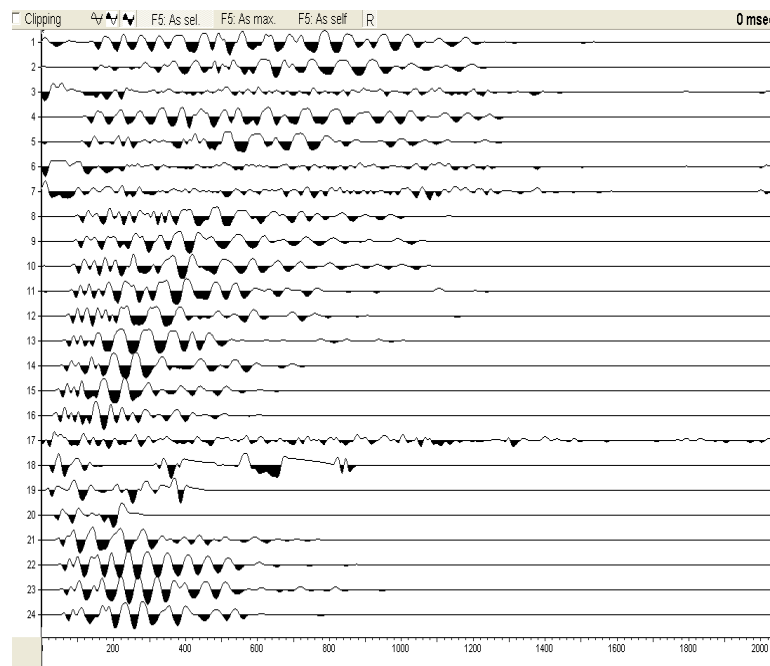


Fig. 111: Shot is located at 165 meters after the first geophone in the profile B of line 2

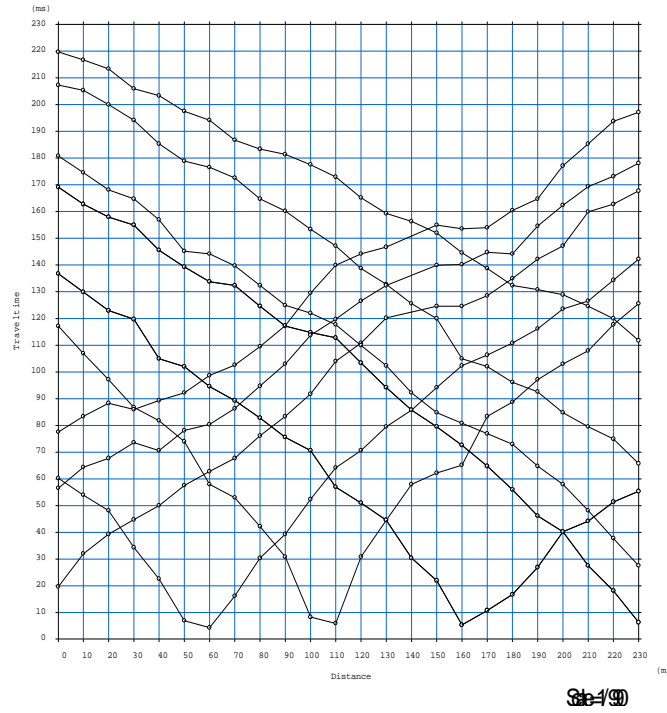


Fig. 112: Travel time curves of profile B in line 2

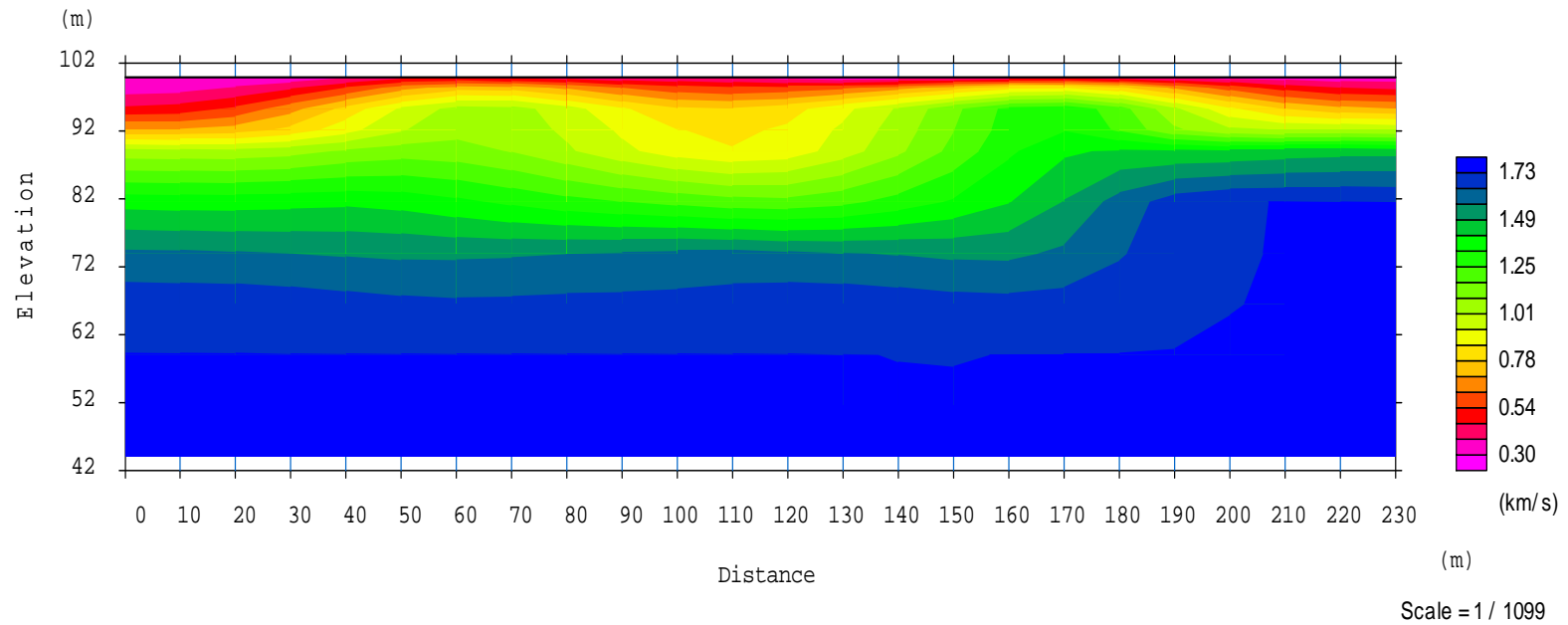


Fig. 113: Obtained velocity model not affected by topography in the profile B of line 2

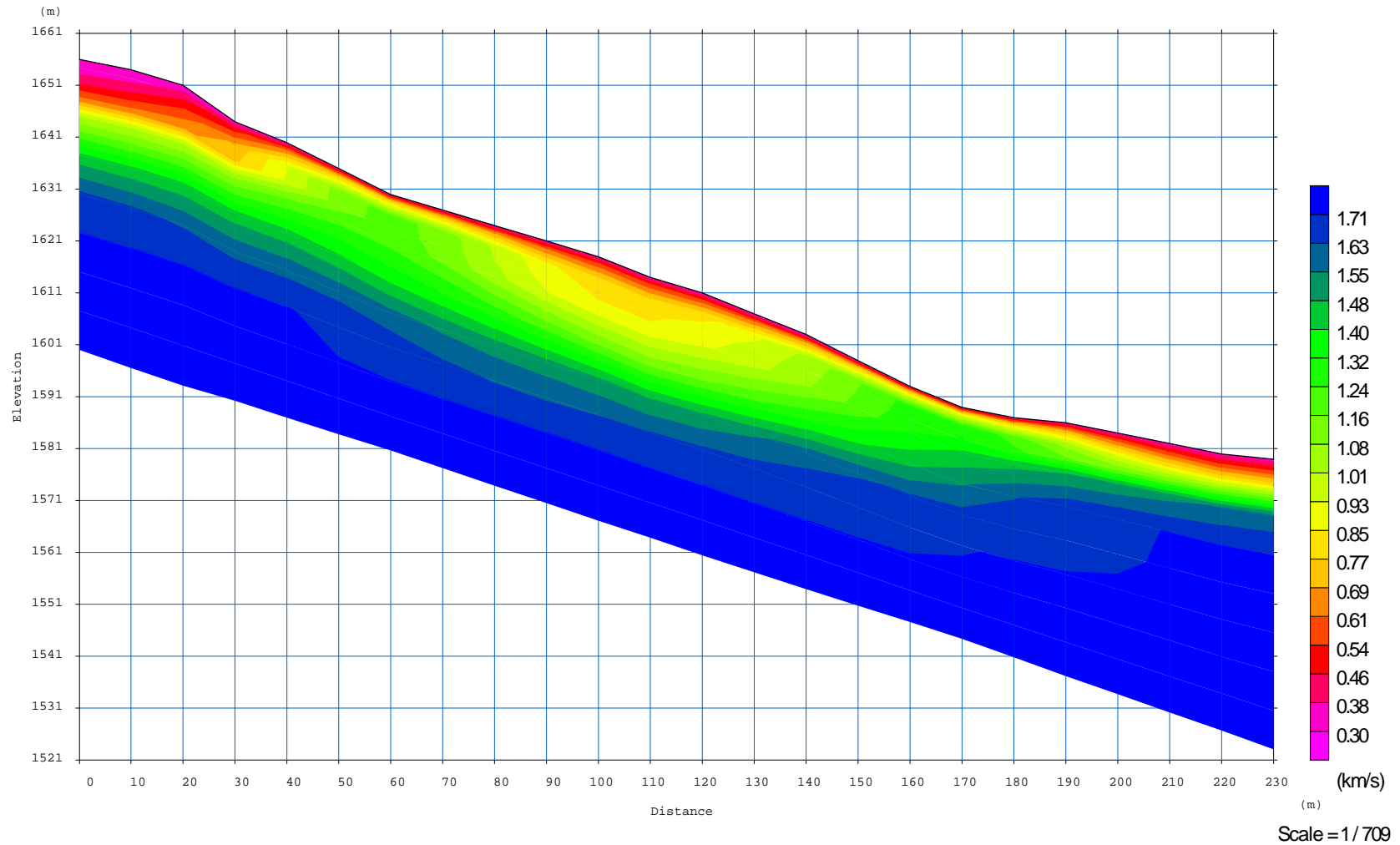


Fig. 114: Obtained velocity model affected by topography in the profile B of line 2

Along the profile B of line 2, three layers with different velocities were detected. These layers, from top to the bottom could be loose soil (overburden), clay and fractured sandstone. Thicknesses of the first and second layers under each Geophone are presented in the below table:

Geophone Number	1	2	3	4	5	6	7	8	9	10	11	12	13	14	15	16	17	18	19	20	21	22	23	24
Thickness of first layer	5.51	4.88	4.49	1.57	1.79	0.93	0	0	0	0	0	0	0.48	0.38	0.91	0.84	0.67	0.33	0.33	1.78	2.77	3.69	3.88	4.31
Thickness of second layer	3.62	6.93	9.03	9.74	10.42	11.22	12.16	14.5	17.08	19.18	20.17	19.11	18.01	16.41	14.3	11.99	9.95	8.93	9.1	8.27	6.47	4.38	2.77	1.83

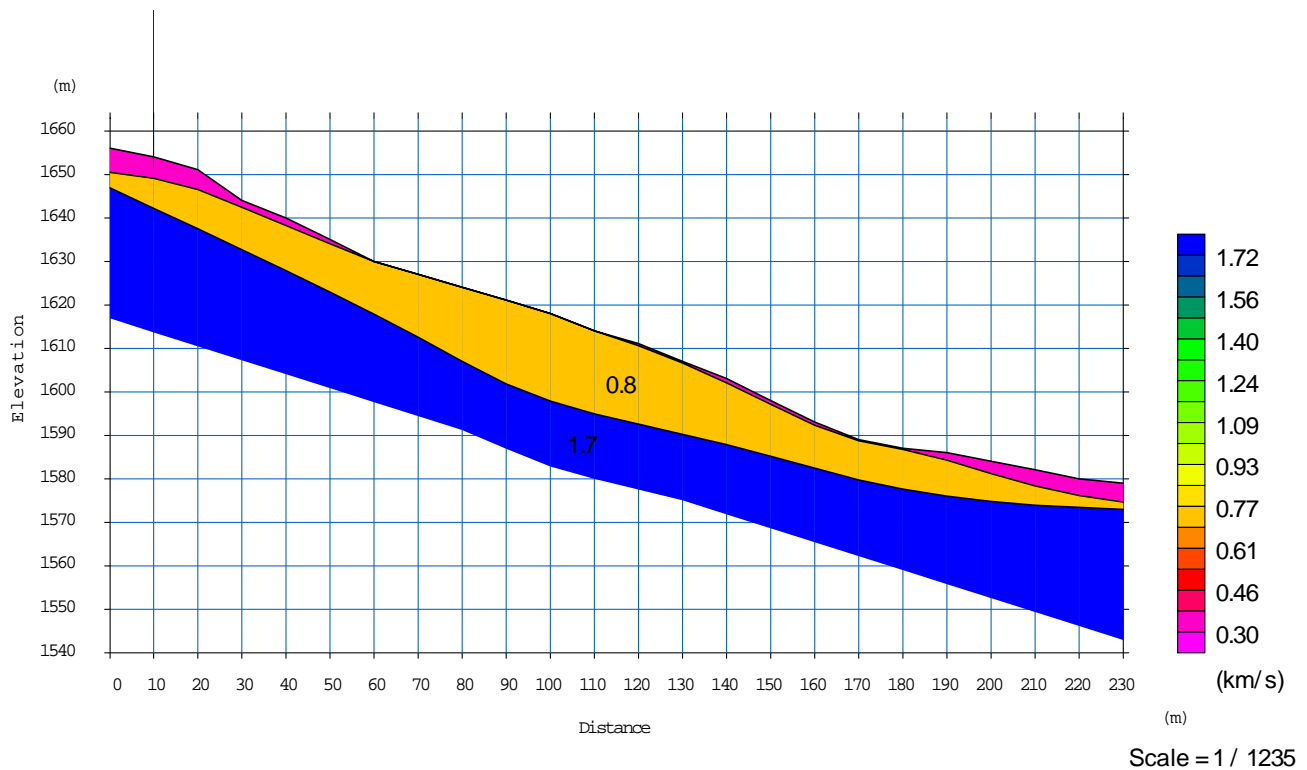


Fig. 115: Obtained velocity model affected by topography in the profile B of line 2 with detection of layer margins

3.9. LINE 2 POROFILE C

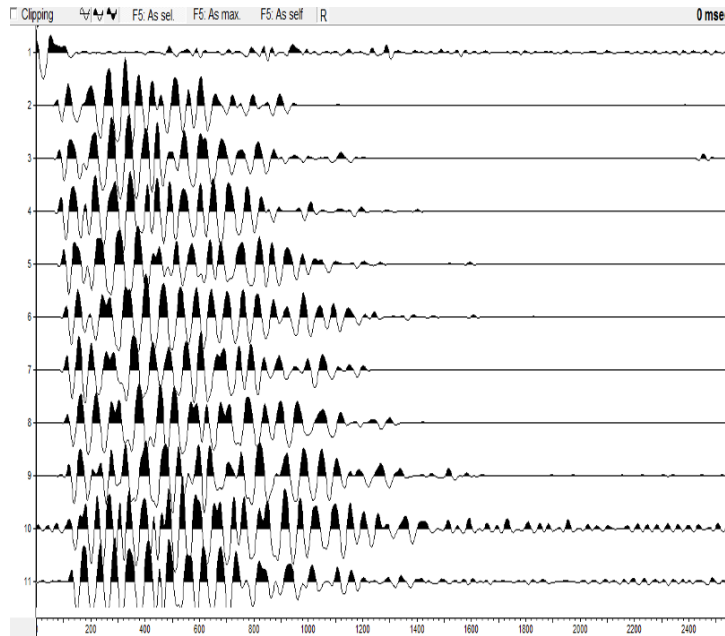


Fig. 116: Shot is located at 55 meters before the first geophone in the profile C of line 2

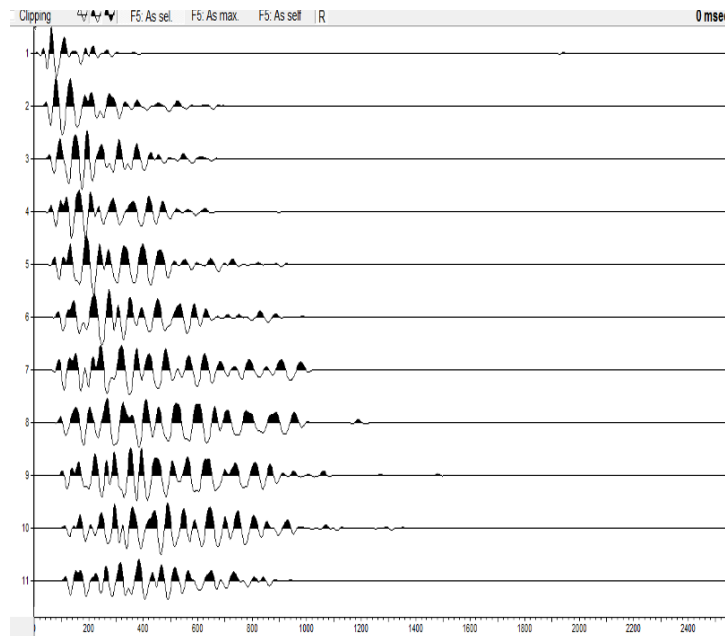


Fig. 117: Shot is located at 10 meters before the first geophone in the profile C of line 2

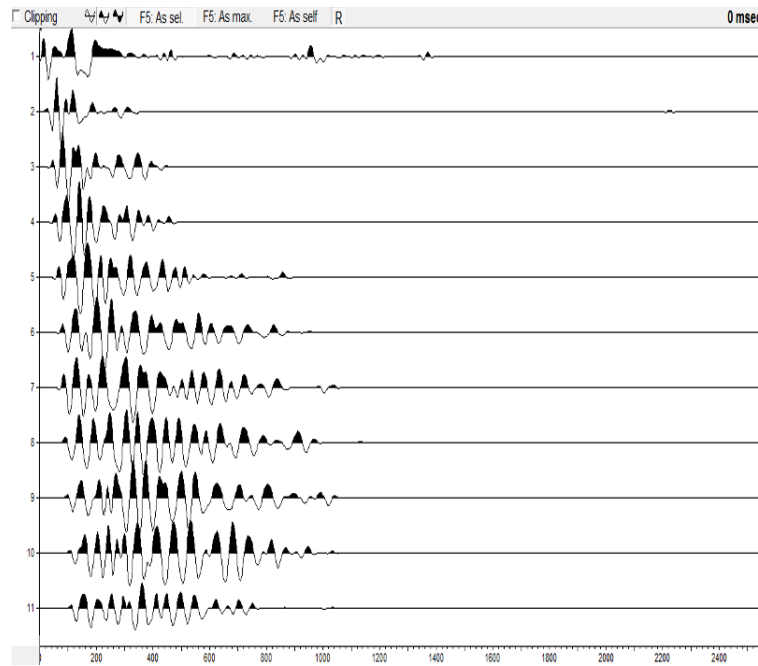


Fig. 118: Shot is located at 1 meter before the first geophone in the profile C of line 2

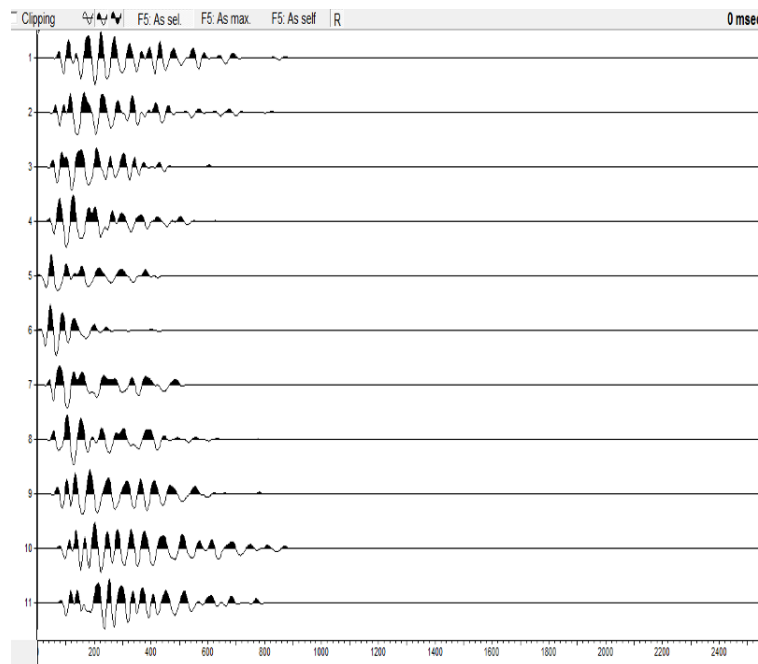


Fig. 119: Shot is located at 45 meters after the first geophone in the profile C of line 2

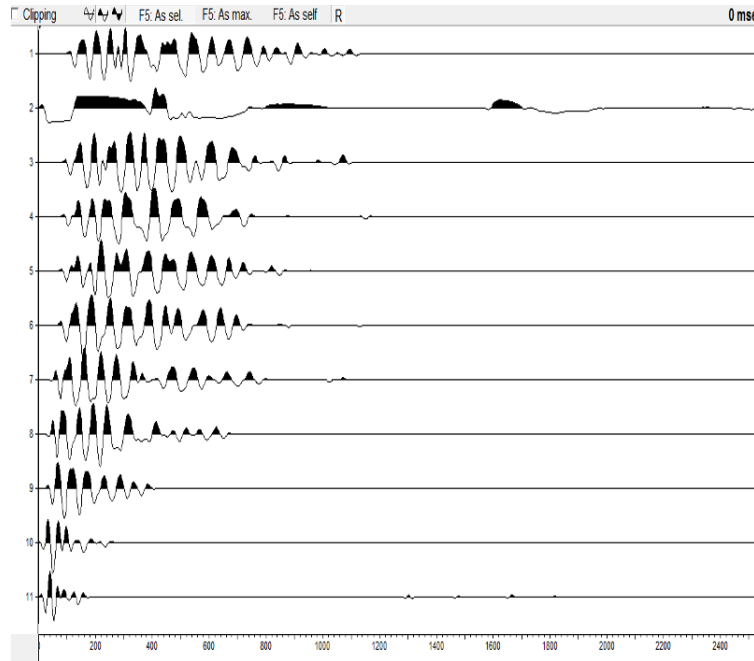


Fig. 120: Shot is located at 95 meters after the first geophone in the profile C of line 2

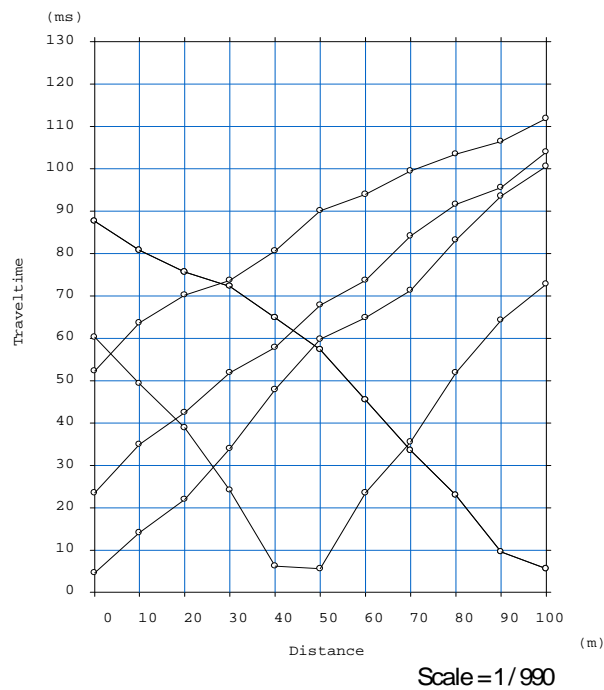


Fig. 121: Travel time curves of 5 shots of profile C in line 2

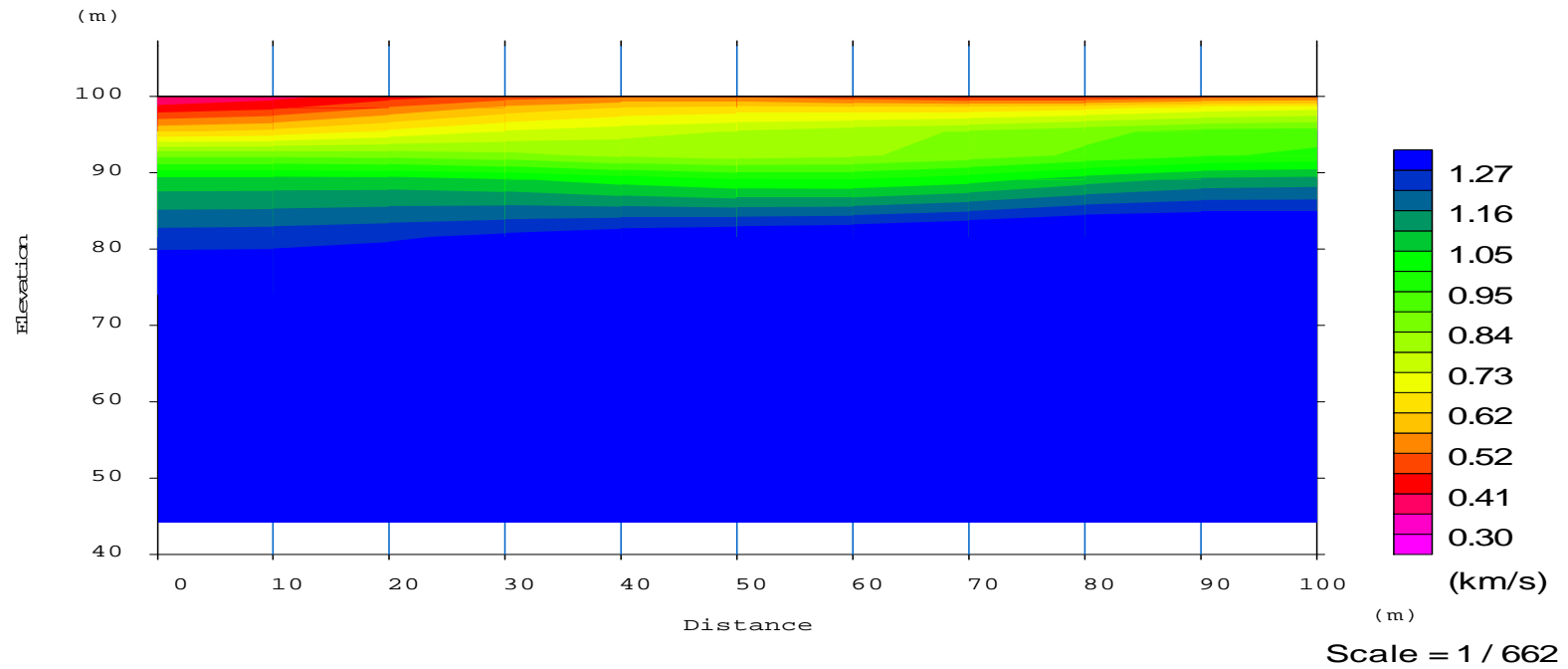


Fig. 122: Obtained velocity model not affected by topography of the profile C in line 2

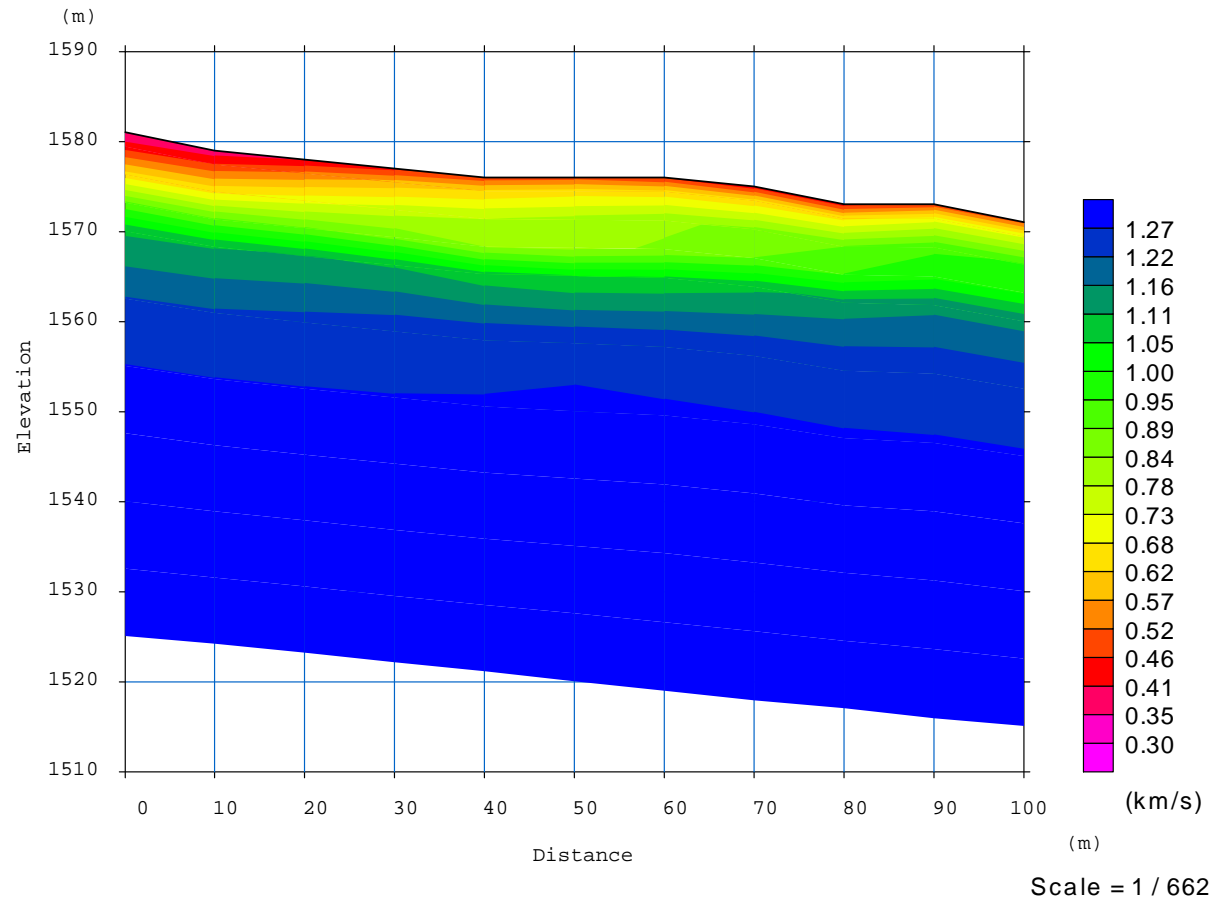


Fig. 123: Obtained velocity model affected by topography of the profile C in line 2

3.10. LINE 2 POROFILE D

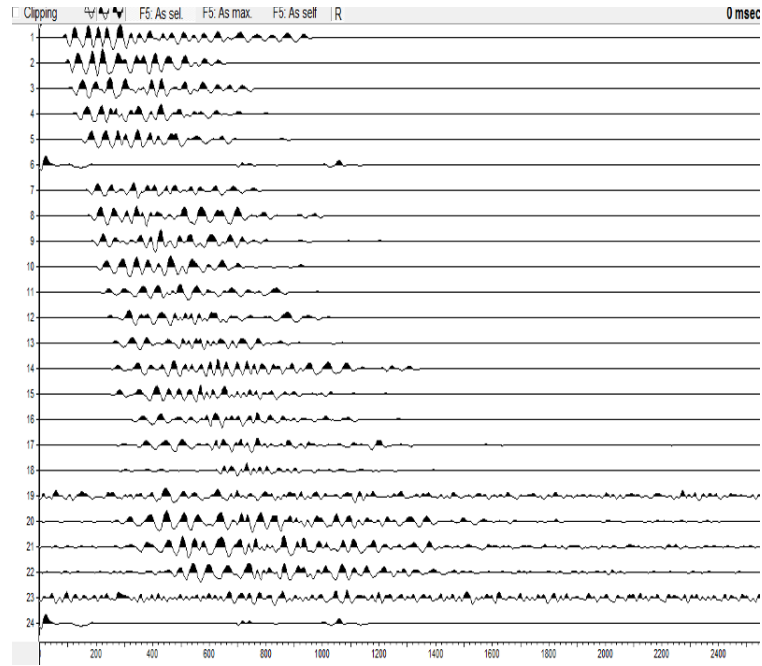


Fig. 124: Shot is located at 50 meters before the first geophone in the profile D of line 2

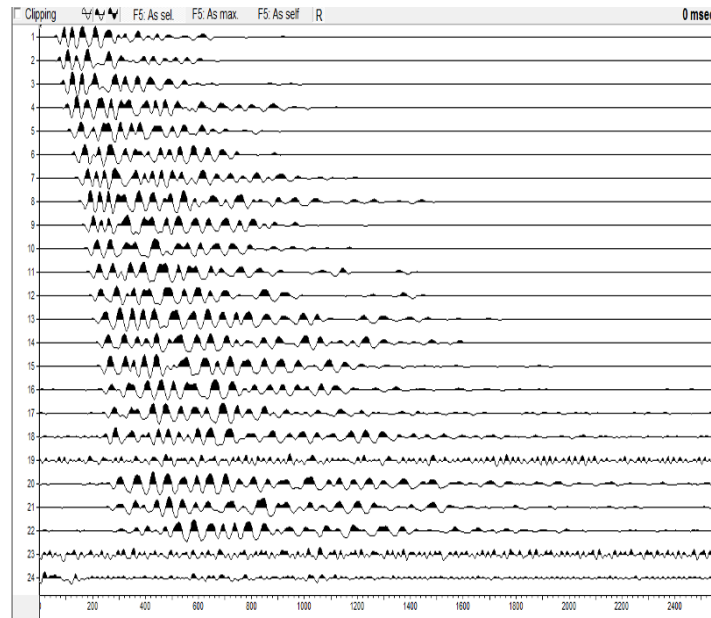


Fig. 125: Shot is located at 30 meters before the first geophone in the profile D of line 2

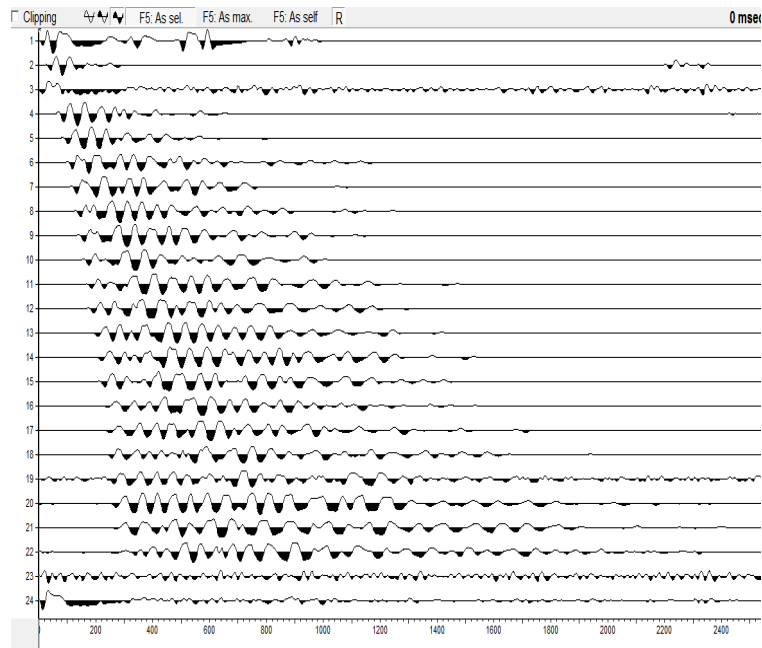


Fig. 126: Shot is located at 1 meter before the first geophone in the profile D of line 2

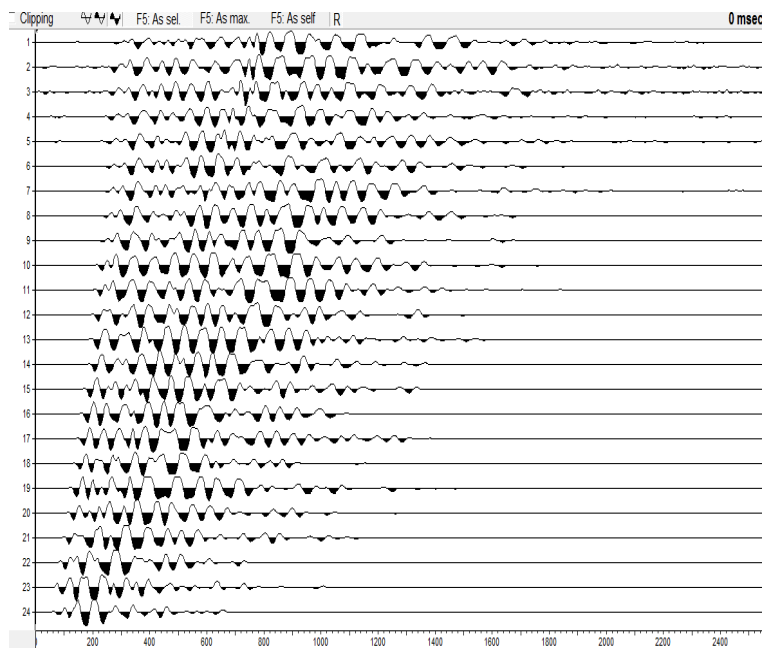


Fig. 127: Shot is located at 280 meters after the first geophone in the profile D of line 2

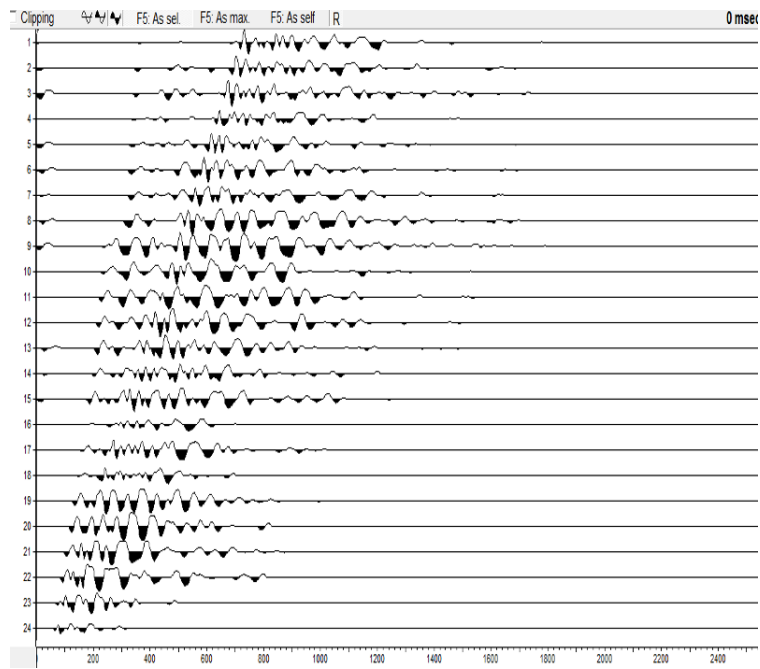


Fig. 128: Shot is located at 260 meters after the first geophone in the profile D of line 2

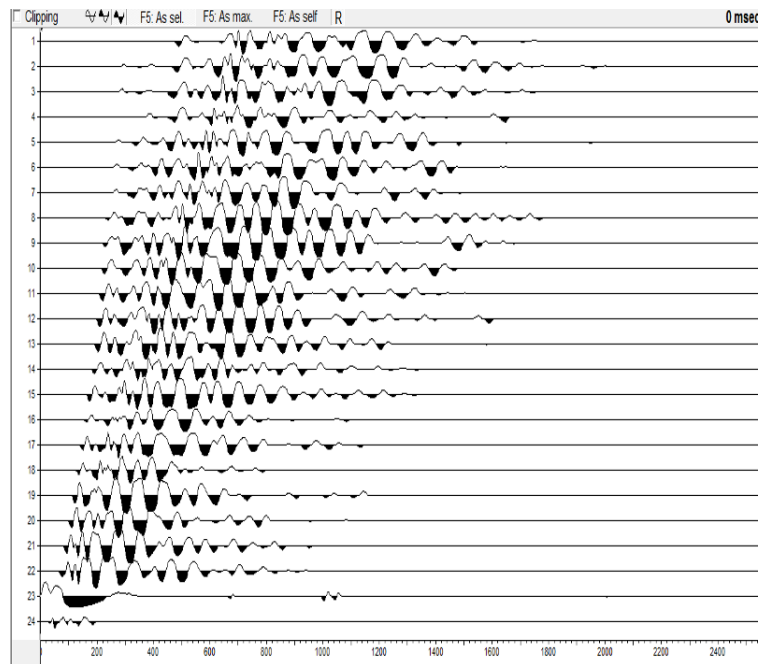


Fig. 129: Shot is located at 240 meters after the first geophone in the profile D of line 2

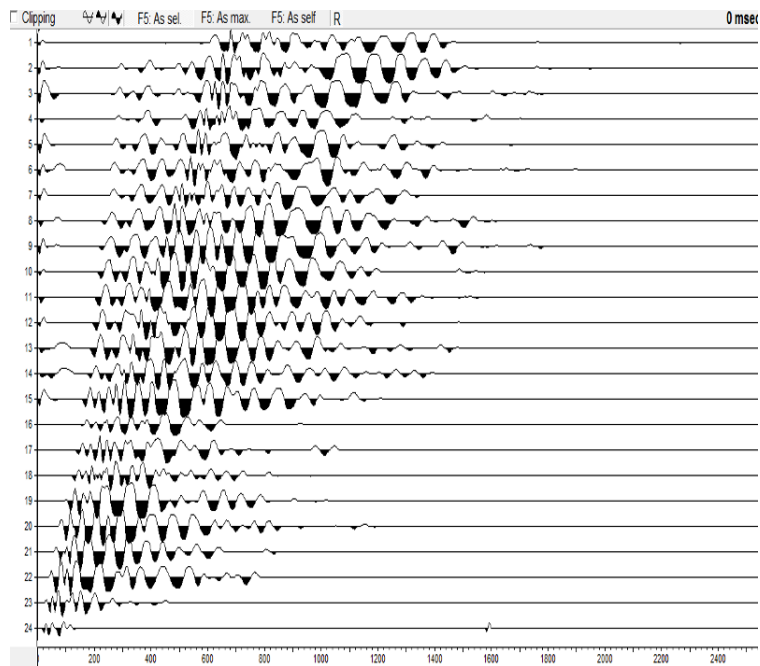


Fig. 130: Shot is located at 231 meters after the first geophone in the profile D of line 2

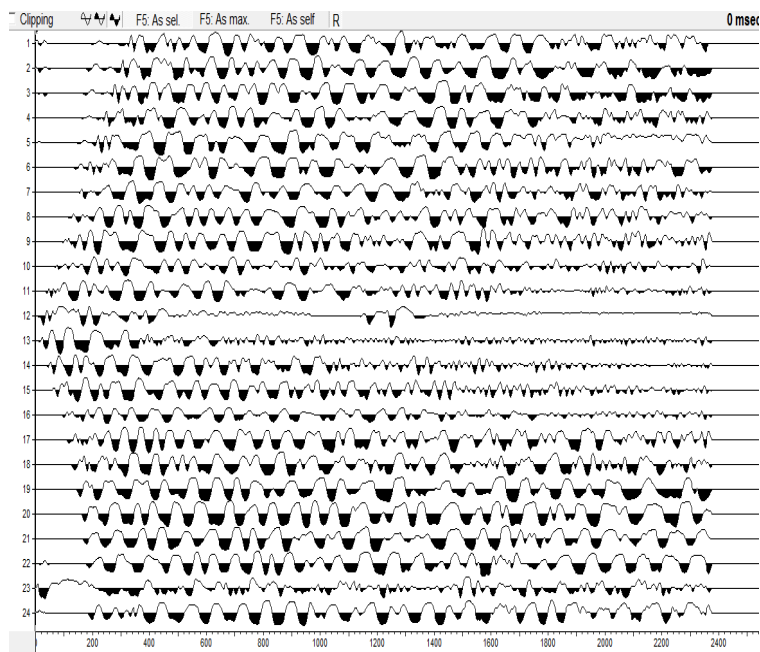


Fig. 131: Shot is located at 115 meters after the first geophone in the profile D of line 2

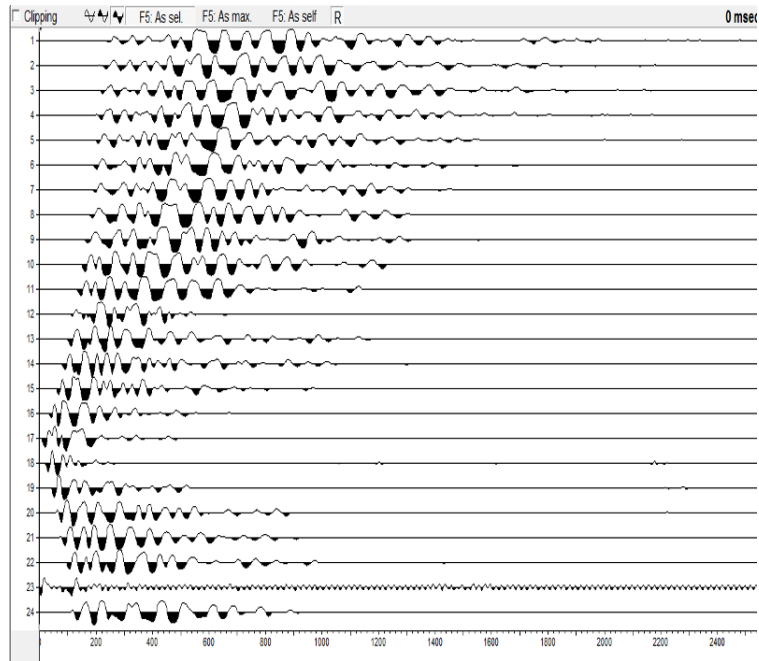


Fig. 132: Shot is located at 165 meters after the first geophone in the profile D of line 2

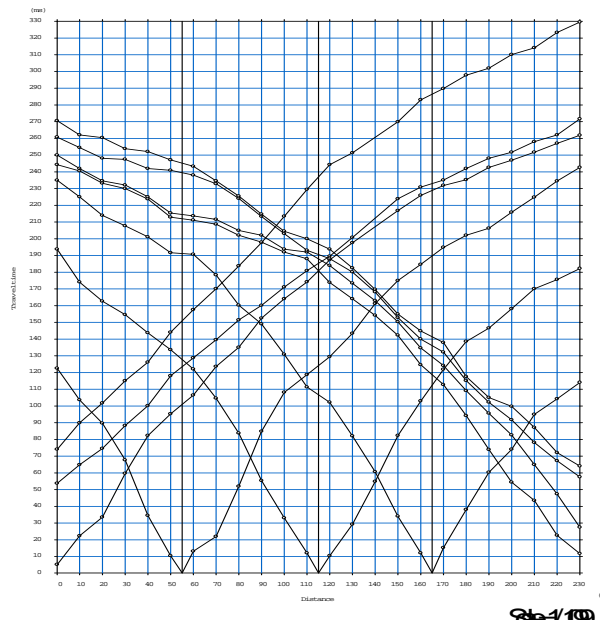


Fig. 133: Travel time curves of 10 shots of profile D in line 2

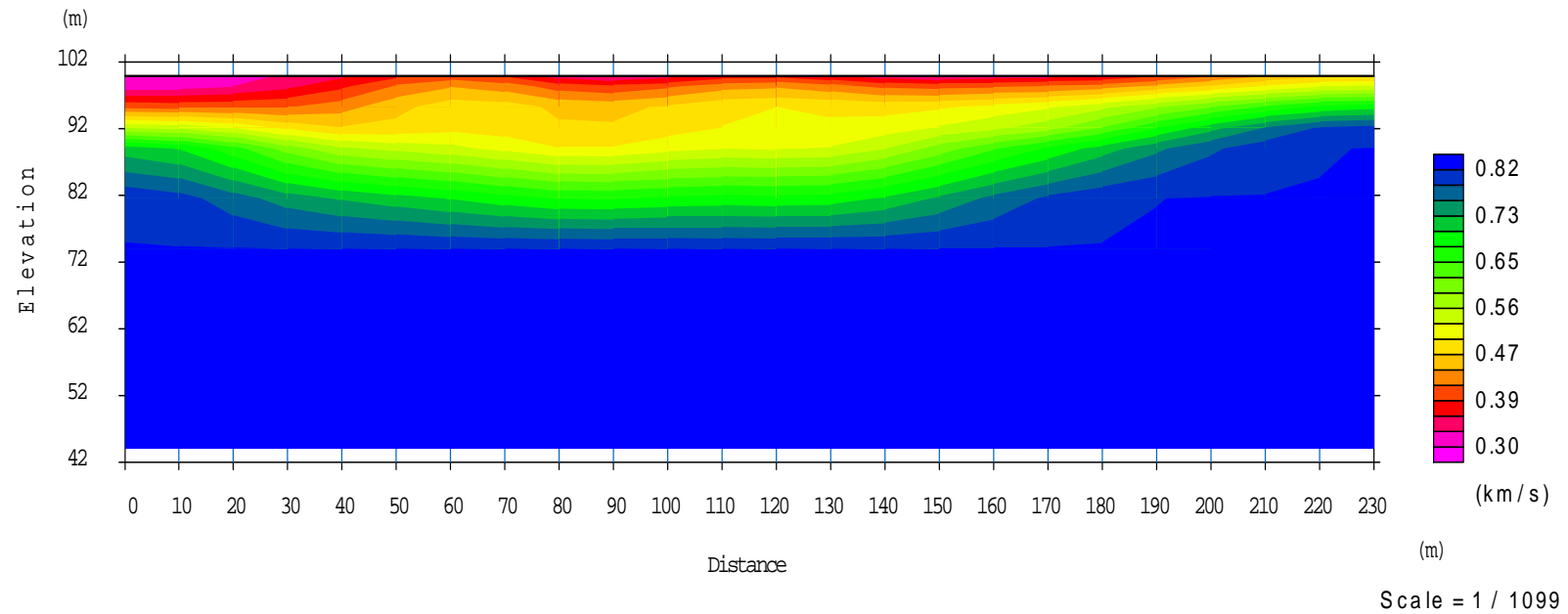


Fig. 134: Obtained velocity model not affected by topography in the profile D of Line 2

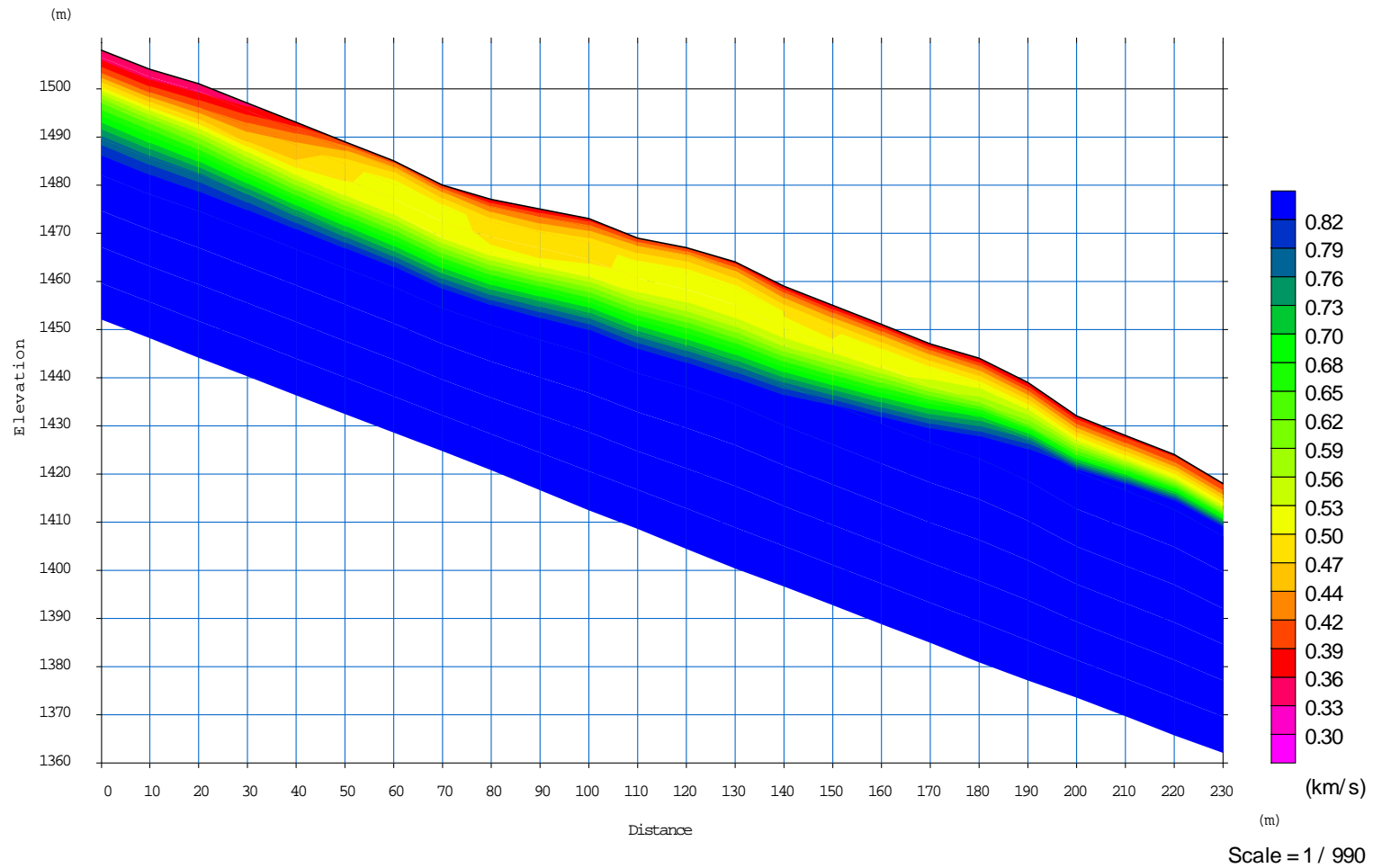


Fig. 135: Obtained velocity model affected by topography in the profile D of Line 2

Along the profile D of line 2, three layers with different velocities were detected. These layers, from top to the bottom could be loose soil (overburden), clay and fractured sandstone. Thicknesses of the first and second layers under each Geophone are presented in the below table:

Geophone Number	1	2	3	4	5	6	7	8	9	10	11	12	13	14	15	16	17	18	19	20	21	22	23	24
Thickness of first layer	11.36	10.11	11.35	12.93	14.73	15.93	16.09	14.53	14.42	14.69	14.78	11.94	11.61	12.78	12.43	12.47	12.78	12.9	14.05	14.56	13.4	14.17	12.95	8.34
Thickness of second layer	1.91	5.47	8.61	11.93	16.29	21.47	27.08	32.56	37.32	40.64	41.77	42.07	41.05	37.2	32.38	27.58	22.18	17.18	12.88	8.2	3.9	0.89	0	0

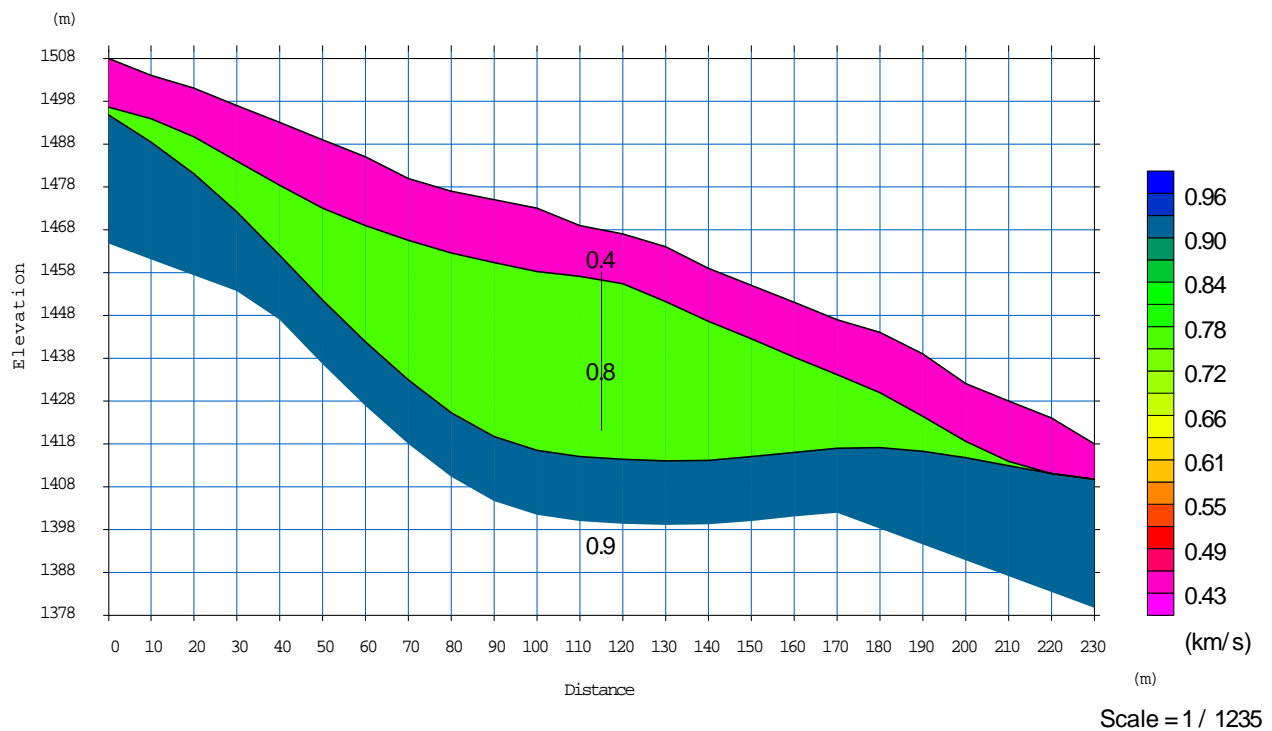


Fig. 136: Obtained velocity model affected by topography in the profile D of line 2 with detection of layer margins

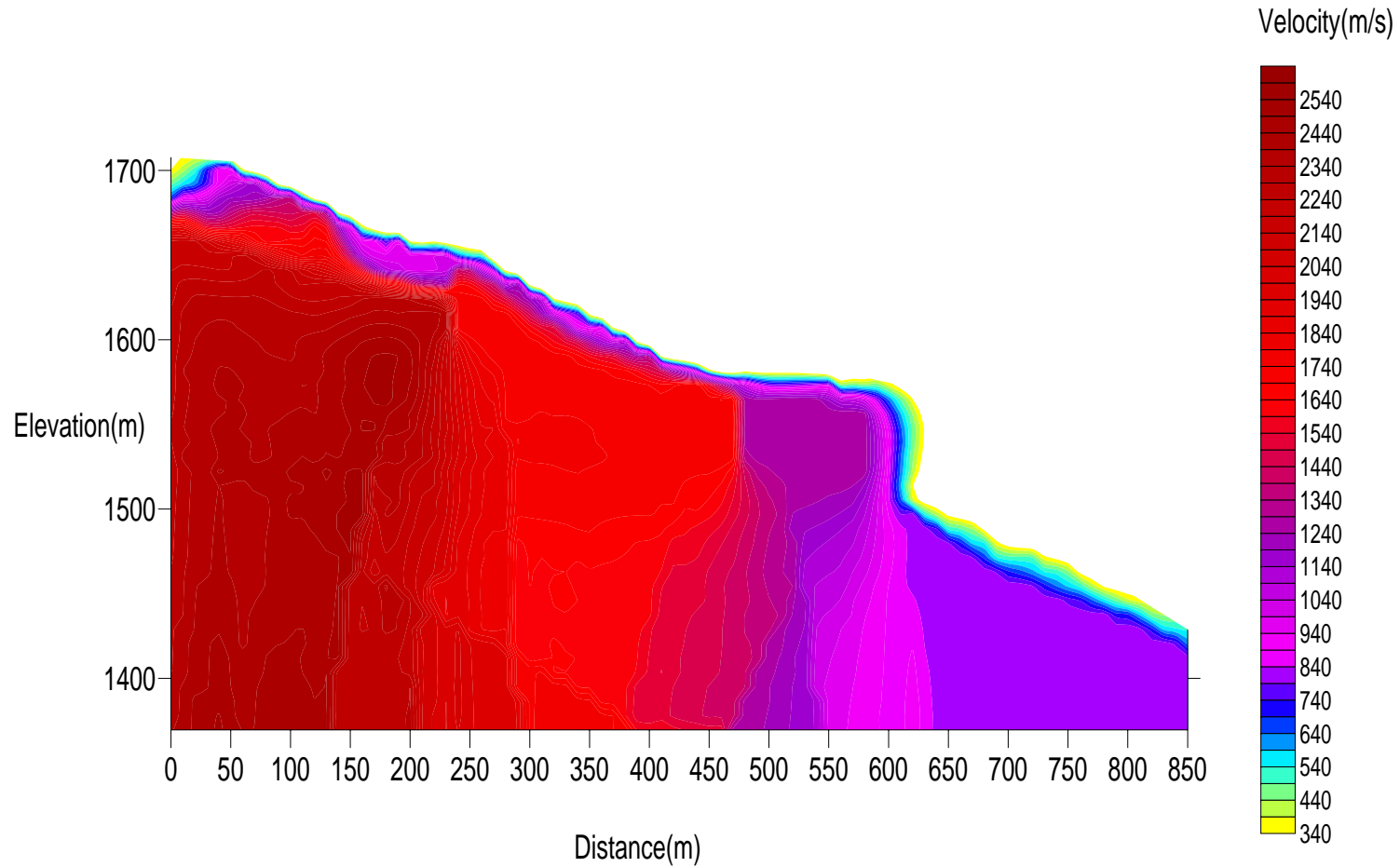


Fig. 137: Obtained velocity model affected by topography along the line 2, interpolated according to Kriging method

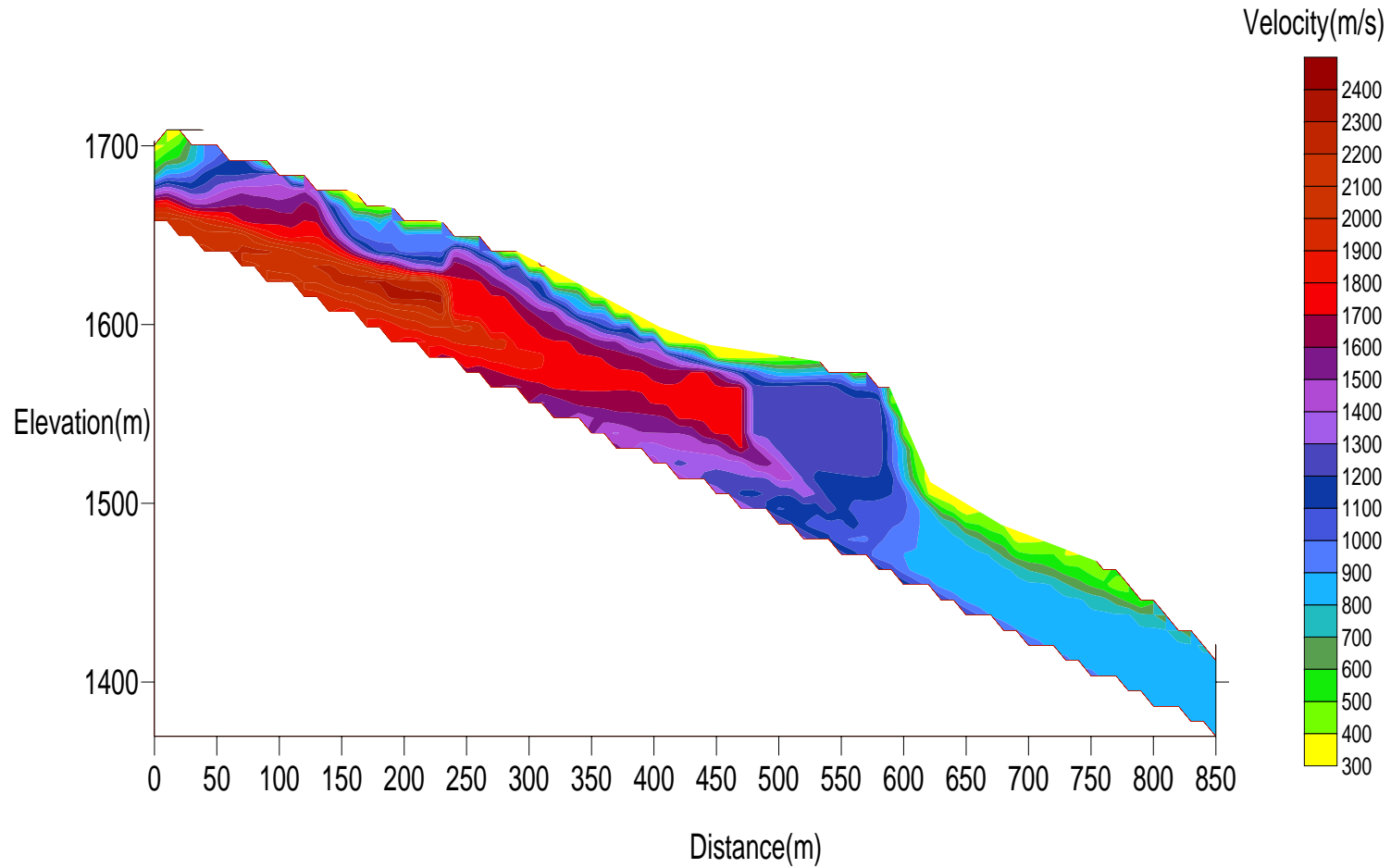


Fig. 138: Obtained velocity model affected by topography in the line 2, interpolated according to Triangular method

3.11. LINE 3 POROFILE A

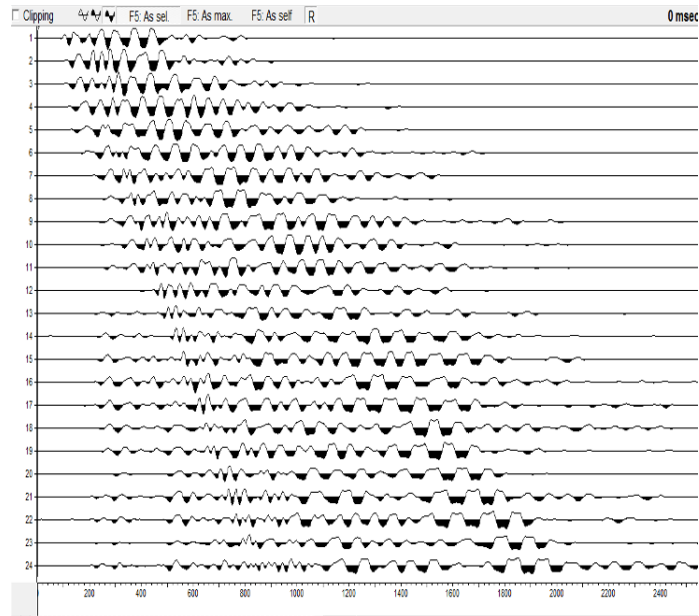


Fig. 139: Shot is located at 55 meters before the first geophone in the profile A of line 3

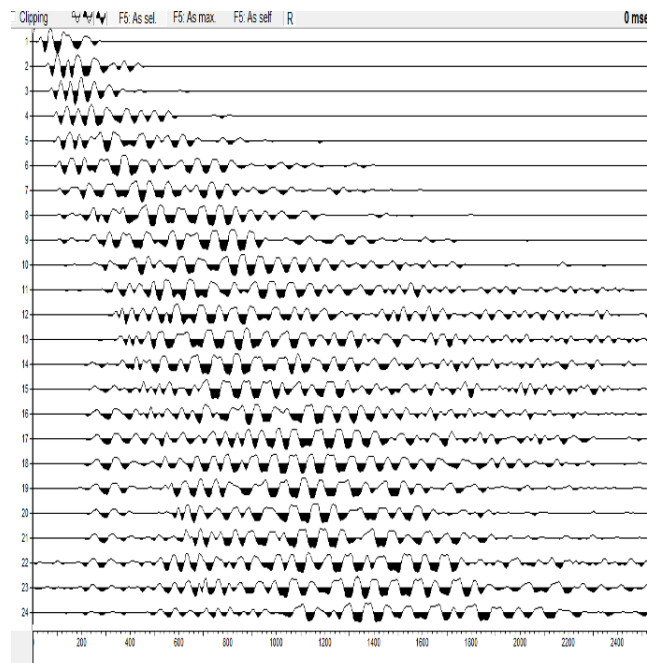


Fig. 140: Shot is located at 10 meters before the first geophone in the profile A of line 3

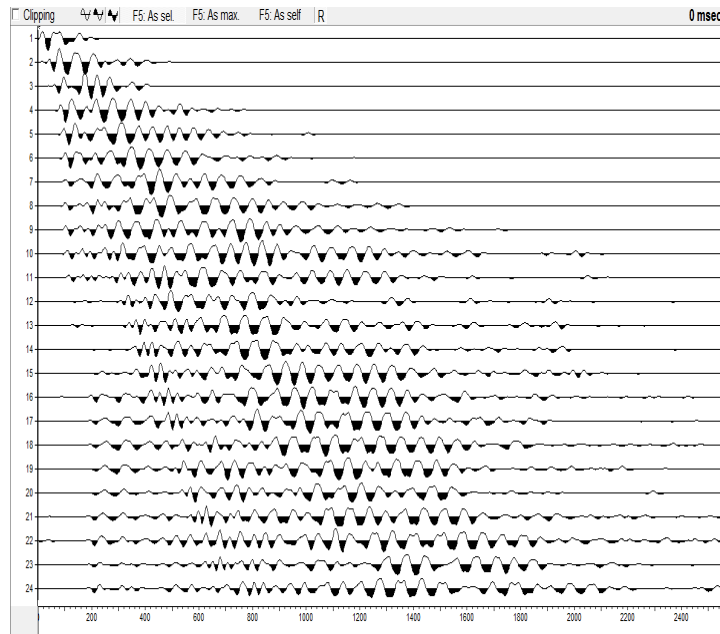


Fig. 141: Shot is located at 1 meter before the first geophone in the profile A of line 3

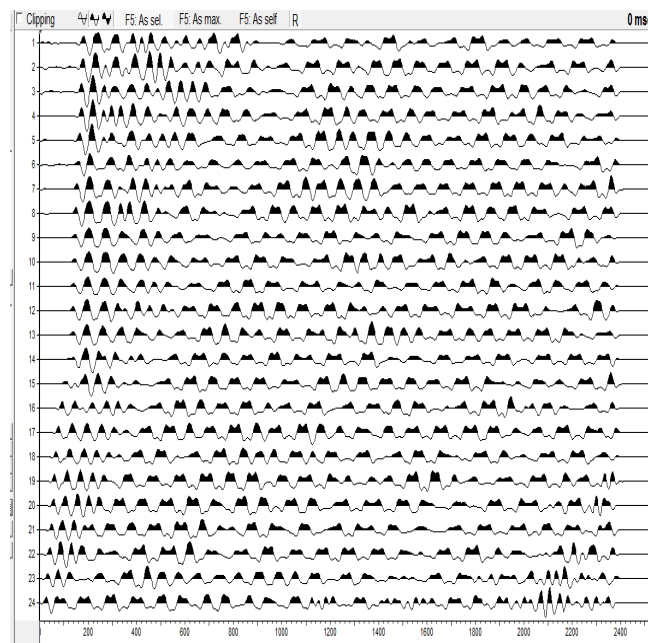


Fig. 142: Shot is located at 231 meters after the first geophone in the profile A of line 3

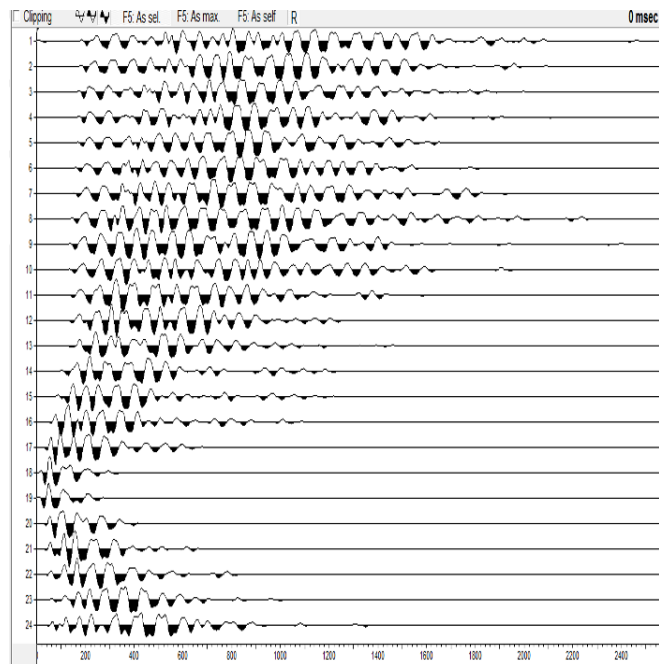


Fig. 143: Shot is located at 175 meters after the first geophone in the profile A of line 3

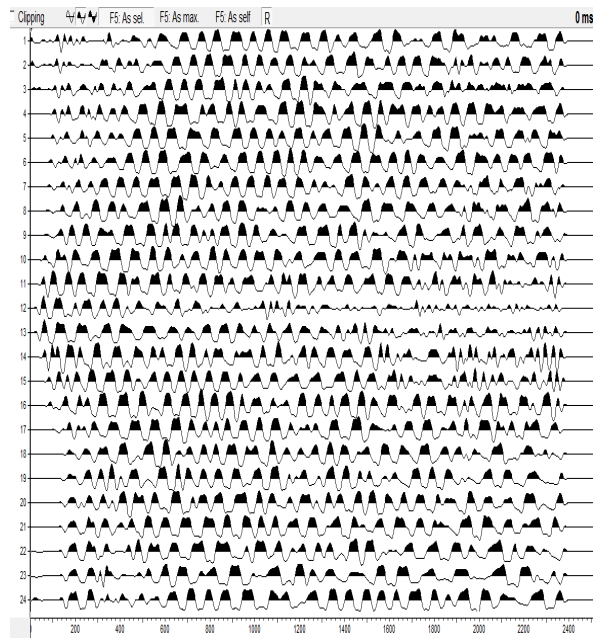


Fig. 144: Shot is located at 115 meters after the first geophone in the profile A of line 3

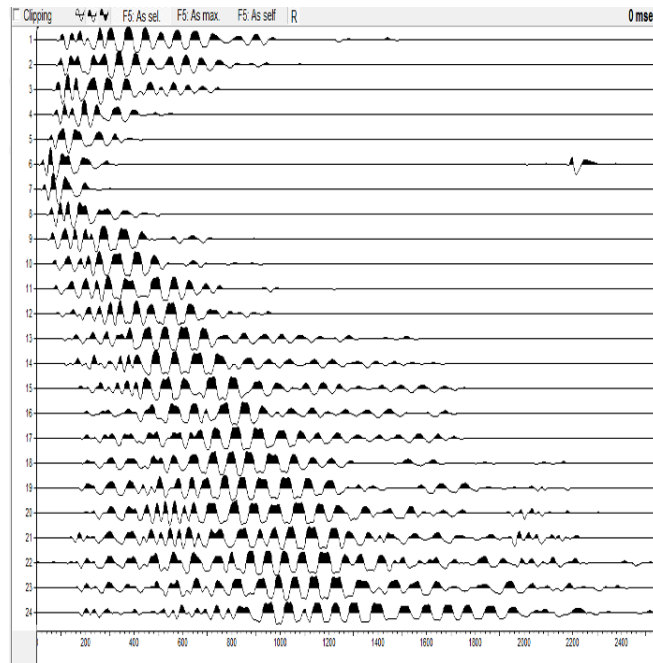


Fig. 145: Shot is located at 55 meters after the first geophone in the profile A of line 3

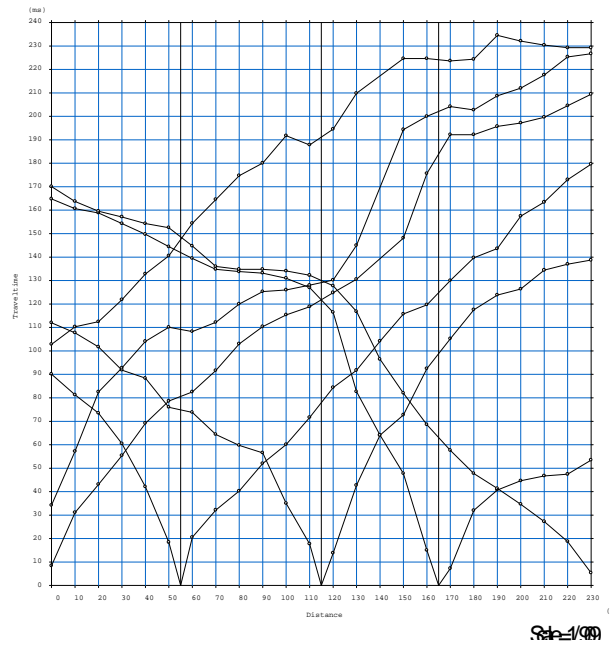


Fig. 146: Travel time curves of 7 shots of profile A of line 3

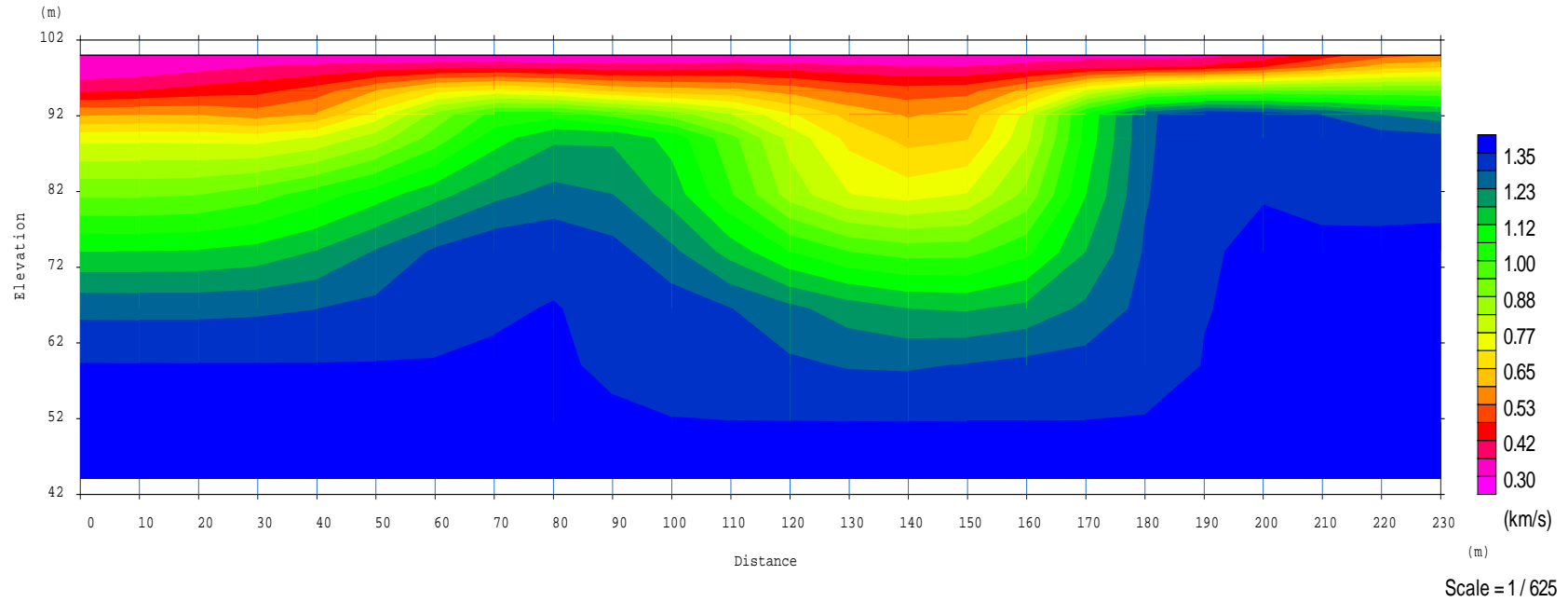


Fig. 147: Obtained velocity model not affected by topography in the profile A of Line 3

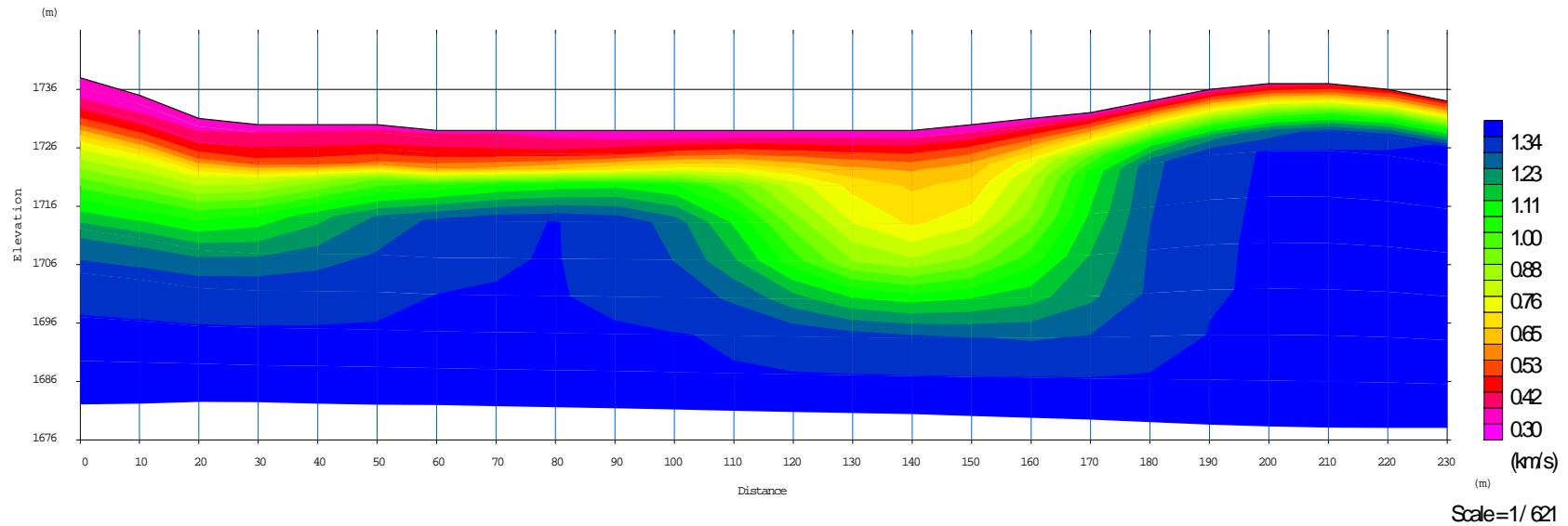


Fig. 148: Obtained velocity model affected by topography in the profile A of Line 3

Along the profile A of line 3, three layers with different velocities were detected. These layers, from top to the bottom could be loose soil (overburden), clay and fractured sandstone. Thicknesses of the first and second layers under each Geophone are presented in the below table:

Geophone Number	1	2	3	4	5	6	7	8	9	10	11	12	13	14	15	16	17	18	19	20	21	22	23	24
Thickness of first layer	7.5	9.86	9.68	10.01	9.32	8.31	7.17	6.68	5.82	4.64	3.26	2.97	3.11	2.63	1.42	0.74	0.38	0	0.65	2.17	3.84	5.46	6.03	5.13
Thickness of second layer	0.84	0	0	0	2.51	5.29	7.48	10.76	14.99	19.15	22.1	22.64	22.68	24.5	28.62	34.13	38.38	39.41	36.22	29.34	20.87	12.66	5.88	0.13

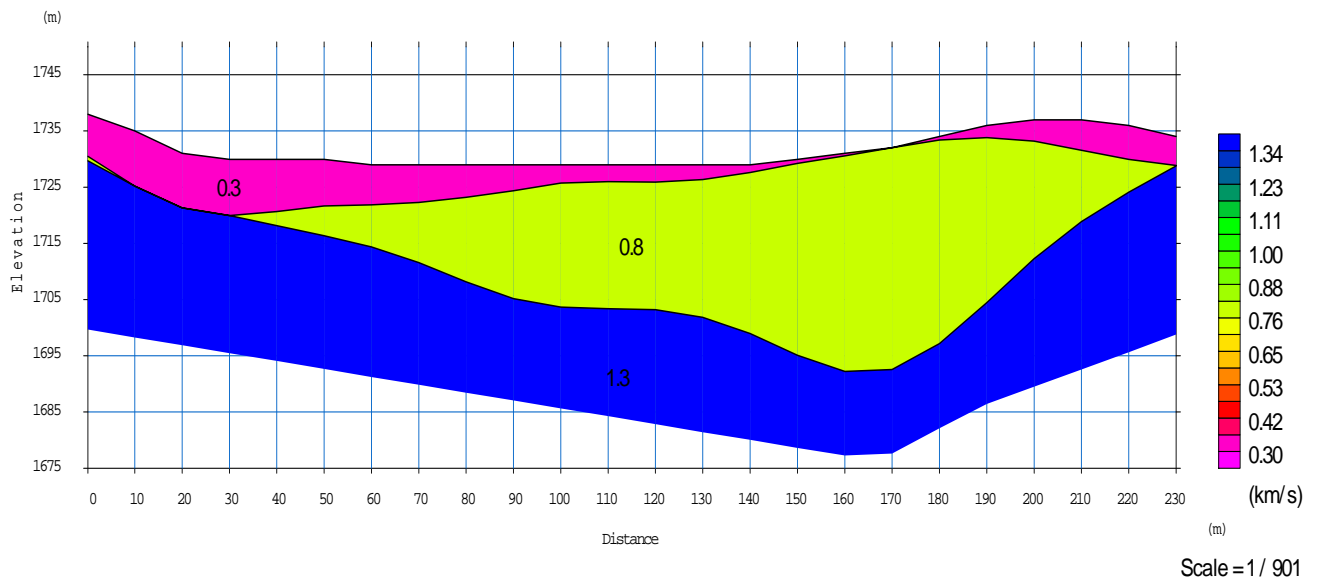


Fig. 149: Obtained velocity model affected by topography in the profile A of line 3 with detection of layer margins



CHAPTER 4

CONCLUSION

4. CONCLUSIONS

Based on the seismic profiles presented in "Chapter 3", the following conclusions can be made:

- Except at the end of the lines 1 and 2, the bedrock at depth of all the three lines are consisted of low velocity fractured rock masses (sandstone/siltstone) while, at shallower depth layers of loose soil (overburden materials) and clayey materials (weathered marl) could be detected.
- In the end of lines 1 and 2, the bedrock at depth are consisted of mixture of low velocity fractured rock masses (sandstone/siltstone) and clayey materials. It seems this mainly due to Ionakhsh fault crossing the lower part of the surveyed area. At shallower depth layers of loose soil (overburden materials) and clayey materials (weathered marl) could be detected.
- Based on the seismic profiles some synclinal structures could be identified that are covered by loose soil/clayey materials.
- No salt body could be detected in the surveyed area from surface to the depth of maximum 80 meters.



APPENDIX 1

PHOTOS



Photo 1: A sample of the geophones used for refraction seismic surveys at Rogun dam site



Photo 2: View of a geophone installed in the ground



Photo 3: A view of the recording equipment used for refraction seismic surveys



Photo 4: Boring and Explosion



Photo 5: A view showing the relatively steep topography along some parts of surveyed area

TECHNO-ECONOMIC ASSESSMENT STUDY FOR ROGUN HYDROELECTRIC CONSTRUCTION PROJECT

PHASE II: PROJECT DEFINITION OPTIONS

Volume 2: Basic Data

Chapter 2: Geology

Part B - Geological Investigation in the Right Bank

Annex 4-2 Report on Microravity Investigations

March 2014



*Joint Stock Company "ROGUN HYDROELECTRICAL POWER PLANT "
The Republic of Tajikistan*



Tunnel Dam Ariana Engineering Co.

Rogun Dam - Complementary Geotechnical Investigations at Right Bank

Final Report on Microgravity Investigations



SADD TUNNEL PARS
Consulting Engineers



SAMANIAN
Technical and Engineering Co.

Report and Revision No.	Date	Prepared by	Checked by Team Leader	Reviewed by Supervisors	Approved by Project Manager
STP No.: Geoph/Rep.01/Rev.0	Nov. 2012	Dr. V.E. Ardestani S. Salimi	H. A. Chehreh	A. Mehinrad A. Farazmand	Kh. Binazadeh
ATD No.:					



Table of content

1. Introduction	5
1.1. Location of the Site	5
1.2. Site Geology	6
2. Microgravity Method	9
2.1. Height of the Points	9
2.2. Time	9
2.3. Latitude	9
2.4. Interpretation Process	10
2.4.1. Gravity Corrections	10
2.4.1.1. Latitude Correction	10
2.4.1.2. Tidal Correction.....	10
2.4.1.3. Free Air Correction.....	11
2.4.1.4. Bouguer Correction.....	11
2.4.1.5. Topographical Correction.....	11
2.4.2. Bouguer Anomaly.....	11
2.5. Filters.....	11
2.5.1. Vertical Gradient	11
2.5.2. Upward Continuation.....	12
2.5.3. Euler Depths.....	12
2.5.4. Analytical Signal	12
2.5.5. Apparent Density	12
2.6. Softwares	13
3. Microgravity Investigations at Right Bank	15

3.1.	Field Procedures of Micro gravity	15
3.2.	Interpretation Strategy	15
3.3.	Interpretation of the Proposed Site.....	16
3.4.	Anomaly No. 1.....	17
3.5.	Three Dimensional Modeling.....	30
4.	Conclusions	43
4.1.	Geological Interpretation.....	43
4.2.	Recommendation.....	44
5.	References	46

List of Table

Table (1): Gravity effect of a rectangle with contrast density	13
Table (2): Coordinates of the center of anomaly No. 1	17
Table (3): Main Characteristics of anomaly No. 1.....	30
Table (4): 3D Coordinates of the center of the anomaly	31
Table (5) : Main geological units observed in Borehole No. DZ-02	43

List of Figure

Fig. (1) : General view of microgravity network	6
Fig. (2) : Geological Map of Rogun dam site	7
Fig. (3) : Effect of height of the point.....	9
Fig. (4): Underground contrast density effect	10
Fig. (5) : Schematic illustrate of free air correction effect	11

Fig. (6) : CG3 gravimeter used for data recording	15
Fig. (7): Reflects the terrain of the surveyed area	18
Fig. (8): Topographical corrections	19
Fig. (9): Bouguer anomalies	20
Fig. (10): Residual gravity anomalies	21
Fig. (11): Anomalies at the depth of 20 meter.....	22
Fig. (12): Anomalies at the depth of 40 meter.....	23
Fig. (13): Anomalies at the depth of 70 meter.....	24
Fig. (14): Anomalies at the depth of 100 meter.....	25
Fig. (15): Anomalies at the depth of 120 meter.....	26
Fig. (16): Anomalies at the Euler depth.	27
Fig. (17): Analytical signal of the anomalies.....	28
Fig. (18): Apparent density Map	29
Fig. (19): Residual Anomalies – window of modeling	31
Fig. (20): Topography- window of modeling.....	32
Fig. (21): The density contrasts after applying the mentioned algorithm at the 1750 horizon	33
Fig. (22): The density contrasts after applying the mentioned algorithm at the 1720 horizon	34
Fig. (23): The density contrasts after applying the mentioned algorithm at the 1700 horizon	35
Fig. (24): The density contrasts after applying the mentioned algorithm at the 1680 horizon	36
Fig. (25): The density contrasts after applying the mentioned algorithm at the 1660 horizon	37
Fig. (26): The density contrasts after applying the mentioned algorithm at the 1640 horizon	38
Fig. (27): The density contrasts after applying the mentioned algorithm at the 1630 horizon	39
Fig. (28): Sections through center of negative anomaly.....	40
Fig. (29): Lateral extension of the anomaly	41



CHAPTER 1

INTRODUCTION

1. Introduction

"Rogun" dam and power plant is under construction on "Vakhsh" river at about 110 kilometers far from north-east of the city of Dushanbe, Tajikistan.

The dam is a rockfill dam with impervious core and in its final stage will be 335 m high. Therefore, it will be the highest dam in the world. Rogun underground powerhouse, with its 6 turbines each with nominal capacity of 600 MW will have a total nominal capacity of 3600 MW for the whole power plant.

According to the planning and scheduling by the Client (Rogun HPP), the first two units (1200 MW) of the Rogun powerhouse shall be commissioned as the first stage of the project. In order to achieve this goal, the river closure shall be done as soon as possible, by which construction of the upstream cofferdam and then stage 1 dam can be effectively started.

This report consists of five chapters and two appendices. The present chapter is dedicated to "Introduction". In "Chapter 2" the introduction to microgravity method is described. "Chapter 3" explains microgravity investigations at right bank of Rogun dam and provides descriptions on the anomalies and its 3D modeling. In "Chapter 4" conclusions and recommendation are provided. Finally, in "Chapter 5" the referenced documents are listed.

1.1. Location of the Site

The area under consideration is located in a mountainous region with a rough topography close to the Rogun in Tajikistan where a dam will be constructed.

A microgravity network is designed for investigating the underground anomalies in the proposed area (Fig. (1)). The base coordinates of the network are $X=25115.88$ and $Y=22305.6$ meters in local coordinate system.

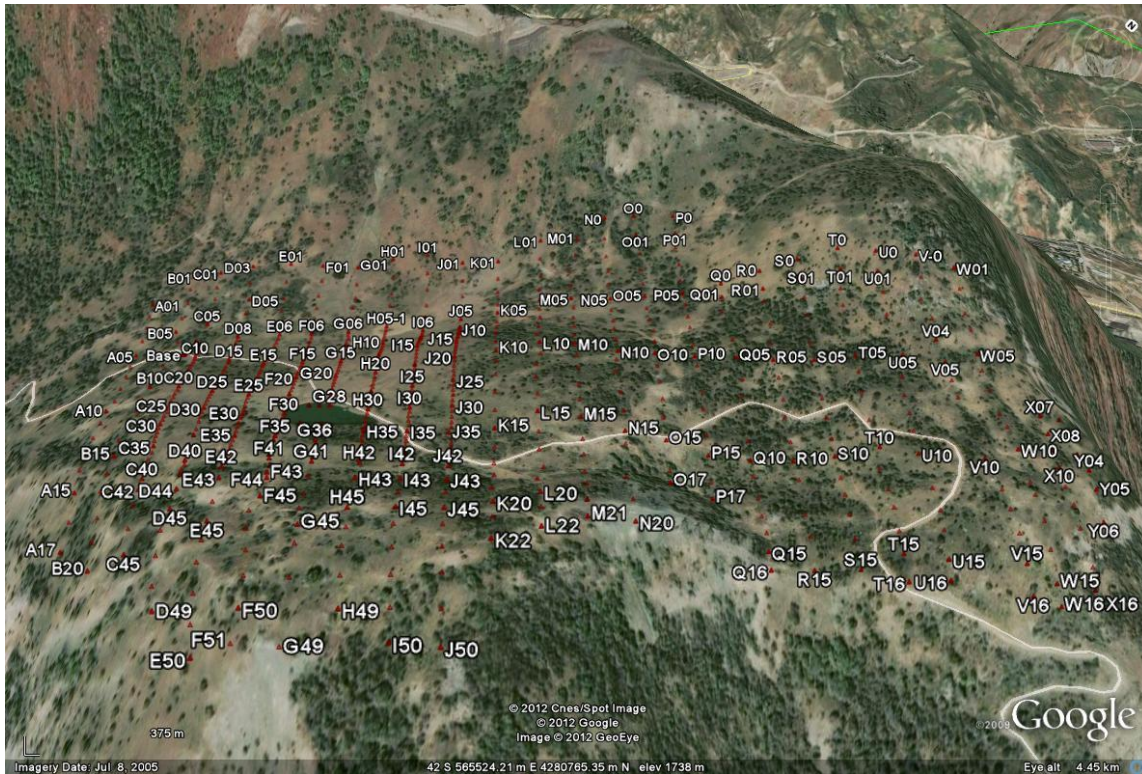


Fig. (1) : General view of microgravity network

1.2. Site Geology

The main Geological units in the surveyed area are as follows [6]:

Cretaceous: silt, mud, sandstone, granodiorite, Conglomerate and limestone.

Triassic: Evaporates (Gypsum and Halite).

The geological map is shown in Fig. (2) [6].

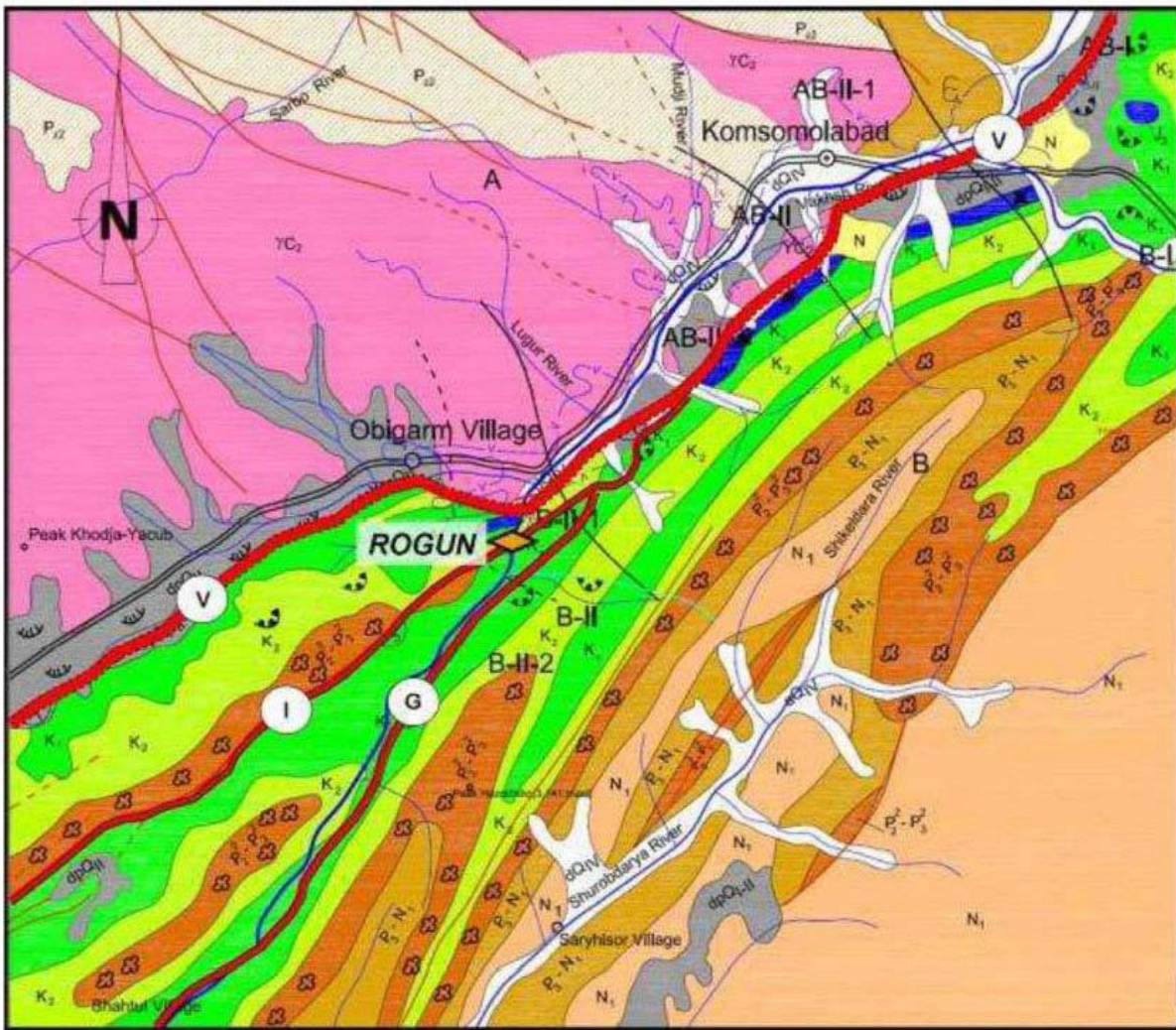


Fig. (2) : Geological Map of Rogun dam site

V = Vakhsh Fault, I = Ionaksh Fault, G = Gulizindan Fault.

Green and yellow green: Cretaceous made of silt, mud and sandstone;

Pink: granodiorite;

Brown: conglomerate and limestone.

Dark blue: Triassic including evaporates (gypsum and halite).



CHAPTER 2

MICROGRAVITY METHOD

2. Microgravity Method

One of the most important physical forces in universe is gravity which can be compute through Newton formula:

$$F = G \frac{m_1 m_2}{d^2}$$

$6.673 * 10^{-8} \text{ gr/cm}^3 \text{ sec}^2$ where G is the gravitational constant and is equal to and m1 and m2 are the attracted and attracter masses.

The base parameter in applied gravity is the acceleration of gravity (g) and its unit is mGal which is equal to 1/100000 meter to squared second. This acceleration of the earth depends on different following factors.

2.1. Height of the Points

The gravity acceleration decreases with increasing the heights.

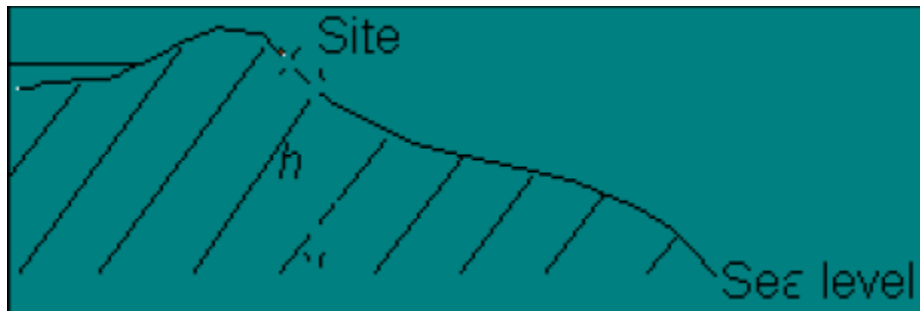


Fig. (3) : Effect of height of the point

2.2. Time

The gravity acceleration changes during the time in a constant location due to the tidal forces of celestial bodies like Moon and Sun.

2.3. Latitude

The amount of gravity acceleration decreases in low latitudes.

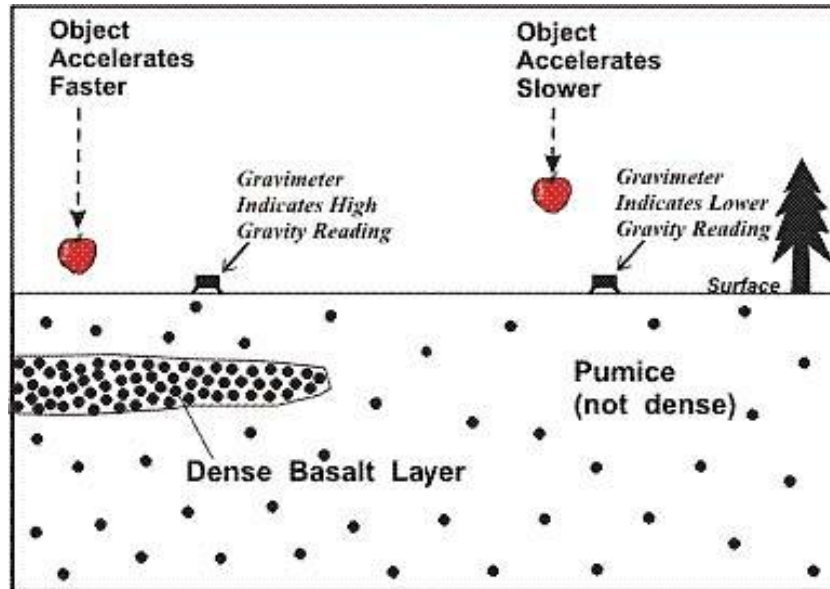


Fig. (4): Underground contrast density effect

Therefore the change in gravity acceleration after correction the other factors such as height, time etc. demonstrate the underground contrast density (Fig. (4)).

2.4. Interpretation Process

2.4.1. Gravity Corrections

2.4.1.1. Latitude Correction

For this correction we use the following formula:

$$\frac{dg}{ds} = 1.37 \sin 2\phi \quad (2)$$

Where ϕ is the average Latitude of the site and dg/ds is the correction in m Gal for 1 mile in north-south direction.

2.4.1.2. Tidal Correction

This correction is done using the repeat gravity measurements in base points and applying the Geosoft software (Ver. 7).

2.4.1.3. Free Air Correction

Measuring the Orthometric heights of the points the following formula is applied Δg (free air) = $0.33086 * h$ (mGal/ meter)



Fig. (5) : Schematic illustrate of free air correction effect

2.4.1.4. Bouguer Correction

The standard formula is used for this correction,

$$\Delta g = 2\pi G\rho h \quad (4)$$

Where h is the thickness of the Bouguer slab (heights of the points) and G is the gravitational constant and ρ is the density of the Bouguer slab.

2.4.1.5. Topographical Correction

This correction is done by using the Digital Terrain Model (DTM) of the area and through Geosoft software.

2.4.2. Bouguer Anomaly

After performing the mentioned correction the Bouguer anomalies are computed by,

$$g\beta = g - \delta f + \delta\beta - \gamma \quad (5)$$

Where g is the observe gravity after drift and tidal corrections and δf and $\delta\beta$ are the free air and Bouguer corrections respectively and γ is the normal gravity which can be computed through standard formula.

2.5. Filters

2.5.1. Vertical Gradient

This filter can be applied to Bouguer gravity anomalies for enhancing the near surface anomalies and through following equation in Geosoft software and by FFT method:

$$\frac{\partial^N g}{\partial z^N} = \frac{1}{4\pi^2} \int_{-\infty}^{+\infty} \int_{-\infty}^{+\infty} G_0(p, q)(p^2 + q^2) \mathbf{exp}[i(px + qy)] dpdq \quad (6)$$

Where p and q are the frequencies, g is the gravity, N is the degree of gradient and $G_0(p, q)$ is the Fourier transform of gravity data.

2.5.2. Upward Continuation

This filter is used for qualitative interpretation and estimation the maximum depths of the anomalies based on the following formula

$$g_z(x, y) = \frac{1}{4\pi^2} \int_{-\infty}^{+\infty} \int_{-\infty}^{+\infty} G_0(p, q) \pm z \sqrt{p^2 + q^2} \mathbf{exp}[i(px + qy)] dpdq \quad (7)$$

Where z is the distance of up-ward continuation.

2.5.3. Euler Depths

This method is used for estimating the minimum to average depths of the anomalies and according the standard formula,

$$(x - x_0) \frac{\partial g}{\partial x} + (y - y_0) \frac{\partial g}{\partial y} + (z - z_0) \frac{\partial g}{\partial z} = Ng \quad (8)$$

Where x_0, y_0, z_0 are the coordinates of a point of the underground anomaly.

2.5.4. Analytical Signal

This filter is suitable for detecting the edbes of the anomalies and can be computes by,

$$|A(x, y)| = \sqrt{\frac{\partial^2 g}{\partial x \partial z} + \frac{\partial^2 g}{\partial y \partial z} + \frac{\partial^2 g}{\partial z^2}} \quad (9)$$

The maximum values of the analytic signal ($A(x, y)$) represent the edges of the anomalies.

2.5.5. Apparent Density

The observed gravity anomalies are simulated by a layer with constant thickness and varying densities. This filter provide a rough estimation of contrast densities,

$$g(x, y, h) = 2\pi Kh \sigma(x, y, h) \quad (10)$$

Where K is the gravitational constant and σ represents the contrast density, g is the gravity effect.

To demonstrate the relation between the resolution of the gravity anomalies and the dimensions of the subsurface sources (anomalies), the gravity effect of a rectangular with contrast density equal to 1 is computed by Talwani formula [3] and demonstrated in Table (1):

Table (1): Gravity effect of a rectangle with contrast density

Minimum Depth (m)	Maximum Depth (m)	Length of the rectangle	Gravity effect (mGal/1000)
11	15	5	25
30	40	5	23
50	60	10	24
100	115	10	18
150	170	10	16
200	220	20	25
300	320	20	17
400	420	25	16
500	525	25	16
600	625	30	16
700	730	30	16
800	830	35	17

Considering the condition of the site if the minimum amount of gravity effect is assumed to be equal to 20 mGal/1000 (micro Gal), for detecting a cavity in 50 meter depth, the average length of it must be about 5 meter.

2.6. Softwares

The commercial software Geosoft (Ver.7) and GMSYS-2D are applied for the aforementioned corrections and filters.

CHAPTER 3

MICROGRAVITY INVESTIGATIONS

AT RIGHT BANK

3. Microgravity Investigations at Right Bank

3.1. Field Procedures of Micro gravity

A Scintrex CG3 gravimeter with a sensitivity of 5 micro gal is used for recording the data (Fig. (6)).



Fig. (6) : CG3 gravimeter used for data recording

Totally 684 gravity points are measured along 25 profiles in the survey site. The distance of the points on the profiles is 10 to 30 meters and the spacing between the profiles is about 50 meters.

3.2. Interpretation Strategy

The main object of the microgravity survey is to check presence of evaporate concentrations. The evaporates (Gypsum and Halite) shows the negative relative anomalies due to their low density in comparison to the host rocks.

After the gravity corrections on observed gravity the Bouguer anomalies are computed. As we are looking for the relative negative gravity anomalies representing the probable

evaporate, the anomalies with blue to dark blues are our desired ones. At the next step and after the computation of Bouguer anomalies the trend effect is removed using the standard method of polynomial fitting (Geosoft) and the residual gravity anomalies are computed consequently. The Euler depths estimate the minimum depth of the anomalies. The up-ward and down-ward filters are used to estimate the maximum depths of the anomalies.

The proposed filters are used for qualitative and quantitative interpretation.

This strategy is used in several microgravity projects in dam sites and some of the results are published in pioneer journals [1] and [2].

3.3. Interpretation of the Proposed Site

The first figure reflects the terrain of the survey area (Fig.7).The topographical corrections (Geosoft) are presented in Fig. (8). After the standard mentioned corrections, the Bouguer anomalies are computed through eqn. (5) and shown on Fig. (9). It is worth to mention that the Bouguer density is considered equal to 2.6 gr/cm^3 according to the report [7]. In this figure the low-density zones are demonstrated by the dark blue color. The residual gravity anomalies are computed and the results are shown in Fig. (10). in this figure five main negative anomalies are numbered. These negative anomalies belong to the low-density zones (probably evaporates) and their detection is our main target at this project.

In Fig. (9) the relative negative anomalies numbers 2,3 and 4 are located in the borders of the gravity network and could be artifacts. For example anomalies numbers 2 and 3 could be generated due to the error in the terrain corrections of the high gradient topography beside them.

Theoretically the gravity network could be expanded (if it is possible in practice) around the anomalies numbers 2,4 and 3 in directions south-east and north-west respectively.

In the other hand by inspecting the terrain of the survey area, we find out high gradient topography in these directions. So concluding that these anomalies (number 2,3 and 4) are generated by topographical effects seems to be reasonable.

Anomaly number 5 is a small low-density zone that most probably is generated by shallow sources.

The most important negative anomaly is anomaly No. 1 which is quite large and locates in the center of the survey area. The center of the anomaly No. 1 is presented in table (2).

Table (2): Coordinates of the center of anomaly No. 1

No.	X (UTM)	Y (UTM)
1	25527.8	22518.8

Applying the up-ward and down-ward methods, the anomalies are shown in deeper horizons in Figs. (11) to (15). The Euler depths are also shown in Fig. (16). the analytic signal of the anomalies is represented in Fig. (17). the apparent density

Map is shown in Fig. (18). This figure is computed for a constant layer with the thickness equal to 50 meters and the values are density contrasts.

3.4. Anomaly No. 1

There is a vast anomaly between profiles K and L. Its center is between points K11 and L12.

Considering the shape of the anomaly, it is generated by a vast low-density zone probably evaporates.

Considering the depth figures (11) to (15), the maximum depth of this anomaly or better to say its depth extension is about 120 m as it can be seen in Fig. (15).

The Euler depths are quite various in different parts of the anomaly (Fig. (16)). Considering the color circles, the depths are form 20 m to 40 m in the borders of the anomaly. Inspecting Fig. (17) the analytical signal is not high at the location of the anomaly number. So the anomaly has not sharp borders. The apparent density map shows a maximum about -0.4 gr/cm^3 density contrast at location of this anomaly.

The depths and density contrast can also be computed through modeling.

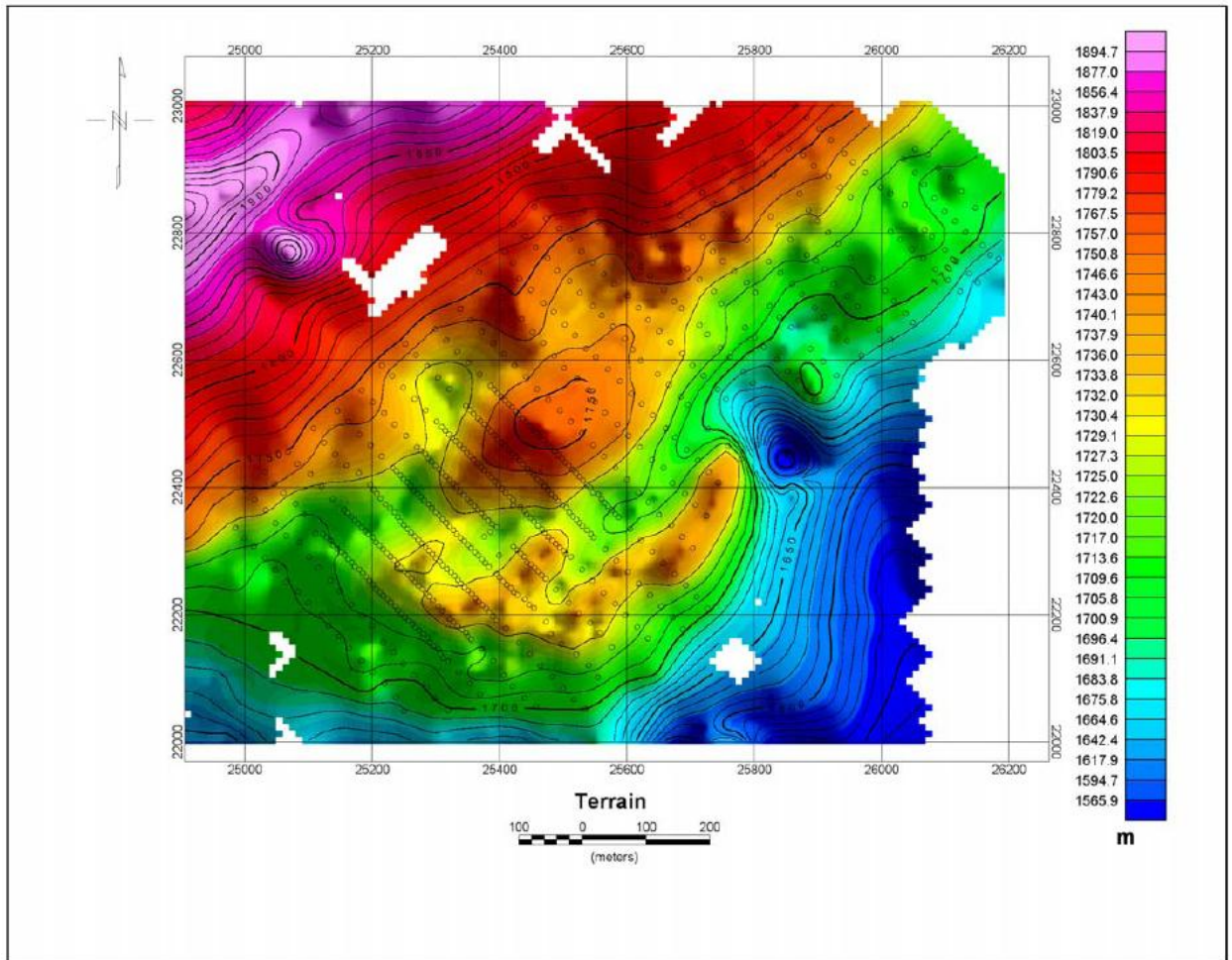


Fig. (7): Reflects the terrain of the surveyed area

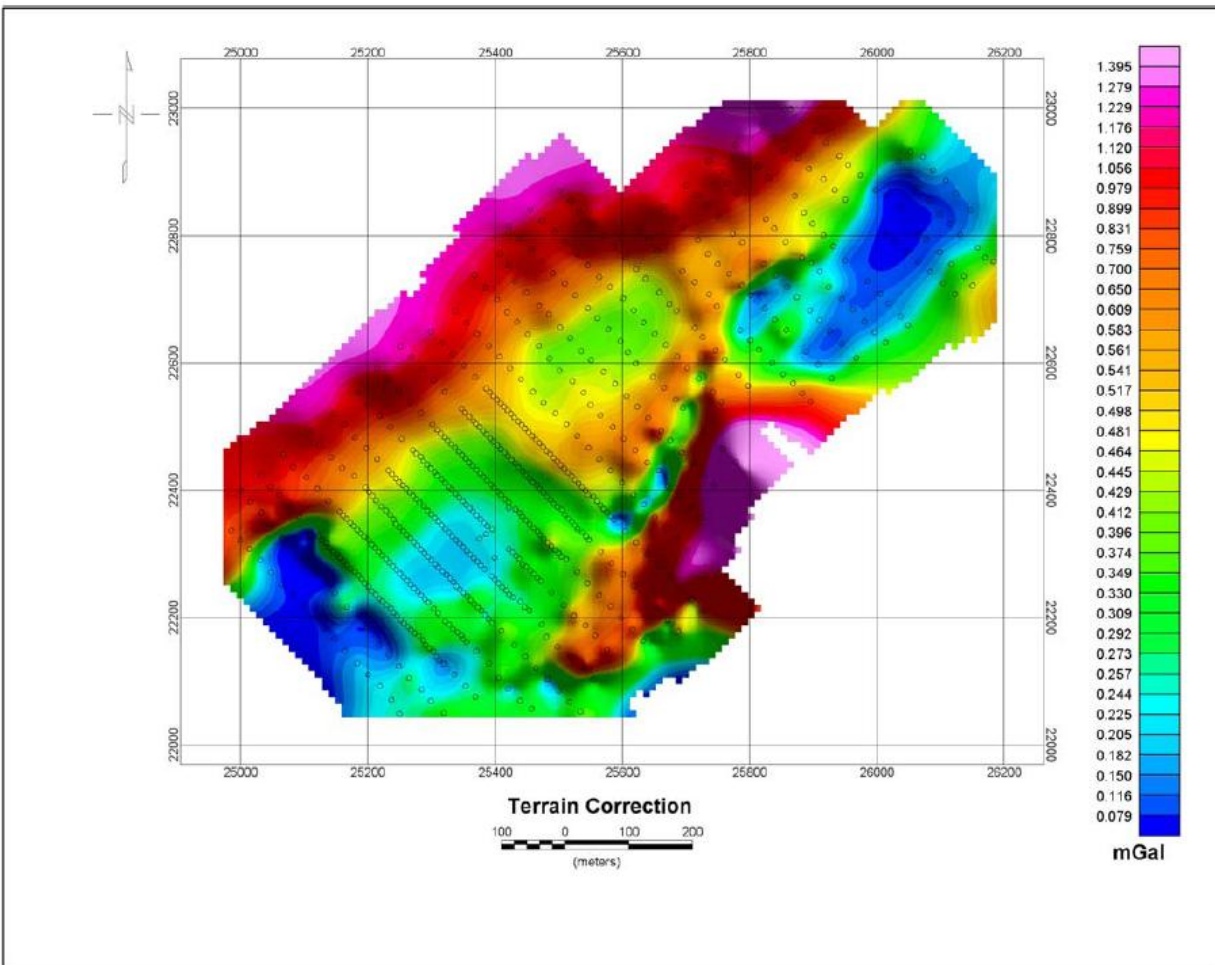


Fig. (8): Topographical corrections

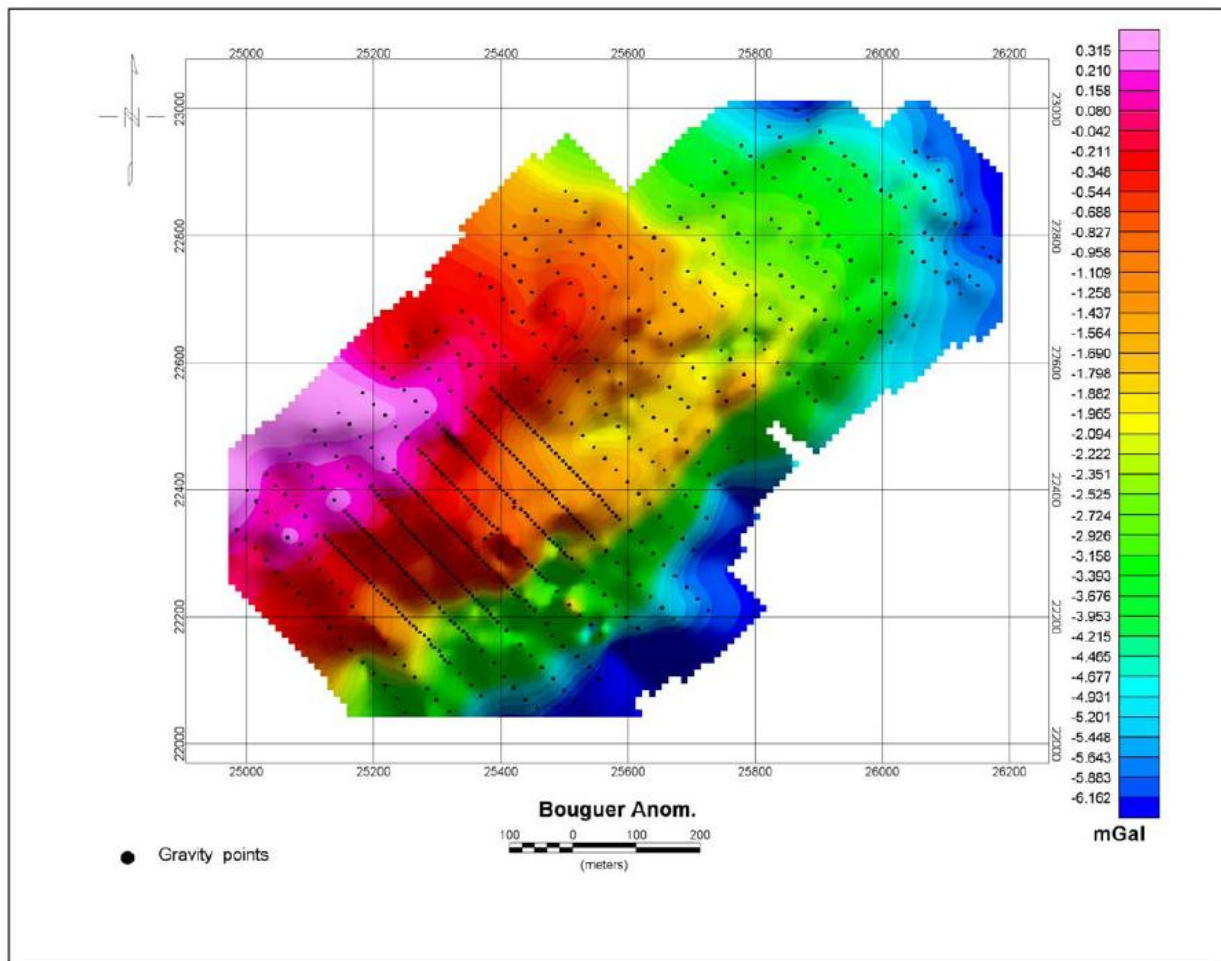


Fig. (9): Bouguer anomalies

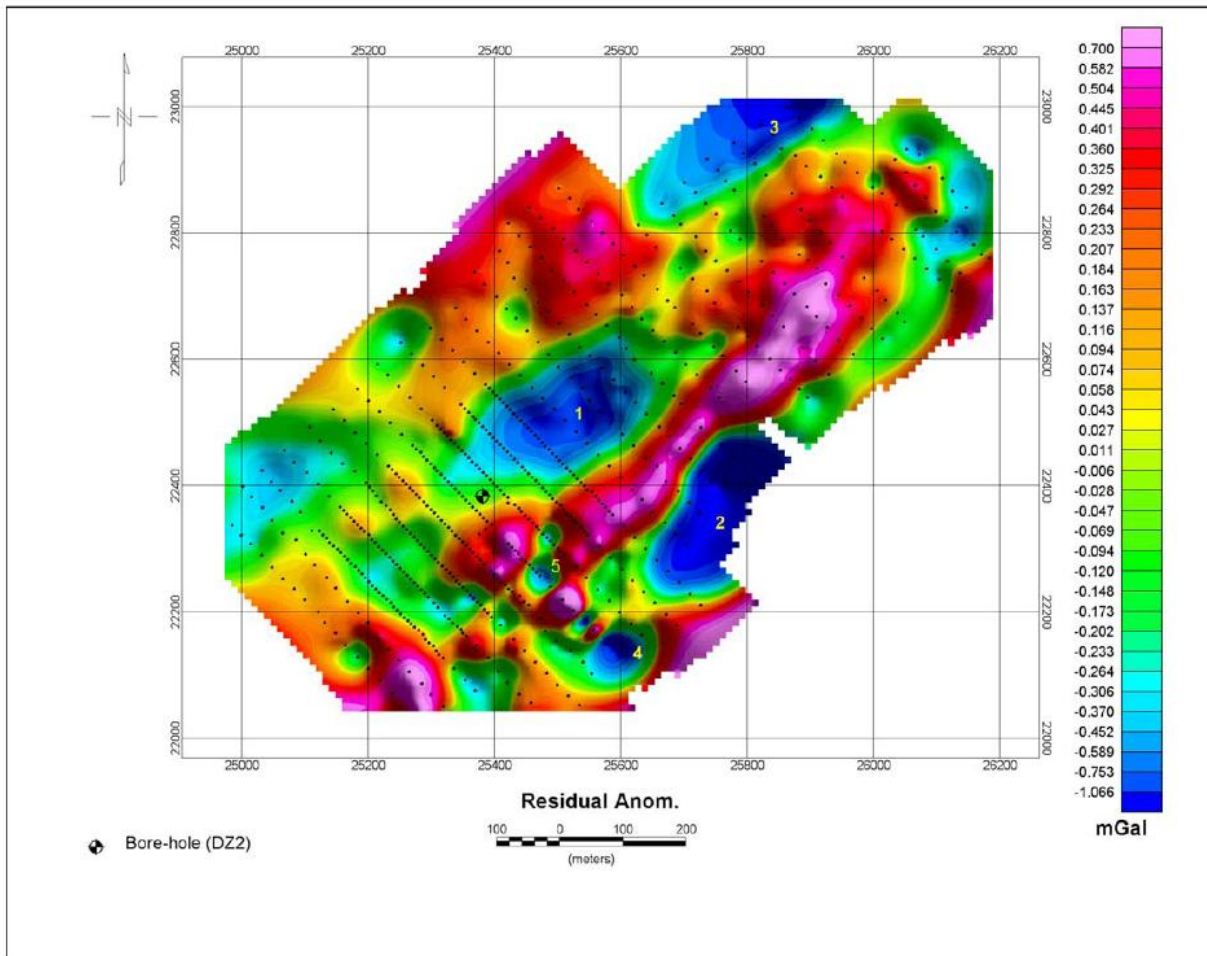


Fig. (10): Residual gravity anomalies

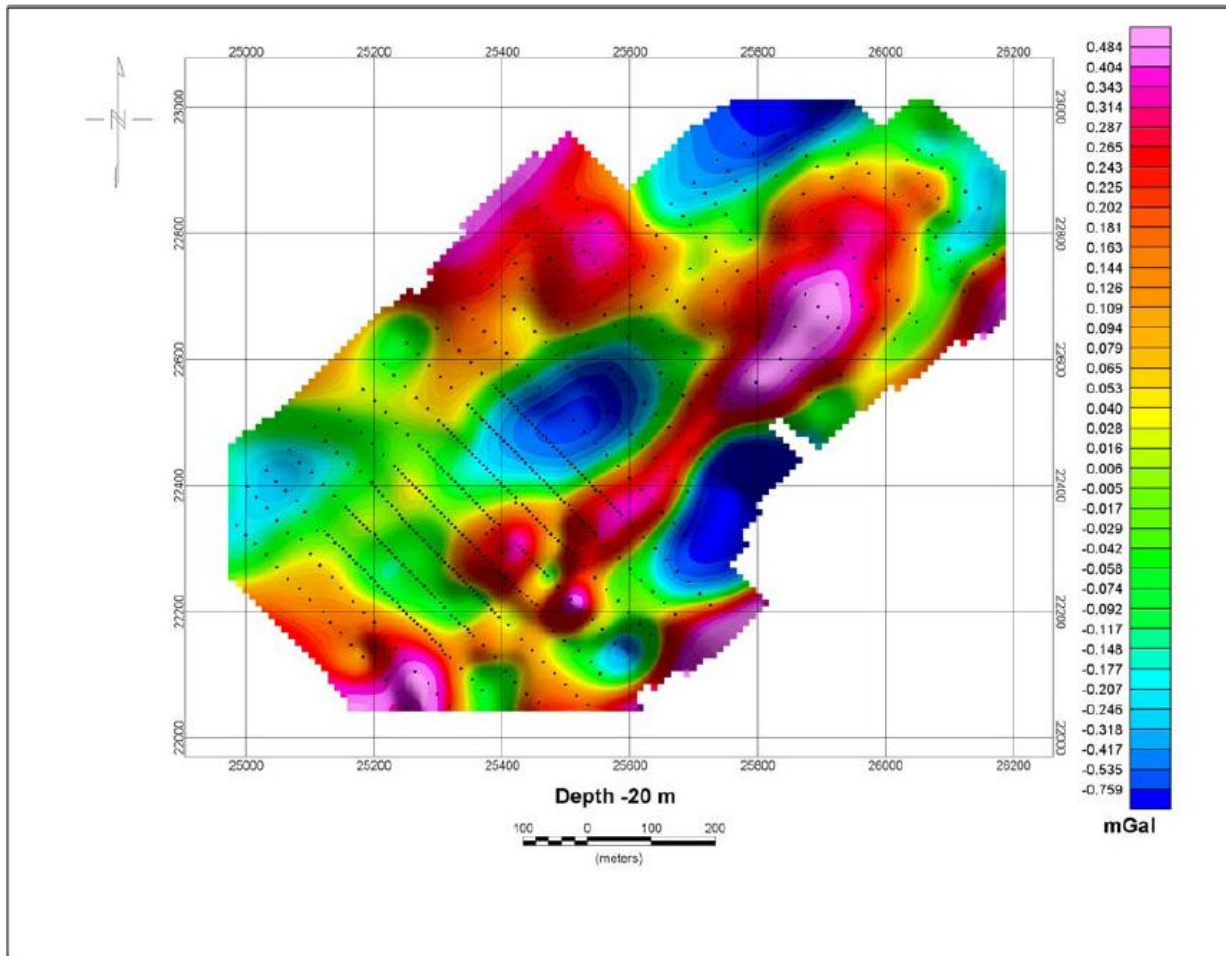


Fig. (11): Anomalies at the depth of 20 meter.

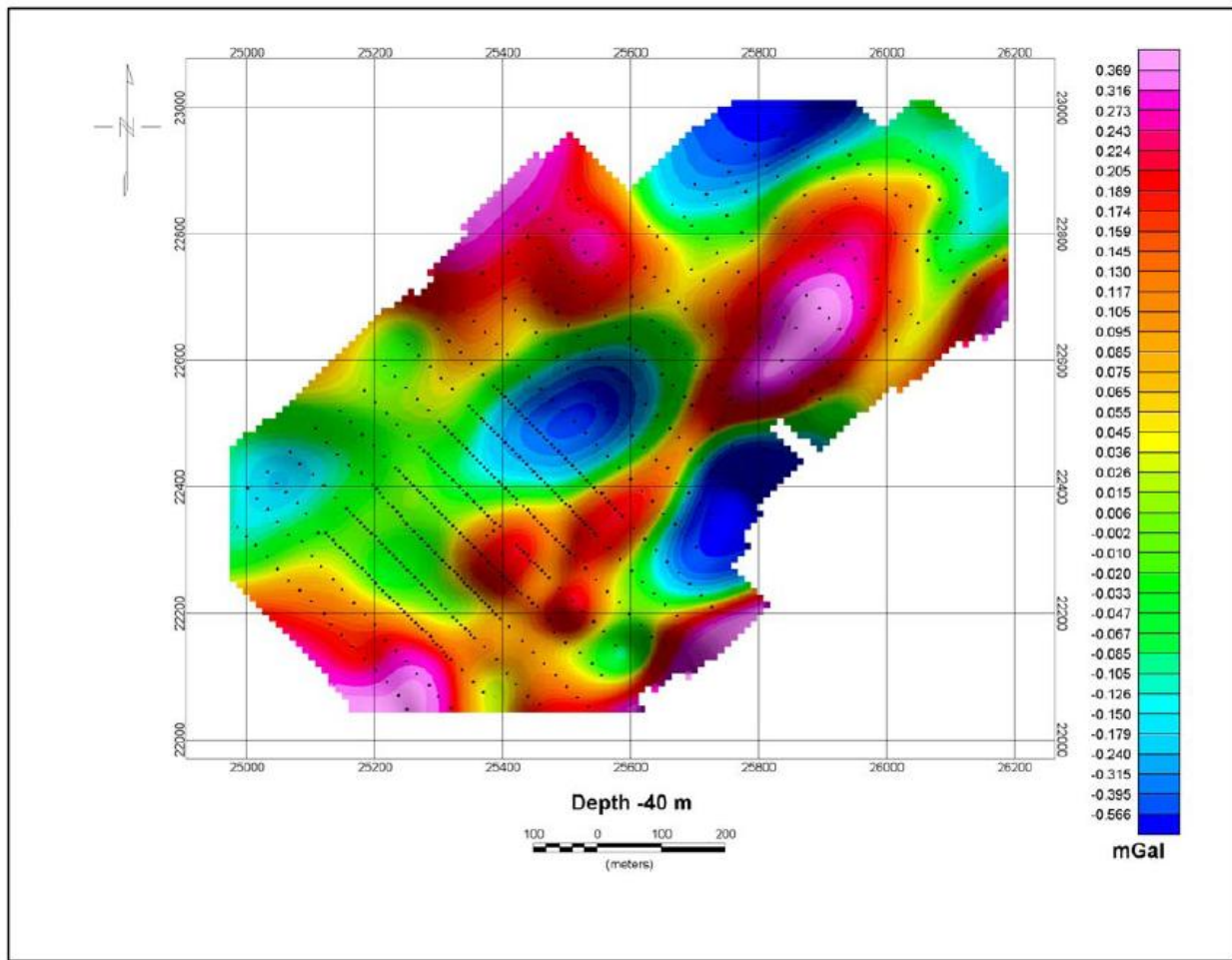


Fig. (12): Anomalies at the depth of 40 meter.

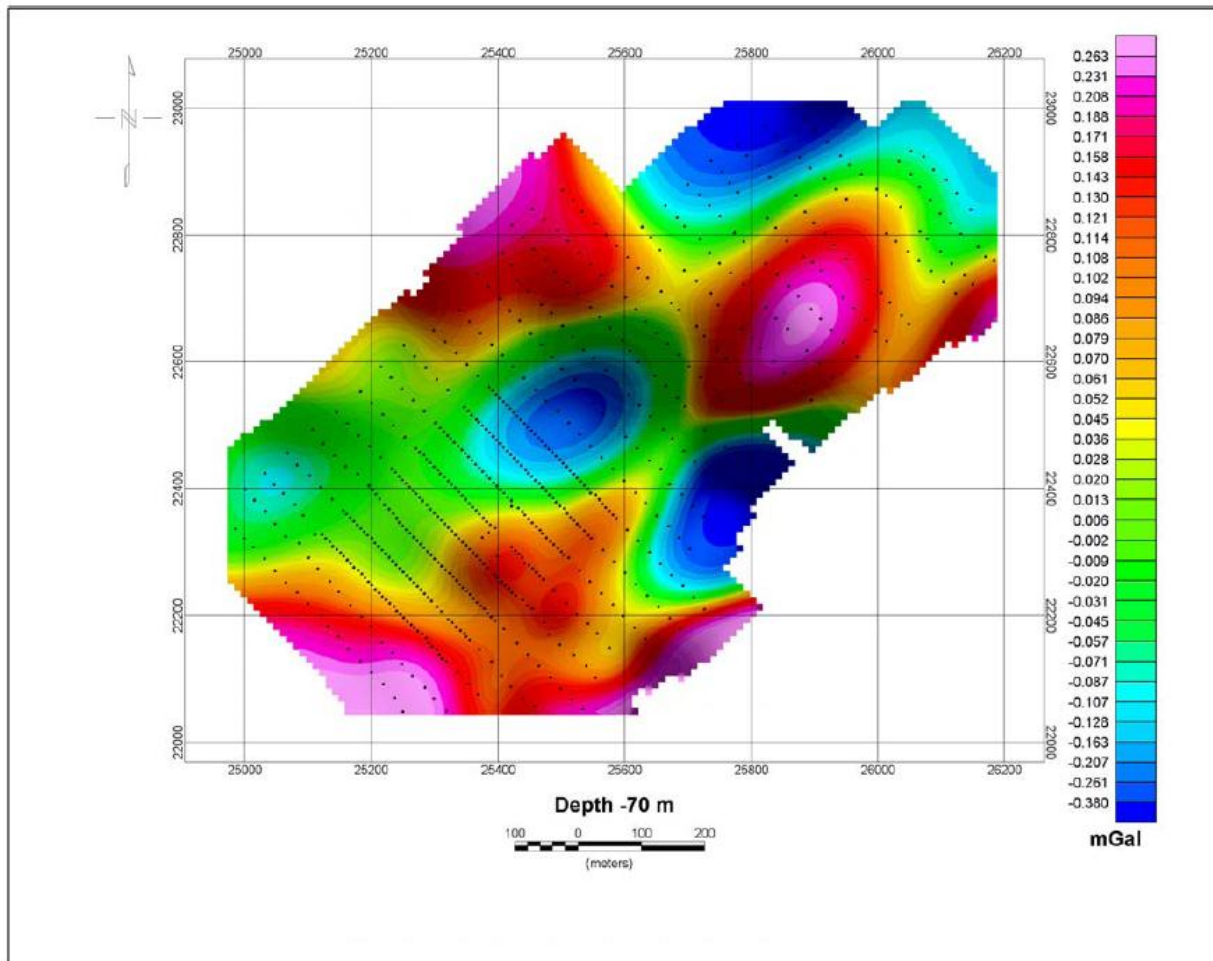


Fig. (13): Anomalies at the depth of 70 meter.

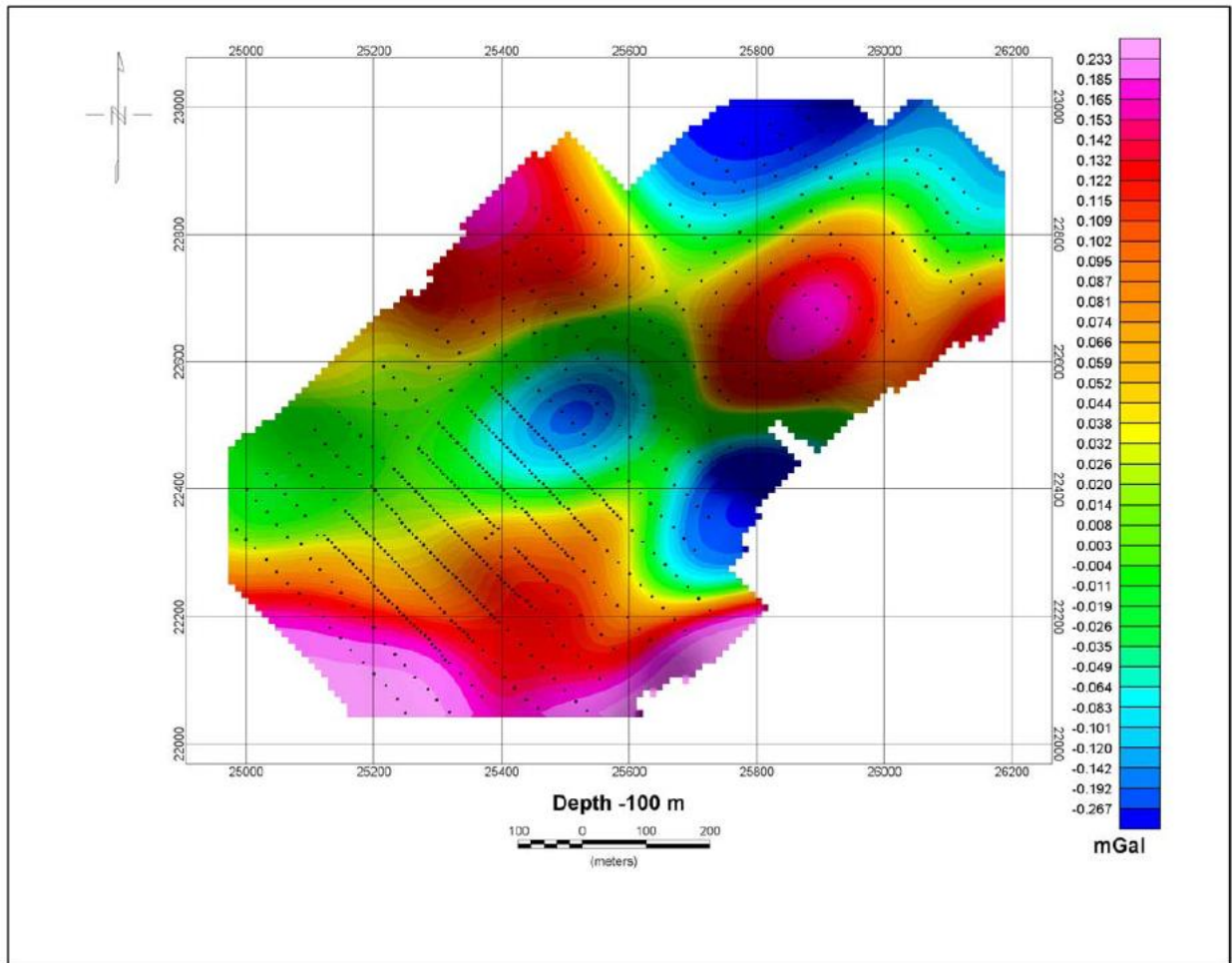


Fig. (14): Anomalies at the depth of 100 meter.

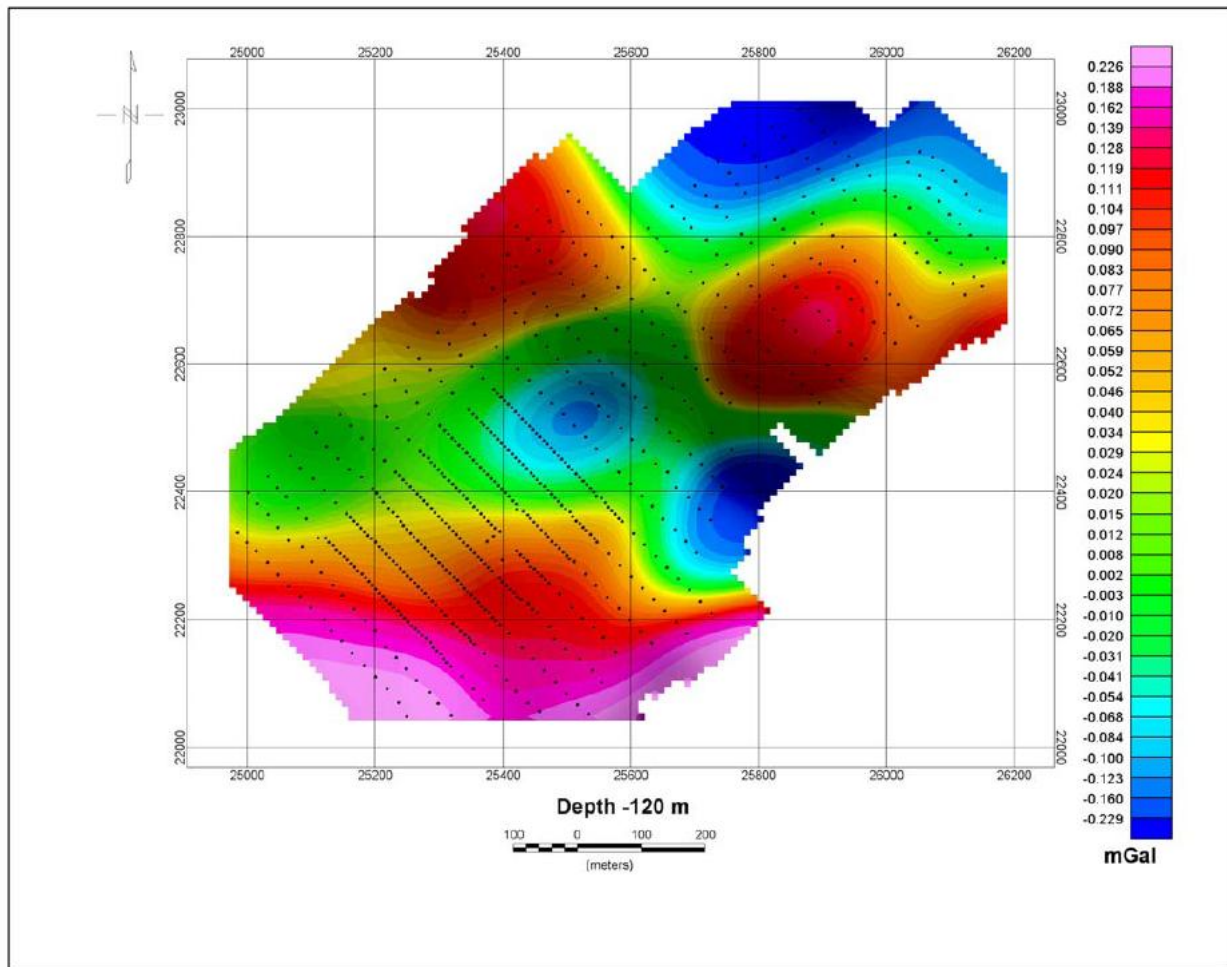


Fig. (15): Anomalies at the depth of 120 meter.

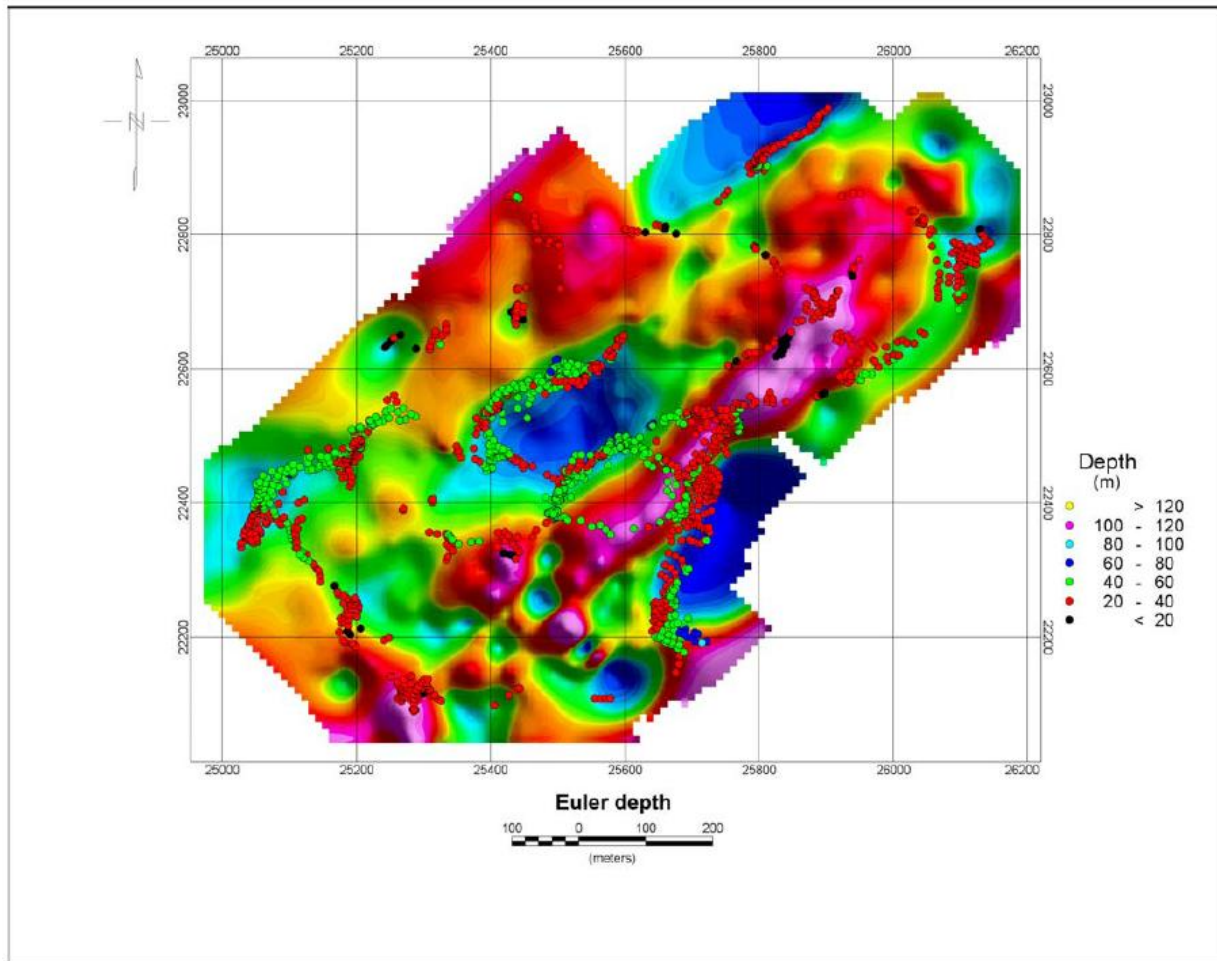


Fig. (16): Anomalies at the Euler depth.

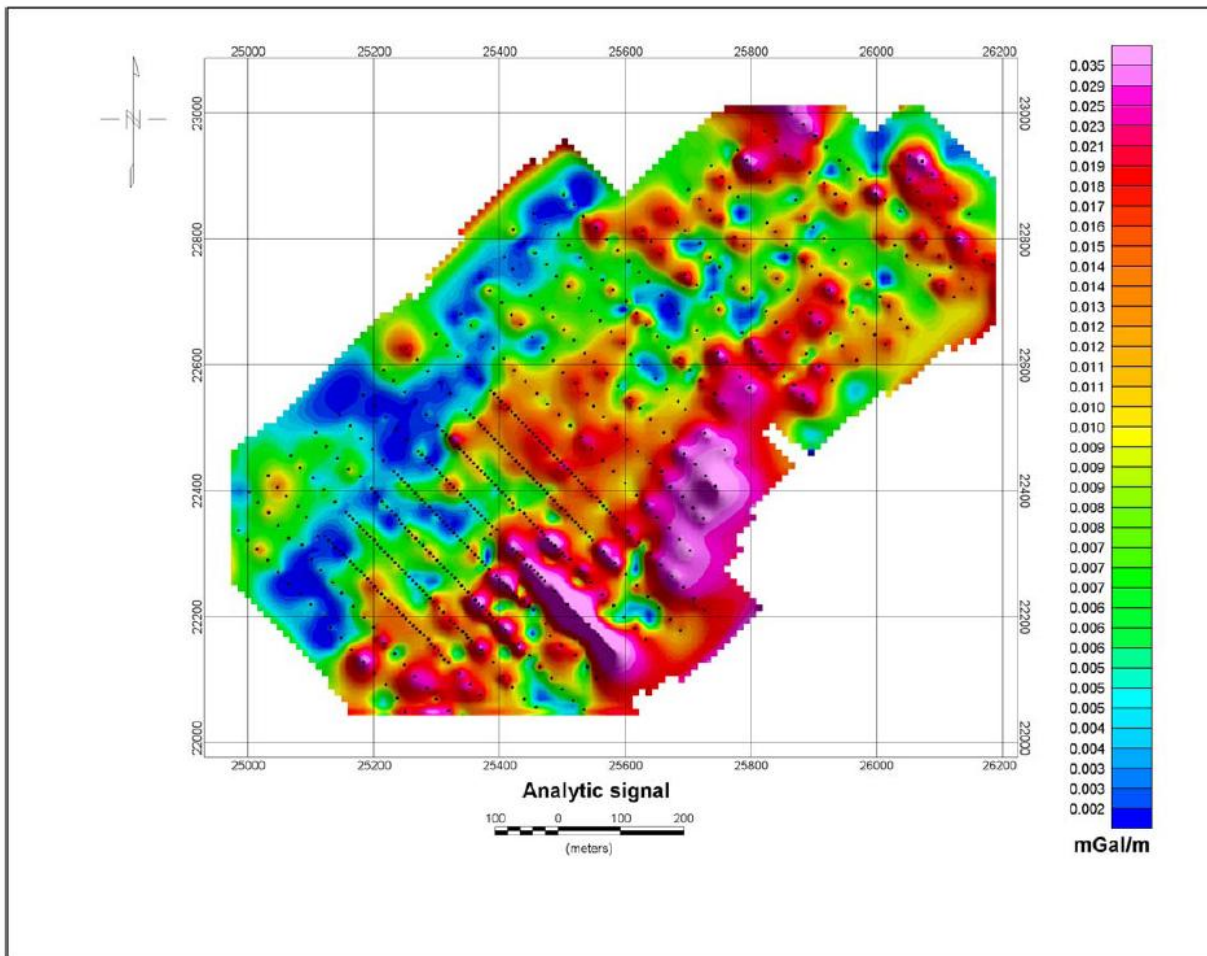


Fig. (17): Analytical signal of the anomalies

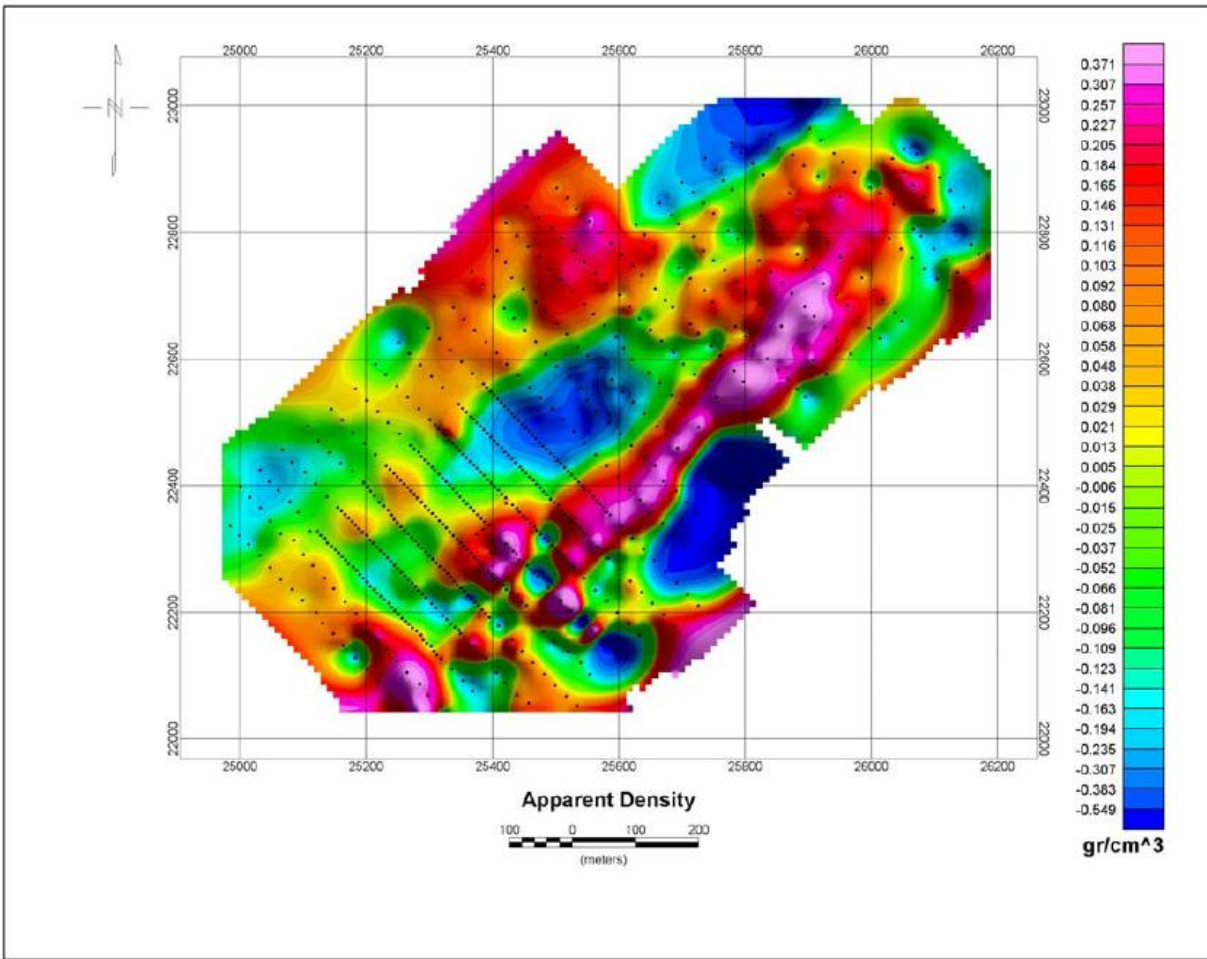


Fig. (18): Apparent density Map

3.5. Three Dimensional Modeling

For estimating the depths and density contrasts as accurate as possible and also validity of the obtained results in former sections, 3-dimensional modeling is carried out by using the new version [5] of the algorithm [4] that has been used by author in different sites successfully and the results are published in pioneer journals [1] and [2].

A window is selected and shown in Fig.(19) for modeling the anomalies of Fig. (10). This window includes the main negative anomaly number1. The topography in the window is demonstrated in Fig. (20). After applying the mentioned algorithm, the density contrasts are computed and shown in Figs. (21) to (27). In these figures sections are provided in x,y and z directions. Inspecting the figures, the low-density zone can be seen in 1630 m horizon.

Considering these figures, the main characteristics of the anomaly are presented in table (3). In this table the depths and density contrast obtained through the depth maps and Euler and apparent density methods are compared to the same values computed by modeling.

Table (3): Main Characteristics of anomaly No. 1

Anomaly number	1
Maximum Height of the ground surface (m)	1754
Minimum depth through modeling (m)	-
Maximum depth through modeling (m)	120-130
Maximum density contrast through apparent Density (gr/cm^3)	-0.4
Maximum density contrast through modeling (gr/cm^3)	-0.4
Minimum depth by Euler (m)	20
Maximum depth by depth maps (m)	120

Note: The sections EW and NS in Figs. (21) to (28) are crossing the center of the anomaly No. 1 with the coordinates reflected in Table (2).

As the values in table (3) show, the derived depths through different methods are very close.

This new algorithm [5] can also estimate the center of negative and positive masses.

The coordinates of the center of the anomalous negative mass of anomaly No. 1 are reflected in Table (4) and the sections crossing these coordinates are shown in Fig. (28).

Table (4): 3D Coordinates of the center of the anomaly

X	Y	Height (m)
25502	22500	1680

It is noted that the coordinates of the center of the anomaly No. 1 (x, y) presented in Table (4) are more accurate than the coordinates given in Table (2).

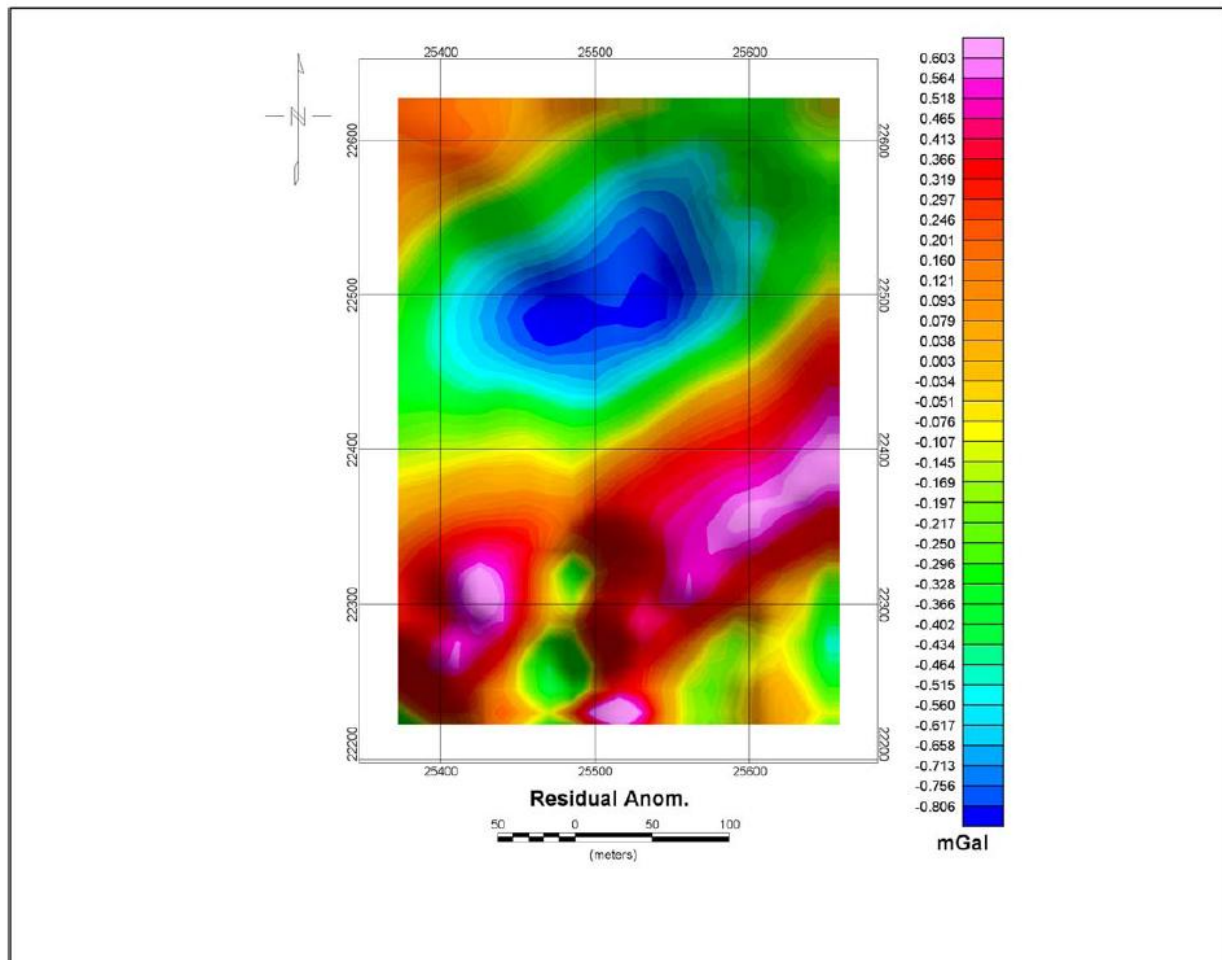


Fig. (19): Residual Anomalies – window of modeling

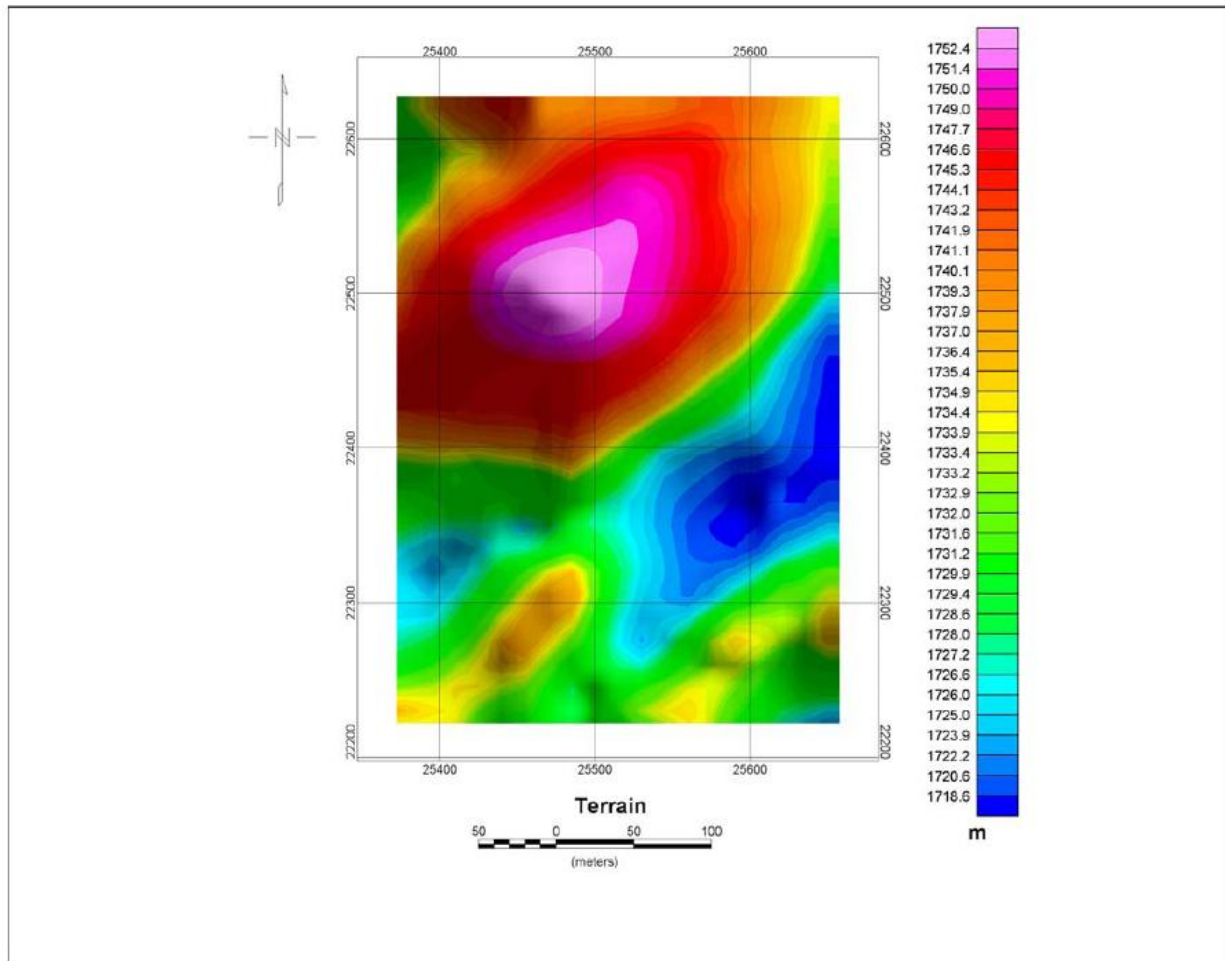
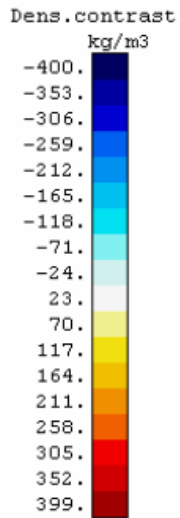


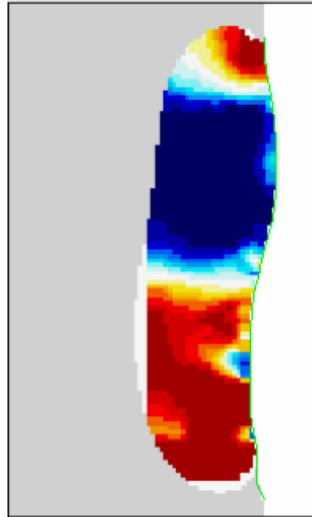
Fig. (20): Topography- window of modeling

GROWTH 2010

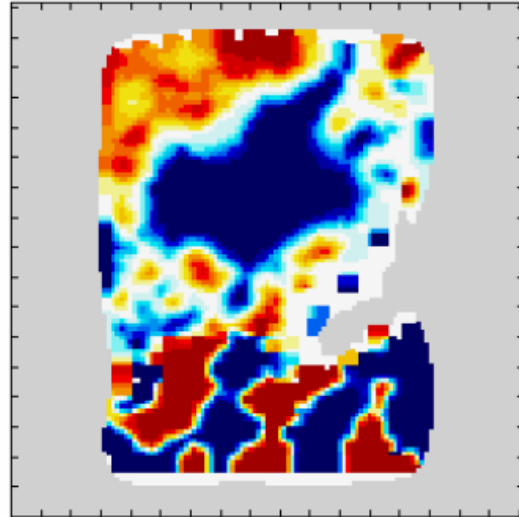
Sections across the 3D contrast density model



NS X= 25527.

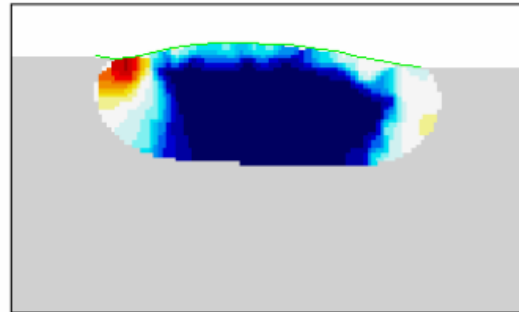


Horizontal 1720.



Axis tick interval: 30. m
Center: 25515. 22425. 1740.
Limits: 25258. 22168. 1757.16
25772. 22682. 1568.41

WE Y= 22518.

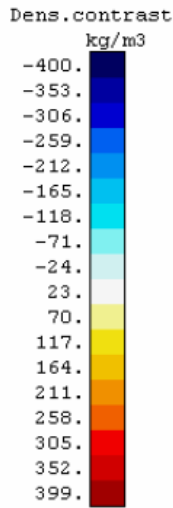


>> exit 0, hor 1, WE 2, SN 3, obli 4 ?

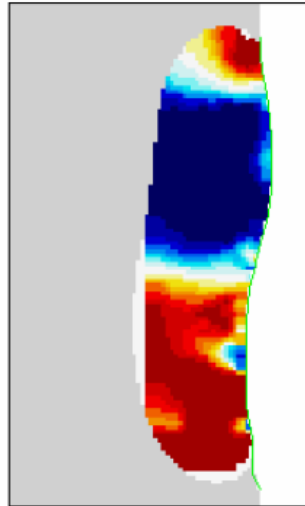
Fig. (22): The density contrasts after applying the mentioned algorithm at the 1720 horizon

GROWTH 2010

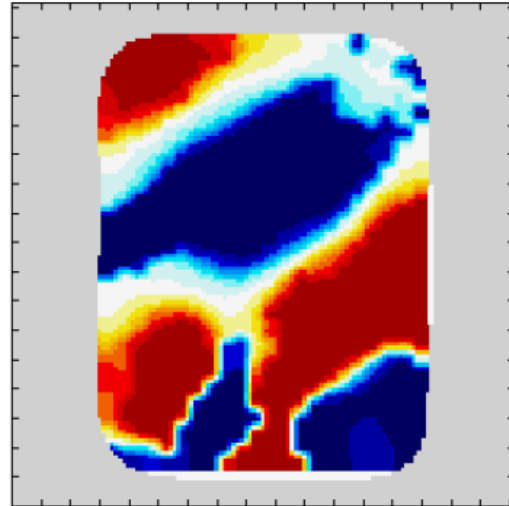
Sections across the 3D contrast density model



NS X= 25527.

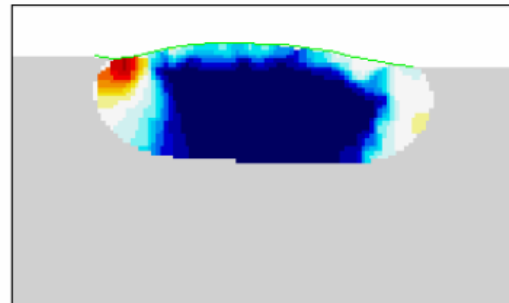


Horizontal 1680.



Axis tick interval: 30. m
Center: 25515. 22425. 1740.
Limits: 25258. 22168. 1757.16
25772. 22682. 1568.41

WE Y= 22518.



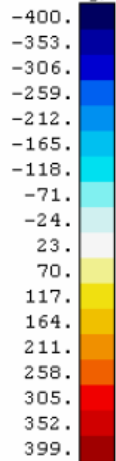
>> exit 0, hor 1, WE 2, SN 3, obli 4 ?

Fig. (24): The density contrasts after applying the mentioned algorithm at the 1680 horizon

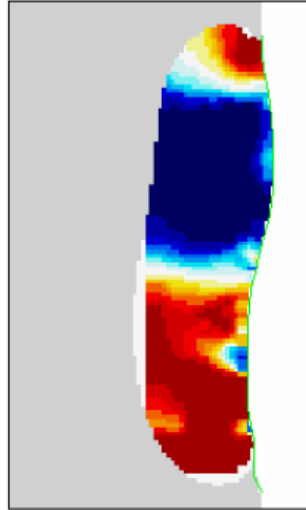
GROWTH 2010

Sections across the 3D contrast density model

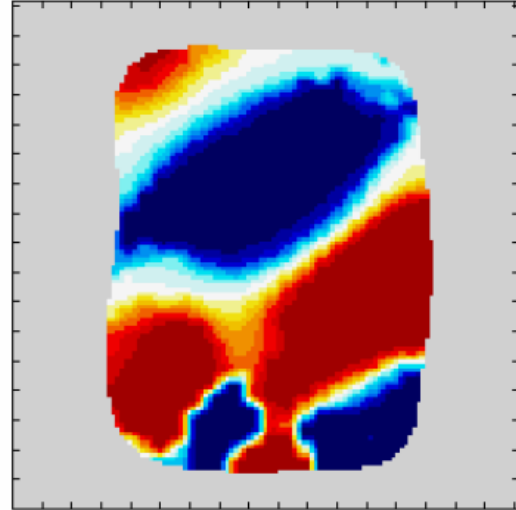
Dens. contrast
kg/m³



NS X= 25527.

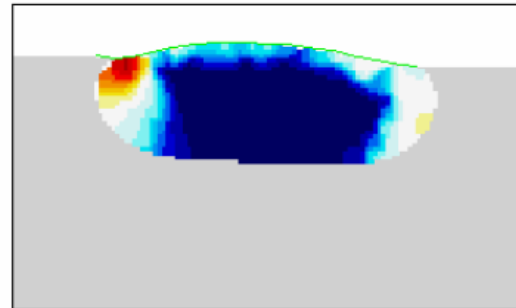


Horizontal 1660.



Axis tick interval: 30. m
Center: 25515. 22425. 1740.
Limits: 25258. 22168. 1757.16
25772. 22682. 1568.41

WE Y= 22518.

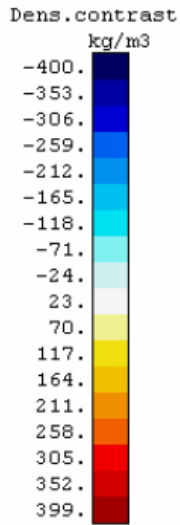


>> exit 0, hor 1, WE 2, SN 3, obli 4 ?

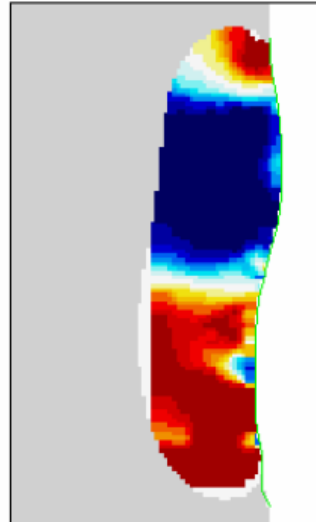
Fig. (25): The density contrasts after applying the mentioned algorithm at the 1660 horizon

GROWTH 2010

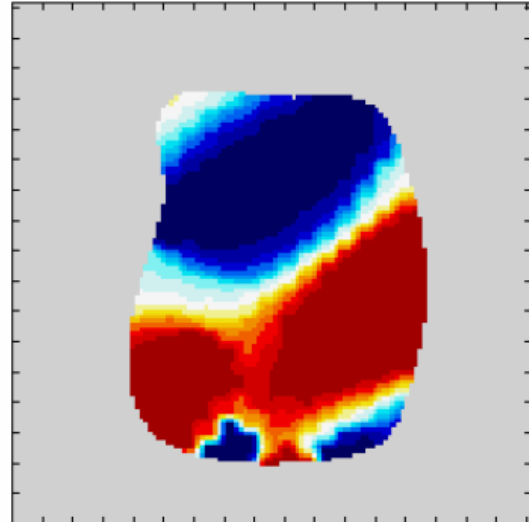
Sections across the 3D contrast density model



NS X= 25527.

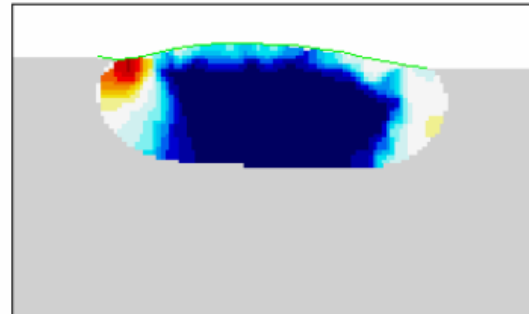


Horizontal 1640.



Axis tick interval: 30. m
Center: 25515. 22425. 1740.
Limits: 25258. 22168. 1757.16
25772. 22682. 1568.41

WE Y= 22518.

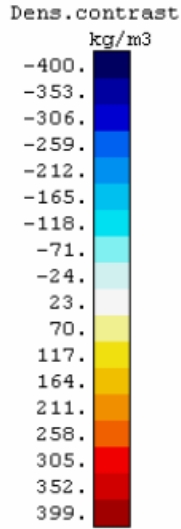


>> exit 0, hor 1, WE 2, SN 3, obli 4 ?

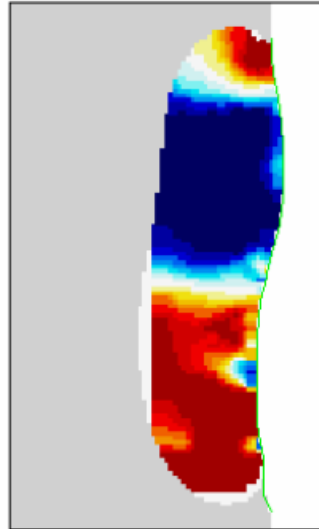
Fig. (26): The density contrasts after applying the mentioned algorithm at the 1640 horizon

GROWTH 2010

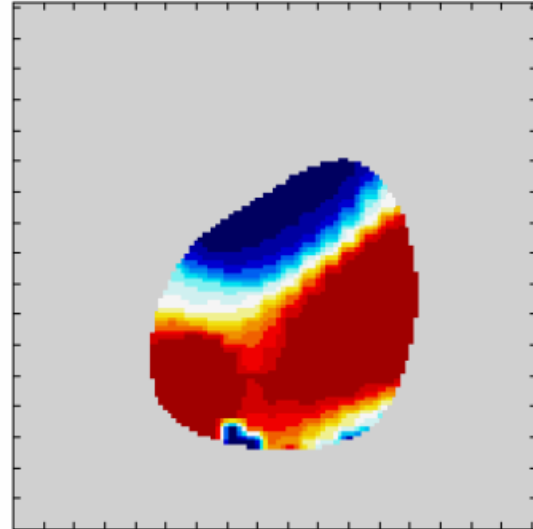
Sections across the 3D contrast density model



NS X= 25527.

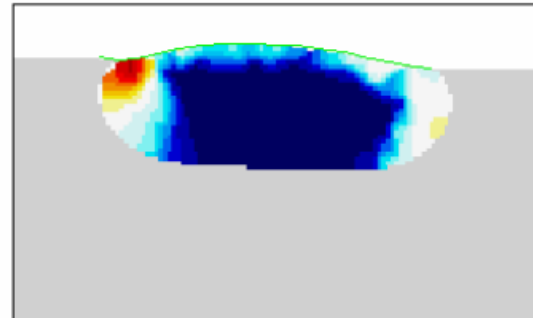


Horizontal 1630.



Axis tick interval: 30. m
Center: 25515. 22425. 1740.
Limits: 25258. 22168. 1757.16
25772. 22682. 1568.41

WE Y= 22518.



>> exit 0, hor 1, WE 2, SN 3, obli 4 ?

Fig. (27): The density contrasts after applying the mentioned algorithm at the 1630 horizon

CHAPTER 4

CONCLUSIONS

4. Conclusions

4.1. Geological Interpretation

The results of the microgravity survey presented in previous sections can be reviewed and correlated to the geological information. One of the most important available geological information is obtained from Borehole DZ-02 which has been almost at the center of the microgravity network (Fig. 8-4).

The main geological units detected in Borehole DZ-02 are summarized in Table (5).

Table (5) : Main geological units observed in Borehole No. DZ-02

Depth (m)		Geological Units
From	To	
0	68	Overburden, Clay with Silt
68	74	Shaley Limestone
74	166	Gypsum and Clay stone sequence

Estimation of the depth of the anomaly No. 1 based on the results of the microgravity survey indicate that the anomaly begins from the shallow depths (nearly 0 in modeling and 20 m in Euler) and continues to about 120 m. Considering the information of Table (5), it is concluded that various geological units can be involved in generating this anomaly.

In accordance with the results of modeling and several other filters (Table 3), it is expected that there is a big low-density zone from near the ground surface to the depth about 120 m.

Considering the coordinates of the center of the negative mass in Table (4), the z coordinate 1680 m, if it is subtracted from the ground elevation at this point (1752 masl), the difference will be 72 m. This depth (72 m) is very close to the border of the overburden and shaley limestone (68 m) observed in Borehole DZ-02 (Table (5)). This may show the importance of the contact surface.

Regarding the question about the cause of this low-density zone (anomaly No. 1) there are two possibilities. The first possibility is the existence of Gypsum and evaporates which are deeply rooted and affected the overlain layers as a concentration.

The second possibility is the cavities and sinkholes with clay infillings in the overburden and particularly in the interface of overburden and shaley limestone and Gypsum sequence.

The Gypsum and evaporates that cause this anomaly might have small cavities, based on our past experience at a site similar to the surveyed area with similar geological units (Clay, Silt, Gypsum and Salt) and considering the maximum density contrast (about -0.4 gr/cm^3) and the closeness of the densities of Clay, silt, Gypsum and salt to this value. The lateral extension of this anomaly is shown in Fig. (9-11).

As it can be recognized from this figure, the anomaly does not extend beyond $X=25650$ in local coordinate (NS section).

4.2. Recommendation

It is recommended to drill a borehole with the depth of at least 120 m at the point with the coordinates indicated in Table (4). Such borehole can be quite informative about the observed anomaly No. 1 and its geological characteristics. However, as the anomaly is caused by a big low-density zone with a density contrast that is not so high (-0.4 gr/cm^3) therefore, intensive changes in geological features of boreholes cores may not be encountered.

CHAPTER 5

REFERENCES

5. References

- [1] Ardestani, V.E., (2008). Modelling the karst zones in a dam site through micro-gravity data, Exploration Geophysics, Vol. 39, pp. 204-209.
- [2] Ardestani, V.E., (2010). Delineating and modelling an underground water conduit by scattered microgravity data and electrical resistivity sounding, Exploration Geophysics, Vol. 41 pp. 210-218.
- [3] Blakely, J.R., (1997). Potential theory in Gravity & Magnetic applications. Cambridge University Press
- [4] Camacho, A.G., Fuensanta, G.M., Viera R, 2002. A 3-D gravity inversion tool based on exploration of model possibilities. Computers & Geosciences, 2002, 28, 191-204.
- [5] Camacho, A.G., Fernandez, J and Gottsman J. 2011. The 3-D gravity inversion package GROWTH2.0 and its application to Tenerife Island, Spain. Computers & Geosciences, 2011, 37, 621-633.
- [6] T-E Assessment study – 2012- final
- [7] Inception Report – May 2011



APPENDIX: A

ROW DATA



Rogun Dam
Complementary Geotechnical Investigations at
Right Bank



SCINTREX V5.2 AUTOGRAV / Field Mode R5.35
Ser No: 211532.
Line: 0. Grid: 1. Job: 0. Date: 12/10/01 Operator: 29490.
GREF.: 0. mGals Tilt x sensit.: 267.3
GCAL.1: 5840.576 Tilt y sensit.: 223.6
GCAL.2: 0. Deg. Latitude: 38.67
TEMPCO.: -0.1488 mGal/mK Deg. Longitude: -69.75
Drift const.: 0.080 GMT Difference: -5.0hr
Drift Correction Start Time: 06:54:31 Cal. after x samples: 999
Date: 12/10/02 On-Line Tilt Corrected = ""

Station	Grav.	SD.	Tilt x	Tilt y	Temp.	E.T.C.	Dur	#	Rej	Time
0.	3688.680*	0.011	4.	6.	-0.52	-0.013	60	0	10:07:59	
1.	3691.370*	0.007	2.	-8.	-0.47	-0.001	60	0	10:32:03	
2.	3691.620*	0.009	-1.	-3.	-0.51	0.004	60	0	10:42:57	
3.	3690.665*	0.011	6.	6.	-0.51	0.008	60	0	10:50:38	
4.	3688.990*	0.012	8.	-2.	-0.50	0.011	60	0	10:57:33	
5.	3686.890*	0.013	8.	-8.	-0.43	0.016	60	0	11:11:59	
6.	3688.970*	0.008	3.	-5.	-0.42	0.021	60	0	11:26:07	
7.	3689.785*	0.013	4.	-3.	-0.45	0.023	60	0	11:34:20	
8.	3689.730*	0.010	0.	-2.	-0.35	0.029	60	0	11:59:45	
9.	3689.895*	0.015	9.	-3.	-0.35	0.030	60	0	12:06:05	
10.	3689.715*	0.013	8.	-2.	-0.33	0.031	60	0	12:12:00	
11.	3690.180*	0.015	3.	-9.	-0.32	0.032	60	0	12:19:14	
12.	3690.655*	0.012	-1.	6.	-0.30	0.032	60	0	12:23:48	
0.	3688.685*	0.014	7.	5.	-0.28	0.032	60	0	12:32:39	
14.	3691.495*	0.016	3.	6.	-0.24	0.032	60	0	12:42:11	
15.	3690.585*	0.016	-1.	6.	-0.23	0.032	60	0	12:48:05	
16.	3688.465*	0.015	-2.	-4.	-0.22	0.031	60	0	12:54:57	
17.	3688.115*	0.011	7.	-9.	-0.17	0.031	60	0	13:03:07	
18.	3687.575*	0.011	-3.	-3.	-0.15	0.030	60	0	13:09:17	
19.	3685.100*	0.010	6.	0.	-0.17	0.028	60	0	13:18:27	
20.	3685.225*	0.011	5.	7.	-0.20	0.027	60	0	13:23:28	
21.	3686.445*	0.013	-0.	-0.	-0.20	0.025	60	0	13:30:22	
22.	3688.180*	0.011	7.	5.	-0.18	0.024	60	0	13:34:56	
0.	3688.715*	0.015	-3.	-0.	-0.13	0.028	60	0	13:21:03	
24.	3688.735*	0.017	0.	2.	-0.21	0.009	60	0	14:19:20	
25.	3689.270*	0.011	1.	9.	-0.15	0.004	60	0	14:28:57	
26.	3689.535*	0.011	6.	-1.	-0.13	0.002	60	0	14:34:03	
27.	3688.815*	0.012	6.	1.	-0.14	-0.005	60	0	14:48:10	
28.	3688.765*	0.013	8.	-5.	-0.16	-0.007	60	0	14:52:46	
29.	3688.485*	0.019	7.	-1.	-0.20	-0.011	60	0	15:00:00	
30.	3688.055*	0.012	-3.	-6.	-0.18	-0.013	60	0	15:04:19	
31.	3687.270*	0.013	3.	5.	-0.15	-0.015	60	0	15:09:15	
32.	3687.700*	0.019	5.	-5.	-0.15	-0.018	60	0	15:13:55	
33.	3687.750*	0.011	2.	1.	-0.14	-0.021	60	0	15:19:28	
34.	3688.320*	0.011	-3.	0.	-0.13	-0.024	60	0	15:24:53	
35.	3687.460*	0.010	-2.	3.	-0.13	-0.027	60	0	15:31:13	
36.	3688.485*	0.008	0.	6.	-0.14	-0.030	60	0	15:35:55	
37.	3690.200*	0.011	8.	-2.	-0.12	-0.032	60	0	15:41:19	
38.	3689.830*	0.017	3.	4.	-0.14	-0.036	60	0	15:48:16	
39.	3689.110*	0.014	2.	-2.	-0.16	-0.039	60	0	15:52:53	
40.	3688.465*	0.010	5.	7.	-0.17	-0.042	60	0	15:57:54	
0.	3688.675*	0.015	6.	-6.	-0.21	-0.071	60	0	17:01:31 42	



Rogun Dam
Complementary Geotechnical Investigations at
Right Bank



 SCINTREX V5.2 AUTOGRAV / Field Mode R5.35
 Ser No: 211532.
 Line: 0. Grid: 1. Job: 0. Date: 12/10/02 Operator: 29490.
 GREF.: 0. mGals Tilt x sensit.: 267.3
 GCAL.1: 5840.576 Tilt y sensit.: 223.6
 GCAL.2: 0. Deg.Latitude: 38.67
 TEMPCO.: -0.1488 mGal/mK Deg.Longitude: -69.75
 Drift const.: 0.080 GMT Difference: -5.0hr
 Drift Correction Start Time: 06:54:31 Cal.after x samples: 999
 Date: 12/10/02 On-Line Tilt Corrected = ""

Station	Grav.	SD.	Tilt x	Tilt y	Temp.	E.T.C.	Dur	#	Rej	Time
0.	3688.665*	0.024	1.	2.	-0.46	-0.055	60	0	09:16:59	
43.	3683.240*	0.009	1.	-6.	-0.41	-0.047	60	0	09:37:10	
44.	3684.315*	0.013	1.	-1.	-0.42	-0.043	60	0	09:44:26	
45.	3686.020*	0.007	-1.	5.	-0.41	-0.041	60	0	09:50:42	
46.	3688.075*	0.008	9.	5.	-0.40	-0.037	60	0	10:00:04	
47.	3688.820*	0.013	9.	-0.	-0.38	-0.033	60	0	10:07:17	
48.	3688.985*	0.011	6.	0.	-0.39	-0.030	60	0	10:15:09	
49.	3688.735*	0.009	5.	-5.	-0.38	-0.028	60	0	10:19:56	
50.	3688.640*	0.009	1.	8.	-0.39	-0.025	60	0	10:25:36	
51.	3688.550*	0.014	3.	-5.	-0.40	-0.023	60	0	10:30:40	
52.	3688.545*	0.008	8.	8.	-0.40	-0.021	60	0	10:34:49	
0.	3688.665*	0.016	-7.	3.	-0.40	-0.019	60	0	10:38:49	
54.	3688.500*	0.014	5.	-5.	-0.39	-0.017	60	0	10:43:11	
55.	3688.455*	0.018	3.	-2.	-0.40	-0.015	60	0	10:47:09	
56.	3688.305*	0.014	-3.	0.	-0.40	-0.013	60	0	10:51:48	
57.	3688.010*	0.014	8.	7.	-0.41	-0.011	60	0	10:56:27	
58.	3687.755*	0.014	-7.	2.	-0.40	-0.009	60	0	11:00:46	
59.	3687.580*	0.010	5.	-1.	-0.40	-0.007	60	0	11:05:29	
60.	3687.305*	0.014	-4.	1.	-0.42	-0.006	60	0	11:10:03	
61.	3686.980*	0.010	7.	3.	-0.44	-0.004	60	0	11:14:11	
62.	3686.595*	0.014	-3.	1.	-0.44	-0.003	60	0	11:18:02	
63.	3686.270*	0.017	9.	2.	-0.43	-0.001	60	0	11:21:52	
64.	3686.055*	0.018	5.	6.	-0.43	-0.000	60	0	11:24:33	
65.	3686.050*	0.016	9.	2.	-0.42	0.001	60	0	11:28:09	
66.	3686.120*	0.019	-0.	-3.	-0.41	0.002	60	0	11:31:46	
67.	3686.050*	0.017	1.	7.	-0.42	0.003	60	0	11:36:16	
68.	3685.890*	0.014	0.	-2.	-0.41	0.005	60	0	11:40:28	
69.	3685.585*	0.012	0.	-7.	-0.41	0.006	60	0	11:44:22	
70.	3685.785*	0.009	8.	5.	-0.40	0.008	60	0	11:48:56	
71.	3685.880*	0.011	-2.	3.	-0.39	0.009	60	0	11:53:12	
72.	3685.795*	0.019	-3.	-4.	-0.38	0.010	60	0	11:56:53	
73.	3685.960*	0.015	3.	6.	-0.38	0.011	60	0	12:00:38	
74.	3686.015*	0.019	3.	0.	-0.38	0.011	60	0	12:04:40	
75.	3686.115*	0.018	1.	-7.	-0.38	0.013	60	0	12:10:27	
76.	3686.165*	0.018	4.	-7.	-0.37	0.014	60	0	12:14:26	
77.	3686.325*	0.012	4.	1.	-0.37	0.014	60	0	12:18:29	
78.	3686.330*	0.019	2.	-2.	-0.37	0.015	60	0	12:23:00	
79.	3686.425*	0.010	6.	-1.	-0.37	0.016	60	0	12:27:42	
80.	3686.095*	0.013	4.	6.	-0.36	0.016	60	0	12:31:23	
81.	3685.850*	0.013	0.	5.	-0.37	0.017	60	0	12:35:37	
82.	3685.890*	0.015	-2.	-1.	-0.38	0.017	60	0	12:41:42	
83.	3686.285*	0.011	9.	-4.	-0.37	0.018	60	0	12:46:12	
84.	3686.615*	0.012	7.	4.	-0.36	0.018	60	0	12:50:58 43	

85. 3686.880* 0.009 -2. -5. -0.37 0.018 60 0 12:55:18
 86. 3685.235* 0.016 4. -2. -0.38 0.018 60 0 13:00:18
 87. 3684.570* 0.018 0. -1. -0.36 0.018 60 0 13:05:18
 88. 3685.130* 0.014 -7. 7. -0.35 0.018 60 0 13:08:50
 89. 3687.100* 0.015 1. -2. -0.33 0.017 60 0 13:21:20
 90. 3686.360* 0.017 5. 7. -0.32 0.017 60 0 13:26:16
 91. 3685.040* 0.010 2. 9. -0.30 0.016 60 0 13:31:01
 92. 3683.520* 0.015 8. -3. -0.25 0.015 60 0 13:37:26
 93. 3684.445* 0.010 -2. 8. -0.32 0.005 60 0 14:23:33
 94. 3686.210* 0.012 0. -4. -0.32 0.003 60 0 14:28:21
 95. 3685.205* 0.012 -5. 5. -0.33 0.001 60 0 14:35:26
 96. 3684.875* 0.017 1. 9. -0.31 -0.001 60 0 14:40:17
 97. 3684.515* 0.012 3. -0. -0.27 -0.003 60 0 14:44:35
 98. 3684.240* 0.010 4. 7. -0.24 -0.005 60 0 14:50:09
 99. 3683.920* 0.010 -7. 2. -0.21 -0.006 60 0 14:54:05
 100. 3683.580* 0.023 -9. -2. -0.21 -0.007 60 0 14:56:46
 101. 3683.430* 0.013 3. 1. -0.21 -0.009 60 0 15:00:29
 103. 3683.615* 0.012 -5. -3. -0.24 -0.013 60 0 15:11:03
 104. 3683.895* 0.020 -7. 9. -0.23 -0.015 60 0 15:14:48
 105. 3684.115* 0.013 6. -1. -0.26 -0.017 60 0 15:19:08
 106. 3684.720* 0.015 9. -3. -0.27 -0.018 60 0 15:22:05
 107. 3685.100* 0.015 2. 1. -0.28 -0.020 60 0 15:26:06
 108. 3685.445* 0.014 -8. 1. -0.29 -0.022 60 0 15:29:47
 109. 3685.500* 0.010 -4. 8. -0.30 -0.023 60 0 15:32:07
 110. 3685.425* 0.011 6. 8. -0.30 -0.024 60 0 15:34:56
 111. 3685.540* 0.012 -3. 0. -0.30 -0.026 60 0 15:39:05
 112. 3685.645* 0.018 1. 1. -0.29 -0.028 60 0 15:43:25
 113. 3685.545* 0.016 3. 7. -0.29 -0.030 60 0 15:47:34
 0. 3688.670* 0.011 -0. 0. -0.29 -0.035 60 0 15:58:19
 115. 3685.465* 0.019 -1. 5. -0.29 -0.039 60 0 16:07:33
 116. 3685.495* 0.013 1. -4. -0.27 -0.041 60 0 16:11:51
 117. 3685.715* 0.022 -1. -0. -0.29 -0.043 60 0 16:17:09
 118. 3686.030* 0.018 -4. -2. -0.32 -0.046 60 0 16:21:26
 119. 3686.270* 0.013 8. -4. -0.34 -0.048 60 0 16:25:30
 120. 3686.705* 0.012 5. -1. -0.35 -0.049 60 0 16:29:55
 121. 3687.290* 0.015 0. 3. -0.37 -0.051 60 0 16:35:00
 122. 3687.665* 0.016 -2. -1. -0.38 -0.053 60 0 16:39:02
 123. 3688.220* 0.013 8. 2. -0.39 -0.055 60 0 16:43:34
 124. 3688.415* 0.014 1. 3. -0.40 -0.057 60 0 16:48:03
 125. 3688.535* 0.014 8. 3. -0.39 -0.059 60 0 16:53:09
 126. 3688.470* 0.016 3. -4. -0.38 -0.061 60 0 16:57:43
 127. 3688.350* 0.016 4. 1. -0.36 -0.062 60 0 17:01:20
 128. 3688.295* 0.016 2. 1. -0.33 -0.064 60 0 17:05:08
 129. 3688.200* 0.012 3. -1. -0.36 -0.065 60 0 17:09:09
 130. 3688.115* 0.010 8. 1. -0.39 -0.066 60 0 17:12:54
 131. 3687.940* 0.018 6. -2. -0.41 -0.068 60 0 17:17:12
 132. 3687.790* 0.017 4. 1. -0.41 -0.069 60 0 17:21:03
 133. 3686.730* 0.016 1. -2. -0.41 -0.070 60 0 17:25:24
 134. 3685.695* 0.019 9. 5. -0.40 -0.072 60 0 17:30:01
 135. 3684.040* 0.018 2. 5. -0.42 -0.073 60 0 17:35:20
 136. 3682.855* 0.018 6. 3. -0.43 -0.075 60 0 17:40:51
 0. 3688.660* 0.019 2. -4. -0.44 -0.077 60 0 17:50:00

 SCINTREX V5.2 AUTOGRAV / Field Mode R5.35
 Ser No: 211532.
 Line: 0. Grid: 1. Job: 0. Date: 12/10/03 Operator: 29490. 44
 GREF.: 0. mGals Tilt x sensit.: 267.3
 GCAL.1: 5840.576 Tilt y sensit.: 223.6
 GCAL.2: 0. Deg.Latitude: 38.67
 TEMPCO.: -0.1488 mGal/mK Deg.Longitude: -69.75
 Drift const.: 0.080 GMT Difference: -5.0hr
 Drift Correction Start Time: 06:54:31 Cal.after x samples: 999
 Date: 12/10/02 On-Line Tilt Corrected = ""

Station	Grav.	SD.	Tilt x	Tilt y	Temp.	E.T.C.	Dur	#	Rej	Time
0.	3688.650*	0.011	-7.	2.	-0.54	-0.062	60	0	09:09:20	
139.	3684.000*	0.011	1.	-3.	-0.50	-0.056	60	0	09:35:04	
140.	3685.040*	0.015	-3.	6.	-0.49	-0.054	60	0	09:40:34	
141.	3685.280*	0.010	-3.	-7.	-0.50	-0.053	60	0	09:43:54	
142.	3685.655*	0.010	1.	-7.	-0.44	-0.050	60	0	09:53:09	
143.	3686.405*	0.013	0.	-2.	-0.44	-0.049	60	0	09:58:17	
144.	3686.935*	0.010	5.	-4.	-0.45	-0.047	60	0	10:03:01	
145.	3687.580*	0.012	-6.	-0.	-0.47	-0.046	60	0	10:07:12	
146.	3687.370*	0.013	6.	6.	-0.47	-0.043	60	0	10:15:37	
147.	3687.515*	0.012	7.	5.	-0.46	-0.042	60	0	10:18:14	
148.	3687.945*	0.014	-3.	9.	-0.45	-0.041	60	0	10:21:16	
149.	3688.060*	0.010	7.	6.	-0.45	-0.040	60	0	10:23:51	
150.	3688.155*	0.011	-2.	2.	-0.45	-0.038	60	0	10:27:59	
151.	3688.205*	0.018	4.	-9.	-0.43	-0.037	60	0	10:32:11	
152.	3688.110*	0.012	-6.	-5.	-0.43	-0.035	60	0	10:37:56	
153.	3687.820*	0.014	-2.	3.	-0.43	-0.033	60	0	10:42:36	
154.	3687.500*	0.011	2.	3.	-0.42	-0.032	60	0	10:46:52	
155.	3686.925*	0.011	8.	3.	-0.40	-0.029	60	0	10:52:48	
156.	3686.220*	0.019	-1.	4.	-0.39	-0.028	60	0	10:56:43	
157.	3686.085*	0.010	8.	2.	-0.39	-0.026	60	0	11:00:32	
0.	3688.670*	0.011	-1.	5.	-0.42	-0.024	60	0	11:06:50	
159.	3685.790*	0.013	0.	-5.	-0.46	-0.022	60	0	11:14:05	
160.	3685.505*	0.014	7.	5.	-0.44	-0.020	60	0	11:18:44	
161.	3685.340*	0.018	-3.	-5.	-0.44	-0.019	60	0	11:21:05	
162.	3685.290*	0.019	8.	-1.	-0.44	-0.019	60	0	11:23:14	
163.	3685.400*	0.014	8.	0.	-0.43	-0.017	60	0	11:27:03	
164.	3685.625*	0.011	3.	-8.	-0.44	-0.016	60	0	11:29:52	
165.	3685.730*	0.016	-9.	0.	-0.45	-0.015	60	0	11:35:48	
166.	3685.725*	0.013	1.	-5.	-0.45	-0.014	60	0	11:38:08	
167.	3685.725*	0.013	8.	5.	-0.44	-0.013	60	0	11:40:30	
168.	3685.720*	0.008	4.	-1.	-0.42	-0.012	60	0	11:44:42	
169.	3685.575*	0.016	8.	1.	-0.40	-0.011	60	0	11:47:20	
170.	3685.190*	0.014	-2.	1.	-0.39	-0.010	60	0	11:50:43	
171.	3684.810*	0.010	8.	2.	-0.39	-0.009	60	0	11:55:26	
172.	3684.515*	0.015	7.	-8.	-0.39	-0.008	60	0	11:59:15	
173.	3683.790*	0.010	-4.	2.	-0.39	-0.007	60	0	12:03:05	
174.	3682.675*	0.010	1.	2.	-0.40	-0.006	60	0	12:06:28	
175.	3682.490*	0.012	0.	9.	-0.42	-0.005	60	0	12:10:51	
176.	3682.905*	0.010	-3.	3.	-0.41	-0.003	60	0	12:18:49	
177.	3683.560*	0.015	8.	7.	-0.39	-0.002	60	0	12:22:08	
178.	3684.150*	0.016	3.	4.	-0.37	-0.002	60	0	12:24:55	
179.	3684.195*	0.015	-9.	3.	-0.35	-0.001	60	0	12:29:22	
180.	3683.180*	0.013	0.	-4.	-0.32	-0.000	60	0	12:33:15	
181.	3682.315*	0.015	1.	3.	-0.32	0.001	60	0	12:40:16	
182.	3684.505*	0.010	3.	9.	-0.35	0.003	60	0	12:50:32	
183.	3683.365*	0.013	1.	4.	-0.33	0.003	60	0	12:53:07	
184.	3684.105*	0.010	3.	6.	-0.33	0.003	60	0	12:56:51	
185.	3684.350*	0.015	-6.	9.	-0.32	0.004	60	0	13:01:18	
186.	3684.675*	0.018	-5.	4.	-0.31	0.004	60	0	13:04:56	

187. 3685.500* 0.016 -8. 4. -0.28 0.004 60 0 13:07:41
 188. 3686.180* 0.015 8. -3. -0.23 0.004 60 0 13:12:06
 190. 3683.125* 0.008 2. 8. -0.24 0.005 60 0 13:21:46
 191. 3682.615* 0.018 1. 5. -0.24 0.005 60 0 13:25:10
 192. 3681.785* 0.012 4. -7. -0.23 0.005 60 0 13:28:16
 193. 3681.985* 0.012 9. 6. -0.22 0.005 60 0 13:34:04
 194. 3682.460* 0.018 6. 0. -0.22 0.004 60 0 13:38:31
 195. 3683.445* 0.011 9. -9. -0.21 0.004 60 0 13:43:26
 0. 3688.670* 0.013 1. 8. -0.30 -0.002 60 0 14:29:54
 197. 3683.190* 0.014 7. 1. -0.25 -0.005 60 0 14:41:11
 198. 3683.305* 0.018 -1. -0. -0.22 -0.007 60 0 14:51:24
 199. 3684.065* 0.011 7. 9. -0.22 -0.008 60 0 14:54:20
 200. 3683.640* 0.015 6. 1. -0.23 -0.009 60 0 14:57:24
 201. 3683.210* 0.011 -0. 5. -0.23 -0.010 60 0 15:00:04
 202. 3683.220* 0.015 -4. 1. -0.23 -0.011 60 0 15:04:15
 204. 3683.740* 0.012 7. -4. -0.23 -0.013 60 0 15:10:55
 205. 3684.345* 0.012 6. -0. -0.24 -0.014 60 0 15:13:16
 206. 3684.775* 0.009 9. 5. -0.26 -0.016 60 0 15:19:34
 207. 3685.215* 0.011 0. 5. -0.26 -0.017 60 0 15:22:12
 208. 3685.715* 0.015 4. 1. -0.26 -0.018 60 0 15:24:49
 209. 3685.910* 0.010 3. 0. -0.27 -0.019 60 0 15:29:17
 210. 3686.120* 0.016 4. 6. -0.28 -0.020 60 0 15:32:01
 211. 3686.250* 0.011 1. 7. -0.30 -0.022 60 0 15:35:48
 212. 3686.420* 0.014 -1. 4. -0.30 -0.023 60 0 15:38:14
 213. 3686.405* 0.012 3. 3. -0.31 -0.024 60 0 15:40:29
 214. 3686.000* 0.014 6. -0. -0.32 -0.025 60 0 15:44:41
 215. 3685.870* 0.010 -3. 6. -0.32 -0.026 60 0 15:47:06
 216. 3685.735* 0.015 5. 3. -0.32 -0.027 60 0 15:50:55
 217. 3685.705* 0.010 9. 6. -0.31 -0.029 60 0 15:54:50
 218. 3685.770* 0.017 9. 1. -0.32 -0.030 60 0 15:57:07
 219. 3685.870* 0.011 10. -6. -0.32 -0.031 60 0 16:00:03
 220. 3686.030* 0.017 9. 1. -0.32 -0.034 60 0 16:06:48
 221. 3686.195* 0.017 -4. 7. -0.32 -0.035 60 0 16:09:50
 222. 3686.365* 0.013 4. -2. -0.34 -0.036 60 0 16:12:16
 223. 3686.605* 0.013 -5. 1. -0.36 -0.039 60 0 16:20:25
 224. 3686.695* 0.016 -5. 1. -0.38 -0.040 60 0 16:23:26
 225. 3686.970* 0.011 -0. 1. -0.37 -0.042 60 3 16:27:27
 226. 3687.275* 0.009 6. -0. -0.37 -0.043 60 0 16:31:40
 227. 3687.590* 0.011 8. 2. -0.37 -0.045 60 0 16:35:27
 228. 3687.735* 0.010 9. -3. -0.37 -0.046 60 0 16:37:53
 229. 3687.830* 0.017 2. 5. -0.39 -0.049 60 0 16:45:25
 230. 3687.815* 0.024 2. 7. -0.39 -0.049 60 1 16:48:05
 231. 3687.790* 0.010 -4. 1. -0.39 -0.051 60 0 16:50:25
 232. 3687.815* 0.012 9. 6. -0.39 -0.051 60 0 16:52:34
 233. 3687.435* 0.013 0. 8. -0.39 -0.052 60 0 16:55:24
 234. 3687.000* 0.018 3. 5. -0.38 -0.053 60 0 16:57:50
 235. 3686.710* 0.014 2. 7. -0.39 -0.054 60 0 17:00:25
 236. 3685.970* 0.014 -1. 2. -0.41 -0.055 60 0 17:04:00
 237. 3685.275* 0.013 3. 7. -0.41 -0.056 60 0 17:06:42
 238. 3684.890* 0.016 0. -5. -0.41 -0.058 60 0 17:10:52
 239. 3684.615* 0.012 -2. 5. -0.41 -0.059 60 1 17:14:15
 240. 3684.110* 0.015 5. 0. -0.40 -0.060 60 0 17:18:22
 241. 3683.275* 0.016 -2. 15. -0.41 -0.062 60 0 17:23:16
 242. 3684.075* 0.015 4. 5. -0.41 -0.063 60 0 17:27:59
 243. 3684.965* 0.018 -1. -1. -0.41 -0.064 60 0 17:30:49
 244. 3685.405* 0.015 1. 6. -0.43 -0.065 60 1 17:35:25
 245. 3686.040* 0.011 3. -0. -0.44 -0.067 60 0 17:39:31
 0. 3688.660* 0.013 1. 2. -0.45 -0.069 60 0 17:47:32 46



Rogun Dam
Complementary Geotechnical Investigations at
Right Bank



 SCINTREX V5.2 AUTOGRAV / Field Mode R5.35
 Ser No: 211532.
 Line: 0. Grid: 1. Job: 0. Date: 12/10/04 Operator: 29490.
 GREF.: 0. mGals Tilt x sensit.: 267.3
 GCAL.1: 5840.576 Tilt y sensit.: 223.6
 GCAL.2: 0. Deg.Latitude: 38.67
 TEMPCO.: -0.1488 mGal/mK Deg.Longitude: -69.75
 Drift const.: 0.080 GMT Difference: -5.0hr
 Drift Correction Start Time: 06:54:31 Cal.after x samples: 999
 Date: 12/10/02 On-Line Tilt Corrected = ""

Station	Grav.	SD.	Tilt x	Tilt y	Temp.	E.T.C.	Dur	#	Rej	Time
0.	3688.605*	0.009	-4.	-7.	-0.67	-0.056	60	0	09:27:03	
248.	3685.975*	0.009	5.	6.	-0.71	-0.055	60	0	09:36:14	
249.	3686.300*	0.013	9.	1.	-0.67	-0.054	60	0	09:41:01	
250.	3686.355*	0.014	-5.	1.	-0.64	-0.054	60	0	09:44:59	
251.	3686.560*	0.010	1.	-5.	-0.68	-0.053	60	0	09:49:30	
252.	3686.800*	0.010	1.	-2.	-0.66	-0.052	60	0	09:53:26	
253.	3686.720*	0.010	9.	2.	-0.69	-0.052	60	0	09:57:17	
254.	3686.460*	0.010	4.	2.	-0.63	-0.051	60	0	10:01:14	
255.	3686.320*	0.012	4.	-9.	-0.67	-0.050	60	0	10:05:13	
256.	3686.170*	0.017	3.	-1.	-0.68	-0.049	60	0	10:10:41	
257.	3685.665*	0.012	3.	-3.	-0.70	-0.048	60	0	10:14:31	
258.	3685.230*	0.009	5.	-5.	-0.72	-0.048	60	0	10:18:28	
259.	3685.040*	0.013	1.	7.	-0.71	-0.047	60	0	10:22:24	
260.	3685.145*	0.012	6.	-0.	-0.71	-0.046	60	0	10:24:52	
261.	3685.335*	0.013	2.	3.	-0.72	-0.046	60	0	10:27:21	
262.	3685.510*	0.013	0.	5.	-0.72	-0.045	60	0	10:31:02	
263.	3685.595*	0.011	2.	-0.	-0.68	-0.044	60	0	10:33:35	
264.	3685.590*	0.016	0.	-5.	-0.68	-0.043	60	0	10:37:49	
265.	3685.580*	0.011	-7.	6.	-0.60	-0.042	60	0	10:41:59	
266.	3685.660*	0.014	2.	5.	-0.64	-0.042	60	0	10:44:37	
267.	3685.735*	0.012	-1.	7.	-0.63	-0.041	60	0	10:48:30	
268.	3685.915*	0.018	4.	-6.	-0.63	-0.040	60	1	10:51:24	
269.	3685.910*	0.014	-1.	6.	-0.68	-0.038	60	0	10:57:52	
270.	3686.225*	0.012	3.	6.	-0.67	-0.037	60	0	11:02:30	
271.	3686.615*	0.010	9.	8.	-0.68	-0.036	60	0	11:05:07	
272.	3686.620*	0.016	7.	-1.	-0.68	-0.036	60	0	11:07:34	
273.	3686.610*	0.016	9.	1.	-0.61	-0.034	60	0	11:12:45	
0.	3688.605*	0.014	4.	6.	-0.68	-0.032	60	0	11:20:37	
275.	3686.085*	0.015	2.	-3.	-0.69	-0.029	60	0	11:33:48	
276.	3686.275*	0.019	6.	4.	-0.68	-0.028	60	0	11:38:15	
277.	3685.640*	0.011	1.	2.	-0.75	-0.027	60	0	11:42:30	
278.	3685.040*	0.014	6.	1.	-0.75	-0.026	60	0	11:47:00	
279.	3684.555*	0.014	6.	-1.	-0.67	-0.024	60	0	11:51:28	
280.	3683.975*	0.010	6.	-5.	-0.65	-0.024	60	0	11:54:44	
281.	3683.285*	0.009	6.	3.	-0.66	-0.022	60	0	12:01:40	
282.	3682.765*	0.010	0.	5.	-0.67	-0.021	60	0	12:07:06	
283.	3682.655*	0.018	5.	6.	-0.66	-0.018	60	0	12:18:34	
284.	3682.850*	0.015	5.	6.	-0.62	-0.018	60	0	12:21:18	
285.	3683.245*	0.018	5.	5.	-0.63	-0.017	60	0	12:25:17	
286.	3683.835*	0.016	6.	2.	-0.64	-0.016	60	0	12:27:36	
287.	3684.700*	0.015	-6.	3.	-0.67	-0.015	60	0	12:32:44	
288.	3683.065*	0.012	5.	2.	-0.64	-0.013	60	0	12:43:37	
289.	3681.040*	0.011	3.	6.	-0.68	-0.013	60	1	12:48:51 47	

290. 3682.655* 0.013 7. 3. -0.64 -0.012 60 0 12:55:39
 291. 3681.365* 0.009 3. -1. -0.64 -0.011 60 0 13:01:18
 294. 3683.135* 0.016 -0. 7. -0.78 -0.009 60 0 13:16:43
 295. 3683.260* 0.012 0. 8. -0.71 -0.009 60 0 13:20:42
 296. 3682.630* 0.014 -1. 1. -0.61 -0.009 60 0 13:25:24
 297. 3682.025* 0.012 -2. 3. -0.62 -0.008 60 0 13:31:11
 298. 3681.450* 0.011 7. 5. -0.55 -0.008 60 0 13:34:12
 299. 3682.990* 0.014 3. -6. -0.59 -0.008 60 0 13:38:45
 300. 3685.635* 0.014 9. 3. -0.40 -0.008 60 0 13:45:23
 301. 3685.115* 0.014 5. 5. -0.31 -0.008 60 0 13:48:17
 302. 3684.505* 0.010 -7. 3. -0.28 -0.008 60 0 13:51:27
 303. 3684.145* 0.010 0. 5. -0.25 -0.008 60 0 13:55:19
 304. 3683.465* 0.014 -2. 2. -0.26 -0.008 60 0 13:58:07
 305. 3682.550* 0.015 3. 2. -0.27 -0.008 60 0 14:00:59
 306. 3682.130* 0.013 2. 9. -0.27 -0.008 60 0 14:05:14
 0. 3688.610* 0.010 0. 1. -0.39 -0.013 60 0 14:51:33
 308. 3683.505* 0.014 4. -2. -0.18 -0.016 60 0 15:08:29
 309. 3684.945* 0.010 3. -4. -0.20 -0.017 60 0 15:13:58
 310. 3685.585* 0.015 -1. -7. -0.23 -0.018 60 0 15:19:02
 311. 3686.205* 0.016 -6. -5. -0.25 -0.019 60 0 15:24:10
 312. 3686.320* 0.019 3. 8. -0.26 -0.020 60 0 15:26:54
 313. 3686.045* 0.018 -3. -2. -0.28 -0.021 60 1 15:30:40
 314. 3685.865* 0.014 -3. 5. -0.28 -0.022 60 0 15:33:01
 315. 3685.575* 0.013 -4. 7. -0.28 -0.023 60 0 15:36:43
 316. 3685.275* 0.010 5. -0. -0.27 -0.023 60 0 15:39:22
 317. 3685.340* 0.012 1. -0. -0.25 -0.024 60 0 15:42:45
 318. 3685.400* 0.017 2. -1. -0.25 -0.025 60 0 15:47:18
 319. 3685.000* 0.015 -1. 9. -0.25 -0.026 60 0 15:50:05
 320. 3684.815* 0.010 0. 9. -0.25 -0.027 60 1 15:54:19
 321. 3684.625* 0.017 2. 9. -0.24 -0.029 60 0 15:58:48
 322. 3684.540* 0.012 9. -6. -0.23 -0.030 60 0 16:03:02
 323. 3684.505* 0.014 -3. 1. -0.24 -0.031 60 0 16:05:54
 324. 3684.285* 0.009 0. 7. -0.24 -0.031 60 0 16:08:26
 325. 3684.070* 0.017 -1. 3. -0.24 -0.032 60 0 16:11:19
 326. 3684.005* 0.014 -1. 8. -0.23 -0.033 60 0 16:13:43
 327. 3683.830* 0.013 4. 4. -0.23 -0.034 60 0 16:16:02
 328. 3683.925* 0.012 4. -5. -0.23 -0.034 60 0 16:18:23
 329. 3684.110* 0.016 4. -5. -0.23 -0.035 60 0 16:20:58
 330. 3684.370* 0.011 -2. -1. -0.23 -0.036 60 0 16:23:22
 331. 3684.850* 0.014 3. -5. -0.25 -0.037 60 0 16:27:54
 332. 3685.535* 0.010 4. -9. -0.26 -0.038 60 0 16:30:37
 333. 3685.970* 0.014 -1. 1. -0.28 -0.039 60 0 16:34:27
 334. 3686.200* 0.019 -6. 2. -0.29 -0.040 60 0 16:36:45
 335. 3686.515* 0.013 0. 0. -0.30 -0.041 60 0 16:39:40
 336. 3686.695* 0.019 3. 3. -0.30 -0.041 60 0 16:41:57
 337. 3686.755* 0.018 1. 4. -0.31 -0.043 60 0 16:46:00
 338. 3686.795* 0.018 3. 3. -0.33 -0.044 60 0 16:48:40
 339. 3686.810* 0.015 5. 6. -0.32 -0.046 60 0 16:56:37
 340. 3686.770* 0.016 3. 6. -0.32 -0.047 60 0 16:59:20
 341. 3686.440* 0.014 -1. 1. -0.32 -0.048 60 0 17:02:32
 342. 3686.245* 0.010 3. 2. -0.32 -0.049 60 0 17:05:27
 343. 3685.280* 0.009 8. 1. -0.34 -0.049 60 0 17:08:24
 344. 3683.215* 0.011 7. 3. -0.34 -0.051 60 0 17:13:52
 345. 3682.460* 0.011 8. 1. -0.33 -0.053 60 0 17:19:28
 346. 3685.290* 0.013 3. 2. -0.32 -0.054 60 0 17:23:36
 347. 3686.540* 0.012 5. -2. -0.33 -0.055 60 0 17:26:41
 348. 3686.700* 0.012 -5. -8. -0.32 -0.056 60 0 17:30:48
 349. 3686.705* 0.013 -8. 1. -0.31 -0.056 60 0 17:33:22 48



Rogun Dam
Complementary Geotechnical Investigations at
Right Bank



0. 3688.640* 0.011 3. 2. -0.33 -0.059 60 0 17:43:29

SCINTREX V5.2 AUTOGRAV / Field Mode R5.35
Ser No: 211532.

Line: 0. Grid: 1. Job: 0. Date: 12/10/05 Operator: 29490.
GREF.: 0. mGals Tilt x sensit.: 267.3
GCAL.1: 5840.576 Tilt y sensit.: 223.6
GCAL.2: 0. Deg.Latitude: 38.67
TEMPCO.: -0.1488 mGal/mK Deg.Longitude: -69.75
Drift const.: 0.080 GMT Difference: -5.0hr
Drift Correction Start Time: 06:54:31 Cal.after x samples: 999
Date: 12/10/02 On-Line Tilt Corrected = ""

Station Grav. SD. Tilt x Tilt y Temp. E.T.C. Dur # Rej Time
0. 3688.790* 0.011 -5. -1. -0.19 -0.042 60 0 09:03:03
352. 3686.885* 0.013 -6. 4. -0.15 -0.046 60 0 09:43:57
354. 3686.680* 0.014 0. 3. -0.13 -0.046 60 0 09:52:34
355. 3686.485* 0.010 7. -6. -0.12 -0.046 60 0 09:55:03
356. 3686.210* 0.012 -1. -5. -0.10 -0.046 60 0 09:59:19
357. 3685.390* 0.014 3. -1. -0.11 -0.046 60 0 10:04:11
358. 3684.975* 0.014 -1. -4. -0.12 -0.046 60 0 10:09:34
359. 3684.180* 0.012 2. -3. -0.14 -0.046 60 0 10:15:01
360. 3683.780* 0.013 -2. 3. -0.15 -0.046 60 0 10:17:30
361. 3683.405* 0.014 7. 2. -0.17 -0.046 60 0 10:20:21
362. 3683.060* 0.010 -1. -2. -0.19 -0.045 60 0 10:22:58
363. 3682.820* 0.010 3. -1. -0.20 -0.045 60 0 10:25:32
364. 3682.415* 0.013 2. -4. -0.16 -0.045 60 0 10:29:41
365. 3682.305* 0.012 1. -5. -0.14 -0.045 60 0 10:32:38
366. 3682.245* 0.012 8. 3. -0.13 -0.044 60 0 10:35:10
367. 3682.185* 0.012 -4. -2. -0.12 -0.044 60 0 10:39:56
368. 3682.205* 0.018 8. 5. -0.11 -0.044 60 0 10:44:00
369. 3682.475* 0.009 -7. 4. -0.12 -0.043 60 0 10:46:36
370. 3682.915* 0.011 2. -6. -0.12 -0.043 60 0 10:49:25
371. 3683.350* 0.013 7. -4. -0.11 -0.043 60 0 10:53:26
372. 3683.530* 0.011 1. -3. -0.11 -0.042 60 0 10:55:50
373. 3683.645* 0.015 -5. 0. -0.10 -0.042 60 0 10:58:00
374. 3683.855* 0.013 4. 1. -0.11 -0.042 60 0 11:01:57
375. 3683.980* 0.009 -1. 1. -0.11 -0.041 60 0 11:04:19
376. 3684.075* 0.013 2. -3. -0.10 -0.041 60 0 11:06:42
377. 3684.090* 0.013 -1. -4. -0.10 -0.040 60 0 11:11:02
378. 3684.005* 0.015 1. -3. -0.10 -0.040 60 0 11:13:50
379. 3684.105* 0.018 -0. 5. -0.10 -0.040 60 0 11:17:01
380. 3684.720* 0.011 3. 1. -0.10 -0.039 60 0 11:22:16
381. 3685.355* 0.016 2. 3. -0.09 -0.038 60 0 11:25:26
382. 3685.670* 0.015 2. -2. -0.07 -0.038 60 0 11:29:39
383. 3685.865* 0.013 9. -2. -0.06 -0.037 60 0 11:34:20
384. 3685.960* 0.009 1. 7. -0.06 -0.036 60 0 11:38:57
385. 3685.700* 0.012 -5. 2. -0.06 -0.036 60 0 11:42:02
386. 3685.870* 0.019 -6. -3. -0.04 -0.035 60 2 11:46:40
387. 3685.905* 0.010 -3. -9. -0.03 -0.034 60 0 11:51:20
388. 3685.770* 0.010 6. 4. -0.03 -0.034 60 0 11:54:39
389. 3685.620* 0.016 5. 5. -0.06 -0.033 60 0 11:59:07
390. 3686.015* 0.019 2. 4. -0.05 -0.032 60 0 12:04:31
391. 3686.445* 0.011 7. -3. -0.04 -0.032 60 0 12:08:19
392. 3682.075* 0.009 0. -8. -0.03 -0.031 60 0 12:14:32
393. 3682.040* 0.012 1. 4. -0.03 -0.030 60 0 12:19:17 49

394. 3682.620* 0.018 -3. -1. -0.03 -0.029 60 0 12:23:11
 395. 3682.635* 0.014 6. -10. -0.01 -0.029 60 0 12:27:40
 396. 3683.415* 0.014 8. 9. 0.00 -0.028 60 0 12:31:16
 397. 3685.515* 0.018 3. 2. -0.00 -0.027 60 0 12:37:24
 398. 3686.745* 0.011 5. -5. 0.01 -0.027 60 0 12:41:32
 399. 3686.175* 0.017 7. 1. 0.01 -0.026 60 0 12:47:09
 400. 3684.550* 0.015 -3. 6. -0.03 -0.024 60 0 13:02:32
 401. 3681.695* 0.013 -5. -5. -0.03 -0.023 60 0 13:06:42
 402. 3679.895* 0.015 4. -3. 0.00 -0.023 60 0 13:11:29
 403. 3680.495* 0.014 7. -6. -0.01 -0.023 60 0 13:14:49
 404. 3682.655* 0.019 -1. -2. -0.01 -0.022 60 0 13:17:43
 405. 3683.135* 0.012 -1. 2. -0.01 -0.022 60 0 13:22:28
 406. 3686.635* 0.010 3. -0. 0.01 -0.021 60 0 13:33:13
 407. 3687.505* 0.014 1. 7. 0.03 -0.021 60 0 13:36:37
 408. 3687.390* 0.013 -9. 1. 0.04 -0.020 60 0 13:41:07
 409. 3686.860* 0.018 6. -5. 0.07 -0.020 60 0 13:46:31
 0. 3688.785* 0.014 -1. 1. 0.08 -0.020 60 0 13:57:07
 411. 3686.605* 0.011 -2. 1. 0.01 -0.026 60 0 15:36:18
 412. 3686.350* 0.012 7. 6. -0.01 -0.026 60 0 15:39:25
 413. 3686.505* 0.017 -1. 2. -0.02 -0.027 60 0 15:41:57
 414. 3686.405* 0.010 -2. 4. -0.03 -0.027 60 0 15:46:47
 415. 3686.260* 0.016 -1. 7. -0.06 -0.028 60 0 15:51:43
 416. 3685.905* 0.014 9. 7. -0.07 -0.029 60 0 15:54:37
 417. 3685.140* 0.013 3. 3. -0.07 -0.029 60 0 15:59:00
 418. 3684.345* 0.018 -5. -9. -0.05 -0.030 60 0 16:01:45
 419. 3683.840* 0.014 3. -1. -0.04 -0.030 60 0 16:05:10
 420. 3683.445* 0.011 -2. -0. -0.04 -0.031 60 0 16:08:02
 421. 3682.980* 0.009 4. 7. -0.04 -0.032 60 0 16:12:11
 422. 3682.225* 0.012 6. 1. -0.05 -0.032 60 0 16:14:55
 423. 3681.680* 0.014 3. -3. -0.03 -0.033 60 0 16:19:22
 424. 3681.300* 0.018 -2. -4. -0.02 -0.034 60 0 16:23:34
 425. 3681.220* 0.017 1. 7. -0.02 -0.035 60 0 16:27:01
 426. 3681.015* 0.013 -0. 4. -0.03 -0.036 60 3 16:31:37
 427. 3680.820* 0.013 -6. 6. -0.02 -0.037 60 0 16:36:04
 428. 3680.560* 0.012 -4. -0. -0.02 -0.037 60 0 16:38:57
 429. 3680.210* 0.012 8. -3. -0.04 -0.038 60 0 16:43:10
 430. 3680.165* 0.012 -3. 2. -0.05 -0.039 60 0 16:48:15
 431. 3680.375* 0.013 7. -7. -0.07 -0.040 60 0 16:53:29
 432. 3680.460* 0.011 -8. -1. -0.08 -0.041 60 1 16:55:53
 433. 3680.530* 0.011 4. -1. -0.08 -0.042 60 0 16:58:29
 434. 3680.740* 0.014 -2. -1. -0.08 -0.042 60 0 17:01:12
 435. 3681.020* 0.015 -1. 6. -0.09 -0.043 60 0 17:03:53
 436. 3681.260* 0.017 -3. 1. -0.10 -0.043 60 0 17:06:07
 437. 3681.635* 0.015 8. -2. -0.10 -0.044 60 0 17:09:03
 438. 3682.210* 0.018 6. -1. -0.12 -0.045 60 0 17:13:08
 439. 3682.560* 0.019 0. -3. -0.11 -0.045 60 0 17:15:50
 440. 3683.115* 0.012 1. 1. -0.13 -0.046 60 0 17:18:51
 441. 3684.195* 0.015 7. 3. -0.15 -0.047 60 0 17:22:12
 442. 3685.450* 0.012 4. 8. -0.15 -0.047 60 0 17:25:33
 443. 3685.820* 0.011 -6. 3. -0.15 -0.048 60 0 17:28:45
 444. 3686.040* 0.012 3. 7. -0.15 -0.048 60 0 17:31:15
 445. 3686.330* 0.012 6. 4. -0.15 -0.049 60 0 17:34:01
 446. 3686.490* 0.025 0. 4. -0.13 -0.050 60 0 17:37:50
 447. 3686.390* 0.016 -1. 4. -0.14 -0.050 60 0 17:40:17
 448. 3685.710* 0.011 -1. -1. -0.14 -0.051 60 0 17:43:23
 449. 3684.430* 0.015 -1. 3. -0.15 -0.052 60 0 17:46:19
 0. 3688.790* 0.013 4. 1. -0.16 -0.053 60 0 17:55:24 50

 SCINTREX V5.2 AUTOGRAV / Field Mode R5.35
 Ser No: 211532.
 Line: 0. Grid: 1. Job: 0. Date: 12/10/06 Operator: 29490.
 GREF.: 0. mGals Tilt x sensit.: 267.3
 GCAL.1: 5840.576 Tilt y sensit.: 223.6
 GCAL.2: 0. Deg.Latitude: 38.67
 TEMPCO.: -0.1488 mGal/mK Deg.Longitude: -69.75
 Drift const.: 0.080 GMT Difference: -5.0hr
 Drift Correction Start Time: 06:54:31 Cal.after x samples: 999
 Date: 12/10/02 On-Line Tilt Corrected = ""

Station	Grav.	SD.	Tilt x	Tilt y	Temp.	E.T.C.	Dur	#	Rej	Time
0.	3688.770*	0.015	-6.	-6.	-0.25	-0.022	60	0	09:04:09	
452.	3682.915*	0.011	-2.	1.	-0.26	-0.025	60	0	09:14:40	
453.	3684.485*	0.014	-4.	2.	-0.23	-0.026	60	0	09:19:15	
454.	3685.270*	0.012	5.	-4.	-0.22	-0.027	60	0	09:22:20	
455.	3685.355*	0.010	-0.	-4.	-0.21	-0.028	60	0	09:26:24	
456.	3685.485*	0.013	1.	-1.	-0.20	-0.028	60	0	09:28:59	
457.	3685.625*	0.011	4.	6.	-0.20	-0.029	60	0	09:33:18	
458.	3684.425*	0.015	2.	-1.	-0.21	-0.030	60	0	09:36:23	
459.	3682.185*	0.009	5.	7.	-0.22	-0.031	60	1	09:40:46	
460.	3681.140*	0.012	0.	2.	-0.22	-0.032	60	0	09:45:28	
461.	3680.410*	0.012	-2.	2.	-0.23	-0.032	60	1	09:48:18	
462.	3680.550*	0.011	2.	1.	-0.22	-0.033	60	0	09:51:55	
463.	3680.365*	0.014	1.	2.	-0.21	-0.033	60	0	09:56:21	
464.	3681.515*	0.012	8.	8.	-0.21	-0.034	60	0	09:59:16	
465.	3683.760*	0.012	-3.	-5.	-0.20	-0.035	60	0	10:04:38	
466.	3685.085*	0.011	0.	-3.	-0.17	-0.035	60	0	10:09:00	
467.	3685.935*	0.013	5.	4.	-0.15	-0.036	60	0	10:12:10	
468.	3686.355*	0.014	3.	-10.	-0.13	-0.036	60	0	10:15:18	
469.	3687.505*	0.013	-2.	6.	-0.11	-0.036	60	0	10:19:23	
470.	3685.455*	0.012	5.	3.	-0.11	-0.037	60	0	10:23:15	
471.	3683.055*	0.009	3.	-1.	-0.12	-0.037	60	0	10:27:57	
472.	3680.140*	0.013	3.	-8.	-0.14	-0.038	60	0	10:31:46	
473.	3679.140*	0.016	-1.	5.	-0.16	-0.038	60	0	10:35:38	
474.	3679.655*	0.011	-2.	3.	-0.15	-0.038	60	0	10:41:48	
475.	3681.700*	0.012	4.	1.	-0.15	-0.038	60	0	10:45:04	
476.	3684.790*	0.013	-1.	-7.	-0.15	-0.039	60	0	10:54:30	
477.	3687.180*	0.010	-1.	-0.	-0.14	-0.039	60	0	10:59:18	
478.	3687.855*	0.018	3.	7.	-0.16	-0.039	60	0	11:08:15	
479.	3686.610*	0.015	3.	0.	-0.15	-0.039	60	0	11:11:34	
480.	3685.590*	0.014	0.	8.	-0.11	-0.039	60	0	11:17:02	
481.	3683.120*	0.011	4.	3.	-0.08	-0.039	60	0	11:20:57	
482.	3681.925*	0.011	0.	1.	-0.06	-0.039	60	0	11:23:51	
483.	3681.360*	0.015	0.	4.	-0.03	-0.039	60	0	11:27:32	
484.	3680.965*	0.011	5.	-6.	-0.01	-0.039	60	0	11:32:12	
485.	3680.720*	0.014	3.	5.	-0.01	-0.039	60	0	11:36:19	
486.	3681.030*	0.016	4.	6.	-0.02	-0.039	60	0	11:40:02	
487.	3682.460*	0.013	5.	-3.	-0.02	-0.039	60	0	11:43:27	
488.	3683.870*	0.012	6.	-1.	-0.02	-0.039	60	0	11:49:19	
489.	3684.320*	0.013	6.	1.	-0.03	-0.039	60	0	11:52:36	
490.	3683.845*	0.011	-3.	8.	-0.02	-0.038	60	0	11:56:47	
491.	3682.365*	0.010	8.	5.	-0.02	-0.038	60	0	12:00:30	
492.	3682.140*	0.011	0.	-1.	0.00	-0.038	60	0	12:04:57	
493.	3682.420*	0.011	2.	2.	0.02	-0.038	60	0	12:09:44	
494.	3682.370*	0.013	7.	2.	0.04	-0.038	60	0	12:13:07	

495. 3680.940* 0.012 -6. 4. 0.03 -0.037 60 0 12:17:49
 497. 3679.940* 0.013 1. 6. 0.03 -0.037 60 0 12:28:58
 498. 3680.720* 0.012 -4. 5. 0.06 -0.036 60 0 12:33:55
 499. 3681.445* 0.010 7. 4. 0.07 -0.036 60 1 12:36:54
 500. 3682.185* 0.014 5. -2. 0.10 -0.036 60 0 12:40:16
 501. 3683.665* 0.012 4. 8. 0.16 -0.036 60 0 12:45:36
 502. 3684.785* 0.016 -6. 7. 0.17 -0.035 60 0 12:49:56
 503. 3684.880* 0.016 7. 8. 0.17 -0.035 60 0 12:54:12
 0. 3688.780* 0.012 2. 6. 0.17 -0.034 60 0 13:05:46
 0. 3688.770* 0.011 -1. 7. -0.00 -0.031 60 0 14:07:56
 506. 3684.310* 0.010 8. -8. 0.07 -0.030 60 0 14:19:16
 507. 3683.675* 0.009 3. 9. 0.08 -0.030 60 0 14:22:33
 508. 3682.390* 0.011 1. -2. 0.08 -0.030 60 0 14:26:18
 509. 3681.610* 0.015 -2. 4. 0.03 -0.030 60 0 14:34:27
 510. 3682.790* 0.011 4. -0. 0.04 -0.030 60 0 14:38:52
 511. 3682.450* 0.011 9. 4. 0.03 -0.030 60 0 14:44:05
 512. 3683.565* 0.012 8. 8. 0.03 -0.030 60 0 14:47:23
 513. 3684.225* 0.009 5. 8. 0.03 -0.030 60 0 14:50:36
 514. 3686.435* 0.009 7. 6. 0.05 -0.030 60 0 14:55:44
 515. 3688.470* 0.012 7. -5. 0.06 -0.030 60 0 15:02:33
 516. 3690.320* 0.011 7. -8. 0.07 -0.030 60 0 15:06:09
 517. 3686.255* 0.009 8. -7. 0.04 -0.031 60 0 15:11:56
 518. 3681.800* 0.013 4. -5. 0.03 -0.031 60 0 15:16:44
 519. 3679.215* 0.018 1. 2. 0.04 -0.031 60 0 15:23:07
 520. 3682.830* 0.014 -6. 2. 0.03 -0.031 60 0 15:29:14
 521. 3683.420* 0.008 -3. -3. 0.02 -0.031 60 0 15:32:34
 522. 3691.185* 0.011 8. 2. 0.06 -0.032 60 0 15:48:08
 523. 3688.245* 0.010 2. -0. 0.03 -0.033 60 0 16:00:34
 524. 3686.890* 0.010 2. 4. 0.02 -0.033 60 0 16:04:08
 525. 3684.685* 0.012 -3. -8. -0.01 -0.034 60 3 16:08:47
 526. 3684.215* 0.010 7. 1. -0.02 -0.034 60 0 16:12:43
 527. 3683.805* 0.012 4. 1. -0.03 -0.034 60 0 16:16:37
 528. 3683.310* 0.017 6. -3. -0.03 -0.035 60 0 16:23:45
 529. 3682.500* 0.011 0. 3. -0.03 -0.036 60 2 16:28:59
 530. 3683.535* 0.012 7. -3. -0.04 -0.036 60 0 16:33:20
 531. 3684.290* 0.016 5. 5. -0.05 -0.036 60 0 16:36:44
 532. 3684.615* 0.015 -4. -8. -0.06 -0.037 60 0 16:39:46
 533. 3684.680* 0.017 -8. 4. -0.06 -0.037 60 0 16:42:57
 534. 3684.310* 0.008 -2. 2. -0.06 -0.038 60 0 16:47:59
 535. 3683.285* 0.015 3. -2. -0.07 -0.038 60 0 16:51:39
 536. 3682.195* 0.015 4. 1. -0.07 -0.038 60 0 16:55:17
 537. 3680.275* 0.015 -5. 1. -0.09 -0.039 60 0 17:00:17
 538. 3678.980* 0.011 6. -1. -0.10 -0.039 60 0 17:03:17
 539. 3677.245* 0.010 9. -3. -0.12 -0.040 60 0 17:06:38
 540. 3677.605* 0.013 4. 3. -0.12 -0.040 60 0 17:10:24
 541. 3679.100* 0.016 3. -3. -0.16 -0.041 60 0 17:16:29
 542. 3680.650* 0.013 -1. -3. -0.17 -0.041 60 0 17:19:41
 543. 3682.080* 0.011 1. 2. -0.17 -0.042 60 0 17:22:47
 544. 3683.040* 0.011 0. -2. -0.18 -0.042 60 0 17:28:14
 545. 3683.710* 0.008 -8. 9. -0.20 -0.043 60 0 17:31:02
 546. 3684.155* 0.012 9. -5. -0.19 -0.043 60 0 17:34:12
 547. 3684.280* 0.010 -9. -4. -0.20 -0.043 60 0 17:37:05
 0. 3688.760* 0.012 -2. 1. -0.17 -0.045 60 0 17:47:59



Rogun Dam
Complementary Geotechnical Investigations at
Right Bank



 SCINTREX V5.2 AUTOGRAV / Field Mode R5.35
 Ser No: 211532.
 Line: 0. Grid: 1. Job: 0. Date: 12/10/07 Operator: 29490. 52
 GREF.: 0. mGals Tilt x sensit.: 267.3
 GCAL.1: 5840.576 Tilt y sensit.: 223.6
 GCAL.2: 0. Deg.Latitude: 38.67
 TEMPCO.: -0.1488 mGal/mK Deg.Longitude: -69.75
 Drift const.: 0.080 GMT Difference: -5.0hr
 Drift Correction Start Time: 06:54:31 Cal.after x samples: 999
 Date: 12/10/02 On-Line Tilt Corrected = ""

Station	Grav. SD	Tilt x	Tilt y	Temp.	E.T.C.	Dur	#	Rej	Time
0.	3688.755*	0.014	-1.	1.	-0.29	0.003	60	0	09:00:22
550.	3683.215*	0.012	-1.	6.	-0.28	-0.000	60	0	09:10:22
551.	3684.405*	0.019	9.	-5.	-0.23	-0.002	60	2	09:15:30
552.	3683.250*	0.019	-7.	-2.	-0.21	-0.006	60	0	09:27:00
553.	3684.410*	0.013	9.	-3.	-0.15	-0.012	60	0	09:45:38
554.	3684.375*	0.016	4.	4.	-0.15	-0.013	60	0	09:51:09
555.	3684.095*	0.014	0.	4.	-0.15	-0.014	60	0	09:54:26
556.	3686.135*	0.016	7.	3.	-0.15	-0.015	60	0	09:57:34
557.	3686.925*	0.014	4.	-1.	-0.15	-0.016	60	0	10:00:47
558.	3685.560*	0.015	2.	-5.	-0.16	-0.018	60	0	10:07:49
559.	3688.770*	0.013	1.	7.	-0.13	-0.019	60	0	10:12:56
560.	3693.075*	0.011	6.	-1.	-0.11	-0.021	60	0	10:19:12
561.	3693.690*	0.018	0.	-8.	-0.09	-0.022	60	0	10:22:23
562.	3693.935*	0.015	-4.	3.	-0.09	-0.023	60	0	10:26:04
563.	3692.255*	0.009	-6.	-3.	-0.11	-0.023	60	0	10:30:06
564.	3689.860*	0.012	-5.	-2.	-0.17	-0.026	60	0	10:42:40
565.	3690.535*	0.012	2.	1.	-0.17	-0.027	60	0	10:45:27
566.	3689.815*	0.019	3.	5.	-0.16	-0.028	60	0	10:48:34
568.	3692.940*	0.013	6.	3.	-0.17	-0.029	60	0	10:57:46
569.	3689.825*	0.016	-4.	3.	-0.19	-0.031	60	0	11:03:40
570.	3687.640*	0.012	5.	8.	-0.18	-0.031	60	0	11:07:21
571.	3686.855*	0.014	0.	1.	-0.14	-0.032	60	0	11:12:58
572.	3686.305*	0.013	8.	7.	-0.12	-0.032	60	0	11:16:04
573.	3686.165*	0.011	-2.	-1.	-0.10	-0.033	60	0	11:20:37
574.	3685.730*	0.013	8.	-1.	-0.09	-0.034	60	0	11:24:55
575.	3684.195*	0.012	8.	3.	-0.09	-0.035	60	0	11:30:18
576.	3683.600*	0.013	5.	-3.	-0.09	-0.035	60	0	11:33:10
577.	3683.135*	0.016	8.	1.	-0.05	-0.036	60	0	11:38:23
578.	3682.945*	0.015	0.	-6.	-0.04	-0.036	60	0	11:43:12
579.	3682.890*	0.014	-4.	1.	-0.04	-0.037	60	0	11:46:01
580.	3682.995*	0.011	7.	-1.	-0.03	-0.037	60	0	11:50:02
581.	3682.945*	0.013	4.	4.	-0.02	-0.038	60	0	11:54:58
582.	3682.480*	0.011	-4.	-7.	-0.02	-0.038	60	0	11:59:46
583.	3682.060*	0.013	5.	2.	-0.02	-0.038	60	0	12:02:57
584.	3678.530*	0.009	8.	-1.	-0.02	-0.039	60	0	12:09:12
585.	3677.010*	0.010	1.	0.	0.01	-0.039	60	0	12:13:02
586.	3675.360*	0.015	8.	-6.	0.02	-0.039	60	0	12:16:41
587.	3678.735*	0.012	-1.	8.	0.03	-0.040	60	1	12:29:07
588.	3681.270*	0.010	3.	5.	0.05	-0.040	60	0	12:32:54
589.	3682.765*	0.013	-5.	-1.	0.08	-0.041	60	0	12:38:28
591.	3681.335*	0.012	2.	-0.	0.03	-0.041	60	0	12:54:36
592.	3684.115*	0.011	8.	5.	0.01	-0.041	60	0	12:59:54
593.	3685.005*	0.009	2.	1.	-0.00	-0.042	60	0	13:04:45
594.	3686.805*	0.013	-8.	-8.	0.01	-0.042	60	0	13:08:37
0.	3688.730*	0.009	-0.	5.	-0.04	-0.042	60	0	13:19:51
597.	3687.635*	0.013	-1.	-0.	-0.01	-0.041	60	0	14:27:32
598.	3688.220*	0.021	-5.	8.	-0.01	-0.041	60	0	14:30:57
599.	3691.590*	0.011	-4.	4.	0.02	-0.041	60	1	14:37:24 53

600. 3692.510* 0.011 4. -3. 0.06 -0.041 60 0 14:42:41
601. 3690.255* 0.011 2. -7. 0.09 -0.040 60 0 14:46:35
602. 3690.475* 0.009 6. -0. 0.14 -0.040 60 0 14:49:32
603. 3688.570* 0.009 0. 1. 0.16 -0.040 60 0 14:53:02
604. 3688.680* 0.012 3. 2. 0.16 -0.040 60 0 14:56:04
605. 3689.990* 0.013 -6. 3. 0.15 -0.040 60 0 15:02:04
606. 3689.945* 0.012 -2. -3. 0.16 -0.040 60 0 15:05:51
607. 3690.010* 0.016 8. -7. 0.17 -0.040 60 0 15:09:27
608. 3691.695* 0.014 1. 2. 0.18 -0.040 60 0 15:13:25
609. 3691.400* 0.011 -1. -2. 0.18 -0.040 60 0 15:18:47
610. 3689.855* 0.015 0. 9. 0.18 -0.040 60 1 15:23:10
611. 3688.070* 0.010 -2. 2. 0.17 -0.040 60 0 15:26:20
612. 3687.265* 0.012 1. 5. 0.18 -0.039 60 0 15:29:57
613. 3684.410* 0.024 4. -3. 0.16 -0.039 60 0 15:36:53
614. 3683.035* 0.018 8. 0. 0.14 -0.039 60 1 15:40:53
615. 3683.265* 0.010 9. 5. 0.12 -0.039 60 0 15:44:20
616. 3681.755* 0.018 7. 4. 0.09 -0.039 60 0 15:47:47
617. 3680.640* 0.011 5. -8. 0.07 -0.039 60 0 15:51:41
618. 3678.410* 0.012 2. 1. 0.07 -0.039 60 0 15:55:24
619. 3675.360* 0.013 2. -1. 0.07 -0.039 60 0 15:59:12
620. 3674.345* 0.016 9. -3. 0.10 -0.039 60 0 16:03:49
621. 3676.270* 0.009 9. 7. 0.10 -0.039 60 2 16:07:01
622. 3679.265* 0.009 2. 4. 0.09 -0.039 60 0 16:10:28
623. 3681.345* 0.015 -3. 4. 0.08 -0.039 60 0 16:13:50
624. 3680.860* 0.011 -2. 1. 0.05 -0.039 60 0 16:20:46
625. 3681.820* 0.014 -0. -2. 0.07 -0.039 60 0 16:24:59
627. 3684.995* 0.015 -6. 8. 0.05 -0.039 60 0 16:32:50
628. 3684.620* 0.010 7. 0. -0.02 -0.039 60 0 16:39:45
629. 3684.675* 0.011 4. 0. -0.02 -0.039 60 0 16:43:02
630. 3683.895* 0.019 0. 1. -0.04 -0.039 60 1 16:47:21
631. 3682.375* 0.012 -1. 5. -0.07 -0.039 60 0 16:51:13
633. 3679.015* 0.011 8. 0. -0.09 -0.039 60 2 17:03:05
634. 3677.400* 0.010 4. 0. -0.09 -0.039 60 0 17:06:04
635. 3673.920* 0.013 7. 1. -0.10 -0.039 60 0 17:09:28
636. 3672.440* 0.011 8. -2. -0.11 -0.039 60 0 17:12:35
637. 3671.455* 0.015 1. 1. -0.13 -0.039 60 0 17:16:20
638. 3672.440* 0.019 -2. -3. -0.14 -0.039 60 0 17:19:17
639. 3676.340* 0.010 3. -1. -0.16 -0.039 60 0 17:23:10
640. 3679.370* 0.012 6. -1. -0.15 -0.039 60 0 17:27:11
0. 3688.720* 0.012 1. 1. -0.22 -0.039 60 0 17:50:16

SCINTREX V5.2 AUTOGRAV / Field Mode R5.35
Ser No: 211532.
Line: 0. Grid: 1. Job: 0. Date: 12/10/08 Operator: 29490.
GREF.: 0. mGals Tilt x sensit.: 267.3
GCAL.1: 5840.576 Tilt y sensit.: 223.6
GCAL.2: 0. Deg.Latitude: 38.67
TEMPCO.: -0.1488 mGal/mK Deg.Longitude: -69.75
Drift const.: 0.080 GMT Difference: -5.0hr
Drift Correction Start Time: 06:54:31 Cal.after x samples: 999
Date: 12/10/02 On-Line Tilt Corrected = ""

Station	Grav.	SD.	Tilt x	Tilt y	Temp.	E.T.C.	Dur	#	Rej	Time
0.	3688.725*	0.012	-3.	5.	-0.32	0.032	60	0	08:46:30	
644.	3686.125*	0.009	0.	4.	-0.33	0.026	60	0	09:02:55	
645.	3687.440*	0.012	6.	3.	-0.30	0.025	60	0	09:07:36 54	
646.	3689.995*	0.009	1.	7.	-0.29	0.023	60	0	09:12:07	
647.	3687.960*	0.014	5.	0.	-0.29	0.022	60	0	09:15:16	
648.	3688.850*	0.016	3.	-2.	-0.28	0.020	60	0	09:19:40	
649.	3688.935*	0.015	5.	1.	-0.29	0.019	60	0	09:22:52	
650.	3688.970*	0.013	-2.	4.	-0.29	0.018	60	0	09:26:06	
651.	3689.795*	0.012	-8.	5.	-0.31	0.017	60	0	09:30:04	
652.	3689.340*	0.013	3.	1.	-0.32	0.015	60	0	09:33:35	
653.	3688.380*	0.014	-2.	-5.	-0.30	0.014	60	0	09:38:20	
654.	3688.395*	0.013	-2.	2.	-0.28	0.013	60	0	09:41:13	
655.	3687.730*	0.015	8.	-7.	-0.27	0.012	60	0	09:44:11	
656.	3686.260*	0.012	-5.	5.	-0.27	0.011	60	0	09:47:13	
658.	3687.015*	0.008	2.	-2.	-0.28	0.008	60	0	09:54:12	
659.	3685.515*	0.013	9.	7.	-0.29	0.006	60	0	09:59:48	
660.	3684.735*	0.009	-4.	5.	-0.28	0.005	60	0	10:02:34	
661.	3683.355*	0.012	5.	1.	-0.29	0.004	60	0	10:05:39	
662.	3683.540*	0.017	5.	-2.	-0.26	0.002	60	0	10:10:15	
663.	3681.675*	0.014	9.	7.	-0.26	0.001	60	0	10:13:54	
664.	3690.550*	0.012	1.	1.	-0.24	-0.004	60	0	10:28:11	
665.	3687.665*	0.016	2.	7.	-0.22	-0.005	60	0	10:32:15	
666.	3686.445*	0.009	4.	4.	-0.21	-0.006	60	0	10:35:13	
667.	3685.910*	0.013	-1.	3.	-0.19	-0.008	60	0	10:38:06	
668.	3686.025*	0.015	1.	-4.	-0.17	-0.009	60	0	10:41:17	
669.	3685.670*	0.013	-7.	0.	-0.18	-0.010	60	0	10:44:50	
670.	3686.150*	0.014	6.	-0.	-0.19	-0.011	60	0	10:48:17	
673.	3684.120*	0.011	6.	1.	-0.17	-0.016	60	0	11:02:27	
674.	3682.640*	0.014	-1.	-3.	-0.16	-0.017	60	0	11:05:34	
675.	3680.680*	0.010	5.	-3.	-0.15	-0.018	60	0	11:09:03	
676.	3680.415*	0.013	7.	3.	-0.12	-0.019	60	0	11:13:46	
677.	3679.460*	0.017	-1.	-5.	-0.11	-0.020	60	0	11:16:47	
678.	3677.120*	0.015	-1.	5.	-0.11	-0.021	60	0	11:20:25	
679.	3672.870*	0.012	-1.	-2.	-0.11	-0.023	60	0	11:25:39	
680.	3670.595*	0.017	3.	5.	-0.10	-0.024	60	0	11:29:02	
681.	3670.275*	0.011	8.	6.	-0.10	-0.025	60	0	11:34:08	
682.	3673.170*	0.012	3.	1.	-0.09	-0.026	60	0	11:37:39	
683.	3677.730*	0.014	-1.	6.	-0.08	-0.027	60	0	11:42:24	
684.	3678.770*	0.012	-3.	4.	-0.06	-0.028	60	0	11:45:54	
685.	3680.680*	0.012	-4.	-6.	-0.04	-0.029	60	0	11:49:22	
686.	3681.780*	0.014	3.	6.	-0.03	-0.030	60	0	11:52:37	
687.	3682.950*	0.010	3.	1.	-0.04	-0.031	60	0	11:56:16	
688.	3684.845*	0.012	3.	6.	-0.06	-0.032	60	0	12:01:11	
689.	3684.720*	0.015	5.	7.	-0.03	-0.033	60	0	12:06:19	
690.	3685.320*	0.013	1.	3.	0.02	-0.035	60	0	12:14:24	
691.	3684.380*	0.011	7.	-1.	0.02	-0.036	60	0	12:18:12	
692.	3684.655*	0.011	0.	4.	0.01	-0.038	60	0	12:25:02	
693.	3685.385*	0.013	-1.	-0.	-0.02	-0.038	60	0	12:28:39	
694.	3687.625*	0.018	7.	5.	-0.03	-0.039	60	0	12:31:50	
695.	3689.960*	0.010	5.	8.	-0.02	-0.040	60	0	12:35:22	
696.	3691.805*	0.015	3.	1.	0.00	-0.041	60	0	12:40:39	
697.	3691.150*	0.022	-2.	4.	0.05	-0.042	60	0	12:46:17	



Rogun Dam
Complementary Geotechnical Investigations at
Right Bank



698. 3689.365* 0.012 1. 6. 0.05 -0.042 60 0 12:50:24
699. 3687.715* 0.012 -1. 2. 0.10 -0.043 60 0 12:55:07
700. 3685.255* 0.010 3. 3. 0.09 -0.044 60 0 12:58:15
701. 3685.850* 0.017 4. 7. 0.09 -0.044 60 0 13:02:30
702. 3686.210* 0.009 5. -5. 0.09 -0.045 60 0 13:05:38
703. 3686.375* 0.017 2. 4. 0.09 -0.045 60 0 13:08:18
704. 3686.370* 0.010 2. 2. 0.07 -0.046 60 0 13:12:55
705. 3685.465* 0.014 6. 8. 0.06 -0.046 60 0 13:15:55
706. 3683.960* 0.017 4. 6. 0.07 -0.046 60 0 13:19:13 55
707. 3682.395* 0.015 4. -8. 0.09 -0.047 60 0 13:23:33
708. 3682.855* 0.014 4. 6. 0.12 -0.047 60 0 13:26:48
709. 3685.770* 0.010 7. -7. 0.12 -0.048 60 0 13:29:58
710. 3685.325* 0.011 7. 7. 0.12 -0.048 60 0 13:32:59
711. 3685.060* 0.012 2. 1. 0.13 -0.048 60 0 13:35:55
712. 3686.380* 0.011 7. -2. 0.13 -0.048 60 0 13:39:23
0. 3688.690* 0.012 -6. -2. 0.11 -0.051 60 0 14:38:15

APPENDIX: B

CORECTED DATA

station	Name	date	time	reading (mGal)	x (m)	y (m)	Height (m)	terrain (mGal)	gravity (mGal)	Free-Air (mGal)	Bouguer (mGal)
1	A17	2012/10/01	10:32:03	3691.371	25249.6	22048.6	1689.66	0.252	2.672	-3.415	-3.415
2	A16	2012/10/01	10:42:57	3691.616	25236.9	22070.4	1691.81	0.244	2.916	-2.733	-2.733
3	A15	2012/10/01	10:50:38	3690.657	25218.8	22091.9	1698.28	0.235	1.957	-2.373	-2.373
4	A14	2012/10/01	10:57:33	3688.979	25200.5	22110.2	1707.04	0.188	0.279	-2.265	-2.265
5	A13	2012/10/01	11:11:59	3686.874	25183.2	22128.1	1717.13	0.19	-1.824	-2.311	-2.311
6	A12	2012/10/01	11:26:07	3688.949	25163.7	22147.4	1710.7	0.113	0.255	-1.543	-1.543
7	A11	2012/10/01	11:34:20	3689.762	25148	22166.3	1708.69	0.116	1.071	-1.137	-1.137
8	A10	2012/10/01	11:59:45	3689.701	25131.1	22183	1710.07	0.094	1.023	-0.903	-0.903
9	A09	2012/10/01	12:06:05	3689.865	25120.9	22199.8	1710.4	0.094	1.191	-0.667	-0.667
10	A08	2012/10/01	12:12:00	3689.684	25099.5	22218.8	1712.19	0.067	1.014	-0.48	-0.48
11	A07	2012/10/01	12:19:14	3690.148	25082.9	22236.4	1710.96	0.067	1.484	-0.261	-0.261
12	A06	2012/10/01	12:23:48	3690.623	25064.8	22251.9	1709.5	0.076	1.962	-0.08	-0.08
14	A05	2012/10/01	12:42:11	3691.463	25047.8	22270.5	1706.21	0.166	2.802	0.089	0.089
15	A04	2012/10/01	12:48:05	3690.553	25031.5	22289.9	1710.71	0.185	1.888	0.092	0.092
16	A03	2012/10/01	12:54:57	3688.434	25013.6	22307.7	1720.85	0.485	-0.236	0.035	0.035
17	A02	2012/10/01	13:03:07	3688.084	24999.3	22321.5	1722.97	0.706	-0.592	0.11	0.11
18	A01	2012/10/01	13:09:17	3687.545	24984.9	22336.7	1726.07	0.796	-1.135	0.2	0.2
19	B01	2012/10/01	13:18:27	3685.072	25001.3	22398.3	1738.91	0.905	-3.613	0.338	0.338
20	B02	2012/10/01	13:23:28	3685.198	25015.3	22381.4	1737.7	0.829	-3.487	0.217	0.217
21	B03	2012/10/01	13:30:22	3686.42	25032.6	22365	1731.17	0.799	-2.26	0.113	0.113
22	B04	2012/10/01	13:34:56	3688.156	25047.7	22344.5	1722.99	0.731	-0.521	0.186	0.186
25	B05	2012/10/01	14:28:57	3689.266	25064.5	22324.6	1717.6	0.117	0.633	0.242	0.242
26	B06	2012/10/01	14:34:03	3689.533	25085.9	22313.9	1716.05	0.083	0.904	0.197	0.197
27	B07	2012/10/01	14:48:10	3688.82	25100.8	22291.1	1718.59	0.058	0.203	0.013	0.013
28	B08	2012/10/01	14:52:46	3688.772	25115.4	22273.9	1718.34	0.05	0.159	-0.081	-0.081
29	B09	2012/10/01	15:00:00	3688.496	25134.5	22254.2	1718.72	0.05	-0.112	-0.276	-0.276
30	B10	2012/10/01	15:04:19	3688.068	25148.5	22237.5	1719.69	0.223	-0.537	-0.503	-0.503
31	B11	2012/10/01	15:09:15	3687.285	25167	22216.3	1721.86	0.285	-1.316	-0.839	-0.839
32	B12	2012/10/01	15:13:55	3687.718	25184.4	22198.4	1719.2	0.08	-0.88	-0.946	-0.946
33	B13	2012/10/01	15:19:28	3687.771	25200	22183.2	1717.96	0.083	-0.823	-1.142	-1.142
34	B14	2012/10/01	15:24:53	3688.344	25216.6	22156.9	1714	0.1	-0.246	-1.371	-1.371
35	B15	2012/10/01	15:31:13	3687.487	25233.2	22141	1715.89	0.127	-1.099	-1.838	-1.838
36	B16	2012/10/01	15:35:55	3688.515	25248.4	22123.1	1709.86	0.202	-0.068	-2.038	-2.038
37	B17	2012/10/01	15:41:19	3690.232	25264.8	22104.7	1701	0.279	1.652	-2.122	-2.122
38	B18	2012/10/01	15:48:16	3689.866	25285	22086.5	1700.36	0.235	1.29	-2.616	-2.616
39	B19	2012/10/01	15:52:53	3689.149	25298.8	22068.9	1700.62	0.25	0.576	-3.277	-3.277
40	B20	2012/10/01	15:57:54	3688.507	25318.9	22050	1699.26	0.342	-0.064	-4.194	-4.194
43	C01	2012/10/02	09:37:10	3683.287	25032	22423.8	1746.78	0.921	-5.373	0.183	0.183
44	C02	2012/10/02	09:44:26	3684.358	25046.4	22405.7	1741.1	0.885	-4.306	0.092	0.092
45	C03	2012/10/02	09:50:42	3686.061	25060.8	22391.8	1732.84	0.866	-2.606	0.108	0.108
46	C04	2012/10/02	10:00:04	3688.112	25079.2	22375	1723.02	0.835	-0.559	0.153	0.153
47	C05	2012/10/02	10:07:17	3688.853	25092.3	22358.1	1719.46	0.492	0.179	0.166	0.166
48	C06	2012/10/02	10:15:09	3689.015	25110.8	22328	1718.44	0.058	0.338	0.117	0.117
49	C07	2012/10/02	10:19:56	3688.763	25122.7	22327.8	1719.54	0.275	0.084	0.088	0.088
50	C08	2012/10/02	10:25:36	3688.665	25127.9	22321.7	1719.83	0.438	-0.016	0.047	0.047
51	C09	2012/10/02	10:30:40	3688.573	25134.5	22316.6	1720.08	0.41	-0.109	0.005	0.005
52	C10	2012/10/02	10:34:49	3688.566	25138.7	22309.4	1719.95	0.387	-0.117	-0.029	-0.029

54	C11	2012/10/02	10:43:11	3688.517	25145.3	22304.1	1719.89	0.368	-0.172	-0.096	-0.096
55	C12	2012/10/02	10:47:09	3688.47	25151.4	22299.1	1719.89	0.353	-0.223	-0.148	-0.148
56	C13	2012/10/02	10:51:48	3688.318	25156.3	22293.9	1720.27	0.336	-0.38	-0.226	-0.226
57	C14	2012/10/02	10:56:27	3688.021	25162.1	22287.9	1721.26	0.317	-0.681	-0.327	-0.327
58	C15	2012/10/02	11:00:46	3687.764	25167.4	22282.4	1722.14	0.305	-0.942	-0.408	-0.408
59	C16	2012/10/02	11:05:29	3687.587	25172.3	22276.2	1722.59	0.295	-1.123	-0.497	-0.497
60	C17	2012/10/02	11:10:03	3687.311	25179.6	22271.5	1723.46	0.287	-1.403	-0.601	-0.601
61	C18	2012/10/02	11:14:11	3686.984	25184.9	22265.8	1724.58	0.28	-1.734	-0.702	-0.702
62	C19	2012/10/02	11:18:02	3686.598	25190.2	22259.9	1725.93	0.278	-2.123	-0.817	-0.817
63	C20	2012/10/02	11:21:52	3686.271	25195.2	22253.6	1726.95	0.274	-2.453	-0.937	-0.937
64	C21	2012/10/02	11:24:33	3686.055	25201	22248	1727.56	0.271	-2.671	-1.032	-1.032
65	C22	2012/10/02	11:28:09	3686.049	25206.2	22240.9	1727.28	0.261	-2.679	-1.097	-1.097
66	C23	2012/10/02	11:31:46	3686.118	25212.2	22235.9	1726.77	0.254	-2.613	-1.135	-1.135
67	C24	2012/10/02	11:36:16	3686.047	25217.2	22229.7	1726.75	0.252	-2.687	-1.212	-1.212
68	C25	2012/10/02	11:40:28	3685.885	25223.2	22225.2	1727.23	0.255	-2.851	-1.28	-1.28
69	C26	2012/10/02	11:44:22	3685.579	25228.9	22219.5	1728.04	0.269	-3.159	-1.423	-1.423
70	C27	2012/10/02	11:48:56	3685.777	25236	22214.1	1726.8	0.251	-2.964	-1.481	-1.481
71	C28	2012/10/02	11:53:12	3685.871	25240.1	22207.5	1726.1	0.25	-2.872	-1.531	-1.531
72	C29	2012/10/02	11:56:53	3685.785	25245.8	22202.4	1726.11	0.252	-2.96	-1.617	-1.617
73	C30	2012/10/02	12:00:38	3685.949	25251.1	22196.3	1725.07	0.252	-2.797	-1.665	-1.665
74	C31	2012/10/02	12:04:40	3686.004	25256.8	22190.6	1724.4	0.254	-2.744	-1.749	-1.749
75	C32	2012/10/02	12:10:27	3686.102	25262.9	22185.6	1723.56	0.258	-2.648	-1.826	-1.826
76	C33	2012/10/02	12:14:26	3686.151	25267.6	22180.6	1722.91	0.264	-2.6	-1.91	-1.91
77	C34	2012/10/02	12:18:29	3686.311	25273.3	22175.5	1721.87	0.27	-2.441	-1.963	-1.963
78	C35	2012/10/02	12:23:00	3686.315	25279.9	22170.8	1721.43	0.279	-2.439	-2.049	-2.049
79	C36	2012/10/02	12:27:42	3686.409	25286.9	22164.2	1720.6	0.283	-2.346	-2.126	-2.126
80	C37	2012/10/02	12:31:23	3686.079	25290.6	22156.3	1721.31	0.29	-2.676	-2.311	-2.311
81	C38	2012/10/02	12:35:37	3685.833	25296.1	22151	1721.67	0.302	-2.923	-2.484	-2.484
82	C39	2012/10/02	12:41:42	3685.873	25303.2	22146.2	1720.87	0.307	-2.884	-2.609	-2.609
83	C40	2012/10/02	12:46:12	3686.267	25307.1	22138.4	1718.6	0.155	-2.49	-2.678	-2.678
84	C41	2012/10/02	12:50:58	3686.597	25311.6	22132	1716.74	0.161	-2.16	-2.726	-2.726
85	C42	2012/10/02	12:55:18	3686.862	25318.8	22126.9	1715.22	0.171	-1.895	-2.772	-2.772
86	C43	2012/10/02	13:00:18	3685.217	25335.9	22110.2	1719.34	0.193	-3.54	-3.577	-3.577
87	C44	2012/10/02	13:05:18	3684.552	25353.5	22092.1	1719.35	0.251	-4.205	-4.239	-4.239
88	C45	2012/10/02	13:08:50	3685.112	25369.1	22075.2	1714.35	0.277	-3.645	-4.699	-4.699
89	D49	2012/10/02	13:21:20	3687.083	25457.7	22056.3	1701.11	0.314	-1.672	-5.426	-5.426
90	D48	2012/10/02	13:26:16	3686.343	25439	22069.2	1706.49	0.287	-2.411	-5.066	-5.066
91	D47	2012/10/02	13:31:01	3685.024	25420.3	22088	1714.66	0.219	-3.73	-4.721	-4.721
92	D46	2012/10/02	13:37:26	3683.505	25405.9	22105.1	1723.38	0.388	-5.247	-4.46	-4.46
93	D45	2012/10/02	14:23:33	3684.44	25389.9	22127.3	1723.11	0.288	-4.297	-3.566	-3.566
94	D44	2012/10/02	14:28:21	3686.207	25370.9	22147	1718.51	0.252	-2.529	-2.734	-2.734
95	D43	2012/10/02	14:35:26	3685.204	25355.1	22161.4	1723.96	0.28	-3.529	-2.625	-2.625
96	D42	2012/10/02	14:40:17	3684.876	25349.5	22166.3	1725.7	0.281	-3.855	-2.596	-2.596
97	D41	2012/10/02	14:44:35	3684.518	25346.9	22171.9	1727.57	0.288	-4.211	-2.57	-2.57
98	D40	2012/10/02	14:50:09	3684.245	25341.1	22176.5	1729.08	0.298	-4.482	-2.534	-2.534
99	D39	2012/10/02	14:54:05	3683.926	25333.8	22181.8	1730.7	0.311	-4.8	-2.52	-2.52
100	D38	2012/10/02	14:56:46	3683.587	25327.8	22188.9	1732.53	0.321	-5.138	-2.486	-2.486
101	D37	2012/10/02	15:00:29	3683.439	25321.3	22193.8	1733.54	0.328	-5.284	-2.427	-2.427
103	D35	2012/10/02	15:11:03	3683.628	25310.4	22206.6	1733.85	0.305	-5.091	-2.17	-2.17
104	D34	2012/10/02	15:14:48	3683.91	25303.6	22213.8	1733.33	0.286	-4.808	-1.993	-1.993

105	D33	2012/10/02	15:19:08	3684.132	25295	22223	1732.95	0.262	-4.584	-1.847	-1.847
106	D32	2012/10/02	15:22:05	3684.738	25289.4	22228.7	1731.1	0.233	-3.977	-1.618	-1.618
107	D31	2012/10/02	15:26:06	3685.12	25283.8	22234.3	1729.99	0.214	-3.594	-1.46	-1.46
108	D30	2012/10/02	15:29:47	3685.467	25278.3	22240.7	1729	0.205	-3.246	-1.313	-1.313
109	D29	2012/10/02	15:32:07	3685.523	25272.8	22245.9	1729.07	0.203	-3.189	-1.243	-1.243
110	D28	2012/10/02	15:34:56	3685.449	25267.1	22251.8	1729.55	0.205	-3.262	-1.218	-1.218
111	D27	2012/10/02	15:39:05	3685.566	25261.7	22257.5	1729.4	0.209	-3.144	-1.131	-1.131
112	D26	2012/10/02	15:43:25	3685.673	25255.9	22263.2	1729.24	0.215	-3.036	-1.054	-1.054
113	D25	2012/10/02	15:47:34	3685.575	25250.3	22268.9	1729.87	0.224	-3.133	-1.022	-1.022
115	D24	2012/10/02	16:07:33	3685.504	25244.8	22274.6	1730.42	0.237	-3.194	-0.973	-0.973
116	D23	2012/10/02	16:11:51	3685.536	25239.2	22280.3	1730.5	0.253	-3.159	-0.922	-0.922
117	D22	2012/10/02	16:17:09	3685.758	25233.7	22286	1729.83	0.258	-2.934	-0.832	-0.832
118	D21	2012/10/02	16:21:26	3686.076	25228.4	22291.8	1728.8	0.269	-2.613	-0.722	-0.722
119	D20	2012/10/02	16:25:30	3686.318	25222.5	22297.3	1728.01	0.283	-2.369	-0.638	-0.638
120	D19	2012/10/02	16:29:55	3686.754	25216.9	22303	1726.41	0.295	-1.93	-0.527	-0.527
121	D18	2012/10/02	16:35:00	3687.341	25211	22309.3	1724.24	0.311	-1.34	-0.379	-0.379
122	D17	2012/10/02	16:39:02	3687.718	25205.9	22314.2	1722.85	0.328	-0.961	-0.283	-0.283
123	D16	2012/10/02	16:43:34	3688.275	25200.9	22322	1720.83	0.36	-0.402	-0.135	-0.135
124	D15	2012/10/02	16:48:03	3688.472	25193.9	22327.1	1720.27	0.375	-0.203	-0.05	-0.05
125	D14	2012/10/02	16:53:09	3688.594	25188.5	22332.1	1720.09	0.388	-0.078	0.038	0.038
126	D13	2012/10/02	16:57:43	3688.531	25183.3	22337.6	1720.54	0.399	-0.139	0.068	0.068
127	D12	2012/10/02	17:01:20	3688.412	25177.6	22343.4	1721.29	0.413	-0.257	0.103	0.103
128	D11	2012/10/02	17:05:08	3688.359	25172.2	22349.1	1721.77	0.431	-0.309	0.149	0.149
129	D10	2012/10/02	17:09:09	3688.265	25166.5	22354.7	1722.34	0.452	-0.401	0.173	0.173
130	D09	2012/10/02	17:12:54	3688.181	25160.9	22360.4	1722.86	0.476	-0.484	0.196	0.196
131	D08	2012/10/02	17:17:12	3688.008	25155.4	22365.9	1723.7	0.499	-0.656	0.195	0.195
132	D07	2012/10/02	17:21:03	3687.859	25138	22382.7	1724.68	0.609	-0.804	0.247	0.247
133	D06	2012/10/02	17:25:24	3686.8	25120.4	22401.9	1729.58	0.699	-1.863	0.187	0.187
134	D05	2012/10/02	17:30:01	3685.767	25103	22420.4	1734.71	0.793	-2.895	0.202	0.202
135	D04	2012/10/02	17:35:20	3684.113	25082.6	22436.5	1742.68	0.893	-4.548	0.173	0.173
136	D03	2012/10/02	17:40:51	3682.93	25067.6	22455.8	1749.03	0.995	-5.731	0.284	0.284
139	E01	2012/10/03	09:35:04	3684.056	25107.6	22492.8	1744.12	1.117	-4.6	0.414	0.414
140	E02	2012/10/03	09:40:34	3685.094	25124.1	22470.2	1738.41	0.89	-3.565	0.285	0.285
141	E03	2012/10/03	09:43:54	3685.333	25141.6	22451.5	1736.95	0.726	-3.328	0.224	0.224
142	E04	2012/10/03	09:53:09	3685.705	25159.4	22434.5	1734.74	0.633	-2.961	0.141	0.141
143	E05	2012/10/03	09:58:17	3686.454	25178.7	22422.4	1731.32	0.568	-2.215	0.191	0.191
144	E06	2012/10/03	10:03:01	3686.982	25196.2	22404.3	1728.5	0.492	-1.689	0.142	0.142
145	E09	2012/10/03	10:07:12	3687.626	25212.8	22383.4	1724.83	0.431	-1.048	0.035	0.035
146	E07	2012/10/03	10:15:37	3687.413	25202.1	22397.1	1726.41	0.473	-1.264	0.14	0.14
147	E08	2012/10/03	10:18:14	3687.557	25207.2	22390.7	1725.59	0.453	-1.122	0.116	0.116
148	E10	2012/10/03	10:21:16	3687.986	25220.6	22374.2	1723.02	0.41	-0.694	0.02	0.02
149	E11	2012/10/03	10:23:51	3688.1	25228	22368	1722.21	0.395	-0.581	-0.032	-0.032
150	E12	2012/10/03	10:27:59	3688.193	25234.8	22361.5	1721.58	0.382	-0.49	-0.07	-0.07
151	E14	2012/10/03	10:32:11	3688.242	25240.2	22354	1721.21	0.371	-0.442	-0.097	-0.097
152	E15	2012/10/03	10:37:56	3688.145	25244.1	22347	1721.28	0.357	-0.541	-0.182	-0.182
153	E16	2012/10/03	10:42:36	3687.853	25249.4	22341.6	1722.34	0.34	-0.835	-0.261	-0.261
154	E17	2012/10/03	10:46:52	3687.532	25255.4	22335.4	1723.54	0.314	-1.157	-0.339	-0.339
155	E18	2012/10/03	10:52:48	3686.954	25260.8	22329.7	1725.71	0.287	-1.737	-0.476	-0.476
156	E19	2012/10/03	10:56:43	3686.248	25266.8	22323.8	1728.39	0.265	-2.444	-0.636	-0.636
157	E20	2012/10/03	11:00:32	3686.111	25272.3	22318	1728.82	0.251	-2.582	-0.686	-0.686

159	E21	2012/10/03	11:14:05	3685.812	25277.8	22312.6	1729.79	0.238	-2.886	-0.792	-0.792
160	E22	2012/10/03	11:18:44	3685.525	25283.2	22306.8	1730.77	0.229	-3.176	-0.883	-0.883
161	E23	2012/10/03	11:21:05	3685.359	25288.8	22301	1731.25	0.224	-3.343	-0.953	-0.953
162	E24	2012/10/03	11:23:14	3685.309	25294.4	22295.5	1731.32	0.215	-3.394	-0.989	-0.989
163	E25	2012/10/03	11:27:03	3685.417	25299.8	22289.6	1730.63	0.205	-3.288	-1.023	-1.023
164	E26	2012/10/03	11:29:52	3685.641	25305.6	22283.9	1729.48	0.195	-3.065	-1.035	-1.035
165	E27	2012/10/03	11:35:48	3685.745	25310.8	22278	1728.76	0.191	-2.963	-1.08	-1.08
166	E28	2012/10/03	11:38:08	3685.739	25317	22272.3	1728.54	0.189	-2.97	-1.132	-1.132
167	E29	2012/10/03	11:40:30	3685.738	25323.7	22266.9	1728.24	0.19	-2.972	-1.195	-1.195
168	E30	2012/10/03	11:44:42	3685.732	25329.3	22261.2	1727.95	0.196	-2.979	-1.262	-1.262
169	E31	2012/10/03	11:47:20	3685.586	25334.5	22255.3	1728.19	0.2	-3.126	-1.358	-1.358
170	E32	2012/10/03	11:50:43	3685.2	25339.3	22248.9	1729.39	0.208	-3.513	-1.501	-1.501
171	E33	2012/10/03	11:55:26	3684.819	25344.4	22243.6	1730.52	0.22	-3.895	-1.653	-1.653
172	E34	2012/10/03	11:59:15	3684.523	25350.1	22238.6	1731.43	0.236	-4.192	-1.765	-1.765
173	E35	2012/10/03	12:03:05	3683.797	25356	22233.1	1733.85	0.273	-4.919	-1.998	-1.998
174	E36	2012/10/03	12:06:28	3682.681	25361.5	22226.8	1737.38	0.339	-6.036	-2.396	-2.396
175	E37	2012/10/03	12:10:51	3682.495	25366.8	22220.8	1737.65	0.363	-6.222	-2.527	-2.527
176	E38	2012/10/03	12:18:49	3682.908	25372.7	22215.4	1735.75	0.315	-5.81	-2.502	-2.502
177	E39	2012/10/03	12:22:08	3683.562	25378.4	22210.7	1733.03	0.271	-5.156	-2.402	-2.402
178	E40	2012/10/03	12:24:55	3684.152	25383.8	22203.9	1730.42	0.255	-4.566	-2.344	-2.344
179	E41	2012/10/03	12:29:22	3684.196	25389.1	22197.9	1729.81	0.265	-4.523	-2.425	-2.425
180	E42	2012/10/03	12:33:15	3683.18	25395.1	22191.5	1732.88	0.294	-5.538	-2.815	-2.815
181	E43	2012/10/03	12:40:16	3682.314	25409.6	22178.9	1734.35	0.416	-6.404	-3.382	-3.382
182	E44	2012/10/03	12:50:32	3684.502	25430.3	22156.3	1724.29	0.311	-4.215	-3.242	-3.242
183	E45	2012/10/03	12:53:07	3683.362	25447.3	22138.5	1726.43	0.372	-5.354	-3.945	-3.945
184	E46	2012/10/03	12:56:51	3684.102	25464.3	22120.4	1720.79	0.428	-4.614	-4.355	-4.355
185	E47	2012/10/03	13:01:18	3684.346	25482.6	22102.4	1716.93	0.187	-4.369	-4.896	-4.896
186	E48	2012/10/03	13:04:56	3684.671	25499.4	22084.3	1712.56	0.238	-4.043	-5.461	-5.461
187	E49	2012/10/03	13:07:41	3685.496	25516.8	22067	1706.1	0.296	-3.217	-5.952	-5.952
188	E50	2012/10/03	13:12:06	3686.176	25534.2	22052	1700.23	0.373	-2.536	-6.467	-6.467
190	F50	2012/10/03	13:21:46	3683.12	25554	22102	1716.96	0.326	-5.588	-6.11	-6.11
191	F49	2012/10/03	13:25:10	3682.61	25539.9	22120.7	1722.39	0.689	-6.097	-5.512	-5.512
192	F48	2012/10/03	13:28:16	3681.78	25520.3	22137.9	1728.76	0.626	-6.926	-5.043	-5.043
193	F47	2012/10/03	13:34:04	3681.98	25497.5	22154	1730.51	0.499	-6.724	-4.484	-4.484
194	F46	2012/10/03	13:38:31	3682.456	25480.3	22169.6	1731.25	0.415	-6.246	-3.854	-3.854
195	F45	2012/10/03	13:43:26	3683.441	25473	22189.2	1729.43	0.331	-5.258	-3.239	-3.239
197	F44	2012/10/03	14:41:11	3683.195	25454.1	22210.6	1732.29	0.297	-5.47	-2.868	-2.868
198	F43	2012/10/03	14:51:24	3683.312	25446.4	22216.1	1732.53	0.281	-5.346	-2.694	-2.694
199	F42	2012/10/03	14:54:20	3684.073	25439.6	22224.9	1730.42	0.258	-4.583	-2.362	-2.362
200	F41	2012/10/03	14:57:24	3683.649	25428.1	22231.6	1732.56	0.26	-5.005	-2.347	-2.347
201	F40	2012/10/03	15:00:04	3683.22	25422.1	22235.9	1734.52	0.27	-5.433	-2.374	-2.374
202	F39	2012/10/03	15:04:15	3683.231	25417.5	22242.4	1734.91	0.273	-5.419	-2.282	-2.282
204	F37	2012/10/03	15:10:55	3683.753	25411	22247.4	1734.72	0.267	-4.892	-1.795	-1.795
205	F36	2012/10/03	15:13:16	3684.359	25405.3	22253.2	1733.73	0.253	-4.285	-1.389	-1.389
206	F35	2012/10/03	15:19:34	3684.791	25399.4	22259.2	1731.8	0.237	-3.849	-1.346	-1.346
207	F34	2012/10/03	15:22:12	3685.232	25394.4	22264.6	1730.31	0.227	-3.406	-1.207	-1.207
208	F33	2012/10/03	15:24:49	3685.733	25383.1	22275.7	1727.29	0.214	-2.903	-1.319	-1.319
209	F32	2012/10/03	15:29:17	3685.929	25377.3	22281.7	1726.84	0.209	-2.704	-1.213	-1.213
210	F31	2012/10/03	15:32:01	3686.14	25372	22287.4	1726.32	0.205	-2.491	-1.105	-1.105
211	F30	2012/10/03	15:35:48	3686.272	25366.1	22293.6	1726.13	0.204	-2.357	-1.009	-1.009

212	F29	2012/10/03	15:38:14	3686.443	25361	22298.8	1725.75	0.209	-2.184	-0.914	-0.914
213	F28	2012/10/03	15:40:29	3686.429	25355.1	22304.8	1726.09	0.206	-2.197	-0.858	-0.858
214	F27	2012/10/03	15:44:41	3686.025	25349.6	22310.5	1727.92	0.202	-2.598	-0.886	-0.886
215	F26	2012/10/03	15:47:06	3685.896	25344.2	22315.9	1728.71	0.202	-2.726	-0.852	-0.852
216	F25	2012/10/03	15:50:55	3685.762	25338.3	22321.5	1729.48	0.203	-2.857	-0.826	-0.826
217	F24	2012/10/03	15:54:50	3685.734	25332.5	22327.5	1729.86	0.206	-2.883	-0.775	-0.775
218	F23	2012/10/03	15:57:07	3685.8	25327.1	22333.4	1729.85	0.211	-2.815	-0.711	-0.711
219	F22	2012/10/03	16:00:03	3685.901	25321.5	22339.1	1729.63	0.218	-2.713	-0.652	-0.652
220	F21	2012/10/03	16:06:48	3686.064	25315.9	22344.7	1729.22	0.228	-2.546	-0.568	-0.568
221	F20	2012/10/03	16:09:50	3686.23	25310.4	22350.8	1728.75	0.242	-2.378	-0.497	-0.497
222	F19	2012/10/03	16:12:16	3686.401	25304.7	22356.5	1728.22	0.257	-2.205	-0.432	-0.432
223	F18	2012/10/03	16:20:25	3686.644	25299.4	22361.8	1727.39	0.274	-1.958	-0.353	-0.353
224	F17	2012/10/03	16:23:26	3686.735	25293.5	22367.7	1727.11	0.291	-1.865	-0.318	-0.318
225	F16	2012/10/03	16:27:27	3687.012	25288.2	22374.2	1726.21	0.313	-1.586	-0.222	-0.222
226	F15	2012/10/03	16:31:40	3687.318	25281.1	22380.5	1725.06	0.34	-1.278	-0.149	-0.149
227	F14	2012/10/03	16:35:27	3687.635	25276.1	22385.7	1723.99	0.363	-0.959	-0.049	-0.049
228	F13	2012/10/03	16:37:53	3687.781	25270.7	22391.2	1723.53	0.387	-0.812	0.005	0.005
229	F12	2012/10/03	16:45:25	3687.879	25265.9	22396.1	1723.26	0.403	-0.711	0.052	0.052
230	F11	2012/10/03	16:48:05	3687.864	25260.1	22401.9	1723.55	0.421	-0.725	0.097	0.097
231	F10	2012/10/03	16:50:25	3687.841	25254.8	22407.5	1723.83	0.444	-0.747	0.131	0.131
232	F09	2012/10/03	16:52:34	3687.866	25248.8	22413.1	1723.96	0.468	-0.721	0.184	0.184
233	F08	2012/10/03	16:55:24	3687.487	25244	22418.5	1725.76	0.472	-1.099	0.173	0.173
234	F07	2012/10/03	16:57:50	3687.053	25237.8	22425.4	1728.01	0.478	-1.532	0.197	0.197
235	F06	2012/10/03	17:00:25	3686.764	25231.9	22430.6	1729.55	0.492	-1.82	0.224	0.224
236	F05	2012/10/03	17:04:00	3686.025	25214.5	22448.5	1733.29	0.546	-2.558	0.248	0.248
237	F04	2012/10/03	17:06:42	3685.331	25197.3	22466	1736.72	0.614	-3.251	0.254	0.254
238	F03	2012/10/03	17:10:52	3684.948	25179.4	22483	1738.81	0.709	-3.633	0.298	0.298
239	F02	2012/10/03	17:14:15	3684.674	25162.1	22503	1740.76	0.871	-3.906	0.424	0.424
240	F01	2012/10/03	17:18:22	3684.17	25145	22520.4	1743.27	1.111	-4.409	0.432	0.432
241	G01	2012/10/03	17:23:16	3683.337	25183.1	22552.5	1746.95	1.019	-5.241	0.35	0.35
242	G02	2012/10/03	17:27:59	3684.138	25200.5	22534.1	1742.99	0.862	-4.439	0.345	0.345
243	G03	2012/10/03	17:30:49	3685.029	25218.3	22516.6	1738.67	0.733	-3.547	0.355	0.355
244	G04	2012/10/03	17:35:25	3685.47	25234.7	22498.9	1736.14	0.624	-3.106	0.283	0.283
245	G05	2012/10/03	17:39:31	3686.107	25252.8	22480.8	1732.85	0.534	-2.468	0.249	0.249
248	G05	2012/10/04	09:36:14	3686.03	25252.8	22480.8	1732.85	0.534	-2.569	0.149	0.149
249	G06	2012/10/04	09:41:01	3686.354	25270.4	22462.9	1730.88	0.463	-2.247	0.07	0.07
250	G07	2012/10/04	09:44:59	3686.409	25276.1	22457.2	1730.42	0.445	-2.194	0.028	0.028
251	G08	2012/10/04	09:49:30	3686.613	25283.4	22452.6	1729.38	0.431	-1.992	0.018	0.018
252	G09	2012/10/04	09:53:26	3686.852	25287.5	22445.5	1728.18	0.421	-1.754	0.01	0.01
253	G10	2012/10/04	09:57:17	3686.772	25293	22440.1	1728.33	0.404	-1.836	-0.04	-0.04
254	G11	2012/10/04	10:01:14	3686.511	25298.9	22434.1	1729.23	0.379	-2.099	-0.12	-0.12
255	G12	2012/10/04	10:05:13	3686.37	25304.8	22428.3	1729.62	0.363	-2.242	-0.184	-0.184
256	G13	2012/10/04	10:10:41	3686.219	25308.7	22423	1730.06	0.35	-2.395	-0.247	-0.247
257	G14	2012/10/04	10:14:31	3685.713	25315.4	22417.5	1731.93	0.331	-2.903	-0.373	-0.373
258	G15	2012/10/04	10:18:28	3685.278	25321.3	22411.2	1733.47	0.322	-3.339	-0.496	-0.496
259	G16	2012/10/04	10:22:24	3685.087	25326.7	22405.7	1734.1	0.307	-3.532	-0.56	-0.56
260	G17	2012/10/04	10:24:52	3685.191	25332.1	22400.4	1733.54	0.29	-3.429	-0.572	-0.572
261	G18	2012/10/04	10:27:21	3685.381	25337.8	22394.3	1732.66	0.275	-3.24	-0.562	-0.562
262	G19	2012/10/04	10:31:02	3685.555	25343.4	22388.3	1731.77	0.265	-3.067	-0.571	-0.571
263	G20	2012/10/04	10:33:35	3685.639	25348.9	22382.6	1731.24	0.257	-2.984	-0.595	-0.595

264	G21	2012/10/04	10:37:49	3685.633	25354.4	22376.8	1731	0.249	-2.992	-0.652	-0.652
265	G22	2012/10/04	10:41:59	3685.622	25360	22371.3	1730.83	0.243	-3.004	-0.7	-0.7
266	G23	2012/10/04	10:44:37	3685.702	25365.5	22365.8	1730.33	0.24	-2.925	-0.722	-0.722
267	G24	2012/10/04	10:48:30	3685.776	25370.8	22360.4	1729.79	0.238	-2.853	-0.759	-0.759
268	G25	2012/10/04	10:51:24	3685.955	25376.8	22354.3	1728.75	0.238	-2.675	-0.794	-0.794
269	G26	2012/10/04	10:57:52	3685.948	25382	22348.3	1728.51	0.238	-2.683	-0.852	-0.852
270	G27	2012/10/04	11:02:30	3686.262	25387.8	22343.2	1726.92	0.241	-2.371	-0.862	-0.862
271	G28	2012/10/04	11:05:07	3686.651	25395.3	22338.4	1725.17	0.25	-1.983	-0.831	-0.831
272	G29	2012/10/04	11:07:34	3686.656	25385.4	22330.8	1725.11	0.24	-1.978	-0.839	-0.839
273	G30	2012/10/04	11:12:45	3686.644	25375.4	22323.1	1725.15	0.229	-1.991	-0.845	-0.845
275	G31	2012/10/04	11:33:48	3686.114	25399.1	22293.7	1725.73	0.237	-2.53	-1.265	-1.265
276	G32	2012/10/04	11:38:15	3686.303	25421.4	22307.8	1727.28	0.248	-2.343	-0.761	-0.761
277	G33	2012/10/04	11:42:30	3685.667	25427.5	22302.1	1729.48	0.256	-2.981	-0.95	-0.95
278	G34	2012/10/04	11:47:00	3685.066	25432.8	22296.9	1731.15	0.267	-3.583	-1.213	-1.213
279	G35	2012/10/04	11:51:28	3684.579	25438.3	22291.9	1733.15	0.281	-4.072	-1.294	-1.294
280	G36	2012/10/04	11:54:44	3683.999	25442.7	22282.8	1735.39	0.308	-4.653	-1.419	-1.419
281	G37	2012/10/04	12:01:40	3683.307	25449.2	22279.5	1737.04	0.35	-5.348	-1.776	-1.776
282	G38	2012/10/04	12:07:06	3682.786	25454.9	22274	1737.01	0.346	-5.87	-2.305	-2.305
283	G39	2012/10/04	12:18:34	3682.673	25460.4	22268.3	1735.79	0.334	-5.986	-2.67	-2.67
284	G40	2012/10/04	12:21:18	3682.868	25466	22262.5	1733.8	0.314	-5.792	-2.881	-2.881
285	G41	2012/10/04	12:25:17	3683.262	25471.9	22256.8	1731.14	0.303	-5.398	-3.029	-3.029
286	G42	2012/10/04	12:27:36	3683.851	25488.2	22239.8	1726.6	0.33	-4.81	-3.366	-3.366
287	G43	2012/10/04	12:32:44	3684.715	25508.1	22219.2	1731.02	0.39	-3.946	-1.602	-1.602
288	G44	2012/10/04	12:43:37	3683.078	25524.2	22202.2	1736.69	0.561	-5.584	-2.085	-2.085
289	G45	2012/10/04	12:48:51	3681.053	25542	22187.6	1728.93	0.521	-7.609	-5.692	-5.692
290	G46	2012/10/04	12:55:39	3682.667	25556.8	22171.9	1731.24	0.634	-5.995	-3.606	-3.606
291	G47	2012/10/04	13:01:18	3681.376	25576.3	22149	1724.21	0.747	-7.286	-6.329	-6.329
294	H49	2012/10/04	13:16:43	3683.144	25632.7	22163.2	1717.8	0.27	-5.517	-5.867	-5.867
295	H48	2012/10/04	13:20:42	3683.269	25615.8	22181.1	1721.14	0.776	-5.391	-5.061	-5.061
296	H47	2012/10/04	13:25:24	3682.639	25597.5	22199.4	1726.65	0.673	-6.02	-4.566	-4.566
297	H46	2012/10/04	13:31:11	3682.033	25581.7	22217.6	1731.21	0.607	-6.625	-4.243	-4.243
298	H45	2012/10/04	13:34:12	3681.458	25563.2	22234.8	1735.5	0.568	-7.199	-3.941	-3.941
299	H44	2012/10/04	13:38:45	3682.998	25545.3	22253.7	1731.56	0.453	-5.658	-3.203	-3.203
300	H43	2012/10/04	13:45:23	3685.643	25529.2	22271.2	1722.73	0.439	-3.011	-2.357	-2.357
301	H42	2012/10/04	13:48:17	3685.123	25511.7	22291.2	1726.49	0.354	-3.53	-2.11	-2.11
302	H41	2012/10/04	13:51:27	3684.513	25504.1	22295.4	1730.15	0.354	-4.139	-1.972	-1.972
303	H40	2012/10/04	13:55:19	3684.153	25500.1	22300.7	1731.09	0.362	-4.497	-2.139	-2.139
304	H39	2012/10/04	13:58:07	3683.473	25494.4	22306	1734.1	0.388	-5.176	-2.205	-2.205
305	H38	2012/10/04	14:00:59	3682.558	25488.2	22312.1	1737.8	0.459	-6.09	-2.364	-2.364
306	H37	2012/10/04	14:05:14	3682.138	25482.7	22317.1	1739.61	0.472	-6.508	-2.414	-2.414
308	H36	2012/10/04	15:08:29	3683.521	25476.5	22322.7	1734.63	0.38	-5.097	-2.017	-2.017
309	H35	2012/10/04	15:13:58	3684.962	25470.2	22329.6	1729.62	0.32	-3.655	-1.597	-1.597
310	H34	2012/10/04	15:19:02	3685.603	25466.6	22334.7	1727.51	0.315	-3.012	-1.383	-1.383
311	H33	2012/10/04	15:24:10	3686.224	25460	22340.6	1725.37	0.339	-2.389	-1.198	-1.198
312	H32	2012/10/04	15:26:54	3686.34	25454.1	22346.5	1725.24	0.307	-2.273	-1.108	-1.108
313	H31	2012/10/04	15:30:40	3686.066	25448.4	22352.6	1726.58	0.29	-2.545	-1.106	-1.106
314	H30	2012/10/04	15:33:01	3685.887	25442.5	22358.8	1727.72	0.28	-2.724	-1.052	-1.052
315	H29	2012/10/04	15:36:43	3685.598	25438.8	22364.1	1728.99	0.277	-3.011	-1.081	-1.081
316	H28	2012/10/04	15:39:22	3685.298	25432	22369.7	1730.54	0.274	-3.31	-1.064	-1.064
317	H27	2012/10/04	15:42:45	3685.364	25421.4	22372.3	1730.68	0.271	-3.243	-0.969	-0.969

318	H26	2012/10/04	15:47:18	3685.425	25421.2	22380.7	1730.71	0.282	-3.181	-0.901	-0.901
319	H25	2012/10/04	15:50:05	3685.026	25415.2	22385.8	1732.49	0.282	-3.579	-0.936	-0.936
320	H24	2012/10/04	15:54:19	3684.842	25409.4	22392.2	1733.52	0.288	-3.762	-0.908	-0.908
321	H23	2012/10/04	15:58:48	3684.654	25403.8	22397.7	1734.54	0.292	-3.948	-0.887	-0.887
322	H22	2012/10/04	16:03:02	3684.57	25398.3	22403.8	1735.2	0.296	-4.031	-0.835	-0.835
323	H21	2012/10/04	16:05:54	3684.536	25393.1	22408.7	1735.54	0.3	-4.064	-0.798	-0.798
324	H20	2012/10/04	16:08:26	3684.316	25386.9	22415.4	1736.67	0.307	-4.283	-0.787	-0.787
325	H19	2012/10/04	16:11:19	3684.102	25381.7	22420.4	1737.72	0.313	-4.496	-0.787	-0.787
326	H18	2012/10/04	16:13:43	3684.038	25375.9	22426.4	1738.31	0.321	-4.559	-0.731	-0.731
327	H17	2012/10/04	16:16:02	3683.864	25370.8	22431.9	1739.13	0.333	-4.733	-0.736	-0.736
328	H16	2012/10/04	16:18:23	3683.959	25364.8	22437.7	1738.97	0.342	-4.637	-0.673	-0.673
329	H15	2012/10/04	16:20:58	3684.145	25359.2	22443.5	1738.37	0.353	-4.45	-0.608	-0.608
330	H14	2012/10/04	16:23:22	3684.406	25353.6	22449.4	1737.48	0.365	-4.189	-0.527	-0.527
331	H13	2012/10/04	16:27:54	3684.887	25348.3	22454.7	1735.66	0.374	-3.706	-0.416	-0.416
332	H12	2012/10/04	16:30:37	3685.573	25343.1	22460.6	1732.96	0.393	-3.02	-0.28	-0.28
333	H11	2012/10/04	16:34:27	3686.009	25337	22466.5	1731.43	0.41	-2.583	-0.155	-0.155
334	H10	2012/10/04	16:36:45	3686.24	25330.9	22472.3	1730.47	0.422	-2.351	-0.119	-0.119
335	H09	2012/10/04	16:39:40	3686.556	25325.1	22478.1	1730.36	0.433	-2.034	0.176	0.176
336	H08	2012/10/04	16:41:57	3686.736	25320.4	22483.3	1728.85	0.46	-1.854	0.048	0.048
337	H07	2012/10/04	16:46:00	3686.798	25314.6	22489.3	1728.79	0.479	-1.791	0.098	0.098
338	H06	2012/10/04	16:48:40	3686.839	25309	22495.1	1728.75	0.5	-1.749	0.132	0.132
339	H05-1	2012/10/04	16:56:37	3686.856	25301	22503.4	1728.78	0.536	-1.73	0.157	0.157
340	H05	2012/10/04	16:59:20	3686.817	25283.7	22521.2	1729.36	0.634	-1.769	0.236	0.236
341	H04	2012/10/04	17:02:32	3686.488	25266.1	22539	1731.06	0.746	-2.097	0.254	0.254
342	H03	2012/10/04	17:05:27	3686.294	25248.5	22556.8	1731.92	0.929	-2.291	0.237	0.237
343	H02	2012/10/04	17:08:24	3685.329	25231	22574.9	1735.95	1.13	-3.255	0.094	0.094
344	H01	2012/10/04	17:13:52	3683.266	25214.9	22591.7	1745.63	1.18	-5.318	0.004	0.004
345	I01	2012/10/04	17:19:28	3682.513	25251.6	22625.7	1747.59	1.198	-6.07	-0.35	-0.35
346	I02	2012/10/04	17:23:36	3685.344	25268.5	22608.2	1735.25	1.168	-3.239	-0.032	-0.032
347	I03	2012/10/04	17:26:41	3686.595	25286.1	22590.2	1729.9	0.999	-1.987	0.128	0.128
348	I04	2012/10/04	17:30:48	3686.756	25303.4	22572.3	1729.25	0.791	-1.826	0.157	0.157
349	I05	2012/10/04	17:33:22	3686.761	25320.8	22554.7	1729.15	0.648	-1.821	0.142	0.142
352	I05	2012/10/05	09:43:57	3686.931	25320.8	22554.7	1729.15	0.648	-1.816	0.147	0.147
354	I06	2012/10/05	09:52:34	3686.726	25346.7	22528.2	1729.52	0.538	-2.025	0.014	0.014
355	I07	2012/10/05	09:55:03	3686.531	25352.9	22521.5	1730.21	0.531	-2.221	-0.043	-0.043
356	I08	2012/10/05	09:59:19	3686.256	25359	22515.5	1731.28	0.518	-2.498	-0.101	-0.101
357	I09	2012/10/05	10:04:11	3685.436	25366	22508.5	1734.91	0.482	-3.321	-0.184	-0.184
358	I10	2012/10/05	10:09:34	3685.021	25369.7	22504.4	1736.2	0.472	-3.738	-0.339	-0.339
359	I11	2012/10/05	10:15:01	3684.226	25375.6	22498.8	1739.38	0.456	-4.536	-0.489	-0.489
360	I12	2012/10/05	10:17:30	3683.826	25381.1	22493.1	1740.94	0.443	-4.937	-0.572	-0.572
361	I13	2012/10/05	10:20:21	3683.451	25386.6	22487.6	1742.3	0.43	-5.314	-0.671	-0.671
362	I14	2012/10/05	10:22:58	3683.105	25392	22481.7	1743.59	0.419	-5.661	-0.755	-0.755
363	I15	2012/10/05	10:25:32	3682.865	25397.4	22475.8	1744.45	0.413	-5.902	-0.82	-0.82
364	I16	2012/10/05	10:29:41	3682.46	25403.3	22470.3	1745.83	0.416	-6.309	-0.946	-0.946
365	I17	2012/10/05	10:32:38	3682.35	25408.6	22464.4	1746.15	0.413	-6.421	-0.993	-0.993
366	I18	2012/10/05	10:35:10	3682.289	25414.6	22458.9	1746.22	0.413	-6.483	-1.04	-1.04
367	I19	2012/10/05	10:39:56	3682.229	25420.2	22453.1	1746.18	0.417	-6.545	-1.112	-1.112
368	I20	2012/10/05	10:44:00	3682.249	25425.6	22447.4	1745.89	0.421	-6.527	-1.152	-1.152
369	I21	2012/10/05	10:46:36	3682.518	25431.3	22441.8	1744.5	0.415	-6.259	-1.168	-1.168
370	I22	2012/10/05	10:49:25	3682.958	25436.8	22435.8	1742.59	0.4	-5.821	-1.118	-1.118

371	I23	2012/10/05	10:53:26	3683.393	25444	22429	1740.49	0.387	-5.388	-1.113	-1.113
372	I24	2012/10/05	10:55:50	3683.572	25448.1	22424.1	1739.72	0.379	-5.21	-1.092	-1.092
373	I25	2012/10/05	10:58:00	3683.687	25453.6	22418.6	1738.87	0.37	-5.096	-1.151	-1.151
374	I26	2012/10/05	11:01:57	3683.897	25459.1	22412.7	1737.78	0.361	-4.888	-1.165	-1.165
375	I27	2012/10/05	11:04:19	3684.021	25465.3	22407.7	1736.9	0.356	-4.765	-1.223	-1.223
376	I28	2012/10/05	11:06:42	3684.116	25470.3	22401.7	1736.19	0.347	-4.671	-1.273	-1.273
377	I29	2012/10/05	11:11:02	3684.13	25475.9	22395.8	1735.77	0.346	-4.658	-1.346	-1.346
378	I30	2012/10/05	11:13:50	3684.045	25481.3	22390	1735.73	0.358	-4.745	-1.441	-1.441
379	I31	2012/10/05	11:17:01	3684.145	25486.9	22384.8	1734.97	0.355	-4.646	-1.497	-1.497
380	I32	2012/10/05	11:22:16	3684.759	25491.9	22378.5	1732.15	0.343	-4.034	-1.459	-1.459
381	I33	2012/10/05	11:25:26	3685.393	25497.9	22373.1	1729.37	0.339	-3.401	-1.393	-1.393
382	I34	2012/10/05	11:29:39	3685.708	25504.9	22369	1727.78	0.343	-3.088	-1.404	-1.404
383	I35	2012/10/05	11:34:20	3685.902	25509.4	22361.5	1726.37	0.339	-2.896	-1.5	-1.5
384	I36	2012/10/05	11:38:57	3685.996	25514.9	22354.9	1726.05	0.327	-2.803	-1.472	-1.472
385	I37	2012/10/05	11:42:02	3685.736	25520.4	22350.3	1726.72	0.325	-3.064	-1.598	-1.598
386	I38	2012/10/05	11:46:40	3685.905	25525.5	22344.5	1725.6	0.33	-2.897	-1.659	-1.659
387	I39	2012/10/05	11:51:20	3685.939	25529.7	22339.9	1725.19	0.335	-2.864	-1.708	-1.708
388	I40	2012/10/05	11:54:39	3685.804	25536.9	22333.6	1725.35	0.345	-3	-1.811	-1.811
389	I41	2012/10/05	11:59:07	3685.653	25543	22327.2	1725.42	0.357	-3.153	-1.951	-1.951
390	I42	2012/10/05	12:04:31	3686.047	25547.3	22321.8	1723.44	0.367	-2.76	-1.961	-1.961
391	I43	2012/10/05	12:08:19	3686.477	25565.8	22303.4	1720.22	0.5	-2.331	-2.188	-2.188
392	I44	2012/10/05	12:14:32	3682.106	25583.4	22285.2	1735.53	0.637	-6.703	-3.44	-3.44
393	I45	2012/10/05	12:19:17	3682.07	25601	22267.6	1734.16	0.606	-6.74	-3.756	-3.756
394	I46	2012/10/05	12:23:11	3682.649	25618.2	22249.6	1730.11	0.65	-6.162	-4.003	-4.003
395	I47	2012/10/05	12:27:40	3682.664	25636	22231.5	1727.45	0.771	-6.147	-4.531	-4.531
396	I48	2012/10/05	12:31:16	3683.443	25653.5	22214	1721.19	0.918	-5.369	-5.029	-5.029
397	I49	2012/10/05	12:37:24	3685.542	25671.6	22195.8	1709.54	0.396	-3.271	-5.304	-5.304
398	I50	2012/10/05	12:41:32	3686.772	25687.8	22177.9	1701.77	0.506	-2.041	-5.659	-5.659
399	J50	2012/10/05	12:47:09	3686.201	25726.5	22210.2	1703.67	0.584	-2.612	-5.843	-5.843
400	J49	2012/10/05	13:02:32	3684.574	25709.2	22228.2	1712.87	0.473	-4.24	-5.595	-5.595
401	J48	2012/10/05	13:06:42	3681.718	25692.2	22246.8	1726.55	1.198	-7.096	-5.662	-5.662
402	J47	2012/10/05	13:11:29	3679.918	25674.4	22264.1	1736.35	1.134	-8.895	-5.466	-5.466
403	J46	2012/10/05	13:14:49	3680.518	25656.6	22281.7	1737.23	0.9	-8.295	-4.685	-4.685
404	J45	2012/10/05	13:17:43	3682.677	25639.3	22299.8	1731.8	0.648	-6.136	-3.634	-3.634
405	J44	2012/10/05	13:22:28	3683.157	25621.7	22317.6	1731.43	0.598	-5.655	-3.228	-3.228
406	J43	2012/10/05	13:33:13	3686.656	25604.6	22335.4	1718.88	0.201	-2.155	-2.284	-2.284
407	J42	2012/10/05	13:36:37	3687.526	25586.9	22353.6	1716.85	0.133	-1.284	-1.828	-1.828
408	J41	2012/10/05	13:41:07	3687.41	25581.6	22358.7	1717.75	0.118	-1.399	-1.76	-1.76
409	J40	2012/10/05	13:46:31	3686.88	25575.8	22365.2	1720.52	0.372	-1.928	-1.725	-1.725
411	J39	2012/10/05	15:36:18	3686.631	25570.1	22370.6	1721.8	0.407	-2.154	-1.69	-1.69
412	J38	2012/10/05	15:39:25	3686.376	25565.1	22376.1	1723.22	0.398	-2.408	-1.653	-1.653
413	J37	2012/10/05	15:41:57	3686.532	25560	22382.6	1722.96	0.406	-2.251	-1.549	-1.549
414	J36	2012/10/05	15:46:47	3686.432	25554.4	22389.9	1723.73	0.428	-2.35	-1.491	-1.491
415	J35	2012/10/05	15:51:43	3686.288	25546.2	22392.4	1724.48	0.44	-2.492	-1.48	-1.48
416	J34	2012/10/05	15:54:37	3685.934	25542.3	22399.2	1726.21	0.459	-2.845	-1.481	-1.481
417	J33	2012/10/05	15:59:00	3685.169	25536.8	22404.7	1729.72	0.457	-3.608	-1.529	-1.529
418	J32	2012/10/05	16:01:45	3684.375	25530.9	22410.6	1733.31	0.468	-4.401	-1.59	-1.59
419	J31	2012/10/05	16:05:10	3683.87	25525.3	22416.5	1735.72	0.473	-4.905	-1.602	-1.602
420	J30	2012/10/05	16:08:02	3683.476	25520	22422.2	1737.68	0.478	-5.298	-1.596	-1.596
421	J29	2012/10/05	16:12:11	3683.012	25514.3	22427.8	1739.93	0.486	-5.76	-1.599	-1.599

422	J28	2012/10/05	16:14:55	3682.257	25508.4	22434.2	1743.12	0.504	-6.514	-1.703	-1.703
423	J27	2012/10/05	16:19:22	3681.713	25502.9	22439.2	1745.5	0.519	-7.057	-1.762	-1.762
424	J26	2012/10/05	16:23:34	3681.334	25497.7	22445	1747.34	0.521	-7.434	-1.764	-1.764
425	J25	2012/10/05	16:27:01	3681.255	25491.9	22450.6	1748.12	0.506	-7.512	-1.682	-1.682
426	J24	2012/10/05	16:31:37	3681.051	25486.4	22456.7	1749.32	0.5	-7.714	-1.64	-1.64
427	J23	2012/10/05	16:36:04	3680.857	25480.2	22461.6	1750.36	0.5	-7.906	-1.621	-1.621
428	J22	2012/10/05	16:38:57	3680.597	25475.2	22467.7	1751.68	0.507	-8.165	-1.611	-1.611
429	J21	2012/10/05	16:43:10	3680.248	25469.2	22474.1	1753.27	0.522	-8.513	-1.633	-1.633
430	J20	2012/10/05	16:48:15	3680.204	25464.3	22479.5	1753.75	0.52	-8.555	-1.577	-1.577
431	J19	2012/10/05	16:53:29	3680.415	25458.2	22485.3	1753.27	0.497	-8.342	-1.464	-1.464
432	J18	2012/10/05	16:55:53	3680.501	25452.8	22490.8	1753.23	0.489	-8.255	-1.385	-1.385
433	J17	2012/10/05	16:58:29	3680.572	25447.1	22496.7	1753.24	0.49	-8.183	-1.311	-1.311
434	J16	2012/10/05	17:01:12	3680.782	25441.8	22502.3	1752.68	0.49	-7.972	-1.215	-1.215
435	J15	2012/10/05	17:03:53	3681.063	25435.9	22508	1751.84	0.49	-7.691	-1.103	-1.103
436	J14	2012/10/05	17:06:07	3681.303	25430.1	22513.7	1751.06	0.497	-7.45	-1.022	-1.022
437	J13	2012/10/05	17:09:03	3681.679	25424.8	22519.8	1749.62	0.499	-7.073	-0.937	-0.937
438	J12	2012/10/05	17:13:08	3682.255	25419.4	22525.5	1747.57	0.497	-6.496	-0.779	-0.779
439	J11	2012/10/05	17:15:50	3682.605	25413.8	22531	1746.09	0.514	-6.145	-0.73	-0.73
440	J10	2012/10/05	17:18:51	3683.161	25408.5	22536.6	1743.71	0.522	-5.588	-0.658	-0.658
441	J09	2012/10/05	17:22:12	3684.242	25402.7	22542.2	1739.25	0.521	-4.506	-0.484	-0.484
442	J08	2012/10/05	17:25:33	3685.497	25397	22547.9	1734.15	0.546	-3.25	-0.267	-0.267
443	J07	2012/10/05	17:28:45	3685.868	25391.3	22554	1732.68	0.551	-2.878	-0.196	-0.196
444	J06	2012/10/05	17:31:15	3686.088	25385.8	22559.6	1731.91	0.549	-2.657	-0.131	-0.131
445	J05	2012/10/05	17:34:01	3686.379	25368.5	22577.3	1730.87	0.601	-2.365	-0.053	-0.053
446	J04	2012/10/05	17:37:50	3686.54	25351	22595.5	1730.37	0.717	-2.203	0.009	0.009
447	J03	2012/10/05	17:40:17	3686.44	25333.6	22613.3	1731.18	0.863	-2.303	0.073	0.073
448	J02	2012/10/05	17:43:23	3685.761	25316.2	22631.2	1734.17	1.02	-2.981	0.005	0.005
449	J01	2012/10/05	17:46:19	3684.482	25298.4	22649.1	1739.48	1.184	-4.259	-0.191	-0.191
452	K01	2012/10/06	09:14:40	3682.94	25338.6	22680.6	1746.8	1.016	-5.815	-0.255	-0.255
453	K02	2012/10/06	09:19:15	3684.511	25354.6	22662.8	1739.82	0.928	-4.244	-0.106	-0.106
454	K03	2012/10/06	09:22:20	3685.297	25371.9	22644.8	1735.78	0.808	-3.459	-0.144	-0.144
455	K04	2012/10/06	09:26:24	3685.383	25389.9	22626.5	1735.41	0.656	-3.373	-0.134	-0.134
456	K05	2012/10/06	09:28:59	3685.513	25406.8	22609.6	1734.85	0.563	-3.244	-0.12	-0.12
457	K06	2012/10/06	09:33:18	3685.654	25423.4	22591.5	1733.76	0.525	-3.104	-0.202	-0.202
458	K07	2012/10/06	09:36:23	3684.455	25440.9	22574	1738.31	0.472	-4.303	-0.474	-0.474
459	K08	2012/10/06	09:40:46	3682.216	25459.2	22554.6	1747.39	0.449	-6.543	-0.862	-0.862
460	K09	2012/10/06	09:45:28	3681.172	25476	22537.9	1751.21	0.446	-7.588	-1.129	-1.129
461	K10	2012/10/06	09:48:18	3680.442	25494.6	22521	1753.02	0.467	-8.319	-1.491	-1.491
462	K11	2012/10/06	09:51:55	3680.583	25511.7	22503.4	1751.5	0.477	-8.179	-1.66	-1.66
463	K12	2012/10/06	09:56:21	3680.398	25529.3	22485	1750.94	0.555	-8.365	-1.96	-1.96
464	K13	2012/10/06	09:59:16	3681.549	25546.5	22466.6	1745.46	0.576	-7.214	-1.927	-1.927
465	K14	2012/10/06	10:04:38	3683.795	25563.8	22448.4	1735.5	0.528	-4.97	-1.713	-1.713
466	K15	2012/10/06	10:09:00	3685.12	25581.4	22430.7	1729.29	0.478	-3.646	-1.655	-1.655
467	K16	2012/10/06	10:12:10	3685.971	25599.6	22412	1724.72	0.445	-2.796	-1.736	-1.736
468	K17	2012/10/06	10:15:18	3686.391	25617.5	22392.8	1721.87	0.458	-2.377	-1.898	-1.898
469	K18	2012/10/06	10:19:23	3687.541	25633.5	22377.4	1716.01	0.141	-1.228	-1.944	-1.944
470	K19	2012/10/06	10:23:15	3685.492	25650.3	22357.6	1722.73	0.603	-3.278	-2.623	-2.623
471	K20	2012/10/06	10:27:57	3683.092	25669.5	22341	1730.26	0.752	-5.679	-3.489	-3.489
472	K21	2012/10/06	10:31:46	3680.178	25686.4	22322.8	1738.5	1.015	-8.594	-4.725	-4.725
473	K22	2012/10/06	10:35:38	3679.178	25703	22304.9	1739.09	1.24	-9.595	-5.606	-5.606

474	L22	2012/10/06	10:41:48	3679.693	25724.5	22355.9	1738.3	1.23	-9.082	-5.255	-5.255
475	L21	2012/10/06	10:45:04	3681.738	25707.6	22373	1734.06	1	-7.038	-4.074	-4.074
476	L20	2012/10/06	10:54:30	3684.829	25690.8	22390.6	1724.4	0.791	-3.95	-2.956	-2.956
477	L19	2012/10/06	10:59:18	3687.219	25671.1	22406.2	1716.7	0.187	-1.561	-2.137	-2.137
478	L18	2012/10/06	11:08:15	3687.894	25657.4	22430.6	1715.02	0.174	-0.889	-1.807	-1.807
479	L17	2012/10/06	11:11:34	3686.649	25639.1	22443.2	1721.06	0.554	-2.135	-1.822	-1.822
480	L16	2012/10/06	11:17:02	3685.629	25620.1	22462.7	1726.04	0.585	-3.157	-1.828	-1.828
481	L15	2012/10/06	11:20:57	3683.159	25602	22481.1	1737.48	0.605	-5.628	-1.967	-1.967
482	L14	2012/10/06	11:23:51	3681.964	25585	22499	1743.15	0.555	-6.824	-2.007	-2.007
483	L13	2012/10/06	11:27:32	3681.399	25565.1	22517.4	1746.67	0.502	-7.39	-1.856	-1.856
484	L12	2012/10/06	11:32:12	3681.004	25549.6	22534.3	1749.18	0.48	-7.786	-1.741	-1.741
485	L11	2012/10/06	11:36:19	3680.759	25539.3	22553.3	1750.81	0.477	-8.032	-1.654	-1.654
486	L10	2012/10/06	11:40:02	3681.069	25521.4	22571	1750.41	0.458	-7.723	-1.427	-1.427
487	L09	2012/10/06	11:43:27	3682.499	25500.8	22587.7	1745.42	0.415	-6.294	-1.015	-1.015
488	L08	2012/10/06	11:49:19	3683.909	25485.3	22606.9	1740.1	0.407	-4.886	-0.691	-0.691
489	L07	2012/10/06	11:52:36	3684.359	25468.8	22626.9	1738.86	0.432	-4.437	-0.495	-0.495
490	L06	2012/10/06	11:56:47	3683.883	25451.6	22644.5	1741.12	0.499	-4.914	-0.512	-0.512
491	L05	2012/10/06	12:00:30	3682.403	25434.1	22664.5	1747.65	0.592	-6.395	-0.662	-0.662
492	L04	2012/10/06	12:04:57	3682.178	25418.9	22679.6	1748.98	0.651	-6.621	-0.616	-0.616
493	L03	2012/10/06	12:09:44	3682.458	25403.3	22698.9	1748.26	0.742	-6.342	-0.485	-0.485
494	L02	2012/10/06	12:13:07	3682.408	25384.2	22718.1	1748.98	0.929	-6.393	-0.388	-0.388
495	L01	2012/10/06	12:17:49	3680.977	25367.7	22737.9	1755.31	1.107	-7.825	-0.531	-0.531
497	M01	2012/10/06	12:28:58	3679.977	25407.7	22771	1758.52	1.061	-8.827	-0.879	-0.879
498	M02	2012/10/06	12:33:55	3680.756	25420.9	22752.5	1754.97	0.888	-8.049	-0.823	-0.823
499	M03	2012/10/06	12:36:54	3681.481	25431	22727.9	1751.82	0.75	-7.324	-0.74	-0.74
500	M04	2012/10/06	12:40:16	3682.221	25448.8	22710.3	1748.28	0.669	-6.585	-0.724	-0.724
501	M05	2012/10/06	12:45:36	3683.701	25468.9	22689.7	1741.54	0.613	-5.105	-0.617	-0.617
502	M06	2012/10/06	12:49:56	3684.82	25484.6	22676.4	1736.57	0.574	-3.987	-0.512	-0.512
503	M07	2012/10/06	12:54:12	3684.915	25502.1	22655.9	1735.91	0.474	-3.893	-0.551	-0.551
506	M08	2012/10/06	14:19:16	3684.34	25518	22639.1	1737.78	0.41	-4.473	-0.751	-0.751
507	M09	2012/10/06	14:22:33	3683.705	25535.2	22618.4	1739.8	0.396	-5.108	-0.975	-0.975
508	M10	2012/10/06	14:26:18	3682.42	25550.7	22604.8	1744.43	0.407	-6.393	-1.315	-1.315
509	M11	2012/10/06	14:34:27	3681.64	25570.2	22585.8	1746.7	0.456	-7.173	-1.633	-1.633
510	M12	2012/10/06	14:38:52	3682.82	25588.6	22566.9	1741.19	0.44	-5.993	-1.575	-1.575
511	M13	2012/10/06	14:44:05	3682.48	25606.8	22547.7	1741.24	0.505	-6.332	-1.905	-1.905
512	M14	2012/10/06	14:47:23	3683.595	25623.2	22531.1	1735.98	0.539	-5.217	-1.863	-1.863
513	M15	2012/10/06	14:50:36	3684.255	25640.4	22513.3	1732.28	0.621	-4.557	-1.956	-1.956
514	M16	2012/10/06	14:55:44	3686.465	25661	22492.7	1721.79	0.662	-2.346	-1.884	-1.884
515	M17	2012/10/06	15:02:33	3688.5	25675.1	22478.5	1711.74	0.331	-0.31	-1.897	-1.897
516	M18	2012/10/06	15:06:09	3690.35	25693.5	22458.8	1703.28	0.524	1.54	-1.77	-1.77
517	M19	2012/10/06	15:11:56	3686.286	25711.2	22442.2	1719.02	0.563	-2.523	-2.625	-2.625
518	M20	2012/10/06	15:16:44	3681.831	25728	22423.7	1734.17	1.323	-6.977	-3.992	-3.992
519	M21	2012/10/06	15:23:07	3679.246	25743.1	22407.3	1740.12	1.586	-9.561	-5.363	-5.363
520	N20	2012/10/06	15:29:14	3682.861	25778.8	22444.3	1726.89	2.51	-5.945	-4.443	-4.443
521	N19	2012/10/06	15:32:34	3683.451	25758.1	22465.2	1727.77	1.881	-5.354	-3.673	-3.673
522	N18	2012/10/06	15:48:08	3691.217	25726.7	22491.6	1698.4	0.593	2.416	-1.889	-1.889
523	N16	2012/10/06	16:00:34	3688.278	25695.3	22529.4	1712.63	0.355	-0.52	-1.924	-1.924
524	N15	2012/10/06	16:04:08	3686.923	25684	22542.4	1719.38	0.558	-1.874	-1.903	-1.903
525	N14	2012/10/06	16:08:47	3684.719	25665.5	22561.4	1730.16	0.598	-4.077	-1.909	-1.909
526	N13	2012/10/06	16:12:43	3684.249	25648.2	22577.9	1733.22	0.483	-4.546	-1.753	-1.753



Rogun Dam
Complementary Geotechnical Investigations at
Right Bank





Rogun Dam
Complementary Geotechnical Investigations at
Right Bank





Rogun Dam
Complementary Geotechnical Investigations at
Right Bank



691	W11	2012/10/08	12:18:12	3684.416	26066.9	22805	1715.59	0.078	-4.289	-5.089	-5.089
692	W12	2012/10/08	12:25:02	3684.693	26078.4	22793.9	1713.61	0.088	-4.013	-5.218	-5.218
693	W13	2012/10/08	12:28:39	3685.423	26099.2	22773.6	1708.52	0.162	-3.284	-5.526	-5.526
694	W14	2012/10/08	12:31:50	3687.664	26117.2	22755.2	1697.82	0.281	-1.043	-5.465	-5.465
695	W15	2012/10/08	12:35:22	3690	26137	22736.3	1686.51	0.385	1.292	-5.436	-5.436
696	W16	2012/10/08	12:40:39	3691.846	26150.4	22721.7	1677.32	0.451	3.137	-5.464	-5.464
697	X16	2012/10/08	12:46:17	3691.192	26183.5	22759.4	1678.66	0.444	2.482	-5.847	-5.847
698	X15	2012/10/08	12:50:24	3689.407	26170.4	22765.6	1686.73	0.33	0.696	-5.988	-5.988
699	X14	2012/10/08	12:55:07	3687.758	26158.5	22780.9	1694.58	0.26	-0.954	-6.037	-6.037
700	X13	2012/10/08	12:58:15	3685.299	26131.4	22801.3	1706.6	0.152	-3.414	-6.048	-6.048
701	X12	2012/10/08	13:02:30	3685.894	26115.1	22818.5	1706.52	0.101	-2.82	-5.471	-5.471
702	X11	2012/10/08	13:05:38	3686.255	26098.5	22833.8	1706.81	0.09	-2.46	-5.05	-5.05
703	X10	2012/10/08	13:08:18	3686.42	26082.7	22855.1	1707.43	0.094	-2.296	-4.76	-4.76
704	X09	2012/10/08	13:12:55	3686.416	26066	22875.3	1708.54	0.13	-2.301	-4.539	-4.539
705	X08	2012/10/08	13:15:55	3685.511	26052.2	22895	1712.71	0.142	-3.207	-4.594	-4.594
706	X07	2012/10/08	13:19:13	3684.006	26033.7	22916.1	1719.33	0.231	-4.712	-4.751	-4.751
707	Y01	2012/10/08	13:23:33	3682.442	26052.3	22931.9	1723.27	0.359	-6.278	-5.513	-5.513
708	Y02	2012/10/08	13:26:48	3682.902	26072.5	22923.5	1719.75	0.233	-5.818	-5.771	-5.771
709	Y03	2012/10/08	13:29:58	3685.818	26088.2	22902.8	1708.85	0.212	-2.903	-5.079	-5.079
710	Y04	2012/10/08	13:32:59	3685.373	26108.4	22886.4	1709.1	0.145	-3.349	-5.473	-5.473
711	Y05	2012/10/08	13:35:55	3685.108	26125	22865.8	1708.47	0.152	-3.615	-5.867	-5.867
712	Y06	2012/10/08	13:39:23	3686.428	26146.8	22839.8	1701.47	0.15	-2.296	-5.976	-5.976